

7-2021

Nutrient Sources, Loads and Trends Vary Spatially and Temporally within the Poteau River Watershed and Lake Wister, Oklahoma

Abbie Lasater
University of Arkansas, Fayetteville

Follow this and additional works at: <https://scholarworks.uark.edu/etd>



Part of the [Environmental Monitoring Commons](#), [Environmental Studies Commons](#), [Fresh Water Studies Commons](#), and the [Water Resource Management Commons](#)

Citation

Lasater, A. (2021). Nutrient Sources, Loads and Trends Vary Spatially and Temporally within the Poteau River Watershed and Lake Wister, Oklahoma. *Graduate Theses and Dissertations* Retrieved from <https://scholarworks.uark.edu/etd/4198>

This Dissertation is brought to you for free and open access by ScholarWorks@UARK. It has been accepted for inclusion in Graduate Theses and Dissertations by an authorized administrator of ScholarWorks@UARK. For more information, please contact scholar@uark.edu.

Nutrient Sources, Loads and Trends Vary Spatially and Temporally within the Poteau River
Watershed and Lake Wister, Oklahoma

A dissertation submitted in partial fulfillment
of the requirements for the degree of
Doctor of Philosophy in Engineering with a concentration in Biological Engineering

by

Abbie Lasater
University of Arkansas
Bachelor of Science in Chemical Engineering, 2017

July 2021
University of Arkansas

This dissertation is approved for recommendation to the Graduate Council.

Brian E. Haggard, Ph.D.
Dissertation Director

Benjamin R. K. Runkle, Ph.D., P.E.
Committee Member

Jung Ae Lee-Bartlett, Ph.D.
Committee Member

Lauren Greenlee, Ph.D.
Committee Member

Abstract

Excess inputs of nutrients and sediments jeopardize drinking water sources, aquatic life habitats, and aesthetic quality of freshwater resources for recreation. The purpose of this dissertation was to analyze long-term water quality trends and loads in the Upper Poteau River Watershed (UPRW) and the Lake Wister Watershed (LWW), and analyze internal phosphorus (P) loads in Lake Wister, Oklahoma. Additionally, this dissertation sought to review the literature for methods of prioritizing subwatersheds for watershed management using watershed models, implement a cost efficient method to remotely monitor streamflow and estimate constituent loads in small-scale watersheds, and finally, to validate the Soil Water Assessment Tool (SWAT) at the small-scale watershed using the aforementioned monitoring data.

Water quality changed over time in the watersheds impacted by both point and nonpoint sources in the UPRW. At the James Fork, total P (TP) did not change and orthophosphate (OP) increased over time, while P decreased at the Poteau River; nitrogen (N) increased at both. Finally, sediment concentrations decreased over time at both the Poteau River and James Fork, with decreasing shifts also occurring in the early 2000's. In the LWW, the largest magnitude of loads came from the Poteau River, and while the magnitude of constituent loads from the Fourche Maline is less, increasing P is a concern. The relatively undisturbed Black Fork watershed contributes the least amount of loads to Lake Wister, and concentrations are decreasing or not changing over time.

In Lake Wister, after 5 aluminum sulfate (alum) treatments across 6 years, sediment P fluxes under anaerobic conditions were not significantly different than prior to any alum treatments. The lack of overall improvement in anaerobic P fluxes over time is likely due to the magnitude of P and sediment loads entering Lake Wister from the LWW, where 92% of the total

P load to Lake Wister from 2010 to 2020 was from external sources. Therefore, while alum treatments provide short term reductions in P fluxes at Quarry Island Cove, the effectiveness was short, suggesting external sources of P must be addressed.

When watershed models are used for subwatershed prioritization, model calibration is often conducted at minimal sites on the large watershed scale and model outputs on the subwatershed scale or smaller are used for prioritization, but little data exists to validate the small-scale model outputs. Therefore, a method was developed to monitor streamflow and estimate constituent loads in small-scale watersheds by using inexpensive pressure transducers to collect continuous records of stage, deploying SonTek-IQs during high flow events, and developing rating curves with stage and discharge data. The small-scale watershed data was then used to validate a SWAT model, which mostly resulted in unsatisfactory performances.

Ultimately, it is important to continue monitoring in the UPRW and LWW to ensure constituent concentrations do not exceed levels of concern. Watershed sources of P must be addressed in addition to internal sources of P in Lake Wister. Finally, it is important to continue exploring subwatershed prioritization techniques and improving watershed model outputs on the small watershed scale.

Acknowledgements

I could not have completed this dissertation without the love and support of my friends and family. I would like to thank all the people who provided support and guidance throughout my time at the University of Arkansas. I would like to thank my advisor, Dr. Brian E. Haggard, for his time, patience, and guidance throughout this process. Thank you for challenging me to become a better scientist. I would like to thank my committee members, Dr. Benjamin Runkle, Dr. Jung Ae Lee-Bartlett, and Dr. Lauren Greenlee, and a previous committee member, Dr. Kieu Le for their additional support in completing this degree. Many people have positively influenced my life to get me where I am today, and I am very grateful for this opportunity and education.

Dedication

To my mother, Cindy Lasater, father, Mark Lasater, and brothers, Aaron Lasater and Sam
Samful

Table of Contents

Introduction.....1

Study Site Description.....3

**Chapter 1: Water Quality Trends and Shifts Variable across Constituents at the Upper
Poteau River Watershed in Arkansas5**

 Abstract.....5

 Introduction.....6

 Methods.....8

Study Site Description.....8

Data Analyses.....11

 Results.....14

Poteau River.....14

James Fork.....16

Black Fork.....18

Point Source Effluents.....24

 Discussion.....26

 Conclusions.....32

 References.....33

Chapter 2: Water Quality Trends and Loads Identify Management Needs in the Lake

Wister Watershed.....36

 Abstract.....36

 Introduction.....37

 Methods.....38

Study Site Description.....39

Data Analyses.....40

 Results.....43

Poteau River.....43

Fourche Maline.....44

Black Fork.....45

 Discussion.....50

 Conclusions.....53

 References.....53

Chapter 3: Magnitude of External Phosphorus Loading Likely Reduces Effectiveness of Aluminum Sulfate Treatments for Management of Sediment Phosphorus Flux56

 Abstract.....56

 Introduction.....57

 Study Site Description.....59

Methods.....	61
Results.....	63
<i>Alum Treatment Experiment in Cores and Cove in 2014</i>	63
<i>Sediment P Fluxes in Quarry Island Cover over Time</i>	65
Discussion.....	69
Conclusions.....	75
References.....	76

Chapter 4: Prioritizing Subwatersheds for Water Quality and Watershed Management

using Watershed Models.....82

Abstract.....	82
Introduction.....	83
Methods.....	85
Watershed Prioritization Techniques using Models.....	85
Challenges of Watershed Models for Prioritization.....	87
Conclusions.....	92
References.....	93

Chapter 5: Cost Efficient Method to Remotely Monitor Streamflow and Estimate

Constituent Loads in Small-Scale Watersheds.....101

Abstract.....	101
---------------	-----

Introduction.....	102
Methods.....	105
<i>Study Site Description</i>	105
<i>Data Collection</i>	107
<i>Rating Curve Development</i>	109
<i>Constituent Load Estimations</i>	110
Results.....	112
<i>Selection of SonTek-IQ Data</i>	112
<i>Rating Curve Development</i>	114
<i>Constituent Load Estimations</i>	120
Discussion.....	122
<i>Rating Curve Development</i>	122
<i>Constituent Load Estimations</i>	128
Conclusions.....	132
References.....	132
Appendix.....	139
<i>Appendix A</i>	139
<i>Appendix B</i>	145

<i>Appendix C</i>	156
<i>Appendix D</i>	167

Chapter 6: Validation of the Soil Water Assessment Tool (SWAT) at Small-Scale

Watersheds Mostly Unsatisfactory.....178

Abstract.....	178
Introduction.....	179
Methods.....	180
<i>Study Site Description</i>	180
<i>SWAT/QSWAT Model Description</i>	183
<i>QSWAT Model Setup</i>	183
<i>QSWAT Model Sensitivity Analysis, Calibration, and Validation</i>	187
Results.....	189
<i>Calibration at Site 1</i>	189
<i>Calibration at Site 5</i>	194
<i>Calibration at Site 10</i>	197
<i>Validation at Small-Scale Watersheds</i>	200
Discussion.....	206
Future Work.....	211
Conclusions.....	212

References.....	212
Appendix A.....	217
Conclusions.....	219

List of Tables

Chapter 1

Table 1. Site IDs (corresponding to Figure 1), names, USGS station numbers, locations, watershed areas, and land use in the Upper Poteau River Watershed.....	9
Table 2. USGS parameter codes, constituents, percentage of censored values, and data availability for each site in the Upper Poteau River Watershed.....	12
Table 3. Optimal LOESS span, LOESS RMSE, linear model slope, linear model p-value, seasonal Kendall's test (SKT) Sens slope, and seasonal Kendall's test p-value for trends in flow adjusted concentrations (FACs) for each parameter of interest at the Poteau River, James Fork, and Black Fork.....	20

Chapter 2

Table 1. Site ID's (corresponding to Figure 1), names, USGS station numbers, locations, watershed areas, and land use in the Lake Wister Watershed.....	40
Table 2. USGS parameter codes, constituents, percentage of censored values, and data availability for each site in the Lake Wister Watershed.....	41

Chapter 4

Table 1. Watershed models used for subwatershed prioritization, country the study was conducted, total watershed size, scale of calibration and validation, number of sites for calibration and validation, parameters used for calibration, scale of subwatershed prioritization, parameters used for prioritization and citations. For the priority scale, values with ~ are average values based on the total watershed size and the number of delineated subwatersheds. If the scale or number of sites used for calibration and validation were not discussed in the study, it is listed as "Unknown." SY= Sediment Yield, TP= Total Phosphorus, TN= Total Nitrogen, Q= Flow/Runoff, SL= Sediment Loads, SS=Suspended Solids, GW= Groundwater, ST=Soil Type, LC= Land Cover.....	99
---	----

Chapter 5

Table 1. Monitoring site ID's (corresponding to Figure 1), names, locations, watershed areas, and land use in the Upper Poteau River Watershed.....	107
Table 2. Generalized Additive Models for Load Estimations, where $s()$ is a spline based smooth function of the predictor variable, and $ti()$ produces a tensor product interaction. Q is log transformed daily or instantaneous flow, and DOY is the day of year.....	111
Table 3. Percentage of stage measurements outside the range of flow and water quality samples, and equivalent number of days with values greater than or less than flow and water quality samples over the three year period (1,095 total days).....	116
Table 4. Slopes of 2-point regression for projecting below the range of measured data, percentage of total flow projected below measured data, average Manning's n estimated using HEC-RAS and used to project flow above the range of measured data, percentage of total flow	

projected above measured data, and LOESS RMSE's for the range of measured data. NA's are listed for sites where SonTek-IQ's were not deployed.....117

Chapter 6

Table 1. Monitoring site ID's (corresponding to Figure 1), names, locations, watershed areas, and land use in the Upper Poteau River Watershed.....	182
Table 2. Performance ratings for evaluating model results (Moriassi et al. 2007).....	189
Table 3. Top five sensitive parameters (descriptions in Appendix A) for each process (flow, sediments, total nitrogen (TN), total phosphorus (TP)), calibration method, and calibrated values at Site 1.....	190
Table 4. Calibration statistics at Site 1 for each constituent (flow, sediments, total nitrogen (TN), total phosphorus (TP)) and average simulated and observed values on the daily, monthly and annual scale.....	191
Table 5: Top five sensitive parameters (descriptions in Appendix A) for each process (flow, sediments, total nitrogen (TN), total phosphorus (TP)), calibration method, and calibrated values at Site 5.....	195
Table 6: Calibration statistics at Site 5 for each constituent (flow, sediments, total nitrogen (TN), total phosphorus (TP)) and average simulated and observed values on the daily, monthly and annual scale.....	196
Table 7: Top five sensitive parameters (descriptions in Appendix A) for each process (flow, sediments, total nitrogen (TN), total phosphorus (TP)), calibration method, and calibrated values at Site 10.....	198
Table 8: Calibration statistics at Site 10 for each constituent (flow, sediments, total nitrogen (TN), total phosphorus (TP)) and average simulated and observed values on the daily, monthly and annual scale.....	199
Table 9: Validation statistics for each constituent (flow, sediments, total nitrogen (TN), total phosphorus (TP)) and average simulated and observed values on the daily scale.....	201
Table 10: Validation statistics for each constituent (flow, sediments, total nitrogen (TN), total phosphorus (TP)) and average simulated and observed values on the monthly scale.....	203
Table 11: Validation statistics for each constituent (flow, sediments, total nitrogen (TN), total phosphorus (TP)) and average simulated and observed values on the annual scale.....	205

List of Figures

Chapter 1

Figure 1. Upper Poteau River Watershed in Arkansas; numbers near stream gages correspond with site IDs in Table 1.....	8
Figure 2. Trends in Flow Adjusted Concentrations (FACs) of Total Nitrogen (TN), Total Phosphorus (TP), Suspended Sediments (SS), Nitrate+Nitrite (NN), and Orthophosphate (OP) at the Poteau River. The FACs were truncated from -1 to 1 for consistency. This may cause a few data points to be missing from the figure, but all data were included in trend analysis. Significant change points are identified by solid vertical lines, the grey areas are the 95% confidence intervals around the change points, and significant linear model slopes are identified by solid blue lines. A timeline of events related to Nonpoint Source Discharge Elimination System (NPDES) permits and other significant milestones for the point sources on the Poteau River is shown in Figure A.....	21
Figure 3. Trends in Flow Adjusted Concentrations (FACs) of Total Nitrogen (TN), Total Phosphorus (TP), Suspended Sediments (SS), Nitrate+Nitrite (NN), and Orthophosphate (OP) at the James Fork. The FACs were truncated from -1 to 1 for consistency. This may cause a few data points to be missing from the figure, but all data were included in trend analysis. Significant change points are identified by solid vertical lines, the grey areas are the 95% confidence intervals around the change points, and significant linear model slopes are identified by solid blue lines. A timeline of events related to Nonpoint Source Discharge Elimination System (NPDES) permits and other significant milestones for the point sources on the James Fork is shown in Figure A.....	22
Figure 4. Trends in Flow Adjusted Concentrations (FACs) of Total Nitrogen (TN), Total Phosphorus (TP), Suspended Sediments (SS), Nitrate+Nitrite (NN), and Orthophosphate (OP) at the Black Fork. The FACs were truncated from -1 to 1 for consistency. This may cause a few data points to be missing from the figure, but all data were included in trend analysis. Significant change points are identified by solid vertical lines, the grey areas are the 95% confidence intervals around the change points, and significant linear model slopes are identified by solid blue lines.....	23
Figure 5. Effluent Concentrations of Ammonia (NH ₃), Total Phosphorus (TP), and Total Suspended Solids (TSS) from the Waldron Waste Water Treatment Plant (WWTP, A-C) and the Tyson Foods, Inc. (D-F) between 1993 and 2019. Blue line represents the linear model slope of the data.....	24
Figure 6: Effluent Concentrations of Ammonia (NH ₃) and Total Suspended Solids (TSS) from the Mansfield Waste Water Treatment Plant (WWTP, A-B) and the Huntington WWTP (C-D) between 2014 and 2019. Blue line represents linear model slope of the data.....	25
Figure 8. Chicken operations and count by county in the Upper Poteau River Watershed from the USDA National Agricultural Statistics Service (NASS, https://www.nass.usda.gov/Quick_Stats).....	31

Chapter 2

Figure 1. Lake Wister Watershed in Arkansas and Oklahoma; numbers near stream gages correspond with Table 1.....	39
Figure 2. Average annual concentrations (dots) and flow normalized concentrations (blue line from WRTDS at the Poteau River near Loving, OK for total nitrogen (TN), nitrate plus nitrite as N (NN), total phosphorus (TP), orthophosphate (OP), and suspended sediment (SS) concentration; slopes and p-values are shown for trends in flow normalized concentrations.....	46
Figure 3: Average annual concentrations (dots) and flow normalized concentrations (blue lines) from WRTDS at the Fourche Maline for total nitrogen (TN), nitrate plus nitrite as N (NN), total phosphorus (TP), orthophosphate (OP), and suspended sediment (SS) concentration; slopes and p-values are shown for trends in flow normalized concentrations.....	47
Figure 4: Average annual concentrations (dots) and flow normalized concentrations (blue lines) from WRTDS at the Black Fork for total nitrogen (TN), nitrate plus nitrite as N (NN), total phosphorus (TP), orthophosphate (OP), and suspended sediment (SS) concentration; slopes and p-values are shown for trends in flow normalized concentrations.....	48
Figure 5: Total nitrogen (TN), nitrate plus nitrite (NN), total phosphorus (TP), orthophosphate (OP), suspended sediment (SS) loads, average annual discharge and total annual precipitation at the Black Fork (Site 2), Fourche Maline (Sites 3 and 4), and the Poteau River near Loving (Site 1) using WRTDS.....	49

Chapter 3

Figure 1. Lake Wister in Oklahoma; Quarry Island Cove is on the north shore of Lake Wister.....	60
Figure 2. Soluble reactive phosphorus (SRP) mass in overlying water over time in cores collected on July 31 st , 2014. Aluminum sulfate and sodium aluminate (alum addition) was added to the cores at equal rates to Quarry Island Cove on August 18 th . Average P fluxes for the anaerobic and aerobic cores are shown above the lines. Average P flux after the alum addition was not significantly different than zero under both aerobic and anaerobic conditions.....	64
Figure 3. All sediment phosphorus (P) fluxes measured under aerobic and anaerobic conditions (A). Sediment P fluxes one week before, one week after, and one month after alum treatments under aerobic (B) and anaerobic conditions (C). Different letters indicate statistically different means ($p < 0.05$).....	66
Figure 4. Average sediment phosphorus (P) fluxes \pm standard deviation under aerobic (top panel) and anaerobic (right panel) conditions each year of sample collection. Vertical dotted lines indicate timing of alum treatment, and 2010 estimates of P fluxes are from Haggard et al., 2012.	67
Figure 5. Sediment phosphorus (P) fluxes under anaerobic conditions from July each year of sample collections. Different letters indicate significantly different means ($p < 0.05$).....	69
Figure 6. Annual, external loads of total phosphorus (TP), soluble reactive phosphorus (SRP), and suspended sediment (SS) from the Black Fork, Fourche Maline and Poteau River entering Lake Wister between 2009 and 2020, adapted from Chapter 2.....	74

Chapter 5

- Figure 1. Monitoring sites in the Upper Poteau River Watershed in Arkansas. Site numbers correspond to site ID's in Table 1.....106
- Figure 2. A) Pressure transducer installation on a bridge post, B) atmospheric pressure transducer attached to a tree outside of floodplain, C) SonTek-IQ attached to concrete block in stream channel, D) SonTek-IQ in stream channel, and E) ammo can attached to tree outside of the flood plain to store battery. Photos by B.J. Austin and A.L Lasater, used with permission108
- Figure 3. Combination of baseflow measurements and data selected from SonTek-IQ continuous measurements for rating curve development where A) includes baseflow measurements and peak flows, B) includes baseflow measurements, peak flows and 75% of peak flows, and C) includes baseflow measurements, peak flows, 75% of peak flows, and 50% of peak flows. D) Hysteresis showing peak flow occurring approximately one hour before peak stage, and E) final selection of data from SonTek-IQ for rating curve development. Data consists of averages around the peak, 75% of peak, and 50% of peak stages and flows and baseflow measurements.....113
- Figure 4. All stage measured, stage measured by flow, and stage sampled for water quality analyses across all non-USGS sites. The bold value in the top left corner of each plot corresponds to site numbers in Table 1. The values above stage measured by flow and stage sampled indicate the percentage of stage data measured by flow and water quality analyses, respectively.....115
- Figure 5. Final rating curves for all non-USGS sites with measured flow data. The bold value in the top left corner of each plot corresponds to site numbers in Table 1. Models were developed using LOESS regression across the range of measured flow data, 2-point regression to project flow less than the minimum measured value, and Manning's equation to project flow greater than the maximum measured value.....118
- Figure 6. Manual and SonTek-IQ measured flows with predicted flows from rating curves. The bold value in the top left corner of each plot corresponds to site numbers in Table 1.....119
- Figure 7. Frequencies of best fit generalized additive models (GAM) 1-5, corresponding to GAMs listed in Table 2, for each load estimation methods (1-3) and for each parameter: total nitrogen (TN), total phosphorus (TP), nitrate plus nitrite (NN), soluble reactive phosphorus (SRP), total suspended solids (TSS), fluoride (Fl), chloride (Cl), and sulfate (SO₄).....121

Chapter 6

- Figure 1. Monitoring sites in the Upper Poteau River Watershed in Arkansas; numbers near streamgages correspond to site ID's in Table 1.....182
- Figure 2. Observed daily streamflow, sediment, total nitrogen (TN), and total phosphorus (TP) loads versus SWAT simulated values at calibration sites; numbers represent Site IDs listed in Table 1.....191
- Figure 3. Observed monthly streamflow, sediment, total nitrogen (TN), and total phosphorus (TP) loads versus SWAT simulated values at calibration sites; numbers represent Site IDs listed in Table 1.....192

Figure 4. Observed annual streamflow, sediment, total nitrogen (TN), and total phosphorus (TP) loads versus SWAT simulated values at calibration sites; numbers represent Site IDs listed in Table 1.....	192
Figure 5. Observed daily streamflow, sediment, total nitrogen (TN), and total phosphorus (TP) loads versus SWAT simulated values at validation sites; numbers represent Site IDs listed in Table 1.....	202
Figure 6. Observed monthly streamflow, sediment, total nitrogen (TN), and total phosphorus (TP) loads versus SWAT simulated values at validation sites; numbers represent Site IDs listed in Table 1.....	204
Figure 7. Observed annual streamflow, sediment, total nitrogen (TN), and total phosphorus (TP) loads versus SWAT simulated values at validation sites; numbers represent Site IDs listed in Table 1.....	206

List of Abbreviations

A	Cross-Sectional Area of Flow
ADEQ	Arkansas Department of Environmental Quality
AGNPS	Agriculture Non-Point Source Pollution Model
AIC	Akaike Information Criterion
Al	Aluminum
Alum	Aluminum Sulfate
ANOVA	Analysis of Variance
ANRC	Arkansas Natural Resource Commission
BMP	Best management practice
CBOD	Carbonaceous Biochemical Oxygen Demand
Cl	Chloride
CWA	Clean Water Act
DEM	Digital Elevation Map
DO	Dissolved Oxygen
DOY	Day of Year
EGRET	Explanation and Graphics for River Trends
ELOHA	Ecological Limits of Hydrologic Alteration
Fl	Fluoride
FN	Flow Normalized
GAM	Generalized Additive Model
GeoWEPP	Geo-Spatial Interface for Water Erosion Prediction Project
GIS	Geographic Information Systems
GW	Groundwater
GWLF	Generalized Watershed Loading Function
HAB	Harmful Algal Bloom
HCT	Hydrologic Characterization Tool
HEC-RAS	Hydrologic Engineering Center's River Analysis System
HIT	High Impact Targeting
HRU	Hydrologic Response Unit

HSPF	Hydrologic Simulation Program Fortran
HUC	Hydrologic Unit Code
HYSTAR	Hydrology Simulation using Time-Area Routing
InVEST SDR	Integrated Valuation of Environmental Services and Trade-Offs Sediment Delivery Ratio
L_d	Daily Loads
L_i	Instantaneous Loads
LOADEST	Load Estimator Platform
LOESS	Locally Weighted Regression
LULC	Land Use/Land Cover
LWW	Lake Wister Watershed
MCDM	Multi-Criteria Decision Making
N	Nitrogen
NaAl(OH)_4	Sodium Aluminate
NH_3	Ammonia
NL	Nutrient Load
NN	Nitrate plus Nitrite
NO_3	Nitrate
NOAA	National Oceanic and Atmospheric Administration
NPDES	National Pollutant Discharge Elimination System
NPS	Non-point source
NSE	Nash-Sutcliffe Efficiency
OP	Orthophosphate
P	Phosphorus
PBIAS	Percent Bias
PRW	Poteau River Watershed
PVC	Polyvinyl Chloride
PVIA	Poteau Valley Improvement Agency
Q	Discharge/Streamflow
Q_d	Mean Daily Flow

QGIS	Open Source Geographic Information System
Q_i	Instantaneous Flow
QSWAT	Open Source Geographic Information System Interface for SWAT
QUAL2kw	Framework for Simulation of Water Quality
R	Hydraulic Radius
RMSE	Root Mean Square Error
RS	Remote Sensing
RSR	Root Mean Square Error Standard Deviation Ratio
S	Slope
SO ₄	Sulfate
SPARROW	Spatially Referenced Regression on Watershed Attributes
SRP	Soluble Reactive Phosphorus
SS	Suspended Sediment
SSURGO	Soil Survey Geographic Soil Database
SWAT	Soil Water Assessment Tool
SWAT-CUP	Soil Water Assessment Tool Calibration and Uncertainty Program
SY	Sediment Yield
TMDL	Total Maximum Daily Load
TN	Total Nitrogen
TP	Total phosphorus
TREX	Two-Dimensional Runoff Erosion and Export
TSS	Total Suspended Solids
UPRW	Upper Poteau River Watershed
USEPA	United States Environmental Protection Agency
USGS	United States Geological Survey
WEPP	Watershed Erosion Prediction Project
WERM	Watershed Erosion Response Model
WLP	Watershed Land prioritization
WP	Wetted Perimeter
WRTDS	Weighted Regression on Time, Discharge, and Season

WRW	Wachusett Reservoir Watershed
WWAT	Water Withdrawal Assessment Tool
WWTP	Waste Water Treatment Plant

List of Submitted Papers

Lasater, A. L., O'Hare, M., and Haggard, B. E. 2021. Water quality trends and shifts variable across constituents at the Upper Poteau River Watershed in Arkansas. Submitted to Transactions of the ASABE. (Dissertation Chapter 1)

Lasater, A. L. and Haggard, B. E. 2021. 2021. Water quality trends and loads identify management needs in the Lake Wister Watershed. Submitted to Agrosystems, Geosciences, & Environment. (Dissertation Chapter 2)

Lasater, A. L., Lee, A. L., and Haggard, B. E. 2021. Magnitude of external phosphorus loading likely reduces effectiveness of aluminum sulfate treatments for management of sediment phosphorus flux. Submitted to Environmental Science & Technology. (Dissertation Chapter 3)

Lasater, A. L., O'Hare, M., Austin, B. J., Scott, E., and Haggard, B. E. 2021. A cost efficient method to remotely monitor streamflow in small-scale watersheds. Submitted to Transactions of the ASABE. (Dissertation Chapter 4)

Introduction

Non-point source (NPS) pollution is a highly recognized threat to freshwater ecosystems (Daniel et al. 1998; Maxted et al. 2009; Ongley et al. 2010), caused by diffuse sources transporting nutrients and sediments into waterbodies primarily through human alteration of landscapes (i.e. urban development and agricultural land use) (Trauth and Xanthopoulos 1997; JunRan et al. 2000; Jonge et al. 2002; Sun et al. 2012). Fertilizers and other chemicals used in agricultural, residential and urban areas enter waterbodies through runoff and seepage, as well as sediments from construction sites and eroding streambanks. External nutrient loading can also originate from point sources, most often through industry and wastewater treatment plant effluent. Excess inputs of nutrients and sediments jeopardize drinking water sources, aquatic life habitats, and aesthetic quality of freshwater ecosystems for recreation (Anderson et al. 2002). With increasing pressures of climate change and population growth, sustainable management of water resources becomes ever more imperative.

Some nutrients entering the waterbody from external sources settle into the bottom sediments through biological assimilation and deposition of suspended solids (Sonzogni et al. 1982; Correll 1998). The bottom sediments can then act as an internal nutrient source, since nutrients are released back into the water column through wind resuspension (Carper and Bachmann 1984), organic matter mineralization (Lovley and Phillips 1986), reductive dissolution under anoxic conditions (Mortimer 1942), or sediment/water equilibrium concentration gradients (Haggard and Sharpley 2006). In particular, sediment release of phosphorus (P) can account for a relatively large fraction of the total P load, especially in eutrophic to hypereutrophic reservoirs (Moore et al. 1998; Haggard et al. 2005a). Sediment P flux is consistently greater during periods of anaerobic conditions compared to aerobic

conditions at the sediment water interface (Correll 1998; Penn et al. 2000; Haggard et al. 2002; Steinman et al. 2004; Haggard et al. 2005a; Sen et al. 2007; Lasater and Haggard 2017), and this internal source of P can maintain water quality issues even when external sources of nutrients are decreased.

Many management strategies focus on external nutrient sources, specifically NPS pollution control through implementation of best management practices (BMPs), which successfully reduce pollutant loads and improve water quality (Merriman et al. 2009; Rao et al. 2009). However, internal sources of nutrients, especially P, are just as important to consider in watershed management strategies (Lasater and Haggard 2017). Sediment P flux is commonly managed by chemical treatment or oxygenation of the water column, causing P to bind to the bottom sediments and reduce internal loading (Kennedy and Cooke 1982; Steinman et al. 2004; Debroux et al. 2012).

Quantifying external and internal pollutant loads, in addition to collecting long-term stage and discharge data, is an essential step towards calibrating and validating watershed models. Watershed models provide a holistic view of hydrologic processes and help to evaluate watershed responses to anthropogenic impacts and changing climates. With advancements in collection of hydrologic data and understanding of physical, chemical and biological processes, these models allow for better understanding on how factors such as population growth, industrialization, urbanization and agriculture, will influence the supply, demand and quality of water (Daniel et al. 2011). Ultimately, watershed models can guide decision making so that management strategies and conservation activities can be effectively implemented to protect water resources.

Study Site Description

The Poteau River Watershed (HUC 11110105) originates on the western edge of Arkansas and flows into Oklahoma, on the southern portion of the Arkansas River Valley. In Arkansas, the Poteau River Watershed drains an area of 1,400 km², which is 56% forested, 21% grassland, 19% transitional and 2% urban/suburban (Arkansaswater.org 2017). The headwaters of the Poteau River originate near Waldron, Arkansas, flowing west into Oklahoma, near Loving, Oklahoma. The two main tributaries of the Poteau River within Arkansas are the Black Fork and the James Fork (to the south and north, respectively).

The Poteau River Watershed has been listed as a priority watershed within the Arkansas Nonpoint Source (NPS) Pollution Management plan since 1998, and thus has been the focus of trans-boundary water quality issues for the last several decades. Several reaches of the Poteau River have been identified as impaired on the 2018 303(d) list for dissolved oxygen, nutrients, anions and turbidity from municipal and industrial point sources and surface erosion (ADEQ 2018). The 2018-2023 NPS Pollution Management Plan aims at reducing pollutant loads in this priority watershed to decrease impairments and restore designated uses (ANRC 2018).

Lake Wister is an impoundment on the Poteau River in Oklahoma, and is on Oklahoma's 303(d) list for algal biomass, pH, total phosphorus (TP) and turbidity (ODEQ 2020). The Lake Wister Watershed covers an area of 2,580 km² and encompasses the southern portion of the Upper Poteau River Watershed (excluding the James Fork watershed, which meets the Poteau River downstream of Lake Wister). The Oklahoma portion of the Lake Wister Watershed is 72% forest, 19% agriculture and 4% urban; similarly, the Arkansas portion is 71% forest, 20% agriculture and 5% urban. The Poteau Valley Improvement Authority (PVIA) actively works to improve water quality in Lake Wister through managing the watershed, the full lake, and Quarry

Island Cove (on the north shore of Lake Wister). Total Maximum Daily Load (TMDL) development concluded that a 78% reduction in TP and a 71% reduction in Total Suspended Solids (TSS) is needed to meet Oklahoma's water quality standards (Scott and Patterson 2018).

The majority of the Upper Poteau River Watershed falls within the Arkansas Valley, which is an alluvial valley between the Ozark Highlands and the Ouachita Mountains. This area is largely underlain with sandstone, shale and siltstone, and poultry and livestock farming are important agricultural land uses. The Black Fork portion of the Upper Poteau River Watershed falls within the Ouachita Mountains, which consists of ridges and hills formed by erosion of sandstone, shale and chert. This area is dominated by loblolly pine and shortleaf pine, and is important for the logging industry. Similarly, the Lake Wister Watershed covers area in the Arkansas Valley and Ouachita Mountains (Woods et al. 2004).

Chapter 1: Water Quality Trends and Shifts Variable across Constituents at the Upper Poteau River Watershed in Arkansas

Abbie L. Lasater¹, Meagan O'Hare¹, and Brian E. Haggard^{1,2}

¹Department of Biological and Agricultural Engineering, University of Arkansas, Fayetteville, AR 72701

²Arkansas Water Resources Center, University of Arkansas, Fayetteville, AR 72701

Abstract

Trend analyses of water quality seek to determine whether concentrations of constituents have increased or decreased over time, which can suggest the effectiveness of management practices or the need for pollutant reduction. The Poteau River Watershed (PRW) is a transboundary watershed across Arkansas and Oklahoma, and in Arkansas, the Poteau River is listed as a priority watershed. The Poteau River flows into Lake Wister, which is an important reservoir for recreation, fishing, and waterfowl hunting for residents and tourists around eastern Oklahoma. The purpose of this study was to analyze long-term (i.e., approximately 25 years) water quality trends across the upper PRW, and to determine how nutrients and sediments have evolved with increasing agriculture and changes in waste water treatment plants in Arkansas. The relatively undisturbed river in the PRW, the Black Fork, showed either decreases or no change in nutrient and sediment concentrations over time (i.e., $\sim 1.0\% \text{ yr}^{-1}$ decrease or less). On the other hand, water quality was changing over time in the two larger watersheds that are impacted by both point and nonpoint sources. At the James Fork, TP did not change and OP increased over time, while P decreased at the Poteau River; N increased at both. Finally, sediment concentrations decreased over time at both the Poteau River and James Fork, with

decreasing shifts also occurring in the early 2000's. The changes over time were not necessarily monotonic, as shifts in flow adjusted concentrations were observed. Point sources in the 2000s reduced their effluent concentrations and regulations were implemented in Arkansas to manage poultry litter applications in nutrient surplus areas (i.e., the UPRW) based on the P index. After these shift changes, water quality did not monotonically change for most sites and parameters over time. Overall, continued monitoring is important, to ensure increasing or unchanging trends do not lead to excessive nutrient concentrations in the watershed.

Introduction

Since the Clean Water Act (CWA) amendment in 1972, federal, state, and local governments have invested billions of dollars to reduce pollutants entering streams and rivers (Keiser and Shapiro 2018). Excess pollutants entering waterbodies can lead to an array of environmental and human health concerns (e.g. excessive plant and algal growth or mercury bioaccumulation through the food chain, Clarkson 1992). The leading source of water quality impairment is nonpoint source pollution, which is most often caused by rainfall runoff across agricultural and urban landscapes (USEPA 2008a). Efforts such as total maximum daily load (TMDL) development, best management practice (BMP) implementation, and stakeholder and citizen education over the last several decades have sought to address diffuse pollutants and improve water quality across the United States.

Monitoring water quality is necessary to assess pollutant concentrations and impacts of conservation activities and watershed management. Long-term water quality and flow data for streams and rivers allow for constituent load estimation, TMDL development, and trend analyses. Trend analyses of water quality seek to determine whether concentrations of constituents have increased or decreased over time, which can suggest the effectiveness of

management practices or the need for pollutant reduction (e.g., see Haggard 2010; Scott et al. 2011). Trends in water quality often occur monotonically, where changes in concentrations are continuous over time, and the typical method involves adjusting constituent concentrations for streamflow and then assessing trends through time (Hirsch et al. 1982; Simpson and Haggard 2018). These trends can inform citizens, watershed managers and government officials of the historical and current state of waterbodies, and the observed changes help to determine future actions for water quality protection.

The Poteau River Watershed (PRW) is a transboundary watershed across Arkansas and Oklahoma. The headwaters of the Poteau River originate near Waldron, Arkansas, then flow west into Oklahoma into Lake Wister, before flowing north to meet the Arkansas River. In Arkansas, the Poteau River it has been listed as a priority watershed within the Arkansas Nonpoint Source (NPS) Pollution Plan since 1998, and has been a focus of trans-boundary water quality issues for the last several decades (ANRC 2018). A TMDL was developed in 2006 for the Poteau River, which concluded a 35% reduction in total phosphorus (TP) from non-point sources was necessary for water quality protection (USEPA 2006). Additionally, municipal and industrial point source reductions have occurred over the past two decades (ANRC 2018).

The purpose of this study is to analyze long-term water quality trends across the upper PRW (UPRW), and to determine how water quality has evolved with increasing agriculture and changes in waste water treatment plants in Arkansas. Monotonic and shift changes in measured water quality parameters will be identified and compared to known watershed management practices and point source reductions through time. This will help determine whether water quality has improved in the area with increasing efforts to minimize point and nonpoint source pollution.

Methods

Study Site Description

The UPRW (HUC 11110105) occupies an area of 1,400 km² in Arkansas (Figure 1). In 2016, land use in the area was 65.3% forested, 25.9% agriculture, 3.7% shrubs/grassland, 6.3% urban/suburban, and 0.8% open water (Dewitz 2019). The headwaters of the Poteau River begin near Waldron, Arkansas, and flow west into Oklahoma, near Loving, Oklahoma. The two main tributaries to the Poteau River within the UPRW are the Black Fork and James Fork. The USGS gauges in the UPRW are on the Black Fork of the Poteau River near Page, Oklahoma, the Poteau River near Cauthron, Arkansas, and the James Fork near Hackett, Arkansas (Figure 1, Table 1). The UPRW is one of 11 NPS priority watersheds in Arkansas (ANRC 2018).

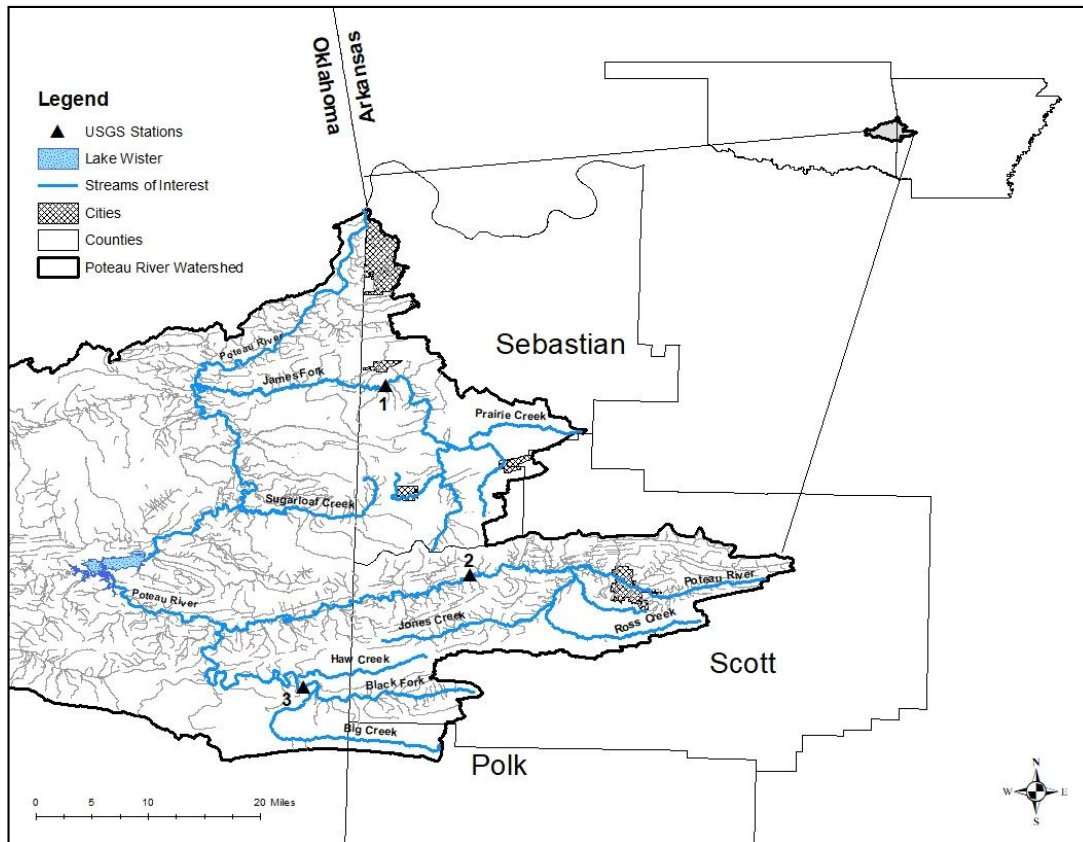


Figure 1: Upper Poteau River Watershed in Arkansas; numbers near streamgages correspond with Site IDs in Table 1.

Table 1: Site IDs (corresponding to Figure 1), names, USGS station numbers, locations, watershed areas, and land use in the Upper Poteau River Watershed

Site ID	Site Name	USGS Station Number	Lat N	Lat W	Watershed Area (km ²)	%F ¹	%U ²	%Ag ³	%G ⁴
1	James Fork near Hackett, AR	7249400	35.162500	94.406944	385	49.7	4.8	33.2	10.9
2	Poteau River near Cauthron, AR	7247000	34.918889	94.299444	527	63.7	5.6	21.3	7.8
3	Black Fork near Page, OK	7247250	34.773610	94.511944	245	88.3	3.5	4.0	4.0

¹ % Forest (%F) includes deciduous, evergreen, and mixed forest; ² % Urban (%U) includes open space, low, medium and high intensity development; ³ % Agriculture (%Ag) includes pasture, hay, and cultivated crops; ⁴ % Grassland (%G) includes grassland and shrubs.

The Poteau River in Arkansas and the Fourche Maline in Oklahoma flow into Lake Wister, an impoundment in Leflore County, Oklahoma (Figure 1), which serves as a drinking water source to about 50,000 people in rural Oklahoma. Lake Wister is also an important reservoir for recreation, fishing, and waterfowl hunting for residents and tourists around eastern Oklahoma. Lake Wister is on Oklahoma's 303(d) list for chlorophyll-a, pH, TP, turbidity and mercury (ODEQ 2020). Historically high algal and cyanobacteria in Lake Wister have led to difficult and costly treatment for drinking water, and has produced several disinfectant by-products. To address water quality concerns in Lake Wister, the Poteau Valley Improvement Agency (PVIA) developed an improvement strategy in 2009, which breaks down restoration into three categories including the watershed, the full lake, and Quarry Island Cove.

An extensive search was conducted in regards to National Pollutant Discharge Elimination System (NPDES) permits and other major changes in the watershed. The Black Fork represents a relatively undisturbed watershed, whereas the Poteau River and James Fork represent

watersheds impacted by point and nonpoint sources. The two major point sources discharging into the Poteau River near Waldron are the Waldron Waste Water Treatment Plant (WWTP) and Tyson Foods, Inc. Permit changes for the Waldron WWTP and Tyson Foods, Inc. have included:

- In 2004, NPDES permits for Tyson, Inc. and Waldron WWTP limited effluent TSS to a monthly average of 15 mg L⁻¹.
- The 2010 permit renewals included an additional effluent limit on TP, resulting in a monthly average of 1.0 and 1.5 mg L⁻¹ for the WWTP and Tyson, respectively.
- No limitations have been set on TN, NN or ammonia (NH₃) for the WWTP; however, since 2004, Tyson's NPDES permit limits TN effluent to 103 mg L⁻¹ monthly average.

Several permitted discharges into tributaries of the James Fork (upstream of the monitoring site) include Huntington and Mansfield WWTPs and West Fraser Inc. (formally known as Travis Lumber Company). In addition, Hartford School District obtained a NPDES permit to discharge in 2004, but it was not renewed in 2009. On the James Fork, limitations on point source effluents with NPDES permits have not changed since first permitting any of the facilities.

These NPDES permits include:

- For the Hartford School District, the NPDES permit limited TSS to a monthly average of 20 mg L⁻¹, but this permit was not renewed after its expiration in 2010.
- The NPDES permit for the Huntington WWTP limits effluent concentrations to a monthly average of 20-30 mg L⁻¹ TSS (depending on the time of year) and 4 mg L⁻¹ NH₃. In January of 2019, the plant was approved for construction to add a second clarifier and include UV disinfection.

- At the Mansfield WWTP, in 2007, an entirely new plant was constructed, and limits on effluents concentrations are monthly averages of 20-30 mg L⁻¹ and 4-6 mg L⁻¹ for TSS and NH₃, respectively.
- At West Fraser Inc., TSS is limited to a monthly average of 35 mg L⁻¹; modifications to the NPDES permit in 2014 included a sedimentation basin that is authorized to discharge overflow into the James Fork after a 10-year, 24-hour or greater storm event.

None of the permits in the James Fork Watershed have limits on effluent P concentrations.

Effluent data from all point sources were obtained from the Arkansas Department of Environmental Quality (DEQ; <https://www.adeq.state.ar.us>) in January, 2021. Simple linear regression and Mann-Kendall trend tests were used to determine trends in reported effluent concentrations over time.

Data Analyses

The long-term data used at each site comes from the USGS National Water Information System database (NWIS; <http://waterdata.usgs.gov/nwis>), which includes flow, stage, and various water quality parameters. Constituents of interest at each site were instantaneous discharge (Q_i), total nitrogen (TN), nitrate plus nitrite (NN), total phosphorus (TP), soluble reactive P (OP) and suspended sediments (SS) (Table 2). These data were generally available from the 1990s to 2020 depending on site and parameter (Table 2). However, water quality data at the Black Fork ended in 2018.

Raw data from the USGS contained censored (i.e., values below detection and/or reporting limits) and estimated values. Estimated values were assumed sufficient, and these values were used in analysis. Less than 15% of the data were censored across all sites and constituents, except for TN and OP at the Black Fork, where 16% and 39% of the data was

censored, respectively (Table 1). Censored values were replaced with the average of the censored values for each parameter to the potential influence of changing reporting limits. The U.S. Environmental Protection Agency suggested using simple substitution methods with data sets less than 15% censored (USEPA 2000). Since less than 15% of the data here was censored for the majority of constituents (except for TN and OP at Black Fork), this method is likely adequate for our data set.

Table 2: USGS parameter codes, constituents, percentage of censored values, and data availability for each site in the Upper Poteau River Watershed.

USGS parameter code	Constituent	Data availability (% Censored)		
		Site 1	Site 2	Site 3
p00600	Total nitrogen (TN), unfiltered, mg L ⁻¹ as N	1975-1981, 1995-2020 (9.2%)	1995-2020 (11.5%)	1991-2018 (16.4%)
p00630	Nitrate plus nitrite (NN), unfiltered, mg L ⁻¹ as N	1977-1994 (0.0%)	NA	NA
p00631	Nitrate plus nitrite (NN), filtered, mg L ⁻¹ as N	1976-1981, 1994-2020 (10.8%)	1995-2020 (11.5%)	1991-2018 (1.4%)
p00665	Total Phosphorus (TP), water, unfiltered, mg L ⁻¹ as P	1972-1981, 1983-2020 (9.6%)	1995-2020 (0.3%)	1992-2018 (9.3%)
p00671	Orthophosphate (OP), water, filtered, mg L ⁻¹ as P	1995-2020 (13.9 %)	1995-2020 (6.2%)	1991-2018 (38.7%)
p80154	Suspended sediment (SS) concentration, mg L ⁻¹	1978-1981, 1995-2020 (0.0%)	1995-2020 (0.0%)	1991-2018 (1.0%)

The database covers several decades where processing and analyses changes occurred for some constituents. Some data were combined to account for changing methods (e.g. switching from filtered to unfiltered samples or for gaps in data availability). At all sites, we combined the

discharge (Q_d , P00060) with the instantaneous discharge (Q_i , P00061) to account for missing Q_i values (< 10 % of data). For the James Fork, we combined the filtered nitrate plus nitrite (NN, p00631) with the unfiltered NN (p00630). There were a few sample dates with both filtered and unfiltered data, and the values were within 10% of each other, so an average of the values was used. At the Poteau and Black Fork, full data sets were available for the filtered NN, so no combination was necessary.

Constituent concentrations were used to evaluate long-term water quality trends, using the following three-step procedure (White et al., 2004):

- Discharge and constituent concentrations were log transformed in order to reduce effects of outliers (Hirsch et al., 1991).
- Constituent concentrations were flow adjusted using a locally weighted regression (LOESS) smoothing technique. LOESS spans were manually inspected, in order to minimize error from the LOESS regression while maximizing the regression's predictive power (Simpson and Haggard, 2018). A range of spans between 0.3 and 0.7 for all constituents was chosen, based on the root mean square errors (RMSE) and visual inspection of the LOESS fits.
- Residuals from the LOESS fit (i.e. the flow-adjusted concentrations, FACs) were analyzed over time in order to evaluate trends, changes in residuals represent a change in constituent concentration over time unrelated to flow. Monotonic trends were examined using linear regression and the nonparametric Seasonal Kendall Test (SKT) based on quarterly data or the median FAC during that quarter. The slopes from these tests were used to estimate the magnitude ($\% \text{ yr}^{-1}$) of any trends (Sen, 1968; Hirsch et al., 1982). Trends with P values less than 0.05 were considered “extremely likely” to increase or

decrease, P values between 0.05 and 0.20 were considered “likely” to increase or decrease, and P values greater than 0.20 were considered “likely not changing” (i.e. as likely increasing or decreasing or not).

Trend analysis was then repeated by removing all censored values to see if the reporting limits influence our trends interpretation. The results from linear regression and the SKT were not different across most of the data, so the results focused on the linear model slopes and p-values.

A nonparametric change point analysis (nCPA) was implemented for all FACs over time, to detect any changes in the time series of data (King and Richardson 2003; Qian et al. 2003). If one or more change point was identified, then the three-step trend analysis was conducted on the time series to the left and right of the point. Additionally, for constituents with gaps in the data sets, a simple t-test or analysis of variance (ANOVA) was used to analyze the difference between means FACs across the groups of data. All data analysis was completed using R, an open source statistical computing environment (R Core Team, 2016).

Results

Poteau River

The Poteau River near Cauthron (Site 2) generally showed the greatest concentrations compared to the James Fork and Black Fork. Over the 25 years of available data, TN concentrations ranged from 0.39 to 2.60 mg L⁻¹, with a median value of 0.76 mg L⁻¹. NN concentrations ranged from 0.02 to 1.74 mg L⁻¹, with a median value of 0.23 mg L⁻¹. TP concentrations ranged from 0.02 to 2.60 mg L⁻¹; however, 98% of the data fell below 0.50 mg L⁻¹ and the median concentration was 0.09 mg L⁻¹. OP concentrations ranged from 0.004 to 2.30 mg L⁻¹, with a median concentration of 0.03 mg L⁻¹, and only one data point (2.30 mg L⁻¹) fell above 0.50 mg L⁻¹. Lastly, SS concentrations ranged from 4 to 970 mg L⁻¹, and the median

concentration was 24 mg L⁻¹. Over the last two years of the study (2019 and 2020), median concentrations of TN, NN, TP, OP, and SS were 0.66, 0.25, 0.05, 0.01, and 10.5 mg L⁻¹, respectively.

All constituent concentrations showed some distinct pattern with increasing discharge. Sediments, P and TN generally increased with discharge, while NN was more variable at higher flows. LOESS was fit to each concentration and discharge relationship with sampling proportions of 0.5 – 0.7 across all constituents (Table 3). All constituents had relatively low RMSEs (<0.50) and spread across time (Table 3, Figure 2), especially TN (RMSE = 0.14).

All nutrient and sediment FACs showed monotonic changes over time, but the direction varied by constituent (Table 3). Flow-adjusted TN significantly increased over time ($p < 0.05$), even though the change was small (0.44 % yr⁻¹). Flow-adjusted NN was the only constituent at this site that showed different results between the linear model and SKT. A slight increase was observed over time with both methods (0.62 and 1.23 % yr⁻¹, SKT and linear model, respectively). However, the SKT suggests only likely increasing ($0.05 < p < 0.20$), while the linear model suggests extremely likely increasing ($p < 0.05$), likely due to the quarterly organization of data with the STK.

In contrast to N, sediment and P were extremely likely improving (i.e. monotonically decreasing) in concentration over time ($p < 0.05$). The greatest magnitude of change occurred in OP FACs, decreasing by -2.55 % yr⁻¹. The decrease in TP was slightly less (-1.53 % yr⁻¹). Sediment FACs were decreasing at a rate of -2.15 % yr⁻¹. Changing FACs each year are relatively small for all constituents (< 3 % yr⁻¹). However, for a change of 2.55 % yr⁻¹, over 25 years of data collection, that's nearly a 65% change in FACs since 1995.

Each constituent showed a shift in FACs (or change point) over time, except for NN (Figure 2). Where shifts occurred, for all constituents, FACs to the left or right were likely not changing over time ($p > 0.20$). For flow-adjusted TP and SS, a shift in FACs occurred in August and October of 2002, resulting in a 22% and 32% decrease in mean TP and SS FACs, respectively. Similarly, a shift occurred in flow-adjusted OP in October 2003, resulting in a 32% decrease. However, for flow-adjusted TN, a shift occurred in May, 2007, with a 9% increase in mean FACs after this time.

James Fork

At the James Fork (Site 1), concentrations were typically lower than the Poteau River. Over the approximately 30 years of available data, TN concentrations ranged from 0.24 to 3.20 mg L⁻¹, with a median value of 0.52 mg L⁻¹. NN concentrations ranged from 0.01 to 1.60 mg L⁻¹, with a median value of 0.11 mg L⁻¹. TP concentrations ranged from 0.01 to 0.80 mg L⁻¹, with a median value of 0.04 mg L⁻¹. OP concentrations ranged from 0.003 to 0.26 mg L⁻¹, with a median value of 0.01 mg L⁻¹. Lastly, SS concentrations ranged from 3 to 642 mg L⁻¹. However, only two values fell above 200 mg L⁻¹, and the median concentration was 27 mg L⁻¹. Over the last two years of the study (2019 and 2020), median concentrations of TN, NN, TP, OP, and SS were 0.51, 0.18, 0.04, 0.01, and 16 mg L⁻¹, respectively.

All constituents at the James Fork showed an increase with increasing discharge. LOESS was fit to each concentration and discharge relationship with sampling proportions of 0.4 – 0.7 (Table 3). All constituents had relatively low RMSEs (<0.40) and spread across time (Table 3, Figure 3). Again, TN expressed the least RMSE of 0.16.

Flow-adjusted TN was likely increasing from 1995 to 2020 ($0.05 < p < 0.20$), with a relatively low magnitude of change (0.29 \% yr^{-1}), and no change point was identified in flow-adjusted TN over time. However, the average flow-adjusted TN was 20% greater between 1975 and 1981 compared to 1995 to 2020 ($p < 0.05$). Flow-adjusted NN was extremely likely increasing from 1995 to 2020 ($p < 0.05$, Table 3). The magnitude of change in flow-adjusted NN was slightly greater than TN (1.25 \% yr^{-1}). Trends in NN were analyzed from 1995 to 2020, where the data set was completely filtered (Table 1). However, with the combined dataset of filtered and unfiltered NN, ANOVA results from the three groups of flow-adjusted data (based on data gaps) showed significant differences. Average, flow-adjusted NN is greatest between 1977 and 1994 and least between 1976 and 1981. Average, flow-adjusted NN from 1994 to 2020 fell between these two groups, but is significantly increasing across time. A shift in flow-adjusted NN occurred in April 1998, with a 38% increase in NN FACs after 1998 compared to 1994 – 1998, but no monotonic trends occurred before or after the change point.

Flow-adjusted OP was likely increasing over time, with a magnitude of change of 0.44 \% yr^{-1} . However, SKT suggests trends in flow-adjusted OP were likely not changing ($p > 0.20$). Two shifts occurred in flow-adjusted OP, one in June 2006 and the other in April 2011. Average flow-adjusted OP was 21% greater after 2011 and 24% less before 2006 compared to between 2006 and 2011. Similar to NN, no monotonic trends occurred in the data set before or after change points in flow-adjusted OP.

Flow-adjusted TP was likely monotonically increasing from 1983 to 2020 ($0.05 < p > 0.2$, Figure 2, A). However, the SKT suggests trends in flow-adjusted TP were likely not changing ($p > 0.20$). Comparing the mean FACs for TP before and after the data gap (Table 1), the average flow-adjusted TP was significantly greater (8% increase) after 1983 compared to the

data between 1972 and 1981 ($p < 0.05$). Additionally, two shifts were identified in FACs over time, one in September 1996 and one in April 2008 (Figure 3, A); however, no monotonic changes occurred before or after the change points. The average flow-adjusted TP was 9% less between the two change points (1996-2008) compared to prior, and 16% less compared to after, giving the slight “U” shape to the FACs over time.

Flow-adjusted SS was the only constituent to be extremely likely improving from 1995 to 2020 (i.e. monotonically decreasing, $-2.27\% \text{ yr}^{-1}$) ($p < 0.05$, Table 3). However, the average flow-adjusted SS after 1995 was not significantly different than the average flow-adjusted SS before 1981 ($p > 0.05$). Two change points were identified relatively close in time, one in June 2002 and the other in January 2005 (Figure 2, E). There was an extremely likely increase in flow-adjusted SS between 2002 and 2005 ($p < 0.05$), but trend analysis across a three-year period is likely unreliable. There were no monotonic trends before 2001 and after 2005. Average flow-adjusted SS was 35% less between 2005 and 2020 than SS FACs between 1995 and 2002.

Black Fork

At the Black Fork (Site 4), concentrations were lower than the Poteau River and the James Fork. Over the 27 years of available data, TN concentrations ranged from 0.11 to 1.3 mg L⁻¹, with a median value of 0.35 mg L⁻¹. NN concentrations ranged from 0.01 to 0.88 mg L⁻¹, with a median value of 0.078 mg L⁻¹. TP concentrations ranged from 0.006 to 0.26 mg L⁻¹, with a median value of 0.022 mg L⁻¹. OP concentrations ranged from 0.003 to 0.18 mg L⁻¹, with a median value of 0.008 mg L⁻¹. Finally, SS concentrations ranged from 0.83 to 146 mg L⁻¹, with a median value of 8.0 mg L⁻¹. At the Black Fork in 2018 (the final year of water quality data), median concentrations of TN, NN, TP, OP, and SS were 0.20, 0.10, 0.01, 0.01 and 4.0 mg L⁻¹, respectively.

All constituents at the Black Fork generally increased in concentration with increasing discharge. LOESS was fit to each concentration and discharge relationship with sampling proportions of 0.4 – 0.6 (Table 3). All LOESS fits for the constituents had relatively low RMSEs (< 0.35), and TN expressed the least RMSE of 0.16 at this site like the Poteau River and the James Fork.

Flow-adjusted TN was extremely likely decreasing over time ($p < 0.001$), with a change of -0.60 \% yr^{-1} (Figure 4, A). One shift in TN FACs occurred in March of 2002, however, FACs to the left or right of the change point were likely not changing over time ($p > 0.20$). The average flow-adjusted TN was 10% greater from 1991-2002 than the average FAC after 2002. Flow-adjusted NN was likely not changing over time ($p = 0.97$; Figure 3 B), and no shift in NN FACs occurred during the study period.

Flow adjusted TP was extremely likely decreasing from 1991-2018 ($p < 0.001$, Figure 4C), and showed the greatest magnitude of change compared to other constituents at the Black Fork (-1.04 \% yr^{-1}). Two shifts were found in flow-adjusted TP over time, one in November 1998 and one in January 2003 (Figure 4). No monotonic changes occurred after the change point in 2003, but there was an extremely likely increase in flow-adjusted TP between 1991 and 2003 ($p = 0.03$). Average flow-adjusted TP between 1998 and 2003 was 23% greater than between 1991 and 1998, and 19% greater than between 2003 and 2020.

Flow-adjusted OP was extremely likely improving over time (i.e. monotonically decreasing) ($p < 0.001$, Table 3), by a magnitude of -0.90 \% yr^{-1} , but nearly 40% of the data are censored. One change point in OP FACs was identified in May of 2000 (Figure 4), however, no monotonic changes occurred before or after the shift. After 2000, average flow-adjusted OP was 17% less than averages before 2000.

Flow-adjusted SS was likely not changing between 1991 and 2018 ($p = 0.52$). A change point in SS FACs was identified in April of 1992 (Figure 4) after only three data points. Flow-adjusted SS after 1992 was likely decreasing at a rate of -0.45 \% yr^{-1} ($p = 0.10$).

Table 3: Optimal LOESS Span, LOESS RMSE, Linear Model Slope, Linear Model P-Value, Seasonal Kendall's Test (SKT) Sens Slope, and Seasonal Kendall's Test P-Value for Trends in Flow Adjusted Concentrations (FACS) for each Parameter of Interest at the Poteau River, James Fork and Black Fork.

Site	Parameter	LOESS Span	LOESS RMSE	Linear Model Slope (%/yr)	Linear Model P-Value	SKT Sens Slope (%/yr)	SKT P-Value
Poteau River at Cauthron, AR	TN	0.70	0.14	0.44	0.02	0.30	0.01
	NN	0.70	0.36	1.23	0.02	0.62	0.05
	TP	0.50	0.29	-1.53	<0.01	-1.37	<0.01
	OP	0.50	0.46	-2.55	<0.01	-2.71	<0.01
	SS	0.60	0.31	-2.15	<0.01	-2.16	<0.01
James Fork	TN	0.40	0.16	0.29	0.15	0.28	0.12
	NN	0.70	0.36	1.25	0.01	0.99	0.01
	TP	0.70	0.26	0.12	0.18	0.04	0.55
	OP	0.70	0.24	0.44	0.05	0.12	0.42
	SS	0.50	0.33	-2.27	<0.01	-2.18	<0.01
Black Fork	TN	0.40	0.16	-0.60	<0.01	-0.66	<0.01
	NN	0.40	0.26	-0.01	0.97	-0.01	0.941
	TP	0.60	0.25	-1.04	<0.01	-1.07	<0.01
	OP	0.40	0.22	-0.90	<0.01	-0.40	<0.01
	SS	0.40	0.32	-0.19	0.52	-0.25	0.28

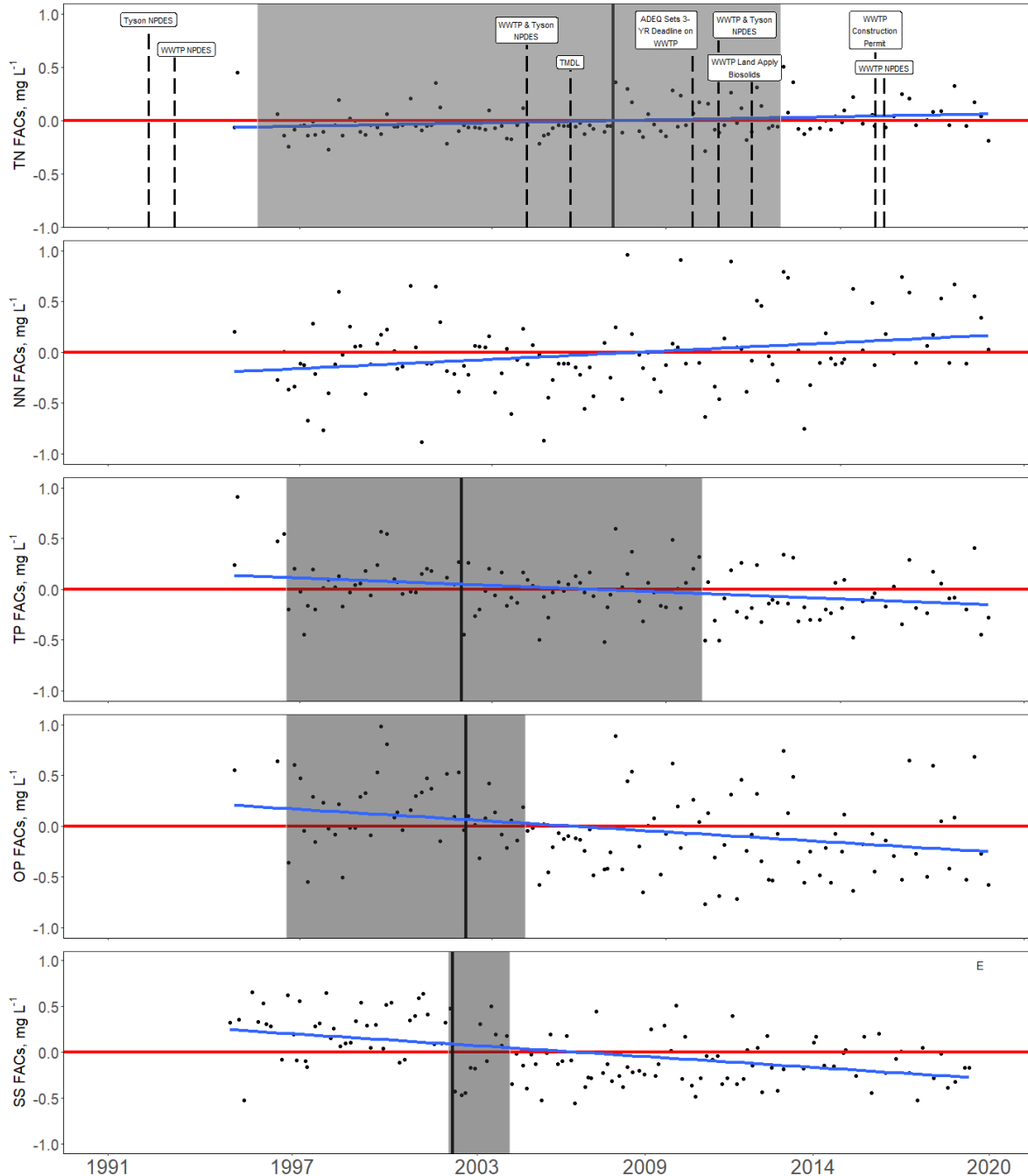


Figure 2: Trends in Flow Adjusted Concentrations (FACs) of Total Nitrogen (TN), Total Phosphorus (TP), Suspended Sediments (SS), Nitrate+Nitrite (NN), and Orthophosphate (OP) at the Poteau River. The FACs were truncated from -1 to 1 for consistency. This may cause a few data points to be missing from the figure, but all data were included in trend analysis.

Significant change points are identified by solid vertical lines, the grey areas are the 95% confidence intervals around the change points, and significant linear model slopes are identified by solid blue lines. A timeline of events related to Nonpoint Source Discharge Elimination System (NPDES) permits and other significant milestones for the point sources on the Poteau River is shown in Figure A.

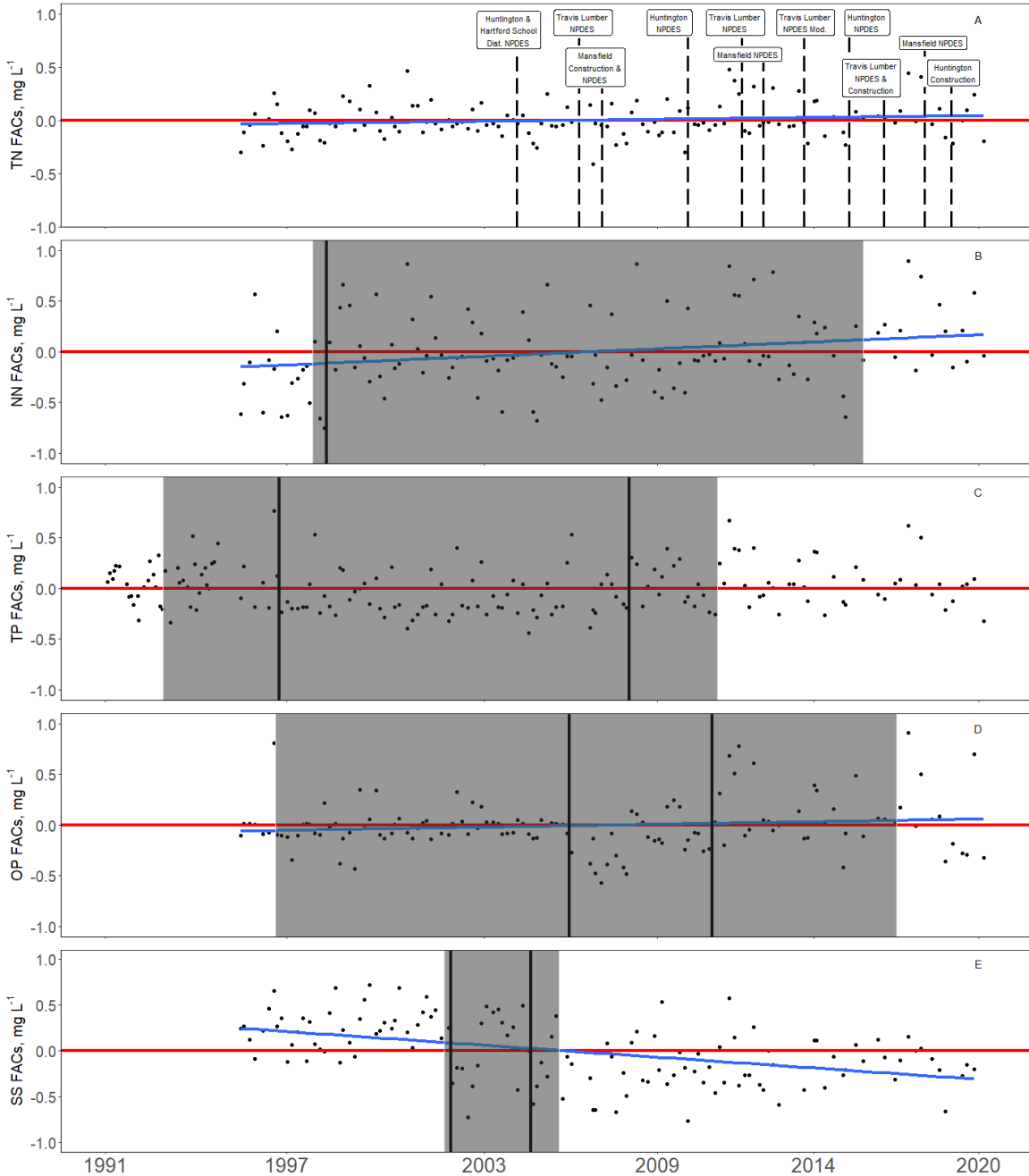


Figure 3: Trends in Flow Adjusted Concentrations (FACs) of Total Nitrogen (TN), Total Phosphorus (TP), Suspended Sediments (SS), Nitrate+Nitrite (NN), and Orthophosphate (OP) at the James Fork. The FACs were truncated from -1 to 1 for consistency. This may cause a few data points to be missing from the figure, but all data were included in trend analysis.

Significant change points are identified by solid vertical lines, the grey areas are the 95% confidence intervals around the change points, and significant linear model slopes are identified by solid blue lines. A timeline of events related to Nonpoint Source Discharge Elimination System (NPDES) permits and other significant milestones for the point sources on the James Fork is shown in Figure A.

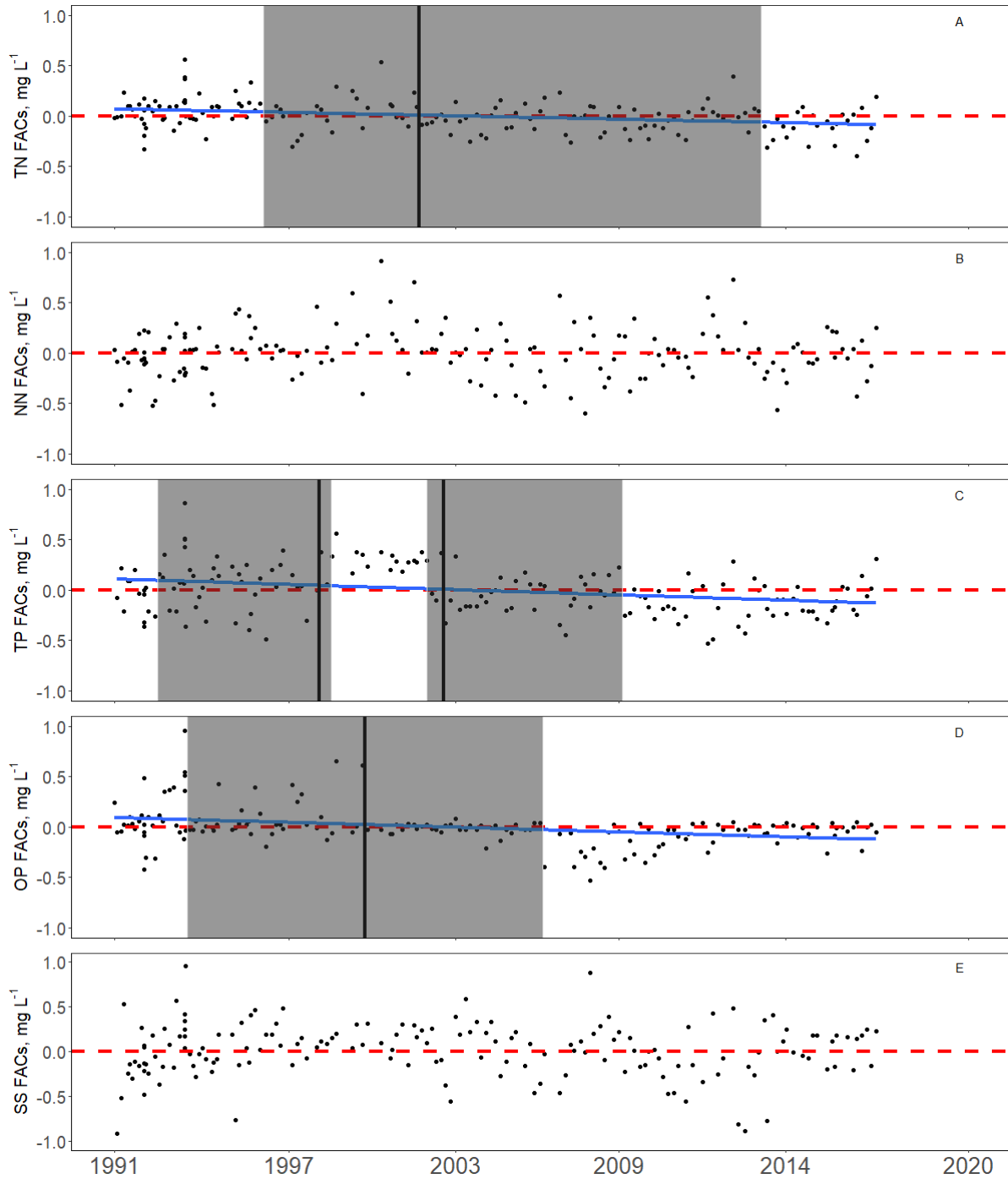


Figure 4: Trends in Flow Adjusted Concentrations (FACs) of Total Nitrogen (TN), Total Phosphorus (TP), Suspended Sediments (SS), Nitrate+Nitrite (NN), and Orthophosphate (OP) at the Black Fork. The FACs were truncated from -1 to 1 for consistency. This may cause a few data points to be missing from the figure, but all data were included in trend analysis.

Significant change points are identified by solid vertical lines, the grey areas are the 95% confidence intervals around the change points, and significant linear model slopes are identified by solid blue lines.

Point Source Effluents

Point sources in the Poteau River watershed include the Waldron WWTP and Tyson, Inc. At the Waldron WWTP, NH_3 concentrations ranged from 0.05 to 23.3 mg L^{-1} with a median of 0.29 mg L^{-1} , TP concentrations ranged from 0.03 to 15.0 mg L^{-1} with a median concentration of 0.79 mg L^{-1} , and TSS concentrations ranged from 0.28 to 29.3 mg L^{-1} with a median concentration of 2.4 mg L^{-1} . At Tyson, Inc., NH_3 concentrations ranged from 0.05 to 5.1 mg L^{-1} with a median of 0.22 mg L^{-1} , TP concentrations ranged from 0.07 to 22.7 mg L^{-1} with a median concentration of 0.88 mg L^{-1} , and TSS concentrations ranged from 0.20 to 370 mg L^{-1} with a median concentration of 1.4 mg L^{-1} . Significant linear decreases have occurred in NH_3 , TP and TSS at Tyson, Inc. and TP and TSS at Waldron WWTP (Figure 5). Additionally, based on Mann-Kendall trend test, significant decreases occurred in all constituents over time at Tyson, Inc. and Waldron WWTP.

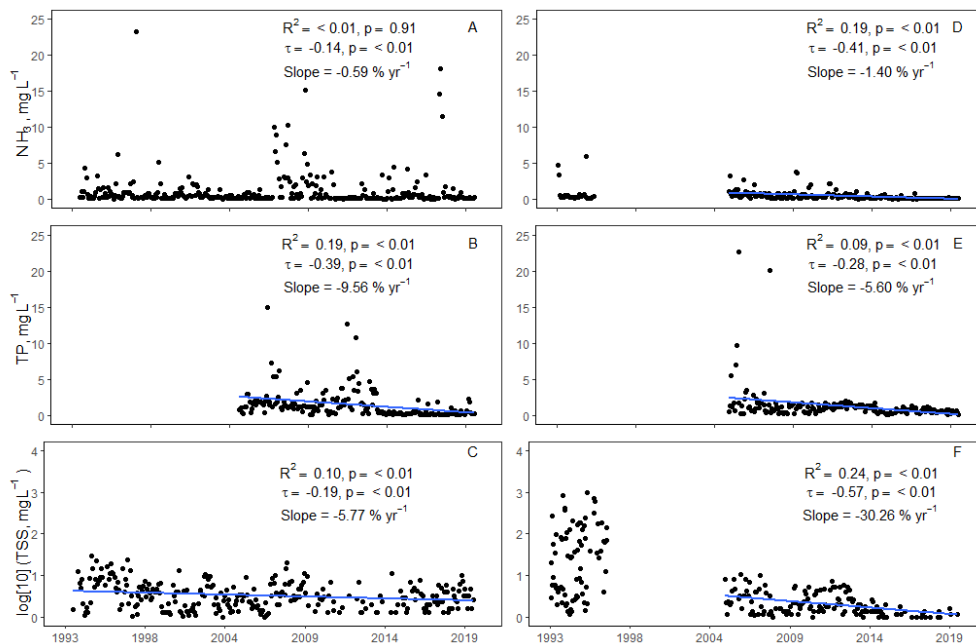


Figure 5: Effluent Concentrations of Ammonia (NH_3), Total Phosphorus (TP), and Total Suspended Solids (TSS) from the Waldron Waste Water Treatment Plant (WWTP, A-C) and the Tyson Foods, Inc. (D-F) between 1993 and 2019. Blue line represents the linear model slope of the data.

In the James Fork watershed, point sources include Mansfield and Huntington WWTP and West Fraser, Inc. At the Mansfield WWTP, NH_3 concentrations ranged from 0.05 to 23.3 mg L^{-1} with a median of 0.29 mg L^{-1} , and TSS concentrations ranged from 1.0 to 20.0 mg L^{-1} with a median concentration of 3.0 mg L^{-1} . At the Huntington WWTP, NH_3 concentrations ranged from 0.06 to 10.5 mg L^{-1} with a median of 0.57 mg L^{-1} , and TSS concentrations ranged from 1.0 to 22.0 mg L^{-1} with a median concentration of 4.8 mg L^{-1} . Based on linear regression and Mann-Kendall trend test, no significant changes occurred in reported constituents over time, except for NH_3 at Huntington, which slightly decreased. At West Fraser, Inc., only a few samples of TSS were reported since 2014, which ranged from 19.1 to 64 mg L^{-1} with a median of 18 mg L^{-1} ; concentrations did not significantly change over time ($p > 0.05$).

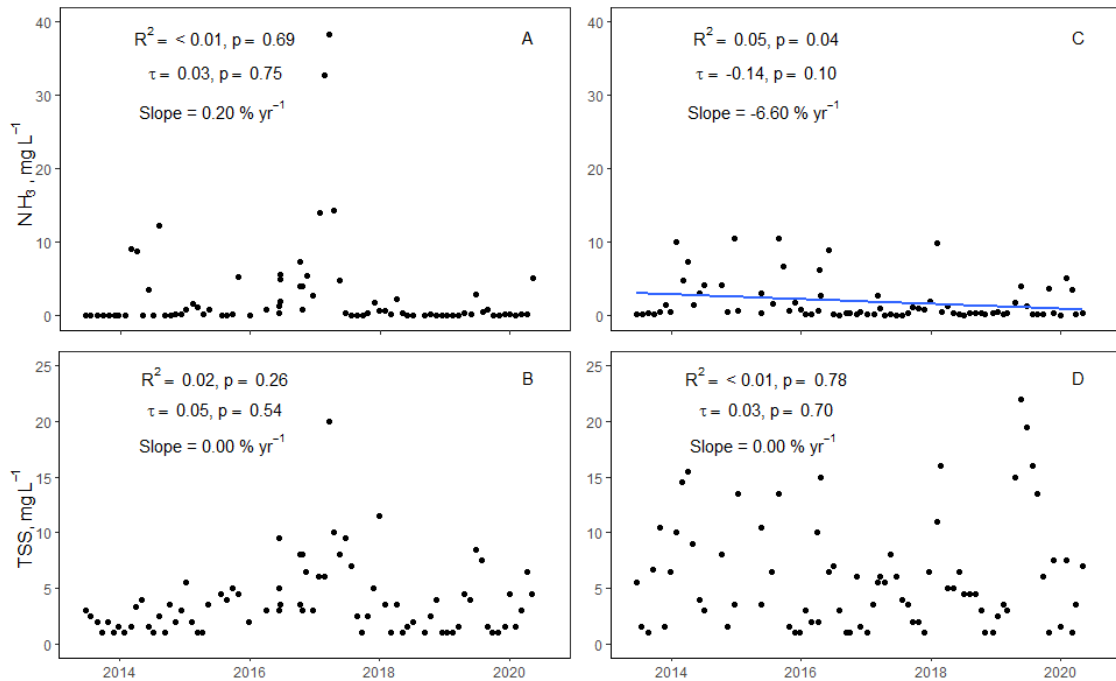


Figure 6: Effluent Concentrations of Ammonia (NH_3) and Total Suspended Solids (TSS) from the Mansfield Waste Water Treatment Plant (WWTP, A-B) and the Huntington WWTP (C-D) between 2014 and 2019. Blue line represents linear model slope of the data.

Discussion

Since water quality has been an ongoing concern in the UPRW, the data presented here provide valuable insight into changes in nutrients and sediments over the last several decades. At the Black Fork, median TN and TP concentrations between 1991 and 2018 were 0.35 mg L^{-1} and 0.02 mg L^{-1} , respectively. Through a literature review of nutrient-biological thresholds across the United States, benthic algal thresholds were determined to be $0.38 - 1.79 \text{ mg L}^{-1}$ and $0.011 - 0.28 \text{ mg L}^{-1}$ for TN and TP, respectively (Evans-White et al. 2013). Median concentrations in the last two years at the Black Fork fell below this range for TN and on the lower end of this range for TP. However, median TP concentrations at the Black Fork fall between 0.006 mg L^{-1} and 0.026 mg L^{-1} TP, where benthic algal response was related to shifts in diatom species rather than nuisance algal conditions (summarized by Evans-White et al. 2013).

While various trends occur across constituents on the Poteau River and the James Fork, median concentrations for all constituents over time are below nutrient thresholds typical for nuisance algal conditions (0.75 , 0.49 , 0.14 , and 0.03 mg L^{-1} for TN, NN, TP and SRP, respectively), determined for the naturally turbid Red River Basin in Arkansas (Haggard et al. 2013). These thresholds may be applicable to the Poteau River, which is also naturally turbid. However, median TN and TP concentrations in the last two years at the James Fork and Poteau River fell within the range for benthic algal thresholds ($0.38 - 1.79 \text{ mg L}^{-1}$ and $0.011 - 0.28 \text{ mg L}^{-1}$ for TN and TP, respectively; Evans-White et al. 2013) reported across the U.S.

Undisturbed watersheds are valuable benchmarks for discerning natural from human-influenced changes in water quality (Murdoch et al. 2005), and nutrients and sediments are often very well retained due to natural vegetation and riparian areas (Lowrance et al. 1984). Trends across seven relatively undisturbed streams in the United States saw both increasing and

decreasing trends in N; however, often times the length of data influenced the direction of trends (Argerich et al. 2013). Additionally, between 2000 and 2014, analysis of minimally disturbed streams across the U.S. found increasing TP concentrations (Stoddard et al. 2016). For the Black Fork, the relatively undisturbed watershed within the UPRW, slight decreases or no changes over time occurred across all flow-adjusted constituents, including after significant shifts in FACs. Our analysis spans nearly 30 years of data at the Black Fork, which likely improves analyses of natural changes over time. It is important to continue water quality monitoring at this site to serve as valuable reference condition for human impacts on regional water quality, but data ended in 2018.

In an analysis of TN and TP concentrations and trends from 2002 to 2012 across 762 sites in the U.S., the majority of sites were above levels of concern (i.e., 0.12 – 2.18 mg L⁻¹ TN and 0.01 – 0.08 mg L⁻¹ TP, varying by ecoregion and based on human health and aquatic life) with undetermined (i.e., minimal rates of change) or decreasing trends (Shoda et al. 2019). TN and TP concentrations at the James Fork and Poteau River fell on the lower end of these ranges, and increasing trends in TN should be closely monitored. Decreasing TP and no change in TP after 2002 at the Poteau River is encouraging, but lack of change in TP at the James Fork should be monitored to observe if increases would occur.

On the James Fork and the Poteau River near Cauthron, water quality is impacted by both point and nonpoint sources. Effluent limitations for point sources have become more stringent over the last several decades (USEPA 2018), and the facilities within the UPRW have made improvement efforts to meet these standards. Effluent concentrations of NH₃, TP and TSS have decreased significantly since 1993 for both facilities in Waldron (Figure 5, $p < 0.001$), except for NH₃ at the WWTP. Notably, in the mid 90's, TSS concentrations from the WWTP and Tyson

reached up to 30 and 400 mg L⁻¹, respectively. With more stringent effluent limitations, the decreasing TSS from these facilities over the last several decades likely contributes to the overall decrease in flow-adjusted suspended sediments at the Poteau River. Similarly, the decreasing effluent P concentrations are likely a big factor contributing to reduced P concentrations at the Poteau River.

In 2006, the TMDL for the Poteau River near Waldron was developed for TP, copper and zinc, with suspected sources of impairment being the Waldron WWTP and Tyson plant; the target concentration for TP in the Poteau River was determined to be 0.1 mg L⁻¹ (FTN Associates 2006). In 2019 and 2020, the median TP concentration was below this target at 0.05 mg L⁻¹. The decreasing shifts in flow-adjusted P and sediment concentrations occurred around the time (or slightly before) of the TMDL development and 2004 permit renewals, which is likely due to the plants preparing to meet new effluent limitations. However, no changes in flow-adjusted P or sediments have occurred since the decreasing shifts in the early 2000s.

While increasing N trends are slight on the Poteau River, this may be due to the lack of limitations on effluent NN concentrations, and since NN is not reported from point source effluents, it could be increasing. While effluent NH₃ concentrations have decreased over time, this could be due to nitrification at WWTPs (Dong et al. 2019), which would lead to increased NN and TN as observed on the Poteau River. Additionally, the Poteau River monitoring site is at least 30 km downstream of the point sources, and uptake lengths for NH₃ are typically between 0.4 and 1.4 km (Haggard et al. 2005b), suggesting reduced N inputs from the effluent would have been nitrified in the river. In 2019 and 2020, fertilizers sold in Scott county were less than 600 tons, which is on the lower end compared to the rest of Arkansas (UADOA 2019, 2020). Therefore, while fertilizer rates often control N concentrations (Liu et al. 2021), it is

more likely that increasing N on the Poteau River is due to point sources than fertilizer inputs. However, it is important to note that while NN is increasing over the entire period of data, TN was likely not changing after the increasing shift in 2007.

In the James Fork Watershed, effluent concentrations of NH_3 and TSS from the Mansfield and Huntington WWTPs have only been reported since 2014. Effluent concentrations of NH_3 and TSS have been relatively stable since 2014, with the only significant decrease occurring in NH_3 from the Huntington WWTP (Figure 6). No effluent data was available from the Hartford School District, and only a few samples of TSS were reported from West Fraser Inc., which have been relatively stable since 2014. These small facilities may be contributing to N increases at the James Fork, similar to processes discussed previously for the Poteau River, since fertilizers use in Sebastian county are also low compared to the rest of Arkansas (UADOA 2019, 2020). However, the impact on P concentrations is more difficult to determine without effluent P data. Additionally, monitoring in HUC-12 subwatersheds within the James Fork watershed between 2011 and 2012 identified streams with high nitrate and TP concentrations as watersheds with permitted discharges (Massey et al. 2013).

Interestingly, our analyses of the data suggested decreasing suspended solids on the Poteau River and James Fork since at least 1994, while the relatively undisturbed Black Fork Watershed suggested likely no changes. Similar decreasing trends were observed for suspended sediment concentrations between 1992 and 2012 on the Poteau River at Loving, Oklahoma in a study conducted by the United States Geological Survey (Oelsner et al. 2017). On the Poteau River and James Fork, decreasing solids could be attributed to more stringent effluent limitations (or limitations at all) for point sources.

In Scott County, which contains the Poteau River Watershed, population has maintained relatively stable, chicken operations have decreased, but chicken counts have remained fairly stable over the last several decades (USDA-NASS 2018) (Figure 8). Stable or increasing poultry counts with decreasing operations likely suggests decreasing farm numbers while operations increase in production capacity. Chicken counts are related to the amount of litter produced, which must be managed in the watershed. Most likely, the litter is land applied within relatively close proximity to the poultry houses. Historically, poultry litter was managed on an N basis (i.e., applied to pastures and hay fields to meet the forage N requirements), which has led to buildup of P in the soils and potential for P loss from the landscape. However, in 2003, Arkansas legislation was implemented to manage poultry litter based on the P Index, which assigns a risk value for P loss in runoff based on P source potential, P transport potential, and BMPs (DeLaune et al. 2004). The P index was updated in 2010 to be more stringent in nutrient surplus areas (Sharpley et al. 2010), which includes the UPRW. Therefore, in addition to the TMDL development and decreases in point source effluents, the decreasing trends in P on the Poteau River, and the shifts in TP and OP in the early 2000's, could be related to implementation of the P index across the watershed.

In Sebastian County, containing the James Fork Watershed, population has increased by about 25% over the last 30 years and chicken counts have continually increased from 1997 to 2017 (USDA-NASS 2018) (Figure 8). In addition to the small point source facilities in the area, increasing population and amount of poultry litter are likely leading to increased N and P concentrations. Subwatersheds with less than 50% forested area and more than 0.9 poultry houses km⁻² were identified as critical source areas for NPS pollution management in Arkansas (McCarty et al. 2018), and while poultry house density is about 0.3 poultry houses km⁻² in the

James Fork watershed, just less than 50% of the watershed area is forested, suggesting land use may be a reason for impairments.

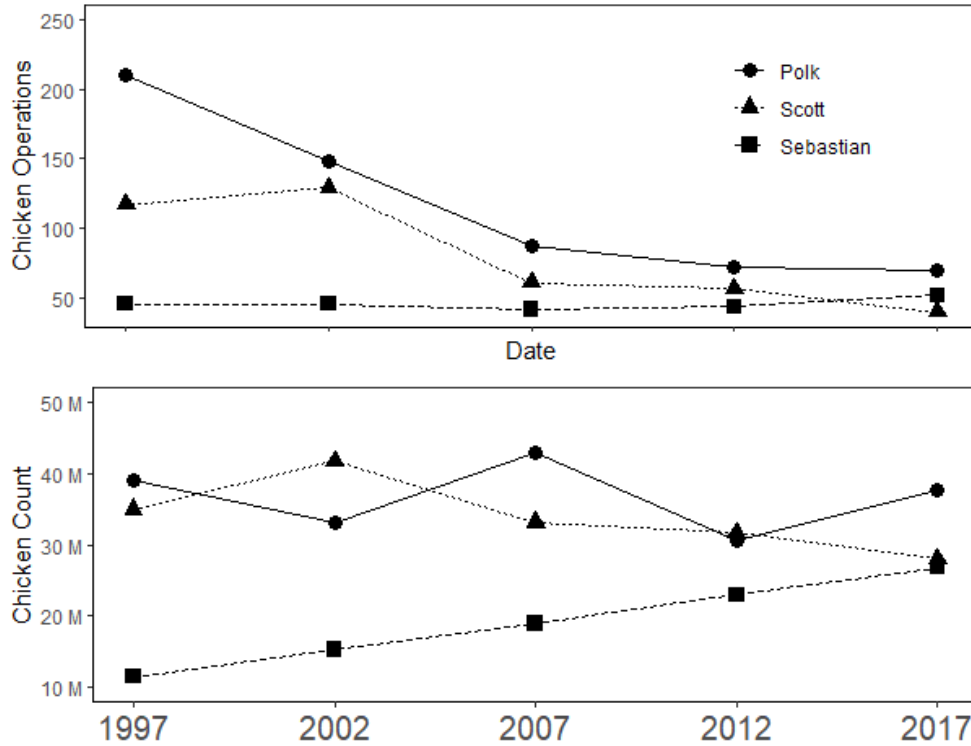


Figure 8: Chicken operations and count by county in the Upper Poteau River Watershed from the USDA National Agricultural Statistics Service (NASS, https://www.nass.usda.gov/Quick_Stats).

Numerous efforts have been made in Scott and Sebastian Counties to reduce sediment and nutrient loading from nonpoint sources into the Poteau River over the last several decades. Between 2002 and 2005, several BMPs were implemented in the watershed (e.g. prescribed grazing, waste management systems, nutrient management), leading to an overall reduction of N, P, and sediment loads by 14,025 kg yr⁻¹, 1,225 kg yr⁻¹, 67 kg yr⁻¹, respectively (USEPA 2005). Also, between 2009 and 2010, the ANRC provided subsidies to transport litter from nutrient surplus areas (including the UPRW) to other approved areas in Arkansas.

In general, the magnitude of decreasing trends were greater than the magnitudes of increasing trends, suggesting that water quality is improving at a faster rate than it may be worsening. Additionally, after shift changes occurred in most constituents, water quality did not monotonically increase or decrease afterwards. Since the passing of the clean water act (CWA) in 1972, water quality across the U.S. has been improving, and over 700 waterbodies have been partially or fully restored (USEPA 2019). Therefore, we expect water quality to improve in this watershed, especially with the numerous efforts to reduce point and nonpoint source pollution going into Oklahoma. For the UPRW, continued monitoring will be important to allow changes in water quality from human activities and watershed management to be captured. Additionally, continued monitoring will contribute to better understanding on how anthropogenic activities are influencing water quality in this watershed.

Conclusions

Long term water quality trends in the Upper Poteau River Watershed in Arkansas identified areas of concern with increasing constituent trends, as well as benefits of management implementation in the watershed. The relatively undisturbed river, the Black Fork, had median nutrient concentrations below typical nuisance algal thresholds and showed either decreases or no change in nutrient and sediment concentrations over time. Water quality monitoring ended in 2018, and resumed monitoring could allow for the Black Fork to serve as a reference for the impacted watersheds in this region.

The James Fork and Poteau River are impacted by both point and nonpoint sources, and median concentrations of TN and TP fall within the benthic algal thresholds. In the James Fork, increases in N and P have occurred, while decreases in sediments were observed. Small WWTPs in the James Fork watershed have no limitations on P, and population and poultry production

have increased over time, likely leading to the increasing FACs. However, after shift changes in nutrient and sediment FACs in the 2000s, no changes have occurred over time.

At the Poteau River, decreases in P and sediments and increases in N have occurred. Shifts in P FACs occurred around 2003, when point sources were making improvements and reducing effluent concentrations, and regulations were implemented in Arkansas to manage poultry litter applications in NSAs (i.e., the UPRW) based on the P index. Additionally, over the last two years, median TP concentrations at the Poteau River fell below the target concentration identified in the TMDL. While effluent NH₃ concentrations were decreasing in the Poteau River watershed, increases in TN and NN might be attributed to increasing nitrification at WWTPs. Ultimately, the regulations and indexes in the UPRW have likely contributed to the decreasing nutrient trends (or minimized the rate of increasing trends). However, it is important to continue monitoring increasing or unchanging trends in FACs across the watershed, to prevent and manage excessive nutrient concentrations.

References

- ANRC (2018) 2018-2023 Nonpoint Source Pollution Management Plan. Arkansas Natural Resource Commission, Little Rock, Arkansas
- Argerich A, Johnson SL, Sebestyen SD, et al (2013) Trends in stream nitrogen concentrations for forested reference catchments across the USA. *Environ Res Lett* 8: doi: 10.1088/1748-9326/8/1/014039
- Clarkson TW (1992) Mercury: Major Issues in Environmental Health. *Environ Health Perspect* 100:31–38
- DeLaune PB, Moore PA, Carman DK, et al (2004) Evaluation of the Phosphorus Source Component in the Phosphorus Index for Pastures. *J Environ Qual* 33:2192–2200. doi: 10.2134/jeq2004.2192
- Dewitz J (2019) National Land Cover Database (NLCD). U.S. Geological Survey
- Dong Y, Yuan H, Zhang R, Zhu N (2019) Removal of ammonia nitrogen from wastewater: A review. *Trans ASABE* 62:1767–1778

- Evans-White MA, Haggard BE, Scott JT (2013) A Review of Stream Nutrient Criteria Development in the United States. *J Environ Qual* 42:1002. doi: 10.2134/jeq2012.0491
- FTN Associates L (2006) TMDLs for Phosphorus, Copper and Zinc for the Poteau River near Waldron, AR. Little Roc
- Haggard BE (2010) Phosphorus Concentrations, Loads, and Sources within the Illinois River Drainage Area, Northwest Arkansas, 1997–2008. *J Environ Qual* 39:2113. doi: 10.2134/jeq2010.0049
- Haggard BE, Scott JT, Longing SD (2013) Sestonic Chlorophyll- Shows Hierarchical Structure and Thresholds with Nutrients across the Red River Basin, USA. *J Environ Qual* 42:437. doi: 10.2134/jeq2012.0181
- Haggard BE, Stanley EH, Storm DE (2005) Nutrient retention in a point-source-enriched stream. *J North Am Benthol Soc* 24:29–47. doi: 10.1899/0887-3593(2005)024<0029:nriaps>2.0.co;2
- Hirsch RM, Slack JR, Smith RA (1982) Techniques of trend analysis for monthly water quality data. *Water Resour Res* 18:107–121
- Keiser DA, Shapiro JS (2018) Consequences of the Clean Water Act and the Demand for Water Quality. *Q J Econ* 134:349–396
- King RS, Richardson CJ (2003) Integrating Bioassessment and Ecological Risk Assessment: An Approach to Developing Numerical Water-Quality Criteria. *Environ Manage* 31:795–809
- Liu W, Yuan Y, Koropecj-Cox L (2021) Effectiveness of nutrient management on water quality improvement: A synthesis of nitrate-nitrogen loss from subsurface drainage. *Trans ASABE* 64:675–689
- Lowrance R, Todd R, Fail, J, et al (1984) Riparian Forests as Nutrient Filters in Agricultural Watersheds. *Bioscience* 34:374–377. doi: 10.2307/1309729
- Mccarty JA, Matlock MD, Scott JT, Haggard BE (2018) Risk indicators for identifying critical source areas in five arkansas watersheds. *Am Soc Agric Biol Eng* 61:1025–1032
- Murdoch PS, McHale MR, Mast MA, Clow DW (2005) The U.S. Geological Survey Hydrologic Benchmark Network
- ODEQ (2020) Oklahoma’s Final Impaired Waterbodies- 303(d) List. Oklahoma Dep Environ Qual
- Oelsner GP, Sprague LA, Murphy JC, et al (2017) Water-Quality Trends in the Nation’s Rivers and Streams 1972-2012- Data Preparation, Statistical Methods, and Trend Results: U.S. Geological Survey Scientific Investigations Report 2017-5006
- Qian SS, King RS, Richardson CJ (2003) Two Statistical Methods for Detecting Environmental Thresholds. *Ecol Modell* 166:87–97

- Scott JT, Haggard BE, Sharpley AN, Romeis JJ (2011) Change Point Analysis of Phosphorus Trends in the Illinois River (Oklahoma) Demonstrates the Effects of Watershed Management. *J Environ Qual* 40:1249–1256. doi: 10.2134/jeq2010.0476
- Sharpley A, Moore P, Daniels M, et al (2010) Arkansas Phosphorus Index. Fayetteville, Arkansas
- Shoda ME, Sprague LA, Murphy JC, Riskin ML (2019) Water-quality trends in U. S. rivers, 2002 to 2012: Relations to levels of concern. *Sci Total Environ* 650:2314–2324. doi: 10.1016/j.scitotenv.2018.09.377
- Simpson ZP, Haggard BE (2018) Optimizing the flow adjustment of constituent concentrations via LOESS for trend analysis. *Environ Monit Assess* 190:
- Stoddard JL, Van Sickle J, Herlihy AT, et al (2016) Continental-Scale Increase in Lake and Stream Phosphorus: Are Oligotrophic Systems Disappearing in the United States? *Environ Sci Technol* 50:3409–3415. doi: 10.1021/acs.est.5b05950
- UADOA (2019) Arkansas Distribution of Fertilizer Sales by County. Little Rock, Arkansas
- UADOA (2020) Arkansas Distribution of Fertilizer Sales by County. Little Rock, Arkansas
- USDA-NASS (2018) Quick Stats. https://www.nass.usda.gov/Quick_Stats/. Accessed 5 Jun 2019
- USEPA (2008) National Water Quality Assessment. <https://www.epa.gov/nps/nonpoint-source-agriculture>
- USEPA (2006) TMDLs for Phosphorus, Copper, and Zinc for The Poteau River Near Waldron, AR. United States Environmental Protection Agency, Dallas, TX
- USEPA (2000) Guidance for Data Quality Assessment. United States Environmental Protection Agency, Washington, DC
- USEPA (2018) Final 2016 Effluent Guidelines Program Plan. Washington, DC
- USEPA (2019) Success Stories about Restoring Water Bodies Impaired by Nonpoint Source Pollution. <https://www.epa.gov/nps/success-stories-about-restoring-water-bodies-impaired-nonpoint-source-pollution>. Accessed 5 Jun 2019

Chapter 2: Water Quality Trends and Loads Identify Management Needs in the Lake Wister Watershed

Abbie Lasater¹, and Brian E. Haggard^{1,2}

¹Department of Biological and Agricultural Engineering, University of Arkansas, Fayetteville, AR 72701

²Arkansas Water Resources Center, University of Arkansas, Fayetteville, AR 72701

Abstract

Trend analyses of water quality seek to determine whether concentrations of constituents have increased or decreased over time, which can show the effectiveness of management practices or the need for pollutant reduction. The Poteau River Watershed (PRW) is a transboundary watershed across Arkansas and Oklahoma, and in Arkansas, the Poteau River has been listed as a priority watershed within the Arkansas Nonpoint Source Pollution Plan since 1998. The Poteau River, Black Fork, and Fourche Maline within the PRW flow into Lake Wister, which is an important reservoir for recreation, fishing, and waterfowl hunting for residents and tourists around eastern Oklahoma. The purpose of this study is to analyze long term trends and loads using the Weighted Regression on Time, Discharge, and Season (WRTDS) to analyze water quality trends and constituent loads from the Poteau River, Black Fork, and Fourche Maline entering Lake Wister. The largest magnitude of loads came from the Poteau River, but flow normalized (FN) phosphorus (P) and sediments have decreased over time, which is a positive impact of watershed management and must be maintained. However, FN nitrogen (N) on the Poteau River has increased over time, and should be the focus of future management

on the Poteau River. While the magnitude of constituent loads from the Fourche Maline are less than the Poteau River, increasing FN P is a concern, and should be prioritized for management in Oklahoma. The relatively undisturbed Black Fork watershed contributes the least amount of loads to Lake Wister, and FN concentrations are decreasing or not changing over time, suggesting a low priority for the Black Fork watershed.

Introduction

Lakes and reservoirs provide many benefits, including wildlife habitats, hydrodynamic energy production, drinking water, and recreation opportunities. However, nutrient pollution to lakes and reservoirs contributes to algal blooms and potential algal toxins, which jeopardizes the quality of these freshwater resources. In 2012, the National Lakes Assessment concluded that 40% of lakes in the United States (U.S.) had excessive total phosphorus (TP) levels and 35% of lakes had excessive total nitrogen (TN) levels. Additionally, the algal toxin microcystin was detected in 39% of lakes (USEPA 2016). Therefore, it is imperative to manage and reduce nutrient pollution in order to sustain lake and reservoir ecosystems, and efforts such as total maximum daily load (TMDL) development, best management practice (BMP) implementation, and stakeholder and citizen education over the last few decades have sought to improve water quality across the United States.

The leading source of water quality impairment is nonpoint source (NPS) pollution, most often caused by rainfall runoff across agricultural and urban landscapes (USEPA 2008a). Point source inputs also contribute to water quality concerns, through effluents from waste water treatment plants (WWTPs) and other industry processes. Nutrients and sediments from external sources (i.e., point and NPS pollution) ultimately accumulate in bottom sediments of lakes and reservoirs, and these nutrients can be released back into the water column under certain

conditions (i.e., internal nutrient sources). Excess nutrients and sediments from internal and external sources lead to accelerated eutrophication and degradation of water resources.

Long-term water quality monitoring is important for assessing nutrient and sediment concentrations entering lakes and reservoirs. Monitoring data allows for constituent load estimations (Malago et al. 2019), total maximum daily load (TMDL) development (Borah et al. 2019), and trend analyses (Shoda et al. 2019), which help analyze impacts of conservation activities and watershed management. In particular, trend analyses of water quality seek to determine whether concentrations of constituents have increased or decreased over time, which can show the effectiveness of management practices or the need for pollutant reduction (e.g., see Haggard 2010; Scott et al. 2011). Estimation of constituent loads help to identify critical source areas, or smaller watersheds which may be contributing disproportionately higher pollutant loads and can be prioritized for management intervention. These trends and constituent loads can inform citizens, watershed managers and government officials of the historical and current state of waterbodies, and help to determine future actions to protect water quality.

The purpose of this study is to analyze long term trends and loads from major tributaries to Lake Wister, Oklahoma, to understand nutrient inputs into the reservoir. Specifically, the Weighted Regression on Time, Discharge, and Season (WRTDS) was used to analyze water quality trends and constituent loads from the Poteau River, Black Fork, and Fourche Maline entering Lake Wister. This analysis will help to inform citizens and stakeholders of changes in water quality over time at the Lake Wister Watershed (LWW), as well as the relative contribution from each major inflow.

Methods

Study Site Description

The LWW encompasses the southern portion of the Poteau River watershed (HUC 11110105), and it occupies an area of 2,580 km² in Arkansas and Oklahoma (Figure 1), that is 72.0% forested, 14.4% agriculture, 7.2% shrubs/grassland, 4.0% urban/suburban, and 1.2% open water. The three main tributaries into Lake Wister are the Poteau River, Black Fork, and Fourche Maline. The headwaters of the Poteau River begin near Waldron, Arkansas, and flow west into Oklahoma, near Loving, Oklahoma. The most downstream USGS gauges with flow and water quality data in the LWW are on the Black Fork of the Poteau River near Page, Oklahoma, the Poteau River near Loving, Oklahoma, and the Fourche Maline near Leflore and Red Oak, Oklahoma (Table 1).

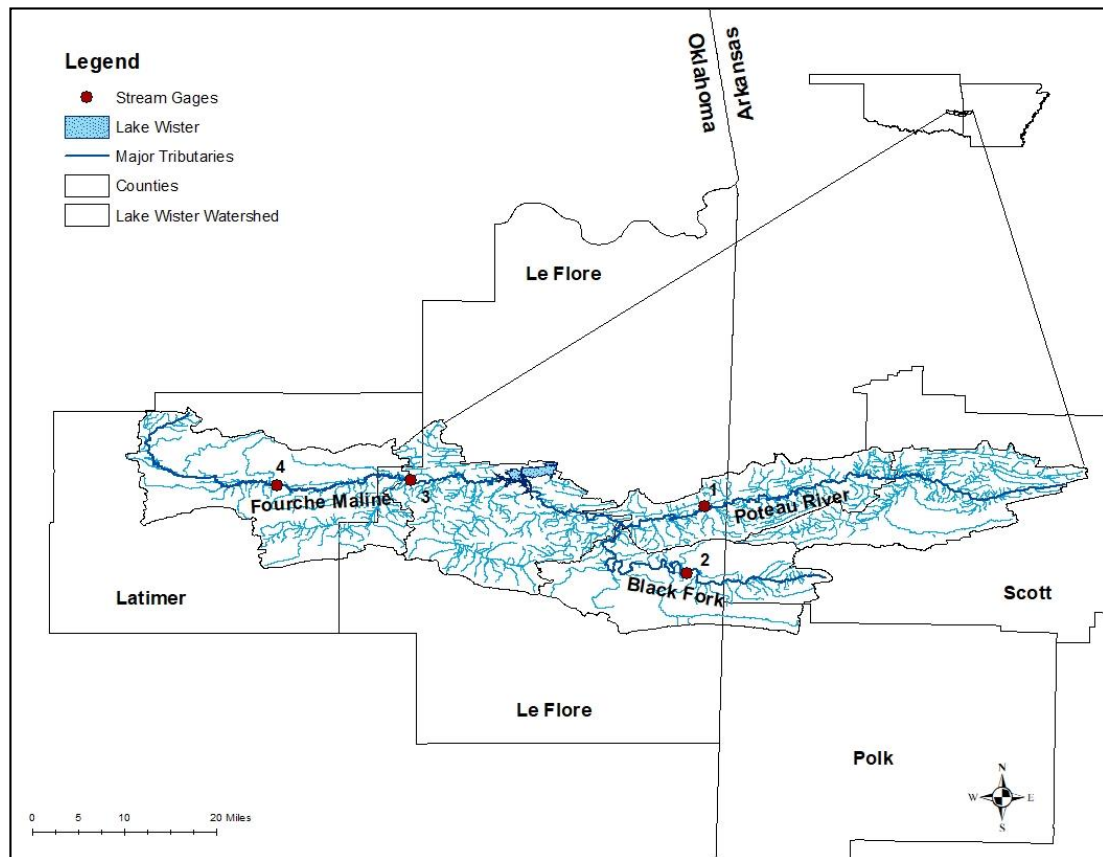


Figure 1: Lake Wister Watershed in Arkansas and Oklahoma; numbers near stream gauges correspond with Table 1.

Table 1: Site ID's (corresponding to Figure 1), names, USGS station numbers, locations, watershed areas, and land use in the Lake Wister Watershed

Site ID	Site Name	USGS Station Number	Lat N	Lat W	Watershed Area (km ²)	%F ¹	%U ²	%Ag ³	%G ⁴
1	Poteau River near Loving, OK	7247015	34.879722	94.483889	697	66.0	5.2	19.7	7.7
2	Black Fork near Page, OK	7247250	34.773610	94.511944	245	88.3	3.5	4.0	4.0
3	Fourche Maline near Leflore, OK	7247650	34.919722	94.945279	692	66.9	3.4	18.9	8.6
4	Fourche Maline near Red Oak, OK	7247500	34.912500	95.155556	303	67.2	4.1	19.5	7.8

¹ % Forest (%F) includes deciduous, evergreen, and mixed forest; ² % Urban (%U) includes open space, low, medium and high intensity development; ³ % Agriculture (%Ag) includes pasture, hay, and cultivated crops. ⁴ % Grassland (%G) includes grassland and shrubs.

Lake Wister is an impoundment in Leflore County, Oklahoma, which serves as a drinking water source to about 50,000 people in rural Oklahoma. Lake Wister is also an important reservoir for recreation, fishing, and waterfowl hunting for residents and tourists around eastern Oklahoma. Lake Wister is on Oklahoma's 303(d) list for chlorophyll-a, pH, TP, turbidity and mercury (ODEQ 2020). Historically high algal biomass and cyanobacteria in Lake Wister have led to difficult and costly treatment for drinking water, and has produced several disinfectant by-products. To address water quality concerns in Lake Wister, the Poteau Valley Improvement Agency (PVIA) developed an improvement strategy in 2009, which breaks down restoration into three categories including the watershed, the full lake, and Quarry Island Cove. PVIA has been working to chemically treat Quarry Island Cove at Lake Wister, develop TMDLs, and implement best management practices (BMPs) in the watershed.

Data Analyses

The long-term data used at each site comes from the USGS National Water Information System database (NWIS; <http://waterdata.usgs.gov/nwis>), which includes flow, stage, and various water quality parameters. Constituents of interest at each site were discharge (Q), total nitrogen (TN), nitrate plus nitrite (NN), total phosphorus (TP), orthophosphate (OP) and suspended sediments (SS) (Table 2). These data were generally available from the 1990s to 2020 depending on site and parameter; however, water quality data at the Black Fork ended in 2018.

Table 2: USGS parameter codes, constituents, percentage of censored values, and data availability for each site in the Lake Wister Watershed.

USGS parameter code	Constituent	Data availability (% Censored)		
		Site 1	Site 2	Site 3
p00600	Total nitrogen, unfiltered (TN), mg L ⁻¹ as N	1993-2020 (6.1%)	1993-2018 (16.4%)	1993-2020 (8.4%)
p00631	Nitrate plus nitrite (NN), filtered, mg L ⁻¹ as N	1993-2020 (6.1%)	1993-2018 (1.4%)	1993-2020 (8.7%)
p00665	Phosphorus (TP), water, unfiltered, mg L ⁻¹ as P	1993-2020 (0.0%)	1993-2018 (9.3%)	1993-2020 (0.8%)
p00671	Orthophosphate (OP), water, filtered, mg L ⁻¹ as P	1993-2020 (3.6%)	1993-2018 (38.7%)	1993-2020 (17.2%)
p80154	Suspended sediment (SS) concentration, mg L ⁻¹	1993-2020 (0.0%)	1993-2018 (1.0%)	1993-2020 (0.0%)

The Weighted Regressions on Time, Discharge, and Season (WRTDS) model (Hirsch et al. 2010; Hirsch and De Cicco 2015) was used to estimate loads and trends at all sites (i.e., the most downstream monitoring sites on tributaries into Lake Wister). For each site and parameter of interest, WRTDS uses weighted regression to estimate mean daily concentrations. For load

estimations, mean daily concentrations are multiplied by mean daily flow, and then summed to determine annual loads.

For trend analysis, mean daily concentrations are flow normalized (FN) to remove the influence of interannual and temporal variability in streamflow. Flow normalization is a method for identifying long-term systematic water quality changes due to anthropogenic activity (point and nonpoint processes) rather than “noise” from variability in streamflow. Trends are reported as the time series of FN annual concentrations (i.e., the average daily FN concentration for each year) and as the percent change in FN concentration relative to initial concentrations. While water quality data at the Black Fork ends in 2018, WRTDS predicts trends and loads through 2020 based on discharge. See Hirsch et al. (2010) for a complete description of the trends and loads methods, including the weighted regression approach and FN process.

Analyses were completed using the EGRET version 3.0.2 R package. The significance of trends in annual FN concentrations were evaluated using a boot strapping method with EGRETci version 2.0.3 R package (Hirsch et al. 2015). Trends with P values less than 0.05 were considered “extremely likely” to increase or decrease, P values between 0.05 and 0.20 were considered “likely” to increase or decrease, and P values greater than 0.20 were considered “likely not changing” (i.e. as likely increasing or decreasing or not).

Raw data from the USGS contained censored values, which typically occurs when the concentration is less than a reporting limit. Less than 15% of the data were censored across all sites and constituents, except for TN and OP at the Black Fork, where 16% and 39% of the data was censored, respectively (Table 1). The WRTDS framework replaces censored values with half of the censored values for each parameter. The U.S. Environmental Protection Agency suggested using simple substitution methods with data sets less than 15% censored (USEPA

2000). Since less than 15% of the data here was censored for the majority of constituents (except for TN and OP at Black Fork), this method was likely adequate for our data set.

On the Fourche Maline, the gauging station on site 6 collects only continuous stage and discharge data. At site 3, there are no continuous stage and discharge data, and only water quality samples and instantaneous discharge measurements. WRTDS requires daily discharge measurements to complete trend and load analyses; therefore, analyses on the Fourche Maline were conducted using mean daily discharge from site 4 and water quality measurements from site 3.

Results

Poteau River

At the Poteau River (Site 1), the most downstream gage on the Poteau River into Lake Wister, annual FN TN concentrations ranged from 0.67 to 0.82 mg L⁻¹, with a median value of 0.76 mg L⁻¹, and FN NN concentrations ranged from 0.17 to 0.28 mg L⁻¹, with a median value of 0.24 mg L⁻¹. Both FN TN and NN showed increasing slopes, however, FN TN was likely not changing ($p = 0.21$), and FN NN was likely increasing ($p = 0.11$) at a rate of 2.60 % yr⁻¹ (Figure 2). The largest magnitude of annual constituent loads occurred on the Poteau River, where the average annual discharge was 9.30 m³s⁻¹ (min = 1.89 m³s⁻¹, max = 17.68 m³s⁻¹). Annual TN loads ranged from 0.05 to 0.66 10⁶ kg yr⁻¹, and annual NN loads ranged from 0.01 to 0.15 10⁶ kg yr⁻¹ (Figure 5).

Annual FN TP concentrations ranged from 0.10 to 0.14 mg L⁻¹, with a median value of 0.11 mg L⁻¹, and FN OP concentrations ranged from 0.03 to 0.08 mg L⁻¹, with a median value of 0.04 mg L⁻¹. Both FN TP and OP likely decreased over time at a rate of -0.97 % yr⁻¹ and -2.70 %

yr⁻¹, respectively (Figure 2). Annual TP loads ranged from 0.01 to 0.16 10⁶ kg yr⁻¹, and annual OP loads ranged from 0.003 to 0.05 10⁶ kg yr⁻¹ (Figure 5).

Finally, annual FN SS concentrations ranged from 26.4 to 45.6 mg L⁻¹, with a median value of 29.3 mg L⁻¹. FN SS concentrations were extremely likely decreasing over time with a change of -1.60 % yr⁻¹ (Figure 2), and annual SS loads ranged from 3.69 to 76.7 10⁶ kg yr⁻¹ (Figure 5). The largest magnitude of loads for all constituents at the Poteau River occurred in 2020, where the largest magnitude of discharge also occurred.

Fourche Maline

At the Fourche Maline (Sites 3 and 4), annual FN TN concentrations ranged from 0.58 to 0.69 mg L⁻¹, with a median value of 0.63 mg L⁻¹, and FN NN concentrations ranged from 0.10 to 0.14 mg L⁻¹, with a median value of 0.11 mg L⁻¹. Both FN TN and NN showed low magnitude slopes, and were likely not changing over time ($p = 0.64$ and 0.82 , respectively, Figure 3). The average annual discharge was 4.10 m³s⁻¹ (min = 1.01 m³s⁻¹, max = 8.20 m³s⁻¹). Annual TN loads ranged from 0.03 to 0.34 10⁶ kg yr⁻¹, annual NN loads ranged from 0.005 to 0.05 10⁶ kg yr⁻¹ (Figure 5).

Annual FN TP concentrations ranged from 0.05 to 0.10 mg L⁻¹, with a median value of 0.08 mg L⁻¹, and FN OP concentrations ranged from 0.01 to 0.02 mg L⁻¹, with a median value of 0.01 mg L⁻¹. FN TP was extremely likely increasing over time ($p < 0.039$) at a rate of 2.80 % yr⁻¹, while FN OP was likely decreasing over time ($p = 0.07$) at a rate of -1.10 % yr⁻¹ (Figure 3). Annual TP loads ranged from 0.003 to 0.08 10⁶ kg yr⁻¹, annual OP loads ranged from 0.001 to 0.01 10⁶ kg yr⁻¹ (Figure 5).

Finally, annual FN SS concentrations ranged from 42.7 to 53.2 mg L⁻¹, with a median value of 44.2 mg L⁻¹. FN SS concentrations had an increasing slope, but were likely not changing over time ($p = 0.59$, Figure 2), and annual SS loads ranged from 2.65 to 66.42 10⁶ kg yr⁻¹. The largest magnitude of loads for all constituents occurred in 2016, which is also when the largest magnitude of discharge occurred.

Black Fork

At the Black Fork (Site 2), annual FN TN concentrations ranged from 0.26 to 0.37 mg L⁻¹, with a median value of 0.34 mg L⁻¹, and FN NN concentrations ranged from 0.08 to 0.11 mg L⁻¹, with a median value of 0.09 mg L⁻¹. FN TN was extremely likely decreasing ($p < 0.039$) at a rate of -1.10 % yr⁻¹, while FN NN was likely not changing ($p = 0.65$, Figure 4). The average annual discharge was 4.87 m³s⁻¹ (min = 0.62 m³s⁻¹, max = 9.60 m³s⁻¹). Annual TN loads ranged from 0.007 to 0.14 10⁶ kg yr⁻¹, and annual NN loads ranged from 0.002 to 0.05 10⁶ kg yr⁻¹ (Figure 5).

Annual FN TP concentrations ranged from 0.02 to 0.03 mg L⁻¹, with a median value of 0.02 mg L⁻¹, and FN OP concentrations ranged from 0.002 to 0.02 mg L⁻¹, with a median value of 0.005 mg L⁻¹. FN TP had a decreasing slope, but was likely not changing over time ($p = 0.22$), while FN OP was extremely likely decreasing over time ($p < 0.039$) at a rate of -3.50 % yr⁻¹ (Figure 4). Annual TP loads ranged from 0.001 to 0.03 10⁶ kg yr⁻¹, annual OP loads ranged from 0.001 to 0.01 10⁶ kg yr⁻¹ (Figure 5).

Finally, annual FN SS concentrations ranged from 8.90 to 12.80 mg L⁻¹, with a median value of 10.9 mg L⁻¹. FN SS was extremely likely decreasing over time ($p = 0.02$) at rate of -1.20 % yr⁻¹ (Figure 4). Annual SS loads ranged from 0.32 to 15.1 10⁶ kg yr⁻¹. The largest magnitude

of loads for each constituent occurred in different years, where the largest magnitude for TN, NN, TP, OP, and SS occurred in 2008, 2016, 2015, 1993, and 2002, respectively (Figure 5).

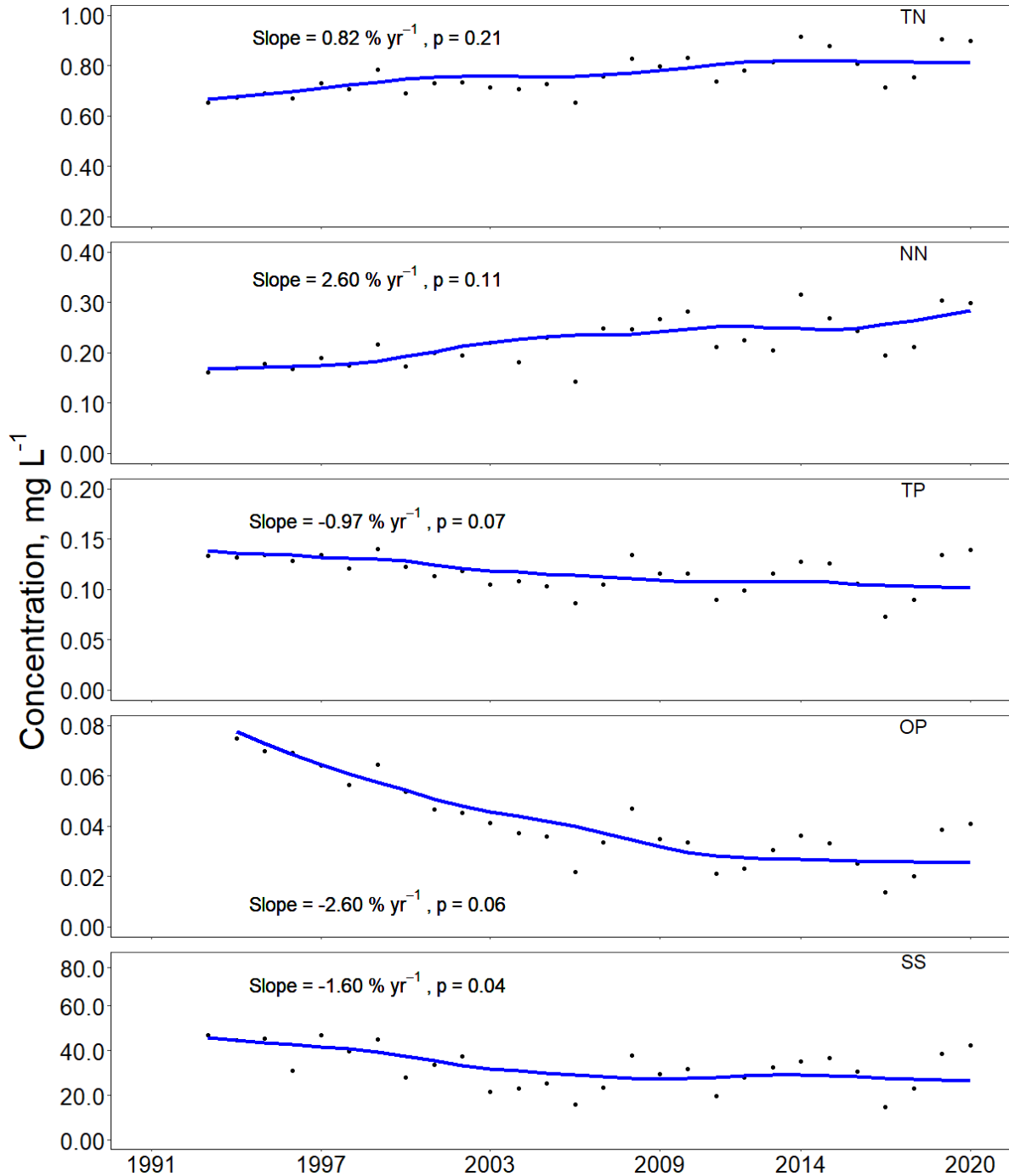


Figure 2: Average annual concentrations (dots) and flow normalized concentrations (blue lines) from WRTDS at the Poteau River near Loving, OK for total nitrogen (TN), nitrate plus nitrite as N (NN), total phosphorus (TP), orthophosphate (OP), and suspended sediment (SS) concentration; slopes and p-values are shown for trends in flow normalized concentrations.

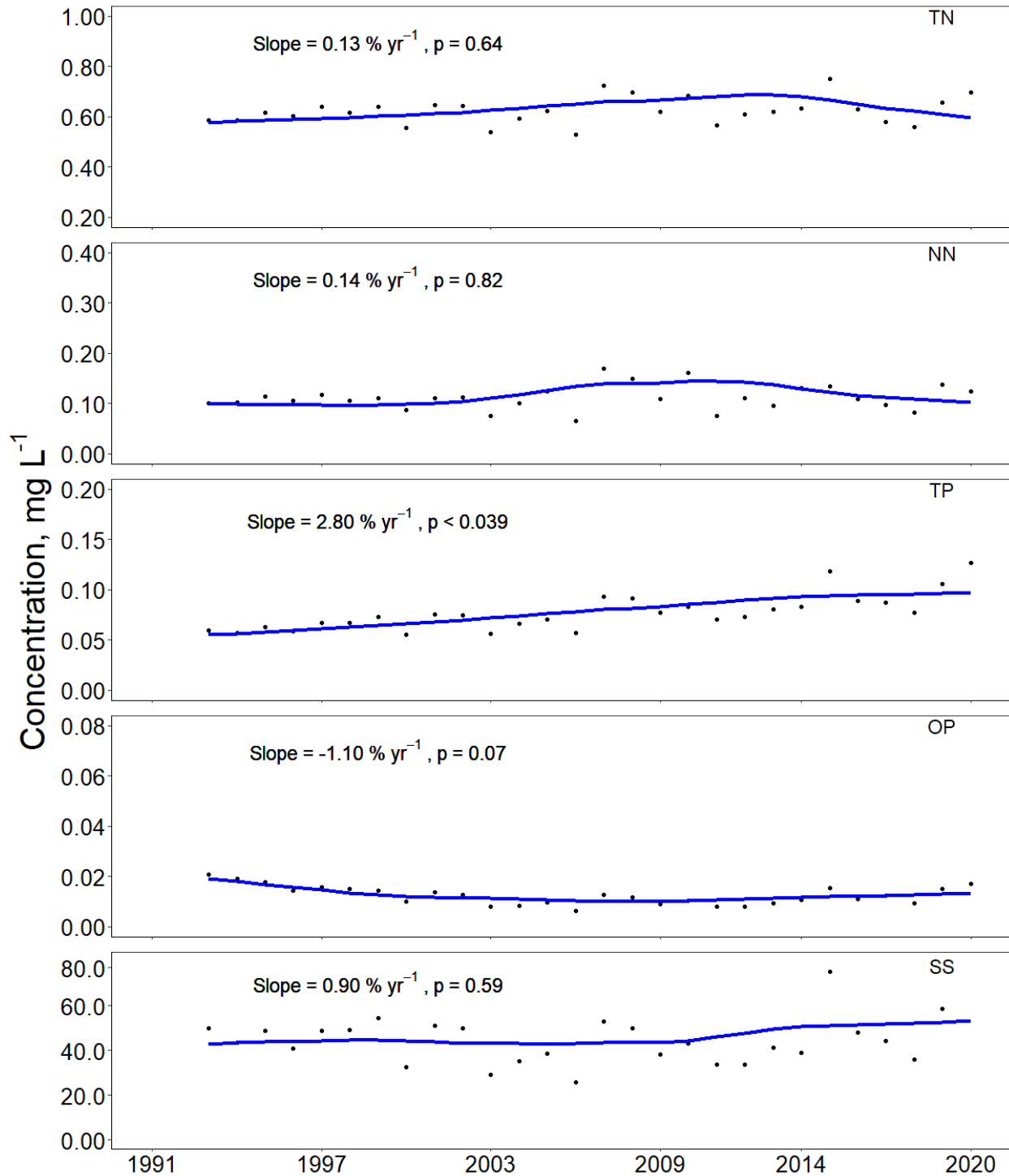


Figure 3: Average annual concentrations (dots) and flow normalized concentrations (blue lines) from WRTDS at the Fourche Maline for total nitrogen (TN), nitrate plus nitrite as N (NN), total phosphorus (TP), orthophosphate (OP), and suspended sediment (SS) concentration; slopes and p-values are shown for trends in flow normalized concentrations.

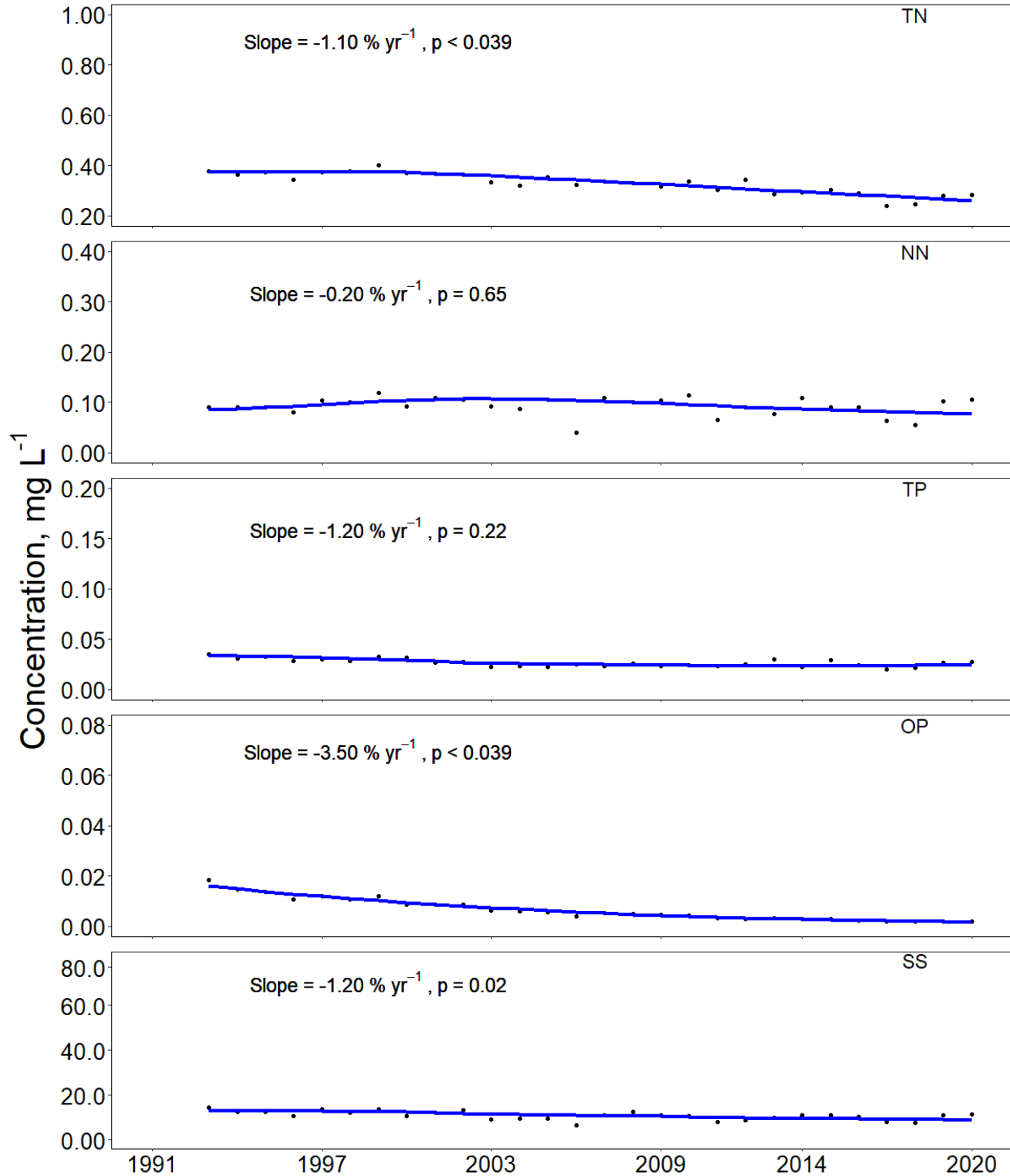


Figure 4: Average annual concentrations (dots) and flow normalized concentrations (blue lines) from WRTDS at the Black Fork for total nitrogen (TN), nitrate plus nitrite as N (NN), total phosphorus (TP), orthophosphate (OP), and suspended sediment (SS) concentration; slopes and p-values are shown for trends in flow normalized concentrations.

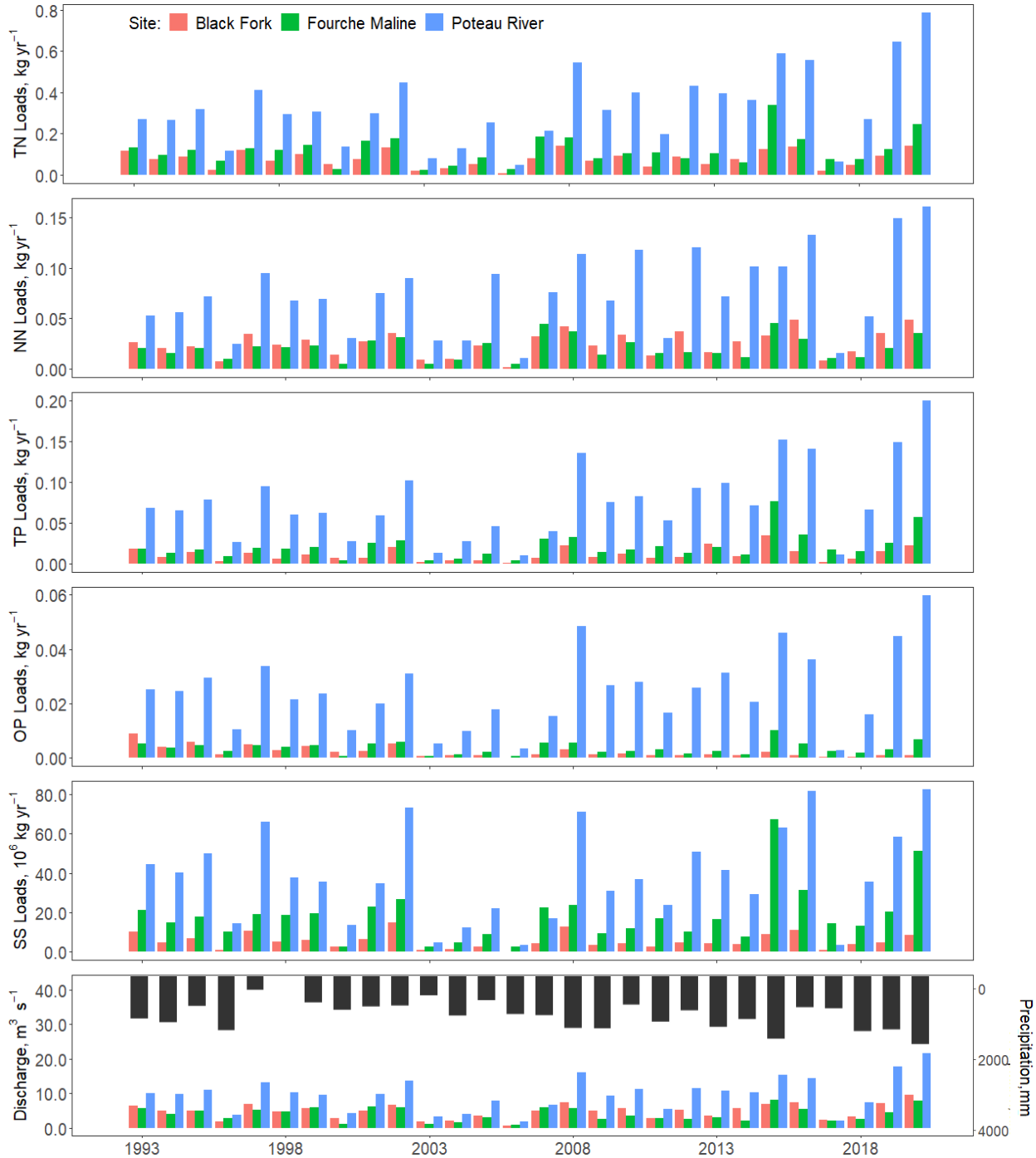


Figure 5: Total nitrogen (TN), nitrate plus nitrite (NN), total phosphorus (TP), orthophosphate (OP), suspended sediment (SS) loads, average annual discharge and total annual precipitation at the Black Fork (Site 2), Fourche Maline (Sites 3 and 4), and the Poteau River near Loving (Site 1) using WRTDS.

Discussion

Lake Wister, Oklahoma, has been considered eutrophic since 1990, and there have been several efforts in the past 10+ years to reduce constituent concentrations and loads into Lake Wister. In 2009, the PVIA developed an improvement strategy, which focused restoration into three zones including the watershed, the full lake, and Quarry Island Cove. Internal loadings of OP to the reservoir were quantified in 2010, and this internal source was determined not to be a dominant P source to the reservoir (Haggard et al. 2012). The maximum P flux in the reservoir was $3.75 \text{ mg m}^{-2} \text{ d}^{-1}$, and assuming half the lake area is anaerobic over sediments about half the time, maximum loads of P from the sediments would be 8,555 kg in 2010. From the watershed, loads of TP and OP were approximately 182,200 and 58,200 kg, respectively, in 2010 (Figure 7). Therefore, about 95% of the TP load and 87% of the OP load to Lake Wister in 2010 was from the watershed, i.e., external sources.

While the watershed was likely the dominant source of nutrients, high algal and cyanobacterial levels in Lake Wister were causing difficult and costly water treatment. Therefore, aluminum sulfate (alum) treatments in Quarry Island Cove began in 2014, and continued almost annually through 2019, to reduce P and organic matter in the water column of the cove. While alum treatments have been used to control the release of P from the sediments in reservoirs for many years (Cooke et al. 1993; Lewandowski et al. 2003a; Huser et al. 2016a), managing both internal and external loads to the reservoir is important for optimal water quality improvement (Burger et al. 2007; Steinman et al. 2007; Zamparas and Zacharias 2014; Kim et al. 2021). WRTDS outputs suggest an annual average of 524,000 kg, 107,100 kg, and 62.4 million kg per year of TN, TP and sediments, respectively, from the Poteau River, Fourche Maline, and Black Fork between 1993 and 2020. Around 65% of the total loads originated from the Poteau

River, and the greatest loads over the study occurred in 2020 (Figure 7). It is important to note that the Poteau River, Fourche Maline and Black Fork watersheds make up about 63% of the Lake Wister watershed, and total loads to Lake Wister would actually be greater than the magnitude estimated in this study. Therefore, management of the external loads entering Lake Wister, in addition to the internal sources, will likely be needed to improve reservoir water quality.

A reservoir model of Lake Wister suggested that a 78% and 71% external load reduction of P and sediments, respectively, was needed to meet water quality standards. Additionally, if internal load reductions of P were achieved through lake management strategies (e.g., alum treatments), then external loads would only need to be reduced by 58% (Scott and Patterson 2018). Between 2011 and 2015, the model predicted an average annual load of TP and sediments to be 221,787 kg per year and 142.5 million kg per year, respectively, from the Poteau River and Fourche Maline. However, WRTDS outputs from this study predicted about half of this amount in the same time period, with an average annual load of TP and sediments to be 138,404 kg per year and 70.3 million kg per year, respectively. These differences are likely attributed to slight differences in regression models used in load estimations, the period of data used to develop regression relationships, and the location of water quality data collection. Scott and Patterson collected water quality data slightly downstream on the Poteau River near Heavener, which also includes the Black Fork watershed. The Poteau River at Heavener has a watershed area of approximately double the Poteau River at Loving (1336 and 697 km² at Heavener and Loving, respectively). Accounting for watershed area, annual loads of TP were 166 and 198 kg per year per km² from Heavener and Loving, respectively, and annual loads of sediments were 0.11 and 0.10 kg per year per km², respectively.

However, the average annual loads of TP and sediments between 2016 and 2020 increased to 155,439 kg per year and 84.6 million kg per year, respectively, according to WRTDS outputs. Constituent loads are highly related to the magnitude of rainfall and discharge; relationships between discharge and constituent loads at the Poteau River and Fourche Maline had R^2 values greater than 0.70 and p-values less than 0.001. Since discharge also increased since 2016 (Figure 5), this is likely the cause of increasing loads during this time.

Several subwatersheds on the Fourche Maline and one on the Poteau River were identified as highest priority for management in the Lake Wister watershed, while subwatersheds on the Black Fork were low priority (Austin et al. 2018), and results from this study agree with this HUC-12 level monitoring. At the Poteau River, FN P and SS concentrations have been decreasing over time while FN N concentrations have been increasing (Figure 2). Water quality trends at the Poteau River were similar near the Arkansas border, which is only about 18 km upstream (see Chapter 1). The decreasing trends in P and sediments are likely due to reductions in point source effluents and regulations implemented in Arkansas to manage poultry litter applications (Chapter 1). However, the increasing FN N should be the focus of management on the Poteau River.

While the largest magnitude of loads occur at the Poteau River, increasing FN P concentrations on the Fourche Maline are still a concern. Austin et al. 2018, identified six subwatersheds as a priority for management on the Fourche Maline based on TP. Therefore, the 2.80 % yr⁻¹ increase in FN TP (Figure 3) on the Fourche Maline should be the focus of management in Oklahoma, likely in the locations identified by Austin et al. 2018.

WRTDS results also suggest the Black Fork to be a low priority watershed, since the Black Fork contributes the least amount of constituent loads to Lake Wister compared to the

Poteau River and Fourche Maline (Figure 5), and FN concentrations have been decreasing or not changing over the last several decades (see also Lasater et al. 2021). The Black Fork watershed is primarily forested, with little human impacts, and is likely not a concern for water quality management in Lake Wister.

Conclusions

Long term water quality trends and loads were analyzed for major tributaries entering Lake Wister, Oklahoma, where water quality has been a concern for several years. The largest magnitude of loads came from the Poteau River, but FN P and sediments have decreased over time, which is a positive impact of watershed management and must continue. However, FN N on the Poteau River has increased over time, and should be the focus of future management on the Poteau River. While the magnitude of constituent loads from the Fourche Maline are less than the Poteau River, increasing FN P is a concern, and should be prioritized for management in Oklahoma. The relatively undisturbed Black Fork watershed contributes the least amount of loads to Lake Wister, and FN concentrations are decreasing or not changing over time, suggesting a low priority for the Black Fork watershed.

References

- Austin BJ, Patterson S, Haggard BE (2018) Water Chemistry During Baseflow Helps Inform Watershed Management: A Case Study of the Lake Wister Watershed, Oklahoma. *J Contemp Water Res Educ* 42–58. doi: 10.1111/j.1936-704X.2018.03292.x
- Borah DK, Padmanabhan G, Kumar S (2019) Total Maximum Daily Load Analysis and Modeling: Assessment and Advancement. *J Hydrol* 24:1–2. doi: 10.1061/(ASCE)HE.1943-5584.0001853
- Burger DF, Hamilton DP, Pilditch CA (2007) Modelling the relative importance of internal and external nutrient loads on water column nutrient concentrations and phytoplankton biomass in a shallow polymictic lake. *Ecol Modell* 211:411–423. doi: 10.1016/j.ecolmodel.2007.09.028

- Cooke GD, Welch EB, Martin AB, et al (1993) Effectiveness of Al, Ca, and Fe salts for control of internal phosphorus loading in shallow and deep lakes. In: *Hydrobiologia*. pp 323–335
- Haggard BE (2010) Phosphorus Concentrations, Loads, and Sources within the Illinois River Drainage Area, Northwest Arkansas, 1997–2008. *J Environ Qual* 39:2113. doi: 10.2134/jeq2010.0049
- Haggard BE, Scott JT, Patterson S (2012) Sediment phosphorus flux in an Oklahoma reservoir suggests reconsideration of watershed management planning. *Lake Reserv Manag* 28:59–69. doi: 10.1080/07438141.2012.659376
- Hirsch RM, Arch SA, Cicco LA De (2015) A bootstrap method for estimating uncertainty of water quality trends. *Environ Model Softw* 73:148–166. doi: 10.1016/j.envsoft.2015.07.017
- Hirsch RM, De Cicco LA (2015) User Guide to Exploration and Graphics for RivEr Trends (EGRET) and dataRetrieval: R Packages for Hydrologic Data. In: *Hydrological Analysis and Interpretation; Section A, Statistical Analysis*. U. S. Geological Survey
- Hirsch RM, Moyer DL, Archfield SA (2010) Weighted Regressions on Time, Discharge, and Season (WRTDS), with an Application to Chesapeake Bay River Inputs. *J Am Water Resour Assoc* 46:857–880
- Huser BJ, Egemose S, Harper H, et al (2016) Longevity and effectiveness of aluminum addition to reduce sediment phosphorus release and restore lake water quality. *Water Res* 97:122–132. doi: 10.1016/j.watres.2015.06.051
- Kim J, Jones JR, Seo D (2021) Factors affecting harmful algal bloom occurrence in a river with regulated hydrology. *J Hydrol Reg Stud* 33:1–14. doi: 10.1016/j.ejrh.2020.100769
- Lasater AL, O'Hare M, Haggard BE (2021) Water Quality Trends and Shifts Variable across Constituents at the Upper Poteau River Watershed in Arkansas. *Trans ASABE* (submitted June 2021)
- Lewandowski J, Schauser I, Hupfer M (2003) Long term effects of phosphorus precipitations with alum in hypereutrophic Lake Susser See (Germany). *Water Res* 37:3194–3204
- Malago A, Bouraoui F, Grizzetti B, De Roo A (2019) Modelling nutrient fluxes into the Mediterranean Sea. *J Hydrol Reg Stud* 22:1–18
- ODEQ (2020) Oklahoma's Final Impaired Waterbodies- 303(d) List. Oklahoma Dep Environ Qual
- Scott JT, Haggard BE, Sharpley AN, Romeis JJ (2011) Change Point Analysis of Phosphorus Trends in the Illinois River (Oklahoma) Demonstrates the Effects of Watershed Management. *J Environ Qual* 40:1249–1256. doi: 10.2134/jeq2010.0476
- Scott JT, Patterson SD (2018) Lake Wister Water Quality Modeling in Support of Nutrient and Sediment TMDL Development

- Shoda ME, Sprague LA, Murphy JC, Riskin ML (2019) Water-quality trends in U. S. rivers, 2002 to 2012: Relations to levels of concern. *Sci Total Environ* 650:2314–2324. doi: 10.1016/j.scitotenv.2018.09.377
- Steinman A, Chu X, Ogdahl M (2007) Spatial and temporal variability of internal and external phosphorus loads in Mona Lake, Michigan. *Aquat Ecol* 43:1–18. doi: 10.1007/s10452-007-9147-6
- USEPA (2016) National Lakes Assessment 2012, A Collaborative Survey of Lakes in the United States. Washington, DC
- USEPA (2008) National Water Quality Assessment. <https://www.epa.gov/nps/nonpoint-source-agriculture>
- USEPA (2000) Guidance for Data Quality Assessment. United States Environmental Protection Agency, Washington, DC
- Zamparas M, Zacharias I (2014) Restoration of eutrophic freshwater by managing internal nutrient loads. A review. *Sci Total Environ* 496:551–562. doi: 10.1016/j.scitotenv.2014.07.076

Chapter 3: Magnitude of External Phosphorus Loading Likely Reduces the Effectiveness of Aluminum Sulfate Treatments for management of Sediment Phosphorus Flux

A. L. Lasater^{1,2}, J. A. Lee³, B. E. Haggard^{1,2}

¹Department of Biological and Agricultural Engineering, University of Arkansas, Fayetteville, AR 72701, USA

²Arkansas Water Resources Center, University of Arkansas System Division of Agriculture, Fayetteville, AR 72701, USA

³Agricultural Statistics Laboratory, University of Arkansas, Fayetteville, AR 72701, USA

Abstract

Aluminum sulfate (alum) treatments have been used for decades to control the release of phosphorus (P) from bottom sediments in lakes and reservoirs. However, the longevity of treatments has varied from less than a year up to 45 years due to insufficient aluminum (Al) dosages applied, saturation of alum flocs, and/or burial of alum flocs by incoming sediments. This study quantified sediment P fluxes under aerobic and anaerobic conditions at Quarry Island Cove at Lake Wister, Oklahoma, before and after treatments which occurred five times between 2014 and 2019. To measure P flux, sediment-water cores were collected from the cove and incubated for 10 days at room temperature under aerobic and anaerobic conditions, and P fluxes were estimated as the slope of increase in P mass over time divided by the area of the core. Sediment P fluxes were consistently greater under anaerobic conditions compared to aerobic conditions. Aerobic P fluxes were not significantly different before or after alum treatments, and the magnitude of P fluxes under aerobic conditions was relatively low throughout the duration of the study ($< 1.47 \text{ mg m}^{-2} \text{ day}^{-2}$). Under anaerobic conditions, P fluxes significantly decreased one week after alum treatments compared to a week before treatment. However, after 5 treatments across 6 years, sediment P fluxes under anaerobic conditions were not significantly different than

prior to any alum treatments in 2010 and 2014 (3 to $4 \text{ mg m}^{-2} \text{ day}^{-2}$). The lack of overall reduction in anaerobic P fluxes over time is likely due to the magnitude of P and sediment loads entering Lake Wister from the watershed, where 92% of the total P load to Lake Wister from 2010 to 2020 was from external sources. Therefore, while alum treatments provide short term reductions in P fluxes at Quarry Island Cove, the effectiveness was short, suggesting external sources of P must be addressed.

Introduction

Cultural eutrophication due to excessive nutrients entering waterways has dramatic consequences to aquatic ecosystems (Smith et al. 1999). Growing population and human activities have led to increases in landscape changes, agricultural production and waste, all of which contribute to shifts in nutrient cycling and increased availability of nitrogen (N) and phosphorus (P) (Anderson et al. 2002). Nutrient enrichment, whether from landscape runoff and/or effluent discharges, increases trophic states of lakes and reservoirs. Increasing trophic states correspond to increased biomass production, which often form nuisance or harmful algal blooms (HABs), contribute to hypoxia, and decrease biodiversity (Hallegraeff 1993; Porter et al. 2013; Glibert 2017).

Increased algal production leads to taste and odor issues in water supplies, as well as potential for HABs related toxins, which are difficult to remove in water treatment processes (Dodds et al. 2008; USEPA 2015). Additionally, seasonal variation in phytoplankton growth and community composition occur, leading to variation in source water quality and treatment approaches throughout the year (Chang et al. 2003; Xu et al. 2010; Rasconi et al. 2015). The costs associated with drinking water treatment can increase greatly due to eutrophication and algal blooms (USEPA 2015). For example, the City of Celina, Ohio, spent nearly \$3.4 million

on operation and maintenance because of nutrient pollution in Grand Lake St. Mary's, but this amount did not include costs associated with aluminum sulfate (alum), lime and sludge disposal (Davenport and Drake 2011). In Waco, Texas, over \$72 million was spent to address poor drinking water quality from 2002 to 2012 due to taste and odor problems, and an estimated \$10.3 million in revenue was lost to the city of Waco (Dunlap et al. 2015). Therefore, proactive efforts to address algal blooms are essential for environmental and economic value of source water.

Algal production in lakes and reservoirs is limited by light, carbon dioxide, and particularly concentrations of N and/or P, or the ratio of N:P (Conley et al. 2009; Paerlet et al. 2016; McCormick et al. 2019). Therefore, to address excess algal production in drinking water sources, remediation efforts typically focus on external loading of nutrients from the watershed or point sources (e.g. best management practices, total maximum daily load development, effluent limitations, etc.), and efforts often address inputs of both N and P (Carey and Migliaccio 2009; Chaubey et al. 2010; Shenk and Linker 2013). However, internal loading of nutrients, specifically P, can lead to continued algal production and source water degradation even when external nutrients are reduced (Doig et al. 2017; Lasater and Haggard 2017; Radbourne et al. 2019). While P concentrations in the bottom sediments ultimately originate from external nutrient sources, legacy P can be released back into the water column through various processes including wind resuspension (Kristensen et al. 1992), reductive dissolution (Mortimer 1942), organic matter mineralization (Anderson and Jensen 1992) and equilibrium P concentrations (EPC) (Haggard and Soerens 2006; Belmont et al. 2009).

Aluminum sulfate (alum, $\text{Al}_2(\text{SO}_4)_3$) treatments have been used for decades to control the release of P from bottom sediments in lakes and reservoirs (Kennedy and Cooke 1982; Smeltzer 1990; Cooke et al. 1993; Lewandowski et al. 2003b; Huser et al. 2016b). Through hydrolysis,

alum produces aluminum (Al) hydroxide flocs that immobilize dissolved and particulate P and settle onto the bottom sediments (Cooke et al. 1993). Several studies have observed significant reductions in water column P concentrations, sediment P release rates, and abundance of algae with the use of alum (Smeltzer 1990; Welch and Cooke 1999; Steinman et al. 2004; Huser et al. 2011). Longevity of alum treatments have varied from less than a year up to 45 years (Huser et al. 2016c). Sodium aluminate ($\text{NaAl}(\text{OH})_4$) is often applied with alum to maintain pH, since the hydrolysis of alum can result in a pH reduction (Smeltzer 1990; Cooke et al. 2005).

The purpose of this study is to measure and analyze sediment P flux at Quarry Island Cove at Lake Wister, Oklahoma, before and after alum/ $\text{NaAl}(\text{OH})_4$ treatments (hereafter, alum treatments). The goal is to determine whether alum treatments are providing an effective remedy to reduce internal P loading. We hypothesize that sediment P release rates will be greater under anaerobic conditions compared to aerobic, and that rates will be greater before the alum treatments compared to after. Additionally, we hypothesize P release rates will decrease over time due to repeated alum treatments.

Study Site Description

Lake Wister is an impoundment on the Poteau River and the Fourche Maline Creek in eastern Oklahoma (Figure 1), covering approximately 29.5 km². The US Army Corps of Engineers (USACE) started dam construction in 1946, and the reservoir was completed and operational by 1949. Lake Wister has an average depth of 2 m and maximum depth of 15 m, and is an important reservoir for drinking water supply, recreation, fishing and waterfowl hunting for residents and tourists around eastern Oklahoma. Lake Wister is listed on Oklahoma's 303(d) list for chlorophyll-a, pH, total phosphorus (TP), turbidity and mercury (ODEQ 2020). To address these water quality concerns, the Poteau Valley Improvement Agency (PVIA) developed an

improvement strategy in 2009, which breaks down restoration into three zones including the watershed, the full lake, and Quarry Island Cove. Quarry Island Cove is at the northeast corner of Lake Wister (Figure 1), and the intake for the PVIA water treatment plant, which distributes drinking water to over 40,000 people in rural Oklahoma, is within the cove.

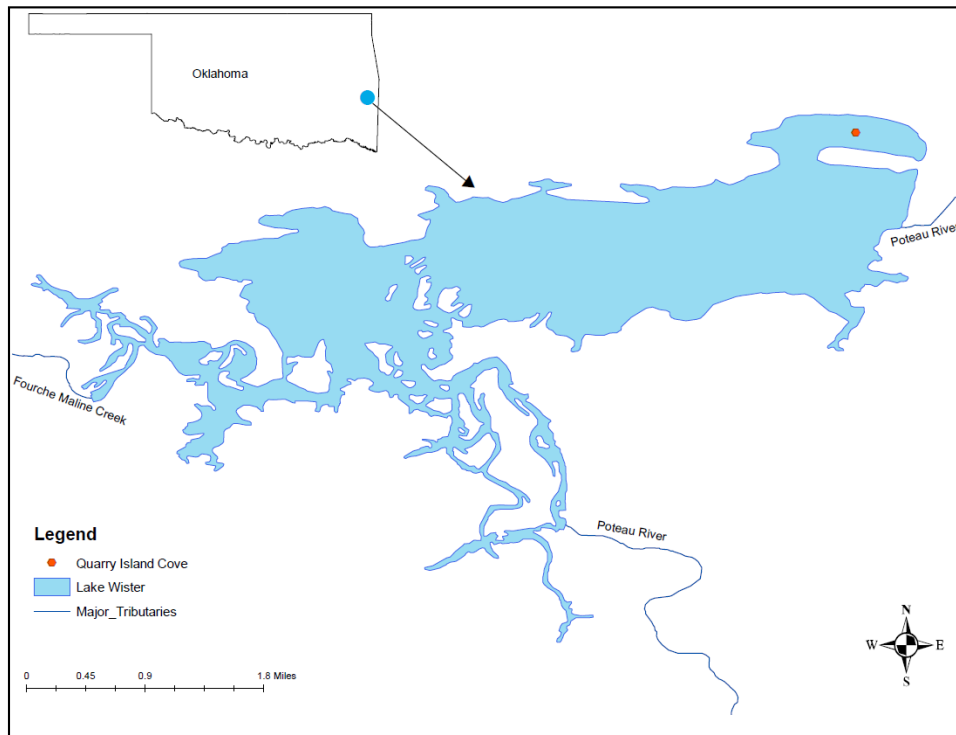


Figure 1: Lake Wister in Oklahoma; Quarry Island Cove is on the north shore of Lake Wister.

Historically high algal and cyanobacteria counts in Quarry Island Cove have led to difficult and costly treatment for PVIA, as well as produced disinfectant by-products. In 2013, monthly sampling showed cyanobacteria counts exceeding $100,000 \text{ cells mL}^{-1}$ across seven of the 12 months (PVIA 2014). Additionally, sediment-water cores collected in July of 2009 showed sediment P release rates up to $3.30 \text{ mg m}^{-2} \text{ day}^{-1}$ under anaerobic conditions (Haggard et al. 2012), which could be contributing to algal blooms in this drinking water source. Over the last several years, the PVIA has been working to treat Quarry Island Cove, in efforts to inactivate P in the surface water and sediments and to prevent excessive algal growth (PVIA 2014).

Methods

The PVIA treated the Quarry Island Cove with alum and NaAl(OH)_4 at a rate of 284 mg m^{-2} alum and 97 mg m^{-2} NaAl(OH)_4 on August 4th and 5th, 2014, July 16th and 27th, 2016, July 27th and 28th, 2017, July 24th and 25th, 2018, and July 30th and 31st, 2019. The treatment was conducted by spraying the alum treatment solution on the surface of the water, allowing the Al hydroxide flocs to settle on the bottom and P to co-precipitate and/or absorb to Al hydroxides formed in the lake water. The NaAl(OH)_4 provided a buffer to maintain pH in the cove, as well as provided additional Al.

Sediment-water cores were collected from Quarry Island Cove on the north shore of Lake Wister (34.947237, -94.723735) before and after alum treatment most years (Figure 1). In 2014, cores were collected on July 31st and August 5th; in 2016, cores were collected on July 21st and August 3rd. In 2017, cores were collected approximately one month after (and not before) the cove was treated with alum (on September 11th, 2017). In 2018, cores were collected on July 16th and August 3rd, and to analyze the impacted of delayed sampling in 2017, cores were collected one month after alum treatment on September 14th, 2018. In 2019, similar to 2018, cores were collected on July 12th, August 6th, and September 9th. The final round of cores were collected on July 27, 2020 to analyze P release rates a year after the last treatment in 2019.

Eight cores were collected on each sampling date using Plexiglas tubes (0.6 m long and 7.9 cm inner diameter) inserted approximately 0.3 m into the sediment with a UWITEC corer. Rubber stoppers were placed on the top of the cores, and caps placed on the bottom end. Properly collected cores had relatively undisturbed sediment and clear overlying water.

Upon return to the laboratory, the depth of the overlying water was adjusted so that each core contained 1 L of water. The cores were then wrapped in Al foil to exclude light and incubated at room temperature (approximately 22°C) for 10 days. All cores were bubbled with air overnight, then half of the cores were incubated under anaerobic conditions (bubbled with N₂) and the other half under aerobic conditions (bubbled with air) for the duration of the experiment. Bubbling with N₂ gas purges the dissolved oxygen (O₂) from the water column and prevents O₂ from diffusing into the water due to positive pressure. Light exclusion in all the cores limits algal growth and uptake of labile P.

In 2014, an additional experiment was conducted on each core collected on July 31st (prior to treating the cove with Al). After approximately 2 weeks of initial incubation, alum and NaAl(OH)₄ were added to each core and incubated an additional 15 days under existing aerobic and anaerobic conditions. Alum treatment rates to the cores were equal to the in-cove treatments on August 5th (284 mg m⁻² alum and 97 mg m⁻² NaAl(OH)₄).

Throughout incubation, water samples were removed from the overlying water of each core at 1 to 3 day intervals. The water was filtered (0.45 µm), acidified using concentrated H₂SO₄, and analyzed for soluble reactive P (SRP) using the automated ascorbic acid reduction technique (APHA, 2005). The overlying water in the cores was maintained at 1 L by adding filtered (0.45 µm) water collected from Lake Wister with a measured SRP concentration.

Sediment P release rates were calculated as changes in P mass in the overlying water as a function of incubation time (mg d⁻¹), divided by the inside area of the sediment-water cores (mg m⁻² d⁻¹). The P mass in the overlying water was corrected for water removal and addition throughout the duration of the experiment. A two-way analysis of variance (ANOVA) was used to analyze the 2014 data, to determine whether release rates were different under aerobic and

anaerobic conditions, and before and after alum treatment in the cores and in the cove. For all years of data, a mixed effect model for split plot design was used to analyze differences in P fluxes under aerobic and anaerobic conditions, and before, one week after and one month after alum treatments in the cove. The mixed effect model was chosen to account for the fixed effects of sample dates and random variation P flux measurements. To understand changes in P fluxes over time, P flux from cores collected in July of each year were compared using the Kruskal-wallis test. All comparisons used an alpha of 0.05.

Results

Alum Treatment Experiment in Cores and Cove in 2014

After one night of aeration, SRP concentrations in the overlying water of all cores ranged from 0.007 to 0.012 mg L⁻¹. Cores under anaerobic conditions reached an average SRP concentration of 0.285 mg L⁻¹ on August 18th (i.e., after 18 days of incubation), while cores under aerobic conditions reached an average of 0.038 mg L⁻¹ SRP. SRP concentrations in the overlying water of anaerobic cores reached a plateau after approximately eight days of incubation. However, SRP concentration in one core plateaued from days 5 to 12, and began to increase again until August 18th (Figure 2).

The slope of SRP mass for anaerobic cores was greater compared to aerobic cores (Figure 2). The average P flux was 6.56 mg m⁻² day⁻¹ (range = 5.03 – 7.51 mg m⁻² day⁻¹) for anaerobic cores, and 0.35 mg m⁻² day⁻¹ (range = 0.00 – 0.57 mg m⁻² day⁻¹) for aerobic cores (Figure 2), and the average P flux under anaerobic conditions was significantly greater than aerobic conditions ($p < 0.001$).

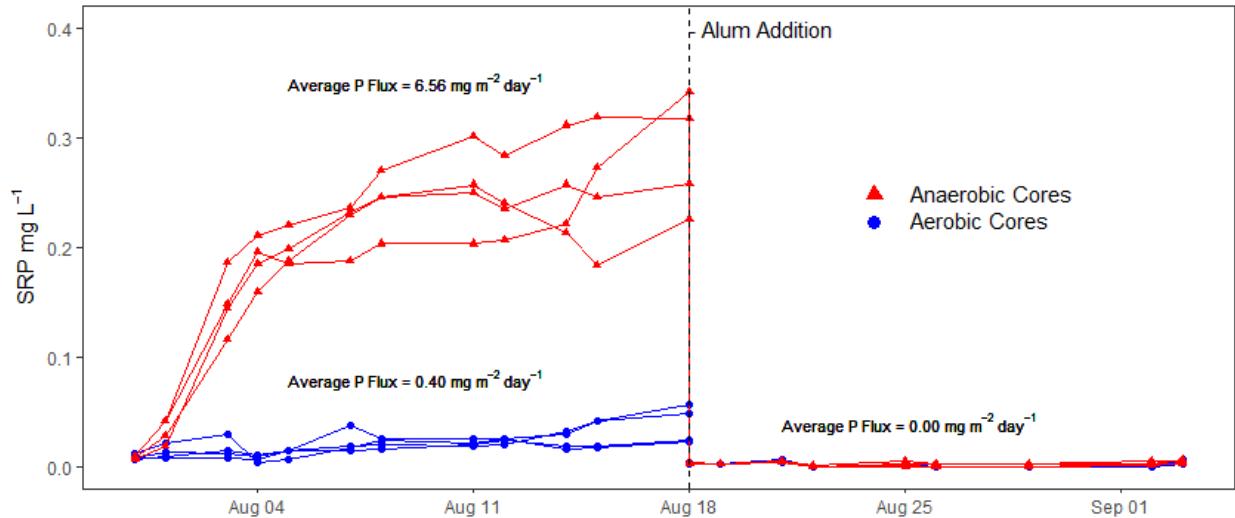


Figure 2: Soluble reactive phosphorus (SRP) mass in overlying water over time in cores collected on July 31st, 2014. Aluminum sulfate and sodium aluminate (alum addition) was added to the cores at equal rates to Quarry Island Cove on August 18th. Average P fluxes for the anaerobic and aerobic cores are shown above the lines. Average P flux after the alum addition was not significantly different than zero under both aerobic and anaerobic conditions.

Following the alum treatment within the cores, SRP concentrations in the overlying water decreased dramatically to a range of 0.003 to 0.004 mg L⁻¹ across anaerobic and aerobic cores. After 15 more days of incubation, the average SRP concentration in the overlying water was 0.002 and <0.001 mg L⁻¹ for cores under anaerobic and aerobic conditions, respectively. The P flux for all cores was 0.00 mg m⁻² day⁻¹ (Figure 2), and the P fluxes under both conditions were not significantly different than the P fluxes of aerobic cores prior to alum treatment.

Following the first alum treatment in Quarry Island Cove, another set of cores were collected from Lake Wister. After one night of aeration, initial SRP concentrations in the overlying water of all cores ranged from 0.011 to 0.021 mg L⁻¹. SRP concentrations in the overlying water of the anaerobic cores reached an average of 0.033 mg L⁻¹, while SRP concentrations in the overlying water of the aerobic cores reached an average of 0.016 mg L⁻¹ SRP. Cores under anaerobic conditions had an average P flux of 0.41 mg m⁻² day⁻² (range = 0.00

–0.94 mg m⁻² day⁻²), and P fluxes under aerobic conditions were not significantly different than anaerobic conditions, with all cores showing no measurable release of P (e.g., 0.00 mg m⁻² day⁻¹).

Sediment P Fluxes in Quarry Island Cover over Time

Combing all years of P flux measurements, including P fluxes measured in 2010 (Haggard et al. 2012), P fluxes were significantly greater under anaerobic (average = 5.12 mg m⁻² day⁻²) compared to aerobic (average = 0.39 mg m⁻² day⁻², Figure 3A). Under aerobic conditions, no significant changes occurred in P fluxes before or after alum treatment, and all P fluxes were less than 1.47 mg m⁻² day⁻² (Figure 3B). Under anaerobic conditions, the average P flux one week before alum treatments was 8.01 mg m⁻² day⁻², and was significantly greater than P fluxes one week and one month after alum treatments (average = 1.87 mg m⁻² day⁻² and 4.02 mg m⁻² day⁻², respectively; Figure 3C).

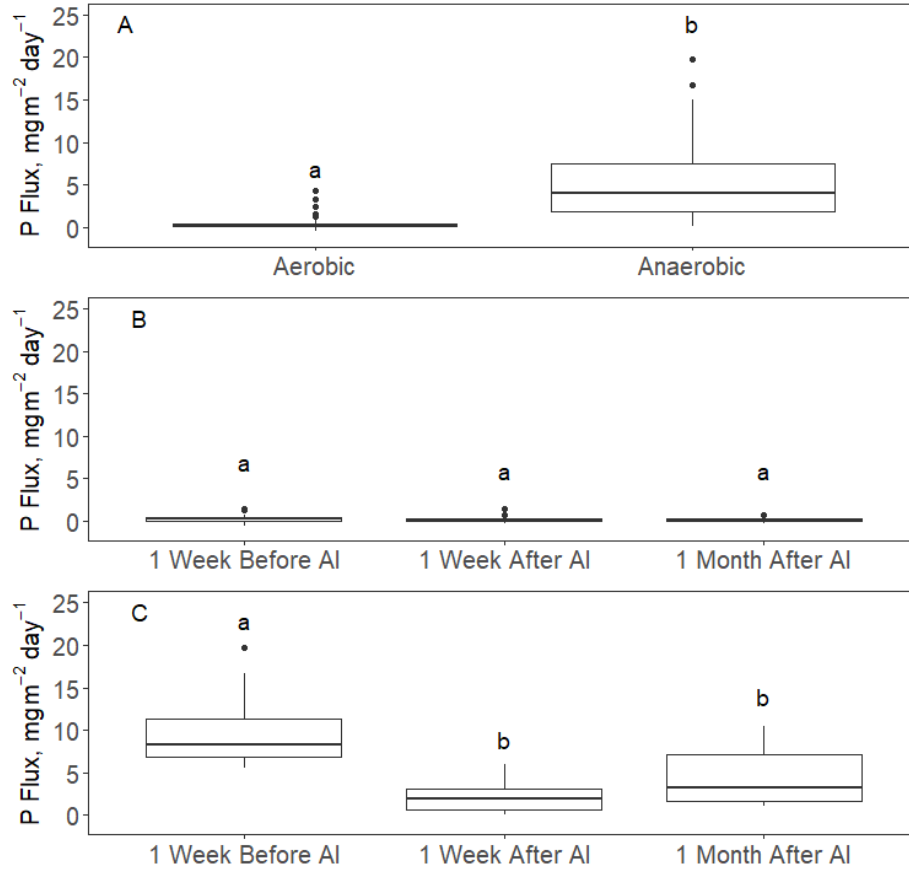


Figure 3. All sediment phosphorus (P) fluxes measured under aerobic and anaerobic conditions (A). Sediment P fluxes one week before, one week after, and one month after alum treatments under aerobic (B) and anaerobic conditions (C). Different letters indicate statistically different means ($p < 0.05$).

In July 2016, two years after the first alum treatment, the average P flux under anaerobic conditions was $15.8 \text{ mg m}^{-2} \text{ day}^{-2}$ (range = $12.9 - 19.7 \text{ mg m}^{-2} \text{ day}^{-2}$), and was the largest magnitude of P fluxes measured in this study (Figure 4). P fluxes under aerobic conditions were significantly less, with an average of $0.66 \text{ mg m}^{-2} \text{ day}^{-2}$ (range = $0.00 - 1.41 \text{ mg m}^{-2} \text{ day}^{-2}$). One week after the second alum treatment, the average P fluxes under anaerobic and aerobic conditions decreased to $3.63 \text{ mg m}^{-2} \text{ day}^{-2}$ (range = $2.70 - 4.60 \text{ mg m}^{-2} \text{ day}^{-2}$), and $0.29 \text{ mg m}^{-2} \text{ day}^{-2}$ (range = $-0.32 - 1.47 \text{ mg m}^{-2} \text{ day}^{-2}$), respectively.

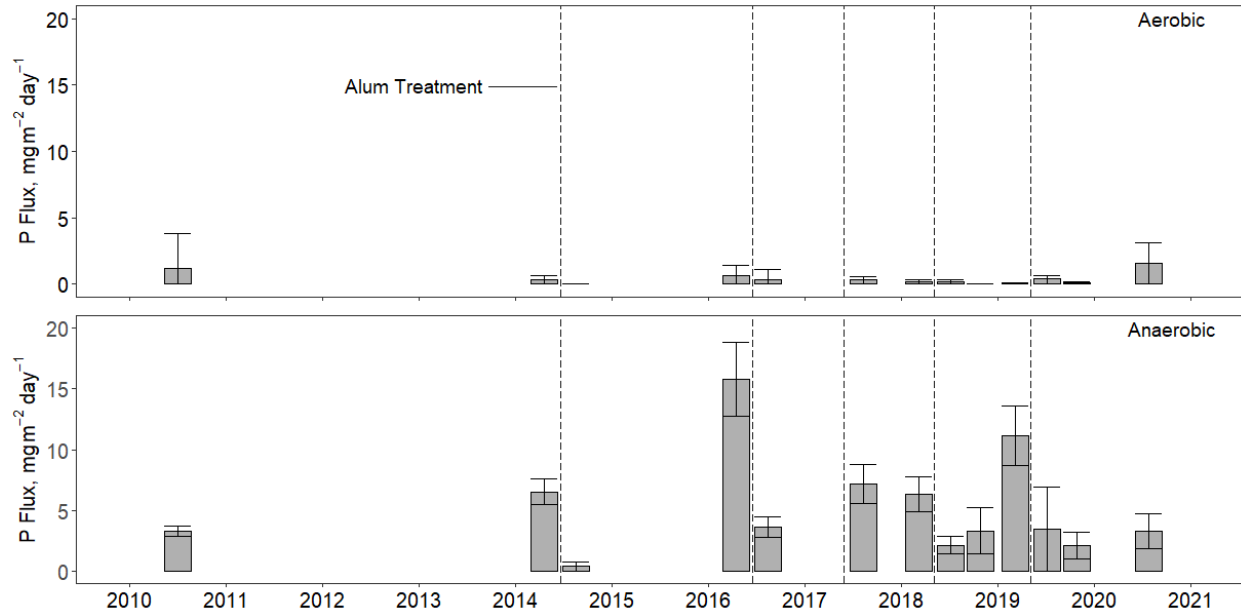


Figure 4: Average sediment phosphorus (P) fluxes \pm standard deviation under aerobic (top panel) and anaerobic (right panel) conditions each year of sample collection. Vertical dotted lines indicate timing of alum treatment, and 2010 estimates of P fluxes are from Haggard et al., 2012.

In September 2017, P fluxes were measured from cores collected one month after the third alum treatment. Under anaerobic conditions, the average P flux was $7.22 \text{ mg m}^{-2} \text{ day}^{-2}$ (range = $5.91 - 9.52 \text{ mg m}^{-2} \text{ day}^{-2}$). P fluxes under aerobic conditions were significantly less, with an average of $0.28 \text{ mg m}^{-2} \text{ day}^{-2}$ (range = $0.00 - 0.57 \text{ mg m}^{-2} \text{ day}^{-2}$, Figure 3).

In July 2018, a year after the third alum treatment, average P fluxes under anaerobic conditions were slightly less (average = $6.32 \text{ mg m}^{-2} \text{ day}^{-2}$; range = $4.71 - 8.00 \text{ mg m}^{-2} \text{ day}^{-2}$) than fluxes measured one month after the third alum treatment. A week following the fourth alum treatment in 2018, P fluxes under anaerobic conditions decreased to an average of $2.17 \text{ mg m}^{-2} \text{ day}^{-2}$ (range = $1.74 - 2.88 \text{ mg m}^{-2} \text{ day}^{-2}$). However, P fluxes measured one month after the fourth alum treatment increased to an average of $3.35 \text{ mg m}^{-2} \text{ day}^{-2}$ (range = $0.95 - 5.31 \text{ mg m}^{-2} \text{ day}^{-2}$). P fluxes under aerobic conditions were significantly less than anaerobic conditions with an average of $0.15 \text{ mg m}^{-2} \text{ day}^{-2}$ (range = $0.00 - 0.38 \text{ mg m}^{-2} \text{ day}^{-2}$), $0.15 \text{ mg m}^{-2} \text{ day}^{-2}$ (range =

0.00 – 0.37 mg m⁻² day⁻²), and -0.06 mg m⁻² day⁻² (range = -0.14 – 0.00 mg m⁻² day⁻²), the week before, week after, and a month after, respectively (Figure 4).

In July 2019, a year after the fourth alum treatment, the average P flux under anaerobic conditions increased to 11.2 mg m⁻² day⁻² (range = 9.26 – 14.6 mg m⁻² day⁻²). Similar to years prior, a week after the alum treatment in 2019, P fluxes decreased to an average of 3.48 mg m⁻² day⁻² (range = 0.00 – 8.56 mg m⁻² day⁻²). One month after the fifth alum treatment, the average P flux decreased to 2.15 mg m⁻² day⁻² (range = 1.15 – 3.74 mg m⁻² day⁻²). Again P fluxes under aerobic conditions were significantly less than anaerobic conditions with an average of -0.29 mg m⁻² day⁻² (range = -0.83 – 0.00 mg m⁻² day⁻²), 0.38 mg m⁻² day⁻² (range = 0.11 – 0.69 mg m⁻² day⁻²), and 0.07 mg m⁻² day⁻² (range = 0.00 – 0.26 mg m⁻² day⁻²), the week before, week after, and a month after, respectively (Figure 4).

In July 2020, a year after the fifth and final alum treatment in Quarry Island Cove, the average P flux under anaerobic conditions increased slightly to 3.32 mg m⁻² day⁻² (range = 1.53 – 4.57 mg m⁻² day⁻²). P fluxes under aerobic conditions were significantly less, with an average of 1.55 mg m⁻² day⁻² (range = 0.13 – 4.35 mg m⁻² day⁻², Figure 4).

To determine whether P fluxes decreased after five alum treatments, sediment P fluxes measured in July of each year were compared. Under aerobic conditions, no significant changes in P fluxes occurred over time. However, under anaerobic conditions, average P fluxes increased from 2010 to 2016, and decreased after 2016 (Figure 5). While P fluxes in 2020 are significantly less than that in 2016, 2020 P fluxes are not significantly different than P fluxes measured in 2010 and 2014 prior to any alum treatments.

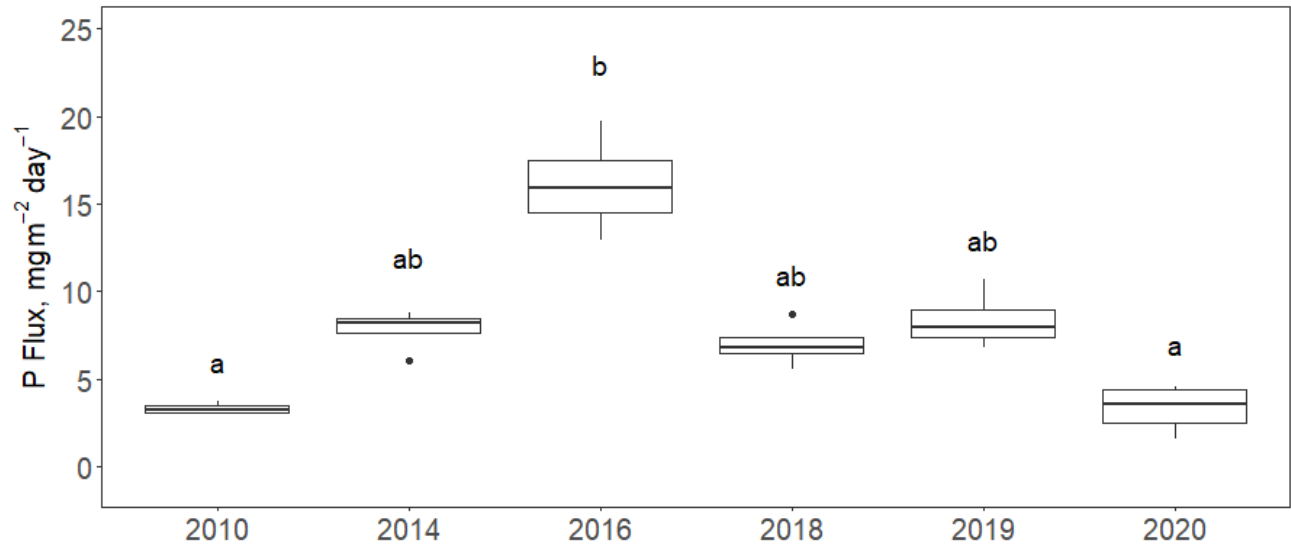


Figure 5: Sediment phosphorus (P) fluxes under anaerobic conditions from July each year of sample collections. Different letters indicate significantly different means ($p < 0.05$).

Discussion

In 2010, prior to any alum treatments in Quarry Island Cove, the average P flux under aerobic conditions was $1.13 \text{ mg m}^{-2} \text{ day}^{-2}$ (Haggard et al. 2012). In 2014, a week before the first alum treatment of Quarry Island Cove, P fluxes under aerobic conditions were even less, with an average of $0.35 \text{ mg m}^{-2} \text{ day}^{-2}$. Sediment P fluxes did not significantly change under aerobic conditions following the alum treatment in 2014, or any year after (Figure 3). Therefore, no effect of alum treatment was observed on P fluxes under aerobic conditions throughout the duration of this study. Additionally, P fluxes were relatively low throughout the study (<0.00 to $1.47 \text{ mg m}^{-2} \text{ day}^{-2}$), and aerobic rates were on the lower end of P fluxes reported in North America for eutrophic and hypereutrophic reservoirs ($<0.00 - 5.00 \text{ mg m}^{-2} \text{ day}^{-2}$) (Holdren and Armstrong 1980; James et al. 1995; Moore et al. 1998; Steinman et al. 2004; Haggard et al. 2005a; Doig et al. 2017; Lasater and Haggard 2017; McCarty 2019).

Alum treatments have been used for decades in lake and reservoir management to control internal release of P (Kennedy and Cooke 1982; Kennedy et al. 1987; Lewandowski et al. 2003b; Huser et al. 2011). When Al salts are added to water, hydrolysis occurs to produce Al hydroxides, which remove P by coagulation of particles, precipitation of AlPO_4 , and/or sorption of P to the Al hydroxide polymers (Recht and Ghassemi 1970; Cooke 1981). Lab experiments involving alum treatments directly to sediment cores have resulted in reduced water column P concentrations and sediment P fluxes under both anaerobic and aerobic conditions (Steinman et al. 2004; Haggard et al. 2005a; Pilgrim et al. 2007). In 2014, P flux was not measurable following alum treatment to the cores collected from Lake Wister, where P concentrations were less than 0.01 mg L^{-1} for the duration of the experiment (Figure 1). While alum treatments in cores at the lab are often immediately effective, P concentrations are typically measured for less than 30 days following treatments. In a study of Green Lake in Washington, sediment P release rates immediately decreased following alum treatment of sediment cores. However, P release rates began to increase again after 32 days of incubation (Degaspero et al. 2009), and release rates were nearly as high as the control by day 48. Therefore, while short term benefits of in-core alum treatments have been observed, the longevity of alum treatments may not be adequately captured in many core incubation experiments.

In 2010, prior to any alum treatments in Quarry Island Cove, P fluxes under anaerobic conditions ranged from 2.95 to $3.75 \text{ mg m}^{-2} \text{ day}^{-2}$, which were within the range of P fluxes measured in other regional reservoirs considered mesotrophic and eutrophic (Haggard et al. 2012). In 2014, P fluxes under anaerobic conditions measured one week prior to the first alum treatment exceeded those in 2010, ranging between 4.90 and $7.37 \text{ mg m}^{-2} \text{ day}^{-2}$. Similar to the lab experiment conducted in 2014, the first alum treatment in Quarry Island Cove in 2014

successfully reduced P fluxes under anaerobic conditions (Figure 3). However, in 2016, two years after the first alum treatment, P fluxes under anaerobic conditions were the greatest ever measured at Quarry Island Cove. Across North America, anaerobic P fluxes in eutrophic lakes and reservoirs often range from 1 to 29 mg m⁻² day⁻² (Nurnberg 1988; Haggard et al. 2005a; Carter and Dzialowski 2012; Steinman and Ogdahl 2015; Doig et al. 2017; Lasater and Haggard 2017), and P fluxes of 9 to 47 mg m⁻² day⁻² have been observed in hypereutrophic lakes and reservoirs (Nurnberg 1988; Auer et al. 1993; Penn et al. 2000; Carter and Dzialowski 2012). Thus, P fluxes at the cove in 2016 were within the range reported for eutrophic and hypereutrophic reservoirs, and it was apparent that the single alum treatment in 2014 did not reduce P fluxes in the long term.

Each year where an alum treatment occurred, P fluxes under anaerobic conditions were reduced immediately following the alum treatment compared to prior to the treatment. However, P fluxes typically increased when measured one or two years after the alum treatment. In 2020, while P fluxes under anaerobic conditions increased only slightly compared to August 2019, P fluxes were similar to those measured in 2010, before the addition of any alum to the cove. Generally, P fluxes throughout the duration of the study increased to a maximum in 2016, then decreased back to original conditions in 2020. Therefore, while short-term effectiveness of alum treatments was observed, five alum treatments across six years did not reduce P fluxes to less than original conditions.

The longevity of alum treatments has been highly variable across studies, ranging from less than 1 year up to 45 years (Welch and Cooke 1999; Lewandowski et al. 2003b; Cooke et al. 2005; Huser et al. 2011, 2016c; James 2017; Augustyniak et al. 2019; James and Bischoff 2019). In a study of 21 lakes across the United States, where alum treatments were successful, internal P

loads were reduced for 4 to 21 years for dimictic lakes and 5 to 11 years for polymictic lakes (Welch and Cooke 1999). Of 114 lakes across the United States, Denmark, Germany and Sweden, the average alum treatment longevity was 21 years for deeper, stratified lakes and 5.7 years for shallow, polymictic lakes (Huser et al. 2016c). The reduced effectiveness of alum treatments (and consequential variability in longevity) is often attributed to insufficient alum dosages applied (Lewandowski et al. 2003b), saturation of alum flocs (James and Bischoff 2019), and/or burial of alum flocs by incoming sediments (Welch and Cooke 1999).

Quarry Island Cove was treated with five smaller doses of alum across several years, assuming the successive smaller doses would be more effective per quantity of material, due to covering over time by incoming fresh sediments (PVIA 2014). However, internal P fluxes were not less than initial conditions by the end of the five alum treatments. In a similar study of hypereutrophic Lake Susser See in Germany, alum was added almost annually from 1977 to 1992. When sediment cores were collected between 1999 and 2002, P release rates were between 10 and 18.5 mg m⁻² day⁻², and there was no improvement to the trophic state of the lake. This was attributed to the small amount of alum added compared to external P loads (Lewandowski et al. 2003b). Additionally, Cooke et al., 2005, suggests that multiple, small doses of alum would not reduce internal P fluxes as well as a single, large dose since the P remaining unfixed by alum each year would resettle and re-enrich the surface sediment layer, allowing for more internal loading of mobile P.

In addition to internal P loadings, external sources from the watershed must be considered for effective lake and reservoir management (Welch and Jacoby 2001; Burger et al. 2007; Steinman et al. 2007; Zamparas and Zacharias 2014). Several studies have suggested reduced effectiveness of alum treatments due to large amounts of P loads entering the waterbody

from the watershed, covering the alum floc on the bottom sediments and adding additional P to be released into the water column (Lewandowski et al. 2003b; James and Bischoff 2019).

Impacts of external load reductions are often delayed due to the P accumulated in the sediments (Søndergaard et al. 2013); therefore, internal loads are addressed after external loads to accelerate lake/reservoir recovery. However, when internal sources are addressed before or without external sources, the attempt to reduce internal sources may be masked by external loading of P (Welch and Cooke 1999; Søndergaard et al. 2003; Haggard et al. 2012).

Annual external loads of P and sediments were quantified from 1993 to 2020 for three major tributaries entering Lake Wister (Poteau River, Black Fork and Fourche Maline; Chapter 2). Between 2009 and 2020, annual external loads expressed a similar pattern to anaerobic P fluxes in Figure 4, where loads increased to a maximum in 2015 and 2016, then decreased again through 2018 (see Figure 5, adapted Lasater et al., 2021). However, in 2019, external loads reached a similar magnitude to loads in 2015 and 2016. Therefore, the high P fluxes observed in 2016 may be attributed to the magnitude of P and sediment loads entering Lake Wister from the watershed in 2015 and 2016. External loads were low in 2017, but increased again in 2018 and 2019 (Figure 6). Anaerobic sediment P fluxes measured in this study were maintained and even slightly decreased between 2018 and 2020 (Figure 5). Therefore, the repetitive alum treatments to the cove may have helped maintain internal P loads through this time. However, the lack of improvement in anaerobic P fluxes compared to initial conditions is likely attributed to large external loads of P and sediments entering Lake Wister and covering and/or saturating the alum floc in the cove.

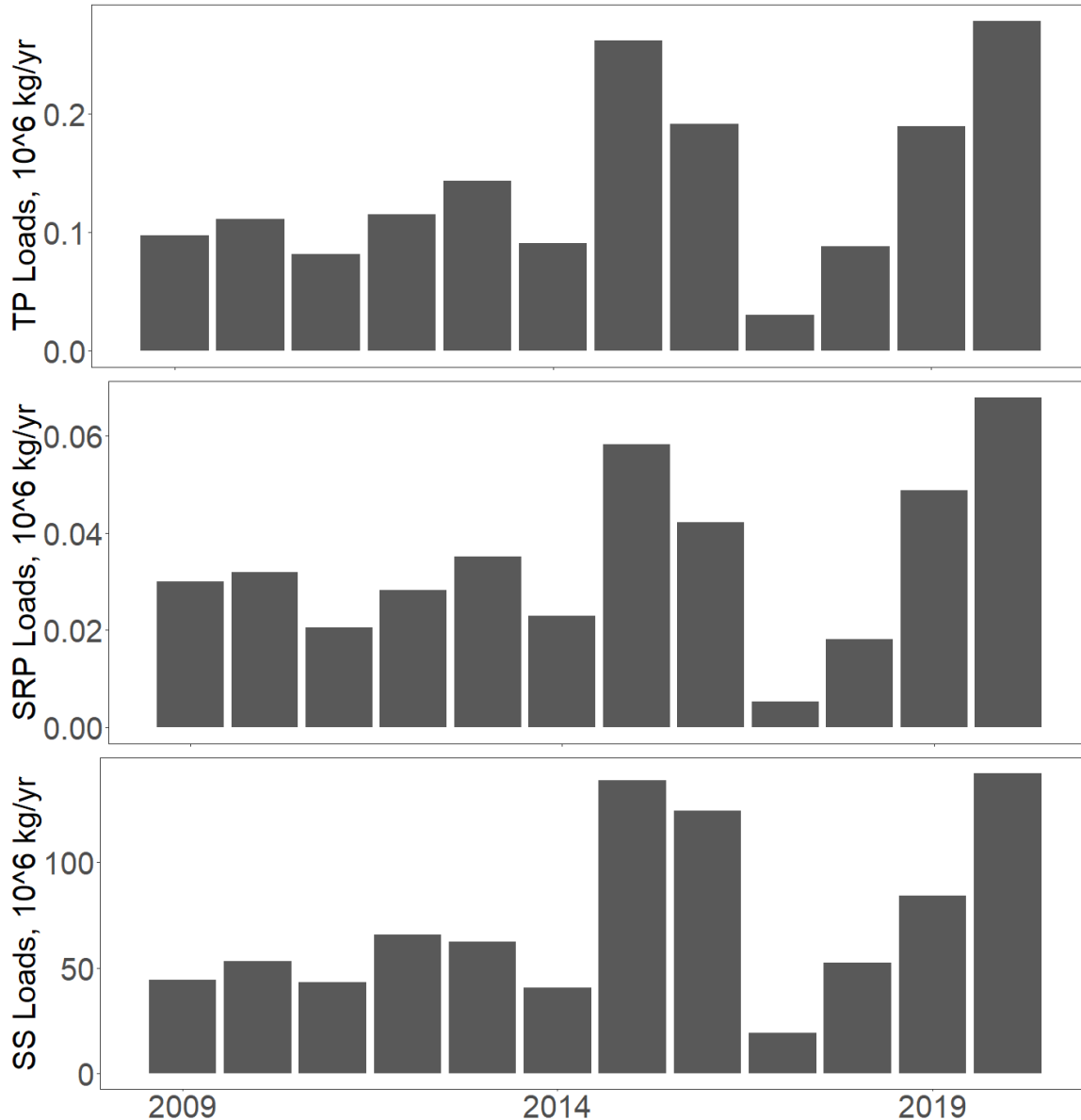


Figure 6: Annual, external loads of total phosphorus (TP), soluble reactive phosphorus (SRP), and suspended sediment (SS) from the Black Fork, Fourche Maline and Poteau River entering Lake Wister between 2009 and 2020, adapted from Lasater et al., 2021.

The average flux of TP entering Lake Wister from the watershed between 2010 and 2020 was $0.17 \text{ mg m}^{-2} \text{ day}^{-1}$ (Lasater and Haggard 2021), while the average P flux from the sediments under anaerobic conditions was $5.25 \text{ mg m}^{-2} \text{ day}^{-1}$. However, in terms of loads, P from the sediments was less due to the difference between lake and watershed area. Total TP loads from the watershed between 2010 and 2020 was 1,580,291 kg, while total P load from these sediments

was 141,542 kg (using the average anaerobic P flux and assuming half of the lake area is anaerobic over the sediments about half of the time). Therefore, about 8% of the total P load to Lake Wister between 2010 and 2020 was from the sediments, and internal P loads were less than 1% of external loads, highlighting the need to address external loads to Lake Wister. After significant reductions in external P loads, internal loads may dominate and respond more effectively to alum treatments (Wang et al. 2019).

The largest magnitude of external P and sediment loads originate from the Poteau River (Figure 5). The Poteau River watershed in Arkansas has been listed as a priority watershed within the Arkansas Nonpoint Source Pollution Plan since 1998 (ANRC 2018), and several reaches of the Poteau River itself have been listed on the Arkansas 303(d) list for impairments from point and nonpoint sources (ADEQ 2018). Therefore, several efforts to improve water quality on the Poteau River in Arkansas have been implemented, including limitations on municipal and industrial point sources and a total maximum daily load (TMDL) developed in 2006. Likely due to these efforts, flow-adjusted sediment and P concentrations have been significantly decreasing in the Poteau River since the early 1990's (Chapter 1), which is positive for Lake Wister. Adversely, flow-adjusted P concentrations in the Fourche Maline have been increasing and flow adjust sediments have not changed (Chapter 2). Ultimately, external loads entering Lake Wister are still likely contributing to internal P fluxes in Quarry Island Cove. With continued watershed management practices and more reductions in external P and sediment loads, the alum treatments would likely be more effective at reducing internal P loads and improving water quality in the cove.

Conclusions

This study quantified sediment P fluxes under aerobic and anaerobic conditions in Quarry Island Cove of Lake Wister, Oklahoma, before and after alum treatments across 6 years. Combining all flux data throughout the study, anaerobic P fluxes were significantly greater than Aerobic P fluxes. Aerobic sediment P fluxes were not significantly different after alum treatments, and the magnitude of P fluxes under aerobic conditions was relatively low throughout the duration of the study ($< 1.47 \text{ mg m}^{-2} \text{ day}^{-2}$). Under anaerobic conditions, alum treatments significantly decreased P fluxes on the short-term (i.e. 1 week after alum treatments). However, after 5 alum treatments across 6 years, sediment P fluxes under anaerobic conditions were not significantly different than prior to any alum treatments in 2010 and 2014. Additionally, P fluxes under anaerobic conditions increased to a maximum of $15.8 \text{ mg m}^{-2} \text{ day}^{-2}$ in 2016, before decreasing back to initial conditions in 2020 (unlike our hypothesis). The lack of overall improvement in anaerobic P fluxes over time is likely due to the magnitude of P and sediment loads entering Lake Wister from the Watershed. Between 2010 and 2019, 92% of the total P loads to Lake Wister were from external sources. Therefore, reductions in external loads prior or in addition to alum treatments would likely improve effectiveness and longevity of alum treatments for reducing sediment P fluxes.

References

- ADEQ, 2018. Arkansas's Final Impaired Waterbodies-303(d) List. Arkansas Department of Environmental Quality, North Little Rock.
- Anderson, D., Glibert, P., Burkholder, J., 2002. Harmful algal blooms and eutrophication: nutrient sources, compositions, and consequences. *Estuaries* 25, 704–726.
<https://doi.org/10.1016/j.hal.2008.08.017>
- Anderson, F.O., Jensen, H.S., 1992. Regeneration of inorganic phosphorus and nitrogen from decomposition of seston in a freshwater sediment. *Hydrobiologia* 228, 71–81.
- ANRC, 2018. 2018-2023 Nonpoint Source Pollution Management Plan. Arkansas Natural Resource Commission, Little Rock, Arkansas.

- Auer, M.T., Johnson, N.A., Penn, M.R., Effler, S.W., 1993. Measurement and verification of rates of sediment phosphorus release for a hypereutrophic urban lake. *Hydrobiologia* 253, 301–309.
- Augustyniak, R., Grochowska, J., Łopata, M., Parszuto, K., 2019. Sorption Properties of the Bottom Sediment of a Lake Restored by Phosphorus Inactivation Method 15 Years after the Termination of Lake Restoration Procedures. *Water* 11, 1–20.
- Belmont, M.A., White, J.R., Reddy, K.R., 2009. Phosphorus Sorption and Potential Phosphorus Storage in Sediments of Lake Istokpoga and the Upper Chain of Lakes, Florida, USA. *J. Environ. Qual.* 38, 987. <https://doi.org/10.2134/jeq2007.0532>
- Burger, D.F., Hamilton, D.P., Pilditch, C.A., 2007. Modelling the relative importance of internal and external nutrient loads on water column nutrient concentrations and phytoplankton biomass in a shallow polymictic lake. *Ecol. Modell.* 211, 411–423. <https://doi.org/10.1016/j.ecolmodel.2007.09.028>
- Carey, R.O., Migliaccio, K.W., 2009. Contribution of wastewater treatment plant effluents to nutrient dynamics in aquatic systems. *Environ. Manage.* <https://doi.org/10.1007/s00267-009-9309-5>
- Carter, L.D., Dzialowski, A.R., 2012. Predicting sediment phosphorus release rates using landuse and water-quality data. *Freshw. Sci.* 31, 1214–1222. <https://doi.org/10.1899/11-177.1>
- Chang, F.H., Zeldis, J., Gall, M., Hall, J., 2003. Seasonal and spatial variation of phytoplankton assemblages, biomass and cell size from spring to summer across the north-eastern New Zealand continental shelf. *J. Plankton Res.* 25, 737–758. <https://doi.org/10.1093/plankt/25.7.737>
- Chaubey, I., Chiang, L., Gitau, M.W., Mohamed, S., 2010. Effectiveness of best management practices in improving water quality in a pasture-dominated watershed. *J. Soil Water Conserv.* 65, 424–437. <https://doi.org/10.2489/jswc.65.6.424>
- Conley, D.J., Paerl, H.W., Howart, R.W., Boesch, D.F., Seitzinger, S.P., Havens, K.E., Lancelot, C., Likens, G.E., 2009. Controlling Eutrophication: Nitrogen and Phosphorus. *Science* (80-.). 323, 1014–1015. <https://doi.org/10.1126/science.1167755>
- Cooke, G.D., 1981. Precipitation and inactivation of phosphorus as a lake restoration technique. USEPA 41.
- Cooke, G.D., Welch, E.B., Martin, A.B., Fulmer, D.G., Hyde, J.B., 1993. Effectiveness of Al, Ca, and Fe salts for control of internal phosphorus loading in shallow and deep lakes, in: *Hydrobiologia*. pp. 323–335.
- Cooke, G.D., Welch, E.B., Peterson, S., Nichols, S.A., 2005. Restoration and Management of Lakes and Reservoirs, 3rd ed. Lewis Publishers.
- Davenport, T., Drake, W., 2011. Grand Lake St. Marys, Ohio- The Case for Source Water Protection: Nutrients and Algae Blooms. *Lakeline* 41–46.

- Degasperi, C.L., Spyridakis, D.E., Welch, E.B., 2009. Alum and Nitrate as Controls of Short-Term Anaerobic Sediment Phosphorus Release: An In Vitro Comparison. *Lake Reserv. Manag.* 8, 49–59. <https://doi.org/10.1080/07438149309354458>
- Dodds, W.K., Bouska, W.W., Eitzmann, J.L., Pilger, T.J., Pitts, K.L., Riley, A.J., Schloesser, J.T., Thornbrugh, D.J., 2008. Eutrophication of U.S. Freshwaters: Analysis of Potential Economic Damages. *Environ. Sci. Technol.* xxx.
- Doig, L.E., North, R.L., Hudson, J.J., Hewlett, C., Lindenschmidt, K.E., Liber, K., 2017. Phosphorus release from sediments in a river-valley reservoir in the northern Great Plains of North America. *Hydrobiologia* 787, 323–339. <https://doi.org/10.1007/s10750-016-2977-2>
- Dunlap, C.R., Sklenar, K.S., Blake, L.J., 2015. A costly endeavor: Addressing algae problems in a water supply. *J. Am. Water Works Assoc.* 107, E255–E262. <https://doi.org/10.5942/jawwa.2015.107.0055>
- Glibert, P.M., 2017. Eutrophication, harmful algae and biodiversity — Challenging paradigms in a world of complex nutrient changes. *Mar. Pollut. Bull.* 124, 591–606. <https://doi.org/10.1016/j.marpolbul.2017.04.027>
- Haggard, B.E., Moore, P. a, Delaune, P.B., 2005. Phosphorus flux from bottom sediments in Lake Eucha, Oklahoma. *J. Environ. Qual.* 34, 724–728. <https://doi.org/10.2134/jeq2005.0724>
- Haggard, B.E., Scott, J.T., Patterson, S., 2012. Sediment phosphorus flux in an Oklahoma reservoir suggests reconsideration of watershed management planning. *Lake Reserv. Manag.* 28, 59–69. <https://doi.org/10.1080/07438141.2012.659376>
- Haggard, B.E., Soerens, T.S., 2006. Sediment phosphorus release at a small impoundment on the Illinois River, Arkansas and Oklahoma, USA. *Ecol. Eng.* 28, 280–287. <https://doi.org/10.1016/j.ecoleng.2006.07.013>
- Hallegraeff, G.M., 1993. A review of harmful algal blooms and their apparent global increase. *Phycologia* 32, 79–99. <https://doi.org/10.2216/i0031-8884-32-2-79.1>
- Holdren, G.C., Armstrong, D.E., 1980. Factors Affecting Phosphorus Release from Intact Lake Sediment Cores. *Environ. Sci. Technol.* 14, 79–87.
- Huser, B., Brezonik, P., Newman, R., 2011. Effects of alum treatment on water quality and sediment in the Minneapolis Chain of Lakes, Minnesota, USA. *Lake Reserv. Manag.* 27, 220–228. <https://doi.org/10.1080/07438141.2011.601400>
- Huser, B.J., Futter, M., Lee, J.T., Perniel, M., 2016. In-lake measures for phosphorus control: The most feasible and cost-effective solution for long-term management of water quality in urban lakes. *Water Res.* 97, 142–152. <https://doi.org/10.1016/j.watres.2015.07.036>
- Huser, Egemose, S., Harper, H., Hupfer, M., Jensen, H., Pilgrim, K.M., Reitzel, K., Rydin, E., Futter, M., 2016. Longevity and effectiveness of aluminum addition to reduce sediment phosphorus release and restore lake water quality. *Water Res.* 97, 122–132. <https://doi.org/10.1016/j.watres.2015.06.051>

- James, W.F., 2017. Phosphorus binding dynamics in the aluminum flocculation layer of Half Moon Lake, Wisconsin. *Lake Reserv. Manag.* 33, 130–142. <https://doi.org/10.1080/10402381.2017.1287789>
- James, W.F., Barko, J.W., Eakin, H.L., 1995. Internal Phosphorus Loading in Lake Pepin Upper Mississippi River. *J. Freshw. Ecol.* 10, 269–276.
- James, W.F., Bischoff, J.M., 2019. Sediment aluminum:phosphorus binding ratios and internal phosphorus loading characteristics 12 years after aluminum sulfate application to Lake McCarrons, Minnesota. *Lake Reserv. Manag.* 2381. <https://doi.org/10.1080/10402381.2019.1661554>
- Kennedy, R.H., Barko, J.W., James, W.F., Taylor, W.D., Godshalk, G.L., 1987. Aluminum sulfate treatment of a eutrophic reservoir: Rationale, application methods, and preliminary results. *Lake Reserv. Manag.* 3, 85–90. <https://doi.org/10.1002/food.19770210811>
- Kennedy, R.H., Cooke, G.D., 1982. Control of lake phosphorus with aluminum sulfate: dose determination and application techniques. *Water Resour. Bull.* 18, 389–395.
- Kristensen, P., Sondergaard, M., Jeppesen, E., 1992. Resuspension in a shallow eutrophic lake. *Hydrobiologia* 228, 101–109.
- Lasater, A.L., Haggard, B.E., 2021. Water Quality Trends and Loads into Lake Wister, Oklahoma. *J. Contemp. Water Res. Educ.* (Submitted June, 2021).
- Lasater, A.L., Haggard, B.E., 2017. Sediment Phosphorus Flux at Lake Tenkiller, Oklahoma: How Important Are Internal Sources? *Agric. Environ. Lett.* 2, 0. <https://doi.org/10.2134/ael2017.06.0017>
- Lasater, A.L., O'Hare, M., Haggard, B.E., 2021. Water Quality Trend Analysis in the Upper Poteau River Watershed. *Trans. ASABE* (submitted June 2021).
- Lewandowski, J., Schausser, I., Hupfer, M., 2003. Long term effects of phosphorus precipitations with alum in hypereutrophic Lake Süsser See (Germany). *Water Res.* 37, 3194–3204. [https://doi.org/10.1016/S0043-1354\(03\)00137-4](https://doi.org/10.1016/S0043-1354(03)00137-4)
- McCarty, J.A., 2019. Sediment phosphorus release in a shallow eutrophic reservoir cove. *Trans. ASABE* 62, 1269–1281. <https://doi.org/10.13031/trans.13309>
- McCormick, A.R., Phillips, J.S., Ives, A.R., 2019. Responses of benthic algae to nutrient enrichment in a shallow lake: Linking community production, biomass, and composition. *Freshw. Biol.* 64, 1833–1847. <https://doi.org/10.1111/fwb.13375>
- Moore, P. a., Reddy, K.R., Fisher, M.M., 1998. Phosphorus Flux between Sediment and Overlying Water in Lake Okeechobee, Florida: Spatial and Temporal Variations. *J. Environ. Qual.* 27, 1428. <https://doi.org/10.2134/jeq1998.00472425002700060020x>
- Mortimer, C.H., 1942. The Exchange of Dissolved Substances Between Mud and Water in Lakes. *Br. Ecol. Soc.* 30, 147–201.

- Nurnberg, G.K., 1988. Prediction of phosphorus release rates from total and reductant- soluble phosphorus in anoxic lake sediments. *Can. J. Fish. Aquat. Sci.* 45, 453–462. <https://doi.org/10.1139/f88-054>
- ODEQ, 2020. Oklahoma’s Final Impaired Waterbodies- 303(d) List. Oklahoma Dep. Environ. Qual.
- Paerl, H.W., Scott, J.T., McCarthy, M.J., Newell, S.E., Gardner, W.S., Havens, K.E., Hoffman, D.K., Wilhelm, S.W., Wurtsbaugh, W.A., 2016. It Takes Two to Tango: When and Where Dual Nutrient (N & P) Reductions Are Needed to Protect Lakes and Downstream Ecosystems. *Environ. Sci. Technol.* 50, 10805–10813. <https://doi.org/10.1021/acs.est.6b02575>
- Penn, M.R., Auer, M.T., Doerr, S.M., Driscoll, C.T., Brooks, C.M., Effler, S.W., 2000. Seasonality in phosphorus release rates from the sediments of a hypereutrophic lake under a matrix of pH and redox conditions. *Can. J. Fish. Aquat. Sci.* 57, 1033–1041. <https://doi.org/10.1139/f00-035>
- Pilgrim, K.M., Huser, B.J., Brezonik, P.L., 2007. A method for comparative evaluation of whole-lake and inflow alum treatment. *Water Res.* 41, 1215–1224. <https://doi.org/10.1016/j.watres.2006.12.025>
- Porter, E.M., Bowman, W.D., Clark, C.M., Compton, J.E., Pardo, L.H., Soong, J.L., 2013. Interactive effects of anthropogenic nitrogen enrichment and climate change on terrestrial and aquatic biodiversity. *Biogeochemistry* 114, 93–120. <https://doi.org/10.1007/s10533-012-9803-3>
- PVIA, 2014. Quarry Island Cove Nutrient Inactivation Project.
- Radbourne, A.D., Elliott, J.A., Maberly, S.C., Ryves, D.B., Anderson, N.J., 2019. The impacts of changing nutrient load and climate on a deep, eutrophic, monomictic lake. *Freshw. Biol.* 64, 1169–1182. <https://doi.org/10.1111/fwb.13293>
- Rasconi, S., Gall, A., Winter, K., Kainz, M.J., 2015. Increasing Water Temperature Triggers Dominance of Small Freshwater Plankton. *PLoS One* 10, e0140449. <https://doi.org/10.1371/journal.pone.0140449>
- Recht, H.L., Ghassemi, M., 1970. Kinetics and mechanism of precipitation and nature of the precipitate obtained in phosphorus removal from wastewater using aluminum (III) and iron (III) salts. *Water Pollut. Control Res. Ser.*
- Shenk, G.W., Linker, L.C., 2013. Development and application of the 2010 Chesapeake Bay Watershed total maximum daily load model. *J. Am. Water Resour. Assoc.* 49, 1042–1056. <https://doi.org/10.1111/jawr.12109>
- Smeltzer, E., 1990. A successful alum/aluminate treatment of lake morey, vermont. *Lake Reserv. Manag.* 6, 9–19. <https://doi.org/10.1080/07438149009354691>
- Smith, V.H., Tilman, G.D., Nekola, J.C., 1999. Eutrophication: impacts of excess nutrient inputs on freshwater, marine, and terrestrial ecosystems. *Environ. Pollut.* 100, 179–196.

- Søndergaard, M., Bjerring, R., Jeppesen, E., 2013. Persistent internal phosphorus loading during summer in shallow eutrophic lakes. *Hydrobiologia* 710, 95–107. <https://doi.org/10.1007/s10750-012-1091-3>
- Søndergaard, M., Jensen, J.P., Jeppesen, E., 2003. Role of sediment and internal loading of phosphorus in shallow lakes. *Hydrobiologia* 506–509, 135–145. <https://doi.org/10.1023/B:HYDR.0000008611.12704.dd>
- Steinman, A., Chu, X., Ogdahl, M., 2007. Spatial and temporal variability of internal and external phosphorus loads in Mona Lake, Michigan. *Aquat. Ecol.* 43, 1–18. <https://doi.org/10.1007/s10452-007-9147-6>
- Steinman, A., Rediske, R., Reddy, K.R., 2004. The reduction of internal phosphorus loading using alum in Spring Lake, Michigan. *J. Environ. Qual.* 33, 2040–2048. <https://doi.org/10.2134/jeq2004.2040>
- Steinman, A.D., Ogdahl, M.E., 2015. TMDL reevaluation: reconciling internal phosphorus load reductions in a eutrophic lake. *Lake Reserv. Manag.* 31, 115–126. <https://doi.org/10.1080/10402381.2015.1014582>
- USEPA, 2015. A Compilation of Cost Data Associated with the Impacts and Control of Nutrient Pollution. EPA 820-F-15-096 1–110.
- Wang, M., Xu, X., Wu, Z., Zhang, X., Sun, P., Wen, Y., Wang, Z., Lu, X., Zhang, W., Wang, X., Tong, Y., 2019. Seasonal Pattern of Nutrient Limitation in a Eutrophic Lake and Quantitative Analysis of the Impacts from Internal Nutrient Cycling. *Environ. Sci. Technol.* 53, 13675–13686. <https://doi.org/10.1021/acs.est.9b04266>
- Welch, E.B., Cooke, G.D., 1999. Effectiveness and longevity of phosphorus inactivation with alum. *Lake Reserv. Manag.* 15, 5–27. <https://doi.org/10.1080/07438149909353948>
- Welch, E.B., Jacoby, J.M., 2001. On Determining the Principal Source of Phosphorus Causing Summer Algal Blooms in Western Washington Lakes. *Lake Reserv. Manag.* 17, 55–65. <https://doi.org/10.1080/07438140109353973>
- Xu, J., Yin, K., Lee, J.H.W., Liu, H., Ho, A.Y.T., Yuan, X., Harrison, P.J., 2010. Long-term and seasonal changes in nutrients, phytoplankton biomass, and dissolved oxygen in deep bay, Hong Kong. *Estuaries and Coasts* 33, 399–416. <https://doi.org/10.1007/s12237-009-9213-5>
- Zamparas, M., Zacharias, I., 2014. Restoration of eutrophic freshwater by managing internal nutrient loads. A review. *Sci. Total Environ.* 496, 551–562. <https://doi.org/10.1016/j.scitotenv.2014.07.076>

Chapter 4: Prioritizing Subwatersheds for Water Quality and Watershed Management Using Watershed Models

Abbie Lasater¹, and Brian E. Haggard^{1,2}

¹Department of Biological and Agricultural Engineering, University of Arkansas, Fayetteville,
AR 72701

²Arkansas Water Resources Center, University of Arkansas, Fayetteville, AR 72701

Abstract

Watershed models are widely used for prioritization of subwatersheds for watershed management. The purpose of this report is to synthesize the literature related to subwatershed prioritization using watershed models, and to evaluate limitations and challenges in targeting subwatersheds using modeling techniques. Most often, watershed model predictions such as sediment yield, erosion rates, runoff and/or nutrient loads are placed into categories or ranked for subwatershed prioritization. However, model calibration is often conducted at minimal sites on the large watershed scale and model outputs on the subwatershed scale or smaller are used for prioritization, but little data exists to validate the small-scale model outputs. Additionally, model setup, calibration and methods chosen for manipulating model outputs can produce conflicting prioritization results. Thus, it is important to define clear prioritization objectives and report techniques used in model setup and prioritization methods. Future work is necessary in determining optimal methods for subwatershed prioritization and the ability of models to predict small-scale watershed data.

Introduction

Of all water on the earth, less than 1% is accessible for human use, and the availability of this water is pertinent to human health, the environment and the economy (Jurkowski 2008). The increasing demand for water due to population growth, combined with anthropogenic impacts on water quantity and quality, all underline the need for sustainable management of water resources. However, financial resources must be focused where needed to improve or maintain water quantity and quality.

A watershed approach for managing water quality and quantity has been used since the 1980s, focusing on an individual geo-hydrological unit to analyze and conserve the natural resources (USEPA 2008b). With limitations in economic and human resources, there is a need to select priority watersheds for implementation of initial remediation efforts (Razavi Toosi and Samani 2017). Watershed prioritization is a process of ranking sensitive watersheds for applications of management practices or restoration techniques, typically on the basis of sub-watersheds within a larger watershed. Sensitive watersheds can include areas where ecosystem services need to be protected, where soil erosion rates are high, or where degradation is caused by human disturbances (Malik and Bhat 2014; Fallah et al. 2016; Aguirre-Salado et al. 2017)

The 1987 amendment to the Clean Water Act expanded the scope of water quality improvements to nonpoint source pollution from previously only addressing point sources (Copeland 2012). This amendment required states to develop management plans and implement programs to reduce runoff from agricultural lands, construction sites and urban areas, resulting in an emphasis on best management practices (BMPs). BMPs are commonly defined as any program, practice, design, or a combination of the latter, which prevent or mitigate nonpoint source pollution (NCFS 2017). Several studies have analyzed the effectiveness of BMPs,

concluding their overall benefit in reducing pollutant loads and improving water quality (e.g. see Park et al. 1994; Arabi et al. 2006; Merriman et al. 2009; Rao et al. 2009). The considerable amount of cost, labor and potential maintenance associated with implementing BMPs emphasizes the need to determine a selective approach for identifying smaller hydrological units and increasing the efficiency of management programs. Watershed prioritization for implementation of BMPs has been carried out through a variety of methods (e.g. watershed modeling, multi-criteria decision making, morphometric analysis; Nooka Ratnam et al. 2005; Legge et al. 2013; Rahaman et al. 2015) using a number of different indicators (e.g. sediment yield, land use, socioeconomic factors; Javed et al. 2009; Newbold and Siikamaki 2009; Ayele et al. 2017).

The early literature for prioritizing watersheds focused on relatively simple physical characteristics of the watershed and water quality issues (Duda and Johnson 1985; Maas et al. 1985; Young et al. 1989; Murray and von Gadov 1991). Watershed characteristics generally consisted of runoff volume and soil erosion rates (Maas et al. 1985; Young et al. 1989; Murray and von Gadov 1991), and water quality concerns were related to areas with high nutrient transport (Duda and Johnson 1985; Maas et al. 1985; Young et al. 1989). By the 1990s, watershed prioritization efforts began integrating remote sensing (RS) and geographic information systems (GIS) (Saha et al. 1992; Sharada et al. 1993; Biswas et al. 1999), powerful tools for delineation of sub-watersheds and analysis of geomorphometric properties (Farhan and Anaba 2016). RS and GIS have developed into widely accepted techniques in watershed characterization and prioritization (Khan et al. 2001; Shrimali et al. 2001; Arun et al. 2005; Katiyar et al. 2006; Martin and Saha 2007; Fallah et al. 2016).

With increased understanding of hydrologic processes and nutrient dynamics, and the integration of RS and GIS, watershed modeling techniques have been increasingly used for subwatershed prioritization in the last couple of decades. Therefore, the purpose of this report is to synthesize the literature related to subwatershed prioritization using watershed models, and to evaluate limitations and challenges in targeting subwatersheds using modeling techniques.

Methods

Studies regarding watershed prioritization using watershed modeling approaches, for the purpose of conservation activities or implementation of BMPs, will be synthesized. To synthesize the current literature, web-based search engines will be used with keywords and phrases such as “watershed prioritization,” “subwatershed prioritization,” “prioritizing watersheds,” “hotspot prioritization,” “prioritizing erosion-prone areas,” “prioritizing critical source areas,” “priority management areas,” “watershed modeling,” and so on. Web-based search engines such as ScienceDirect, Web of Science, and Google Scholar will be used. Literature will be confined to prioritization efforts directly related to watershed management planning (e.g. implementation of BMPs or conservation activities).

Watershed Prioritization Techniques using Models

Various models have been used for prioritizing subwatersheds within a larger watershed for management practices (Table 1). Often times, models are calibrated and validated on the HUC-8 scale or larger, and then the calibrated models are used for predictions on the HUC-12/14 scale or smaller. Model predictions such as sediment yield, erosion rates, runoff and/or nutrient loads are then placed into categories or ranked for prioritization. For example, in the Damador catchment in India (10,878 km²), the Soil Water Assessment Tool (SWAT) was calibrated and

validated at four locations with watershed sizes between 21 and 95 km², then runoff and sediment yield were predicted on the Hydrologic Response Unit (HRU) scale. Sediment yield values for each HRU were then placed into predefined categories of slight (0-5 t ha⁻¹ yr⁻¹), moderate (5-10 t ha⁻¹ yr⁻¹), high (10-20 t ha⁻¹ yr⁻¹), very high (20-40 t ha⁻¹ yr⁻¹), and severe (40-80 t ha⁻¹ yr⁻¹), then graphically displayed to show potential sources and priority areas (Kumar and Mishra 2015).

Other prioritization methods from model outputs include:

- Ranking soil loss, sediment yield, nutrient loads, and/or runoff for each subwatershed, placing into categories (e.g. low, medium, high), then graphically displaying results (Young et al. 1989; Tripathi et al. 2003; Kaur et al. 2004; Pandey et al. 2009; Robertson et al. 2009; Tibebe and Bewket 2010; Besalatpour et al. 2012; Saghafian et al. 2012; Mosbahi et al. 2013; Chen et al. 2014a; Sardar et al. 2014; Noor et al. 2016; Welde 2016; Ayele et al. 2017; Shivhare et al. 2017)
- Placing flow-weighted nutrient and sediment concentrations from subwatersheds into categories using percentile classifications, and graphically displaying the results (Pai et al. 2011b)
- Estimating, ranking, and graphically displaying several subwatershed characteristics separately including sediment yield, runoff yield, sediment delivery ration, soil phosphorus, sediment-phosphorus index, and erosion tolerance index, and comparing high-risk areas of overlap among the parameters (Ghafari et al. 2017).

- Combining multiple model outputs. For example, combining the sediment delivery and erosion risk from the High Impact Targeting (HIT) model, infiltration and groundwater recharge from SWAT, and the sensitivity of groundwater withdrawal from Michigan's Water Withdrawal Assessment Tool (WWAT). Then a knowledge-based weighting system is applied to combine model outputs with categorical criteria (e.g. opportunity for implementing conservation practices, connectivity to main stream, etc.) to calculate priority values for each subwatershed (Legge et al. 2013)
- Combining sediment and/or nutrient load estimations with other qualitative parameters (e.g. community support for conservation, stakeholder value, implementation costs of management practices, land availability, watershed attributes, etc.) to develop a composite criterion, which is then ranked, separated into classes, and graphically displayed (Shriver and Randhir 2006; Jang et al. 2013, 2015).
- Combining with morphometric analysis and/or land use/land cover (LULC) analysis (Ajay et al. 2014; Shivhare et al. 2017).
- Using multi-criteria decision making (MCDM) techniques with various aforementioned prioritization methods (Chung and Lee 2009; Gopinath et al. 2016).

Challenges of Watershed Models for Prioritization

Often times, studies graphically display prioritization results from two or more parameters, but do not further discuss the final prioritization of subwatersheds (e.g. see Kaur et al. 2004; Pai et al. 2011a; Ghafari et al. 2017). One subwatershed may be high priority for one

parameter but low priority for another parameter, but a final weighted prioritization may not be established. To determine the final ranking of subwatersheds in these situations, it may be useful to develop an overall compound parameter or develop other techniques to better account for differences in prioritization across multiple target parameters.

Pai et al. 2011b discussed an important consideration when using stream reach outputs from watershed models. Downstream subwatersheds can express higher priority due to load accumulation, and this must be adjusted for when ranking subwatersheds for prioritization. For example, a study in the Pocono Creek Watershed in Pennsylvania, subwatersheds were prioritized using SWAT for flow concerns (i.e. flood hazard and decreased base flow) (Kalin and Hantush 2009). The authors noted that the geographical proximity of a subwatershed to the watershed outlet affected their prioritization results, and this was visually seen in the priority maps. The bias identified by the authors of this study must be accounted for in all prioritization efforts, since the ultimate goal is to analyze the individual contribution of subwatershed based on management activities, LULC changes, water quality changes, etc., and not the spatial location within the larger watershed. Pai et al. 2011b addressed this bias by subtracting the nutrient and sediment loads from upstream subwatersheds to determine individual subwatershed contributions.

Only a few studies have reported the inclusion of point source contributions in watershed prioritization (Randhir et al. 2001; Saraswat et al. 2009; Pai et al. 2011b). However, the lack of point source information can cause subwatershed priorities to deviate from typical land-use relationships (e.g., a high priority subwatershed that is primarily forested) (Pai et al. 2011a), and underestimate areas with large nonpoint source contributions. The incorporation of point source

data can help to better define small-scale pollution sources and improve precision of watershed modeling and prioritization techniques (Robertson et al. 2009).

More often than not, watershed models are calibrated and/or validated at the larger-scale watershed, and are then used to predict parameters at the subwatershed scale (or smaller) where prioritization is conducted (e.g. see Table 1). However, there is no validation of the model predicted results at the smaller scale. This is challenging, since data are not always available at all (or any) subwatershed outlets to validate the model results. This may cause difficulty in convincing watershed managers and stakeholders to act on model-generated prioritization results (Pai et al. 2011b). Potential solutions include generating small-scale data in order to calibrate/validate the model, or using other surrogate methods to validate the identified priority subwatersheds. For example, Pai et al. 2011b analyzed relationships between model generated subwatershed pollutant concentrations and the subwatershed's percentage of forest and pasture acreage. A positive relationship was identified between pollutant concentration and pasture acreage, while a negative relationship was identified between pollutant concentration and forest acreage. This was consistent with expectations, and provided a simple way to validate the subwatershed prioritization (Pai et al. 2011a).

While the use of additional information or surrogate methods would strengthen prioritization results, watershed models can still provide valuable insight into watershed behaviors and changes, and help identify priority areas of concern. Priority subwatersheds were compared between a calibrated and uncalibrated SWAT model in the Saugahatchee Creek and Magnolia River watersheds in Alabama, and the Zrebar Lake watershed in Iran (Niraula et al. 2012; Imani et al. 2019). Priority areas were similar between calibrated and uncalibrated models across all sites, and non-matching areas were typically lower priority. However, all SWAT

models were calibrated and validated at the watershed outlet, and Niraula et al. 2012 suggests the results may change if the models are calibrated at various locations within the watershed, and further studies are necessary.

On a few occurrences, watershed models were calibrated with one or more parameters, but different parameter(s) were used for prioritization (Shriver and Randhir 2006; Chung and Lee 2009; Tibebe and Bewket 2010; Mosbahi et al. 2013; Chen et al. 2014a; Xu et al. 2016). In these cases, the model was typically calibrated and validated with flow and sediment yields, but then nutrient outputs were used for prioritization. Similar to calibration/prioritization scale differences, it is difficult to assume acceptable model performances when calibration/validation data are not available. Therefore, caution must be taken when prioritizing subwatershed with parameters that have not been calibrated.

Few studies have compared prioritization results from watershed models with other prioritization techniques (e.g., LULC analyses, morphometric analyses, and MCDM). In the Nagwan watershed in India, sediment yield generated from SWAT was used to prioritize subwatersheds and compared to priority subwatersheds determined from a subjective model based on erosivity determinants (e.g., slope, soil type, LULC, etc.). The subjective model produced reverse priorities for 67-93% of the subwatersheds, and the SWAT generated results were considered to be superior due to its ability to account for the impact of landuse and soil types on runoff and erosion (Kaur et al. 2004). In the Kangsabati basin in India, SWAT model outputs were used to validate four different MCDM techniques (i.e., VIKOR, TOPSIS, SAW, and CF). Priority subwatersheds identified by SWAT agreed best with priority subwatersheds from VIKOR, but differed from results generated by TOPSIS, SAW, and CF, likely due to assumptions made in weight assignments for variables (Bhattacharya et al. 2020). However,

again SWAT models in both aforementioned studies were only calibrated and validated at the watershed outlet (Table 1), making it difficult to justify the subwatershed model outputs.

The setup, calibration and validation of watershed models can vary greatly across studies, leading to variable outputs and results. This was evident when four independently developed SWAT models and a SPARROW model were compared for identification of priority areas in the Maumee River watershed in the U.S (Evenson et al. 2021). Most often, the models disagreed regarding priority areas, with only between 16 and 46% of subwatersheds being identified as priority in more than one model. The authors suggest that identification of priority areas using watershed models would benefit from comprehensive uncertainty analyses. This was consistent with a study in the Saugahatchee Creek watershed in Alabama, where SWAT and the Generalized Watershed Loading Function (GWLF) produced varied priority subwatersheds (though not as pronounced as Evensen et al. 2021) (Niraula et al. 2013). Additionally, in the Xiangxi River watershed in China, priority areas differed across SWAT models developed with different DEMs, and in the Mississippi/Atchafalaya River Basin in the U.S., priority areas varied with SPARROW model parametrization (Robertson et al. 2009).

In the Gully Creek Watershed in Canada, SWAT was compared to the event-based Agriculture Non-Point Source (AGNPS) pollution model for identifying priority areas and seasons for sediment and P loading. Both models agreed that summer did not constitute a “hot-moment” for sediment and P, but SWAT identified winter and AGNPS identified spring as hot-moments for sediment and P. This study identifies the need for including seasonal variations in priority areas (Shrestha et al. 2021).

Even with a well calibrated/validated watershed model, the method chosen for manipulating model outputs and determining priority subwatersheds can produce variable

results. For example, in the Saginaw River watershed in Michigan, SWAT model outputs were used to compare four methods for targeting priority subwatersheds, 1) the concentration impact index (CII), 2) Load Impact Index (LII), 3) Load per Subbasin Area Index (LPSAI), and 4), Load per Unit Area Index (LPUAI) (Giri et al. 2012). The CII and LII methods identify priority areas based on pollutant concentration and pollutant loads, respectively, in the subwatershed reaches (including upstream watersheds). The LPSAI method identifies priority areas based on the pollution load for each subbasin, while the LPUAI is based on the average pollutant load per unit area. These different targeting techniques identified different areas for high, medium, and low priority, and based on simulated BMP implementation, various targeting techniques were better at reducing various constituent loads of interest. Therefore, clear objectives for prioritization must be identified (e.g., reducing nitrogen loads), so the appropriate targeting method will be selected.

A drawback of using watershed models for subwatershed prioritization is the complexity and quantity of data required, which may not be practical in data scarce areas (Aher et al. 2014). In this case, other prioritization techniques may need to be explored such as morphometric analyses, land use/land cover analyses, MCDM, or a combination of methods. However, in the hydrologic community, there is an ongoing debate on the use of simple or detailed index-based methods for prioritization, or complex watershed models (Rudra et al. 2020). Thus, continued research on optimal prioritization techniques is necessary.

Conclusions

Watershed models are widely used for prioritization of subwatersheds for watershed management. However, model calibration is often conducted at minimal sites on the large watershed scale and model outputs on the subwatershed scale or smaller are used for

prioritization, but little data exists to validate the small-scale model outputs. The use of additional information or surrogate methods would likely strengthen prioritization results. Additionally, model setup, calibration and methods chosen for manipulating model outputs can produce variable prioritization results. Thus, it is important to define clear prioritization objectives and report techniques used in model setup and prioritization methods. Future work is necessary in determining optimal methods for subwatershed prioritization and the ability of models to predict small-scale watershed data.

References

- Aguirre-Salado C, Miranda-Aragón L, Pompa-García M, et al (2017) Improving Identification of Areas for Ecological Restoration for Conservation by Integrating USLE and MCDA in a GIS-Environment: A Pilot Study in a Priority Region Northern Mexico. *ISPRS Int J Geo-Information* 6:262. doi: 10.3390/ijgi6090262
- Aher PD, Adinarayana J, Gorantiwar SD (2014) Quantification of morphometric characterization and prioritization for management planning in semi-arid tropics of India: A remote sensing and GIS approach. *J Hydrol* 511:. doi: 10.1016/j.jhydrol.2014.02.028
- Arabi M, Govindaraju RS, Hantush MM, Engel BA (2006) Role of watershed subdivision on evaluation of long-term impact of best management practices on water quality. *J Am Water Resour Assoc* 42:513–528
- Arun PS, Jana R, Nathawat MS (2005) A Rulebase Physiographic Characterization of a Drought Prone Watershed Applying Remote Sensing and GIS. *J Indian Soc Remote Sens* 33:189–201
- Ayele G, Teshale E, Yu B, et al (2017) Streamflow and Sediment Yield Prediction for Watershed Prioritization in the Upper Blue Nile River Basin, Ethiopia. *Water* 9:782. doi: 10.3390/w9100782
- Besalatpour A, Hajabbasi MA, Ayoubi S, Jalalian A (2012) Identification and prioritization of critical sub-basins in a highly mountainous watershed using SWAT model. *Eurasian J Soil Sci* 1:58–63
- Bhattacharya RK, Chatterjee N Das, Das K (2020) Sub-basin prioritization for assessment of soil erosion susceptibility in Kangsabati, a plateau basin: A comparison between MCDM and SWAT models. *Sci Total Environ* 734:1–21
- Biswas S, Sudhakar S, Desai V (1999) Prioritisation of Subwatersheds Based on Morphometric Analysis of drainage basin: a remote sensing and gis approach. 155–166

- Chen L, Zhong Y, Wei G, et al (2014) Development of an Integrated Modeling Approach for Identifying Multilevel Non-Point-Source Priority Management Areas at the Watershed Scale. *Am Geophys Union* 50:4095–4109. doi: 10.1002/2013WR015041. Received
- Chung ES, Lee KS (2009) Prioritization of water management for sustainability using hydrologic simulation model and multicriteria decision making techniques. *J Environ Manage* 90:1502–1511. doi: 10.1016/j.jenvman.2008.10.008
- Copeland C (2012) CRS Report for Congress Clean Water Act: A Summary of the Law
- Duda AM, Johnson RJ (1985) Cost-Effective Targeting of Agricultural Nonpoint-Source Pollution Controls. *J Soil Water Conserv* Vol 40, No 1, p 108-111, January-February, 1985 2 Fig, 19 Ref
- Evenson GR, Kalcic M, Wang Y, et al (2021) Uncertainty in critical source area predictions from watershed-scale hydrologic models. *J Environ Manage* 279:111506. doi: 10.1016/j.jenvman.2020.111506
- Fallah M, Kaviani A, Omidvar E (2016) Watershed prioritization in order to implement soil and water conservation practices. *Environ Earth Sci* 75:1–17. doi: 10.1007/s12665-016-6035-1
- Farhan Y, Anaba O (2016) A Remote Sensing and GIS Approach for Prioritization of Wadi Shueib Mini-Watersheds (Central Jordan) Based on Morphometric and Soil Erosion Susceptibility Analysis. *J Geogr Inf Syst* 8:1–19
- Ghafari H, Gorji M, Arabkhedri M, et al (2017) Identification and prioritization of critical erosion areas based on onsite and offsite effects. *Catena* 156:1–9. doi: 10.1016/j.catena.2017.03.014
- Giri S, Nejadhashemi AP, Woznicki SA (2012) Evaluation of targeting methods for implementation of best management practices in the Saginaw River Watershed. *J Environ Manage* 103:24–40. doi: 10.1016/j.jenvman.2012.02.033
- Imani S, Delavar M, Niksokhan MH (2019) Identification of Nutrients Critical Source Areas with SWAT Model under Limited Data Condition. *Water Resour* 46:128–137. doi: 10.1134/S0097807819010147
- Jang T, Vellidis G, Hyman JB, et al (2013) Model for prioritizing best management practice implementation: Sediment load reduction. *Environ Manage* 51:209–224. doi: 10.1007/s00267-012-9977-4
- Jang T, Vellidis G, Kurkalova LA, et al (2015) Prioritizing Watersheds for Conservation Actions in the Southeastern Coastal Plain Ecoregion. *Environ Manage* 55:657–670. doi: 10.1007/s00267-014-0421-9
- Javed A, Yousuf M, Rizwan K (2009) Prioritization of Sub-watersheds based on Morphometric and Land Use Analysis using Remote Sensing and GIS Techniques. *J. Indian Soc. Remote Sens.* 37:261–274
- Jurkowski A (2008) Drinking water: understanding the science and policy behind a critical resource. *Natl. Acad.*

- Kalin L, Hantush MM (2009) An Auxiliary Method to Reduce Potential Adverse Impacts of Projected Land Developments: Subwatershed Prioritization. *Environ Manage* 43:311–325. doi: 10.1007/s00267-008-9202-7
- Katiyar R, Garg PK, Jain SK (2006) Watershed Prioritization and Reservoir Sedimentation Using Remote Sensing Data. *Geocarto Int* 21:55–60. doi: 10.1080/10106040608542393
- Kaur R, Singh O, Srinivasan R, et al (2004) Comparison of a Subjective and a Physical Approach for Identification of Priority Areas for Soil and Water Management in a Watershed – A Case Study of Nagwan Watershed in Hazaribag district of Jharkhand, India. *Environ Model Assess* 9:115–127
- Khan MA, Gupta VP, Moharana PC (2001) Watershed prioritization using remote sensing and geographical information system: a case study from Guhiya, India. *J Arid Environ* 49:465–475. doi: 10.1006/jare.2001.0797
- Kumar S, Mishra A (2015) Critical Erosion Area Identification Based on Hydrological Response Unit Level for Effective Sedimentation Control in a River Basin. *Water Resour Manag* 29:. doi: 10.1007/s11269-014-0909-3
- Legge JT, Doran PJ, Herbert ME, et al (2013) From model outputs to conservation action: Prioritizing locations for implementing agricultural best management practices in a Midwestern watershed. *J Soil Water Conserv* 68:22–33. doi: 10.2489/jswc.68.1.22
- Maas RP, Smolen MD, Dressing SA (1985) Selecting critical areas for nonpoint-source pollution control. *J Soil Water Conserv* 40:68–71
- Malik MI, Bhat MS (2014) Integrated Approach for Prioritizing Watersheds for Management: A Study of Lidder Catchment of Kashmir Himalayas. *Environ Manage* 54:1267–1287. doi: 10.1007/s00267-014-0361-4
- Martin D, Saha SK (2007) Integrated approach of using remote sensing and gis to study watershed prioritization and productivity. *PHOTONIRVACHAK-JOURNAL INDIAN Soc Remote Sens* 35:21–30
- Merriman KR, Gitau MW, Chaubey I (2009) A tool for estimating best management practice effectiveness in Arkansas. *Appl Eng Agric* 25:199–213. doi: 10.13031/2013.26333
- Mosbahi M, Benabdallah S, Boussema MR (2013) Assessment of soil erosion risk using SWAT model. *Arab J Geosci* 6:4011–4019. doi: 10.1007/s12517-012-0658-7
- Murray DM, von Gadow K (1991) Prioritizing mountain catchment areas. *J Environ Manage* 32:357–366. doi: 10.1016/S0301-4797(05)80072-6
- NCFS (2017) What are BMPs?
- Newbold SC, Siikamaki J (2009) Prioritizing conservation activities using reserve site selection methods and population viability analysis. *Ecol Appl* 19:1774–1790. doi: 10.1890/08-0599.1
- Niraula R, Kalin L, Srivastava P, Anderson CJ (2013) Identifying critical source areas of nonpoint source pollution with SWAT and Identifying critical source areas of nonpoint

- source pollution with SWAT and GWLF. *Ecol Modell* 268:123–133. doi: 10.1016/j.ecolmodel.2013.08.007
- Niraula R, Kalin L, Wang R, Srivastava P (2012) Determining nutrient and sediment critical source areas with SWAT: Effect of lumped calibration. *Trans ASABE* 55:137–147. doi: 10.13031/2013.41262
- Nooka Ratnam K, Srivastava YK, Venkateswara Rao V, et al (2005) Check Dam positioning by prioritization micro-watersheds using SYI model and morphometric analysis - remote sensing and GIS perspective. *J Indian Soc Remote Sens* 33:25–38. doi: 10.1007/BF02989988
- Noor H, Vafakhah M, Mohammady M (2016) Comparison of different targeting methods for watershed management practices implementation in Taleghan dam watershed, Iran. *Water Sci Technol Water Supply* 16:1484–1496. doi: 10.2166/ws.2016.048
- Pai N, Saraswat D, Daniels M (2011a) Identifying Priority Subwatersheds in the Illinois River Drainage Area in Arkansas Watershed Using a Distributed Modeling Approach. *Trans ASABE* 54:2181–2196. doi: 10.13031/2013.40657
- Pai N, Saraswat D, Daniels M (2011b) Identifying priority subwatersheds in the Illinois River Drainage Area in Arkansas watershed using a distributed modeling approach. *Trans ASABE* 54:2181–2196. doi: 10.13031/2013.40657
- Pandey A, Chowdary VM, Mal BC, Billib M (2009) Application of the WEPP model for prioritization and evaluation of best management practices in an Indian Watershed. *Hydrol Process* 23:2997–3005. doi: 10.1002/hyp
- Park SW, Mostaghimi S, Cooke RA, McClellan PW (1994) Bmp Impacts on Watershed Runoff, Sediment, and Nutrient Yields. *JAWRA J Am Water Resour Assoc* 30:1011–1023. doi: 10.1111/j.1752-1688.1994.tb03349.x
- Rahaman SA, Ajeez SA, Aruchamy S, Jegankumar R (2015) Prioritization of Sub Watershed Based on Morphometric Characteristics Using Fuzzy Analytical Hierarchy Process and Geographical Information System – A Study of Kallar Watershed, Tamil Nadu. *Aquat Procedia* 4:1322–1330. doi: 10.1016/j.aqpro.2015.02.172
- Randhir TO, O'Connor R, Penner PR, Goodwin DW (2001) A watershed-based land prioritization model for water supply protection. *For Ecol Manage* 143:47–56. doi: 10.1016/S0378-1127(00)00504-1
- Rao NS, Easton ZM, Schneiderman EM, et al (2009) Modeling watershed-scale effectiveness of agricultural best management practices to reduce phosphorus loading. *J Environ Manage* 90:1385–1395. doi: 10.1016/j.jenvman.2008.08.011
- Razavi Toosi SL, Samani JMV (2017) Prioritizing Watersheds Using a Novel Hybrid Decision Model Based on Fuzzy DEMATEL, Fuzzy ANP and Fuzzy VIKOR. *Water Resour Manag* 31:2853–2867. doi: 10.1007/s11269-017-1667-9
- Robertson DM, Schwarx GE, Saad DA, Alexander RB (2009) Incorporating Uncertainty into the Ranking of SPARROW Model Nutrient Yields from the Mississippi/Atchafalaya River Basin Watersheds. *J Am Water Resour Assoc* 45:534–549

- Rudra RP, Mekonnen BA, Shukla R, et al (2020) Currents Status, Challenges, and Future Directions in Identifying Critical Source Areas for Non-Point Source Pollution in Canadian Conditions. *Agriculture* 10:2–25
- Saghafian B, Sima S, Sadeghi S, Jeirani F (2012) Application of unit response approach for spatial prioritization of runoff and sediment sources. *Agric Water Manag* 109:36–45. doi: 10.1016/j.agwat.2012.02.004
- Saha SK, Bhattacharjee C, Laeangzuva, Pande LM (1992) Prioritization of sub-watersheds based on erosion loss estimation- a case study of part of song river watershed, doon valley using satellite data. *Natl Symp Remote Sens Sustain Dev* 181–186
- Saraswat D, Daniels M, Tacker P, Pai N (2009) A Comprehensive Watershed Response Modeling for 12-digit Hydrologic Unit Code “ HUC ” in Selected Priority Watersheds in Arkansas
- Sardar B, Singh AK, Raghuwanshi NS, Chatterjee C (2014) Hydrological Modeling to Identify and Manage Critical Erosion-Prone Areas for Improving Reservoir Life: Case Study of Barakar Basin. *J Hydrol Eng* 19:196–204. doi: 10.1061/(ASCE)HE.1943-5584.0000749
- Sharada D, Kumar M, Venkataratnam L (1993) Watershed prioritisation for soil conservation—a GIS approach. *Geocarto*. doi: 10.1080/10106049309354396
- Shivhare N, Kumar A, Jee P, et al (2017) Identification of critical soil erosion prone areas and prioritization of micro- watersheds using geoinformatics techniques. *Ecol Eng* 0–1. doi: 10.1016/j.ecoleng.2017.09.004
- Shrestha NK, Rudra RP, Daggupati P, et al (2021) A comparative evaluation of the continuous and event-based modelling approaches for identifying critical source areas for sediment and phosphorus losses. *J Environ Manage* 277:1–14. doi: 10.1016/j.jenvman.2020.111427
- Shrimali SS, Aggarwal SP, Samra JS (2001) Prioritizing erosion-prone areas in hills using remote sensing and GIS - a case study of the Sukhna Lake catchment , Northern India. *JAG* 3:54–60
- Shriver DM, Randhir TO (2006) Integrating stakeholder values with multiple attributes to quantify watershed performance. *Water Resour Res* 42:1–15. doi: 10.1029/2005WR004413
- Tibebe D, Bewket W (2010) Surface runoff and soil erosion estimation using the SWAT model in the Keleta Watershed, Ethiopia. *L Degrad Dev* 22:551–564
- Tripathi MP, Panda RK, Raghuwanshi NS (2003) Identification and prioritisation of critical sub-watersheds for soil conservation management using the SWAT model. *Biosyst Eng* 85:365–379. doi: 10.1016/S1537-5110(03)00066-7
- USEPA (2008) Handbook for Developing Watershed Plans to Restore and Protect Our Waters. *High Educ* 7:400

- Welde K (2016) Identification and prioritization of subwatersheds for land and water management in Tekeze dam watershed, Northern Ethiopia. *Int Soil Water Conserv Res* 4:30–38. doi: 10.1016/j.iswcr.2016.02.006
- Xu F, Dong G, Wang Q, et al (2016) Impacts of DEM uncertainties on critical source areas identification for non-point source pollution control based on SWAT model. *J Hydrol* 540:355–367. doi: 10.1016/j.jhydrol.2016.06.019
- Young RA, Onstad CA, Bosch DD, Anderson WP (1989) AGNPS: A nonpoint-source pollution model for evaluating agricultural watersheds. *J Soil Water Conserv* 44:168–173. doi: citeulike-article-id:13481122

Table 1: Watershed models used for subwatershed prioritization, country the study was conducted, total watershed size, scale of calibration and validation, number of sites for calibration and validation, parameters used for calibration, scale of subwatershed prioritization, parameters used for prioritization and citations. For the priority scale, values with ~ are average values based on the total watershed size and the number of delineated subwatersheds. If the scale or number of sites used for calibration and validation were not discussed in the study, it is listed as “Unknown.” SY= Sediment Yield, TP= Total Phosphorus, TN= Total Nitrogen, Q= Flow/Runoff, SL= Sediment Loads, SS=Suspended Solids, GW= Groundwater, ST=Soil Type, LC= Land Cover.

Model(s)	Country	Watershed Size (km ²)	Calibrated/Validated Scale (km ²)	Calibration/Validation Sites	Calibration Parameter(s)	Priority Scale (km ²)	Prioritization Parameter(s)	Citation
SWAT	India	10,878	21 - 95	4	Q/SY	HRU	SY	Kumar and Mishra, 2015
SWAT/QUAL2kw	China	2,027	Unknown	Unknown	Unknown	80 Subwatersheds (~25)	TP Loads	Chen et al. 2014
SWAT	Iran	1,560	1,560	1	Q/Sediment	144 Subwatersheds (~10)	Q/SY	Ghafari et al. 2017
HCT and Benefit/Cost Model	United States	320	None	None	None	20 Subwatersheds (~16)	ΔSL/\$Invested	Jang et al. 2013
HCT and Benefit/Cost Model	United States	Southeast Ecoregion	None	None	None	HUC-8	ΔSL/\$Invested	Jang et al. 2015
SWAT	India	95.76	95.76	1	Q/SY	15 Subwatersheds (~6)	SY	Kaur et al 2004
SWAT/HIT/WWAT	United States	1,156	Subbasin (size unknown)	7	Q	15 Subwatersheds (~77)	SY/GW/ST/LC	Legge et al. 2013
SWAT	India	1,776	Unknown	1	Q/SY	15 Subwatersheds (8-300)	SY	Uniyal et al. 2020
SWAT	Algeria	24,000	Unknown	Unknown	Q	27 Subwatersheds (0.3 - 229.5)	SY	Mosbahi et al. 2013
SWAT	China	10,200	10,200	1	Q/SY	24 Subbasins	Q/SY	Yu et al. 2021
SWAT	China	3,099	None	None	None	27 Subbasins	TN/TP	Xu et al. 2016
SWAT	United States	17,000	17,000	1	Q/SY/NL	252 HUC-12 Subwatersheds	Q/TSS/TN/TP	Evenson et al. 2021
SPARROW	United States	17,000	Unknown	1,100 Stations in US	Q/SY/NL	252 HUC-12 Subwatersheds	Q/TSS/TN/TP	Evenson et al. 2021
SWAT/AGNPS	Canada	14	Unknown	4	Q/SY/P	Subwatersheds	SY/P	Shrestha et al. 2021
SWAT	Iran	900	900	1	Q/SY	37 Subwatersheds (0.09 - 72)	SY	Noor et al 2016
SWAT/GWLF	United States	570	Unknown	1	Q/SY/NL	Subwatersheds	Q/TSS/TN/TP	Niraula et al. 2013
SWAT	United States	1,960	HUC-12 and HUC-8	7 (7 Q, 3 WQ)	Q/S/TP/NO ₃	28 Subwatersheds (HUC-12)	S/TP/NO ₃	Pai et al. 2011
SWAT	India	6,293	~30 - 5,300	4	Q/SY	202 Subwatersheds (~30)	SY	Sardar et al. 2014
SWAT	India, China, Nepal	1,775	Unknown	Unknown	Unknown	17 Subwatersheds (~69)	SY	Shivhare et al. 2017
SWAT	United States	1,870	1,784	1	Q	209 Subwatersheds (~9)	Q/SY/NL/Other	Shriver et al. 2006
SWAT	Iran	5,560	Unknown	2	Q/SY/NL	32 Subwatersheds	SY/TN/TP	Babaei et al. 2019
SWAT	Ethiopia	15,000	Unknown	Unknown	Q	Unknown	Q	Workuet al. 2020
GeoWEPP	Turkey	170	Unknown	Unknown	Unknown	85 Subwatersheds	SY	Dutal and Reis 2020
InVEST SDR	Tunisia	720	Unknown	24 Reservoirs	Sedimentation	17 Subwatersheds	SY	Bouguerra and Jebari 2017
SWAT	India	92.46	92.46	1	Q/SY/NL	12 Subwatersheds (0.54 - 17.23)	SY/NL	Tripathi et al. 2003
SWAT	Iran	830	830	1	Q/SY	26 Subbasins	SY/N/P	Raeisi et al. 2020
SWAT	Ethiopia	29,404	29,404	1	Q/SY	47 Subwatersheds (~625)	SY	Welde 2016
SWAT	Ethiopia	287	287	1	Q/SY	22 Subwatersheds (~13)	SY	Ayele et al. 2017

Table 1 (Cont.)

WLP	United States	906	Unknown 28 (Not validated)	Unknown	Unknown	Unknown	Pollutant Travel Time/Other	Randhir et al. 2001
WEPP	India	28		1	Q/SY	7 Subwatersheds (~4)	SY	Pandey et al. 2009
SWAT	Ethiopia	1,060	1,060	1	Q	20 Subwatersheds (~53)	SY	Tibebe and Bewket 2010
SWAT	Iran	2,133	Unknown	1	Q	55 Subwatersheds (~39)	Q	Besalatpour et al. 2012
SPARROW	United States	Mississippi/Atchafalaya River Basin	> 820	425	TN/TP Q/Climate Data	HUC-8 11 Subwatersheds (~11)	TN/TP	Robertson et al. 2009
HSPF	Korea	287	~72	4			Q/TN/SS/TP/Other	Chung and Lee 2009
SWAT	United States	43491	43491.00	4	Q/P/N	HRU	SY/P	White et al. 2009
WERM	India	995	Unknown	Unknown	Unknown	Unknown	Geomorphic Characteristics	Panhalkar and Pawar 2011
WEPP	Iran	69	69	1	Q/SY	16 Subwatersheds	Q/SY	Saghafian et al. 2015
SWAT	United States	2,400	Unknown	3	Q/ST/P	HRU	SY/P	Busteed et al. 2009
SWAT	India	43,900	Unknown	4	Q/SY	57 Subwatersheds	SY	Pandey and Palmate 2019
SWAT	China	4426	2027	1	Q/SY/P	≤ 500	Pollutant Loads	Wang et al. 2016
HYSTAR	United States	3.29	3.29	1	Weather/Q	Grids	Q	Her and Heatwole, 2018
TREX	Japan	137	Unknown	2	Q/SY	21 Subwatersheds (< 13)	Q/SY	Wei et al. 2017
SWAT	India	2,656	Unknown	1	Q	35 Subwatersheds (< 190)	Q/SY/LULC/Morphometric	Parupalli et al. 2019
SWAT	United States	180 and 44.8	180 and 44.8	1 each	Q/SY/TP/TN	HRU	Q/SY/TP/TN	Niraula et al. 2012
SWAT	Kenya	9,500	Subwatershed	14	Q/SY	HRU/Subwatershed	SY	Hunink et al. 2013
SWAT	United States	142	Unknown	1	Q/SY/N/P	HRU	SY/N/P	Giri et al. 2016
SWAT	United States	22,260	6,060	1	Q/SY/TN/TP	Subbasins	SY/TN/TP	Giri et al. 2012
SWAT	India	84,818	Subwatershed	3	Q/SY	23 Subwatersheds	SY	Dutta and Sen, 2018
SWAT	United States	6,300	Unknown	Unknown	Unknown	68 Subwatersheds	N/P/Socioeconomic Data	Keeler et al. 2019
SWAT	India	9,658	~9,658	1	Q/SY	38 Subwatersheds	SY	Bhattacharya et al. 2020
SWAT	Iran	89	89	1	Q/TN/TP	HRU	Q/TN/TP	Imani et al. 2019
SWAT	United States	3,105	Subbasin (size unknown)	4	Q/P/SY	HRU	P	Winchell et al. 2015
SWAT	Ethiopia	320	Unknown	1	Q	24 Subwatersheds	SY	Naqvi et al. 2019
SWAT	Iran	5,343	5,343	1	Q/TSS	17 Subbasins (1 - 792)	Q/SY	Saghafian et al. 2012

Chapter 5: Cost Efficient Method to Remotely Monitor Streamflow and Estimate Constituent Loads in Small-Scale Watersheds

A.L. Lasater¹, M. O'Hare¹, B.J. Austin², E. Scott³, and B.E. Haggard^{1,2}

¹Biological and Agricultural Engineering Department, University of Arkansas, Fayetteville,
Arkansas 72701

²Arkansas Water Resources Center, University of Arkansas System Division of Agriculture,
Fayetteville, Arkansas 72704

³Ozark Water Watch, Rogers, Arkansas 72756

Abstract

Discharge monitoring stations are often costly and difficult to install, operate and maintain, especially in small streams. The purpose of this study was to introduce a cost-efficient method for remotely monitoring streamflow in small-scale watersheds to provide continuous discharge measurements across multiple sites and flow conditions. Within the Upper Poteau River Watershed (UPRW) in Arkansas, 12 sites were selected at bridge crossings near the outflow of HUC-12 or HUC-14 subwatersheds. A HOBO water level logger was deployed at each site to obtain continuous stage records, and HOBO barometric pressure transducers were installed within 16 km of each sample site to account for fluctuations in atmospheric pressure. SonTek-IQ acoustic Doppler instruments were deployed to measure discharge during high flow events, and roving discharge monitoring stations were installed at each site to allow for easy rotation of the SonTek-IQs among sites between flood events. Once roving discharge monitoring stations are installed at each site, one or more SonTek-IQ can be rotated among sites to capture high-flow discharge measurements; therefore, a SonTek-IQ is not required for every site of interest. The high-flow data captured during SonTek-IQ deployment, and baseflow discharge measurements collected on a monthly basis, were used to develop rating curves with a combination of simple linear regression, locally weighted regression (LOESS), and Manning's

equation. The rating curves well represented measured flows, with Nash-Sutcliffe efficiencies (NSE) ranging between 0.87 and 0.98. Additionally, water quality samples were collected across the range of flow, and constituent loads were estimated using Generalized Additive Models (GAMs), where the best fit GAM was determined to be spline based smooth functions of streamflow (Q) and day of year (DOY). Both instantaneous Q (Q_i) and mean daily Q (Q_d) well predicted constituent loads (NSEs > 0.87), and did not predict significantly different loads across sites (except site 14). Therefore, both Q_i and Q_d were considered adequate for load estimation methods. This method provides an opportunity to collect continuous records of flow across multiple, remote, small-scale watersheds, and in conjunction with constituent concentrations and load estimations, can be used to calibrate and validate watershed models.

Introduction

Earth's freshwater resources are essential for human well-being, ecosystem services and economic activity. While only representing a small fraction of the global water supply, freshwater provides sources for drinking water and irrigation, opportunities for sports and recreation, and habitat for over 100,000 plant and animal species (Aylward et al. 2005; Dudgeon et al. 2006). Due to increasing population and land use changes, human activity has been a major influence on freshwater ecosystems (Sala et al. 2000; Dudgeon et al. 2006). When combined with climate change impacts such as increasing temperatures and variations in hydrologic cycles, large amounts of stress are applied to freshwater quantity and quality (Jimenez Cisneros et al. 2014). Therefore, efforts to monitor freshwater ecosystems are increasingly important for sustainable water management.

Regular, long-term streamflow data can be used to understand changes in hydrology and trends in natural disturbances (e.g. flooding and drought) in freshwater ecosystems (Dai and

Trenberth 2002; Erwin and Hamilton 2005; Haritashya et al. 2006; Peterson et al. 2013; Chen et al. 2014b). This information can help to develop effective policy, allocate water supplies and assess the effectiveness of management practices. For example, the Ecological Limits of Hydrologic Alteration (ELOHA) framework was developed by synthesizing decades of global streamflow data (Poff et al. 2010), and ELOHA is used to determine empirical relationships between flow alterations and ecological responses across streams. This extensive streamflow database and framework has now been applied in numerous case studies to implement policy, manage flows, and achieve river condition goals (Martin et al. 2015; Solans and García de Jalón 2016; Zhang et al. 2016; Stein et al. 2017).

When nutrient and sediment concentrations are monitored in conjunction with streamflow, water quality trends can be evaluated adjusting for discharge (Hirsch et al. 1982; Helsel and Hirsch 1991), and constituent loads can be estimated (Cohn et al. 1989; Migliaccio et al. 2010a). Constituent loads and streamflow measurements are important for calibrating and validating watershed and reservoir models (Silberstein 2006), which can be used to predict various water resource scenarios under the impact of environmental and management changes, as well as develop total maximum daily loads (TMDLs). Watershed models help to establish watershed management plans and pollution prevention strategies (Erwin and Hamilton 2005), as well as identify priority areas of concern within a watershed (e.g. see Tripathi et al. 2003; Pai et al. 2011; Welde 2016).

Discharge monitoring stations are often costly and difficult to install, operate and maintain, especially in small streams. Discharge estimations are typically conducted using the velocity-area method (i.e. velocity across the stream multiplied by the cross sectional area), where velocity is measured through various techniques including current meters, dilution

gauging or acoustic Doppler current profilers (Dobriyal et al. 2017). However, velocity measurements are typically instantaneous and must be collected manually in the stream, which can be dangerous under some flow conditions or difficult in numerous, remote streams. Additionally, it can be difficult to ensure velocity measurements are representative of the entire flow profile of a given stream. Discharge is sometimes estimated using hydrologic control structures (e.g. a weir or flume), where flow is calculated based on changes in flow depth (Turnipseed and Sauer 2010). However, hydrologic control structures are impractical for monitoring numerous, small-scale streams across a watershed.

Due to costs and feasibility associated with discharge estimations, monitoring data is often limited on small-scale streams and watersheds within the area of interest. Therefore, watershed models are often used to predict constituent concentrations and flow conditions at small-scale streams, but data to validate these outputs are typically unavailable (Pai et al. 2011b; Welde 2016; Chapter 4). The purpose of this study is to introduce a cost-efficient method for remotely monitoring streamflow and estimating constituent loads in small-scale watersheds by:

- collecting continuous stage measurements using pressure transducers,
- collecting continuous discharge measurements using roving discharge stations,
- combining stage and discharge data to develop rating curves, and
- using rating curves and constituent concentrations to estimate constituent loads.

This monitoring method provides continuous discharge measurements across multiple streams and flow conditions. The flow data, in conjunction with constituent concentrations and loads, can be used to calibrate and validate watershed models and evaluate water quantity and quality across small-scale watersheds where data is typically limited. This method was implemented

across the Upper Poteau River Watershed (UPRW) in Arkansas, where non-point source pollution is an increasing concern, and identification of priority subwatersheds (i.e. small-scale pollution sources) is imperative (ANRC 2018).

Methods

Study Site Description

The UPRW (HUC 11110105) occupies an area of 1,400 km² in Arkansas (Figure 1). In 2001, land use in the area was 60.0% forested, 6.3% urban, 25.9% agriculture, 3.7% grassland, and 0.8% open water (USGS 2001). In 2016, forested area increased to 65.3%, agriculture area decreased to 21.9%, and urban area was 6.4%, grassland was 4.0%, and open water was 0.9% (USGS 2016). The headwaters of the Poteau River begin near Waldron, Arkansas, and flow west into Oklahoma, near Loving, Oklahoma. The two main tributaries to the Poteau River within the UPRW in Arkansas are the Black Fork and the James Fork.

The UPRW has been listed as a priority watershed within the Arkansas Nonpoint Source Pollution Plan since 1998, and has been a focus of trans-boundary water quality issues for the last several decades (ANRC 2018). In 2017, this 1,400 km² watershed contained over 350 poultry farms and produced nearly 100 million birds (USDA 2017). Portions of the Poteau River are listed on the Arkansas 303 (d) list for dissolved oxygen, turbidity, chlorides, sulfates and total dissolved solids (ADEQ 2018). A TMDL was developed in 2006 for the Poteau River, which concluded a 35% reduction in total phosphorus (TP) from non-point sources was necessary for water quality protection (USEPA 2006).

For this study, 12 sites were selected at bridge crossings near the outflow of HUC-12 or HUC-14 subwatersheds within the UPRW for implementing the streamflow monitoring

technique (Figure 1, Table 1). Sites were selected to represent a range of land use and baseflow water quality conditions. Catchment land use ranged from 23 to 92.3% forested, 1.1 to 7.7% urban, and 0 to 61.4% agriculture (mostly pasture). Barren land represented less than 1% of catchment area for all watersheds, and the remainder of the watershed areas were open water, shrubs, and grasslands (USGS 2016). Catchment area ranged from 7 to 193 km² across all sites (Table 1). Additionally, the three U.S. Geological Survey (USGS) discharge monitoring stations in the UPRW were monitored for water quality parameters (Figure 1, Table 1).

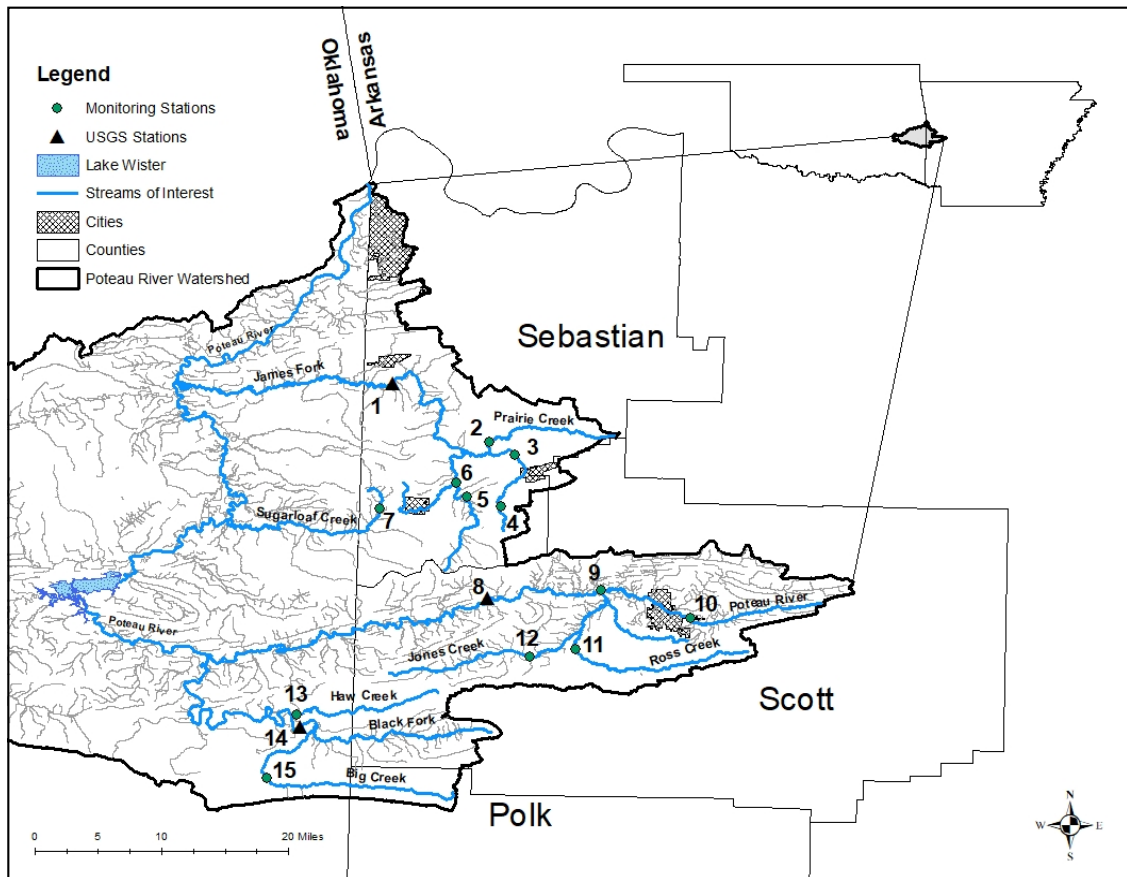


Figure 1: Monitoring sites in the Upper Poteau River Watershed in Arkansas. Site numbers correspond to site ID's in Table 1.

Table 1: Monitoring site ID's (corresponding to Figure 1), names, locations, watershed areas, and land use in the area.

Site ID	Site Name	Lat N	Long W	Watershed Area (km ²)	%F ¹	%U ²	%AG ³
James Fork Watershed- HUC 1111010508							
1	USGS 07249400- James Fork	35 09.755	94 24.424	381	50.3	4.8	40.8
2	Prairie Creek	35 05.709	94 17.776	70	23.0	5.1	61.4
3	Lower Cherokee Creek	35 04.839	94 16.013	80	45.1	6.0	46.4
4	Cherokee Creek Headwaters*	35 01.379	94 16.985	14	84.5	1.1	9.4
5	James Fork Headwaters*	35 01.984	94 19.315	39	84.7	1.2	8.9
6	Lower James Fork*	35 02.820	94 20.302	95	69.9	3.5	18.3
Lower Poteau River Watershed- HUC 1111010506							
7	Upper Sugar Loaf Creek	35 01.177	94 25.285	7	88.6	1.6	1.3
Headwaters Poteau River Watershed- HUC 1111010501							
8	USGS 07247000- Poteau River	34 55.129	94 17.918	527	63.7	5.6	21.3
9	Lower Poteau River*	34 55.666	94 10.124	193	51.6	7.7	32.0
10	Poteau River Headwaters*	34 53.769	94 03.975	39	52.7	5.5	33.1
11	Ross Creek*	34 51.647	94 11.910	77	71.8	4.6	13.9
12	Upper Jones Creek*	34 51.895	94 12.835	73	84.8	2.7	2.2
Black Fork Watershed- HUC 1111010502							
13	Haw Creek	34 47.257	94 30.924	62	90.3	1.8	1.1
14	USGS 07247250- Black Fork	34 46.428	94 30.748	245	88.3	3.5	9.8
15	Big Creek*	34 42.970	94 33.006	60	92.3	6.2	0.0

¹ % Forest (%F) includes deciduous, evergreen, and mixed forest; ² % Urban (%U) includes open space, low, medium and high intensity development; ³ % Agriculture (%Ag) includes pasture, hay, and cultivated crops. *Indicates where a SonTek-IQ was deployed.

Data Collection

A HOBO water level logger (i.e., pressure transducer; Onset Computer Corporation, Bourne, Massachusetts) was deployed at each site (except USGS stations, Sites 1,8, and 14) in December 2017 to obtain continuous stage records, and HOBO barometric pressure transducers were installed within 16 km of each sample site to account for fluctuations in atmospheric pressure. The HOBOs were installed and maintained according to standard operating procedures (OCC 2018), where the HOBO water level loggers were typically suspended within a polyvinyl

chloride (PVC) pipe attached to a bridge post, and atmospheric HOBOS were bound to trees outside of the stream channel (Figure 2A and 2B, respectively). Sensors were set to record measurements on 15-minute intervals, and data were downloaded from the HOBOs on a monthly basis.



Figure 2: A) Pressure transducer installation on a bridge post, B) atmospheric pressure transducer attached to a tree outside of floodplain, C) SonTek-IQ attached to concrete block in stream channel, D) SonTek-IQ in stream channel, and E) ammo can attached to tree outside of the flood plain to store battery. Photos by B.J. Austin and A.L. Lasater, used with permission.

SonTek-IQ acoustic Doppler instruments (SonTek/Xylem Inc., San Diego, California), were deployed to measure discharge during high flow events. SonTek-IQs measure the velocity of water using the Doppler shift and internally calculate discharge once calibrated to the stream channel geometry. Roving discharge monitoring stations were installed at each site to allow for easy rotation of the SonTek-IQs among sites between flood events. Roving discharge monitoring stations include a concrete base staked into the streambed, a container to store the battery and wiring (e.g. an ammo can), and PVC pipe from the concrete base up the stream bank

and to the battery container (Figure 2 C-E). The battery container is attached to a tree outside of the floodplain (Figure 2E).

Once roving discharge monitoring stations are installed at each site, one or more SonTek-IQ can be rotated among sites to capture high-flow discharge measurements; therefore, a SonTek-IQ is not required for every site of interest. Rating curves can be developed for all sites using the high-flow data captured during SonTek-IQ deployment, and baseflow discharge measurements collected on a monthly basis using velocity-area methods, since the SonTek-IQ flow measurements are not reliable when water depths are less than 0.45 m (SonTek-IQ 2017).

Water samples were collected across the range of discharge measurements (i.e., baseflow and stormflow) to estimate constituent loads. Water samples were analyzed at the Arkansas Water Resources Center Water Quality Lab (AWRC WQL) for nitrate-nitrogen ($\text{NO}_3\text{-N}$), chloride (Cl), fluoride (Fl), soluble reactive P (SRP), TP, total nitrogen (TN), total suspended solids (TSS), and sulfate (SO_4^{2-}). The equipment, methods and method detection limits for the certified AWRC lab are available online (AWRC 2021).

Rating Curve Development

Select data from the SonTek-IQs (peak flows, 75% of peak flows, and 50% of peak flows, on the rising and falling limbs) were combined with baseflow discharge measurements (e.g. using velocity-area methods) and the associated instantaneous stage to develop rating curves. Rating curves were developed using simple linear regression, locally weighted regression (LOESS), and Manning's equation. Nonparametric LOESS regression was used to fit the range of measured flow and stage data with a sampling proportion of 0.5. Below the range of

measured flow data, 2-point regression was applied to estimate low flows, and Manning's equation was used for flow estimations above of the range of measured data (Equation 1):

$$Q = \left(\frac{K}{n}\right) AR^{\frac{2}{3}}\sqrt{S}$$

where Q is the flow (ft³/s), K is a constant equal to 1.49 ft^{1/3}/s, n is the surface roughness (s/ft^{1/3}), A is the cross-sectional area of flow (ft²), R is the hydraulic radius (ft), and S is the slope of the channel (ft/ft).

To estimate A and R from Manning's equation, an unsteady flow analysis was conducted in the Hydrologic Engineering Center's River Analysis System (HEC-RAS) (USACE 2016). With inputs including the stream channel survey, LOESS rating curve data, and a stage hydrograph, the unsteady flow analysis computes the A and the wetted perimeter (WP) for a range of user defined depths. The R at each depth is then computed as A divided by the WP.

The best fit model for each rating curve was evaluated using the root mean square error (RMSE), where the lower the RMSE, the better the rating curve. To determine how well the observed data versus the simulated fits the 1:1 line, and to determine relative magnitude of the residual variance, the Nash-Sutcliffe efficiency (NSE) was calculated for each model. An NSE of 1 indicates a perfect match of modelled data to observed data. The rating curve was then used to develop a record of continuous, instantaneous flow on a 15-minute time interval.

Constituent Load Estimations

Generalized additive models (GAM), in the mgcv package in R (R Core Team 2016; Wood 2017), were applied for constituent load estimations using log transformed constituent concentrations, log transformed flow and day of year (DOY) to capture seasonality. Three

primary methods were used to estimate constituent loads to compare the use of instantaneous flow (Q_i) or mean daily flow (Q_d) in load estimation. For the first method (M1), constituent concentrations were multiplied by the corresponding instantaneous flow (Q_i) to get instantaneous load (L_i). For each constituent, several GAMs were generated to explore relationships and interactions between predictor variables Q_i and DOY (Table 2), and the best fit GAM was identified by the minimum Akaike information criterion (AIC) and significance of each predictor variable ($p < 0.05$). Daily loads were estimated by integrating the L_i across each day, and then summed to estimate monthly and yearly loads.

Table 2: Generalized Additive Models for Load Estimations, where $s()$ is a spline based smooth function of the predictor variable, and $ti()$ produces a tensor product interaction. Q is log transformed daily or instantaneous flow, and DOY is the day of year.

ID	Generalized Additive Model
1	$s(Q) + s(\text{DOY})$
2	$ti(Q, \text{DOY})$
3	$ti(Q) + ti(\text{DOY}) + ti(Q, \text{DOY})$
4	$ti(Q) + ti(Q, \text{DOY})$
5	$s(Q)$

For the second method (M2), mean daily flows (Q_d) were estimated by averaging Q_i for each day. The load for each day (L_d) was then estimated by using Q_d to predict L_d from best fit GAM relationship of Q_i and L_i from M1. Daily loads were then summed to estimate monthly and yearly loads. For the last method (M3), loads were estimated by multiplying measured constituent concentrations by the corresponding Q_d , developing a new GAM relationship between loads and Q_d , and using Q_d of each day to predict L_d . Again, L_d was summed to estimate monthly and yearly loads. Across all three methods, 95% confidence intervals were estimated for daily, monthly and yearly load estimations.

Results

Selection of SonTek-IQ Data

Since all instantaneous flow measurements obtained by the SonTek-IQ were not necessary for rating curve development, on first attempt, peak flows and corresponding stages were selected from every high flow event measured. Peak flows were paired with baseflow measurements and LOESS regressed against stage to develop a rating curve for each site. However, the data was sparse and left large gaps in the relation (Figure 3A). On second attempt, peak flows and 75% of peak flows (on the rising and falling limbs of the hydrograph) were paired with baseflow measurements and LOESS regressed (Figure 3B). However, again there was a gap in the data across the mid-range stage measurements. Therefore, peak flows, 75% of peak flows, and 50% of peak flows (on the rising and falling limbs of the hydrograph) were then paired with baseflow measurements and LOESS regressed (Figure 3C). In this scenario, the range of flows better represented the range of stages, leaving less gaps in the data.

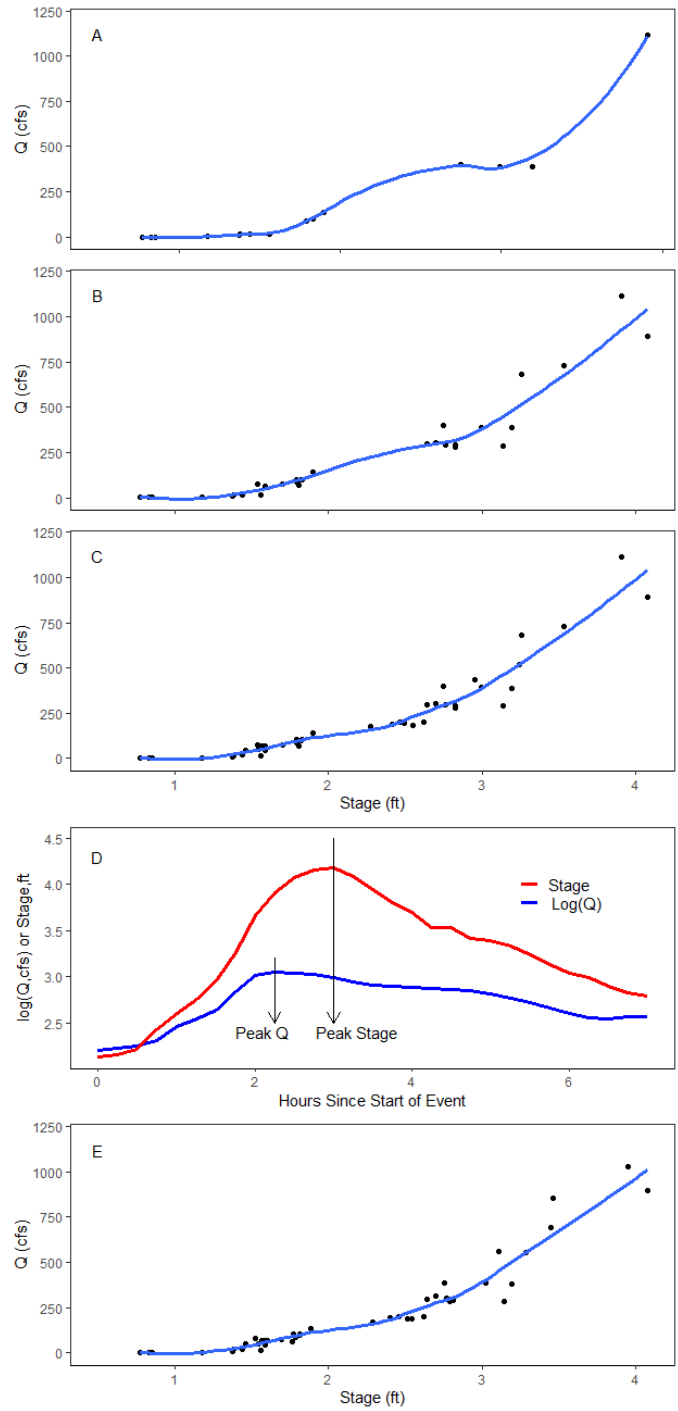


Figure 3: Combination of baseflow measurements and data selected from SonTek-IQ continuous measurements for rating curve development where A) includes baseflow measurements and peak peak flows, B) includes baseflow measurements, peak flows and 75% of peak flows, and C) includes baseflow measurements, peak flows, 75% of peak flows, and 50% of peak flows. D) Hysteresis showing peak flow occurring approximately one hour before peak stage, and E) final selection of data from SonTek-IQ for rating curve development. Data consists of averages around the peak, 75% of peak, and 50% of peak stages and flows and baseflow measurements.

However, upon analysis of individual high-flow events, hysteresis was observed across the majority of sites and events. In the terms of this study, hysteresis typically occurred as a delay in the peak stage following the peak flow (Figure 3D). Peak stages were typically delayed by an hour, so to account for this delay, the final approach for data selection consisted of averaging the five values (on 15-minute intervals) around the selected stages and flows. Therefore, the final rating curves consisted of the averages around the peak flows, 75% of the peak flows, and 50% of the peak flows from the SonTek-IQ, averages around the corresponding stages, and baseflow measurements (Figure 3E). The averaging also helped to minimize noise in the data.

Rating Curve Development

For all sites, the range of measured stage data slightly exceeded the range of measured flow data. Therefore, flow must to be projected when the stage is less than or greater than the range of stage data captured by flow measurements. For sites where SonTek-IQ's were deployed, 89 to 99% of stage data were within the range of measured flow (Figure 4), estimated as the sum of flows below and above the range of measured data divided by the total sum of flows over the 3 year period. Less than 1% of stage data exceeded the maximum stage associated with a measured flow, and less than 11% of stage data fell below the minimum stage associated with a measured flow. This is equivalent to less than 6 days of stage data exceeding maximum measured flow and less than 115 days of stage data below minimum measured flow throughout the 3 years of monitoring (Table 3). Site 15 had the lowest portion of stage data represented by flow (89%), while all other sites with SonTek-IQ deployment had greater than 95% of stage data represented by flow. Sites 3 and 13 did not have baseflow measurements nor

SonTek-IQ deployment, and Sites 2 and 7 only had discharge measured during baseflow conditions.

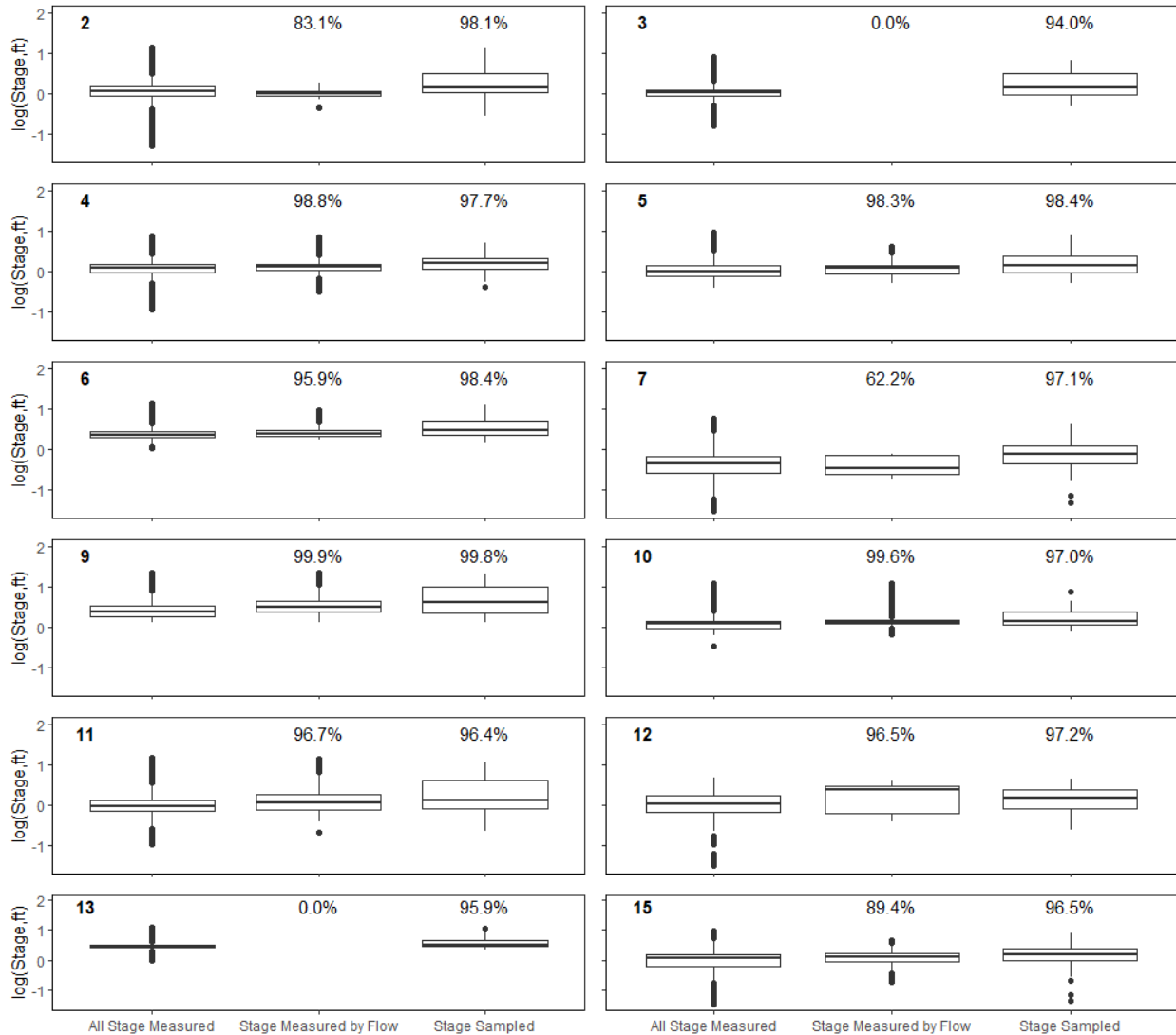


Figure 4: All stage measured, stage measured by flow, and stage sampled for water quality analyses across all non-USGS sites. The bold value in the top left corner of each plot corresponds to site numbers in Table 1. The values above stage measured by flow and stage sampled indicate the percentage of stage data measured by flow and water quality analyses, respectively.

Table 3: Percentage of stage measurements outside the range of flow and water quality samples, and equivalent number of days with values greater than or less than flow and water quality samples over the three year period (1,095 total days).

Site ID	Stage Measurements Outside the Range of Flow				Stage Measurements Outside the Range of Measured Water Quality			
	% Greater	Days Greater	% Less	Days Less	% Greater	Days Greater	% Less	Days Less
2	12.5	134	4.5	49.3	0.0	0.1	1.9	20.5
3	100.0	453	0.0	0.0	0.1	0.3	5.9	26.2
4	0.0	0.0	1.2	12.9	0.1	0.7	2.2	24.5
5	0.5	5.5	1.2	12.9	0.0	0.3	1.6	17.0
6	0.3	2.9	3.9	42.3	0.0	0.3	1.6	17.2
7	17.8	194	20.0	213	0.0	0.4	2.9	30.3
9	0.0	0.0	0.1	0.6	0.2	2.1	0.1	0.6
10	0.0	0.0	0.4	4.6	0.1	0.6	3.0	32.5
11	0.0	0.0	3.3	35.9	0.0	0.5	3.6	39.1
12	0.2	2.4	3.3	35.8	0.0	0.1	2.8	29.9
13	100	1106	0.0	0.0	0.0	0.4	4.0	43.7
15	0.2	2.1	10.4	115	0.0	0.2	3.6	39.1

To project flows below the range of measured data, 2-point regression was used between the minimum measured flow value and the origin. The slopes of 2-point regression ranged from 0.041 to 3.101 ft² s⁻¹ across all sites (Table 4). The 2-point regression was used for less than 11% of the total flow at sites with SonTek-IQ deployment. The maximum percentage of total flow that had to be predicted on the lower end occurred at site 15 (10.4%), but all other sites were less than 5% of the total flow. Therefore, the projections below the range of measured data likely had little influence on estimated total monthly and/or annual flows.

Using A and R values from HEC-RAS, an average *n* was back-calculated using measured flow values and Manning's equation. The average *n*, as well as estimated WP and R values from HEC-RAS, were used to project flow above the range of measured data. Manning's *n* values ranged from 0.002 and 0.071 (Table 4). Across all sites, it was necessary to use Manning's equation to predict high flows for less than 1% of flows.

Table 4: Slopes of 2-point regression for projecting below the range of measured data, percentage of total flow projected below measured data, average Manning’s n estimated using HEC-RAS and used to project flow above the range of measured data, percentage of total flow projected above measured data, and LOESS RMSE’s for the range of measured data. NA’s are listed for sites where SonTek-IQ’s were not deployed.

Site ID	2-Point Regression Slopes	Average Manning’s n	LOESS RMSE
2	NA	NA	NA
3	NA	NA	NA
4	0.041	0.05	183
5	0.953	0.022	52.2
6	0.211	0.031	3.63
7	NA	NA	NA
9	0.306	0.071	210
10	0.080	0.002	153
11	2.371	0.023	379
12	0.109	0.036	25.8
13	NA	NA	NA
15	3.101	0.025	189

For the range of measured stage and flow data, LOESS regression was applied with a sampling proportion of 0.5. The RMSE’s from LOESS regression ranged from 3.6 to 379 across all sites (Table 3). While normal distributions are not required for LOESS regression, the large amount of spread in the data at site 5 justified a square root data transformation (Figure 5). A square root transformation was chosen due to its ability to handle zero values. Final rating curves for each site were developed by combining the 2-point regression, LOESS regression, and Manning’s equation data (Figure 5).

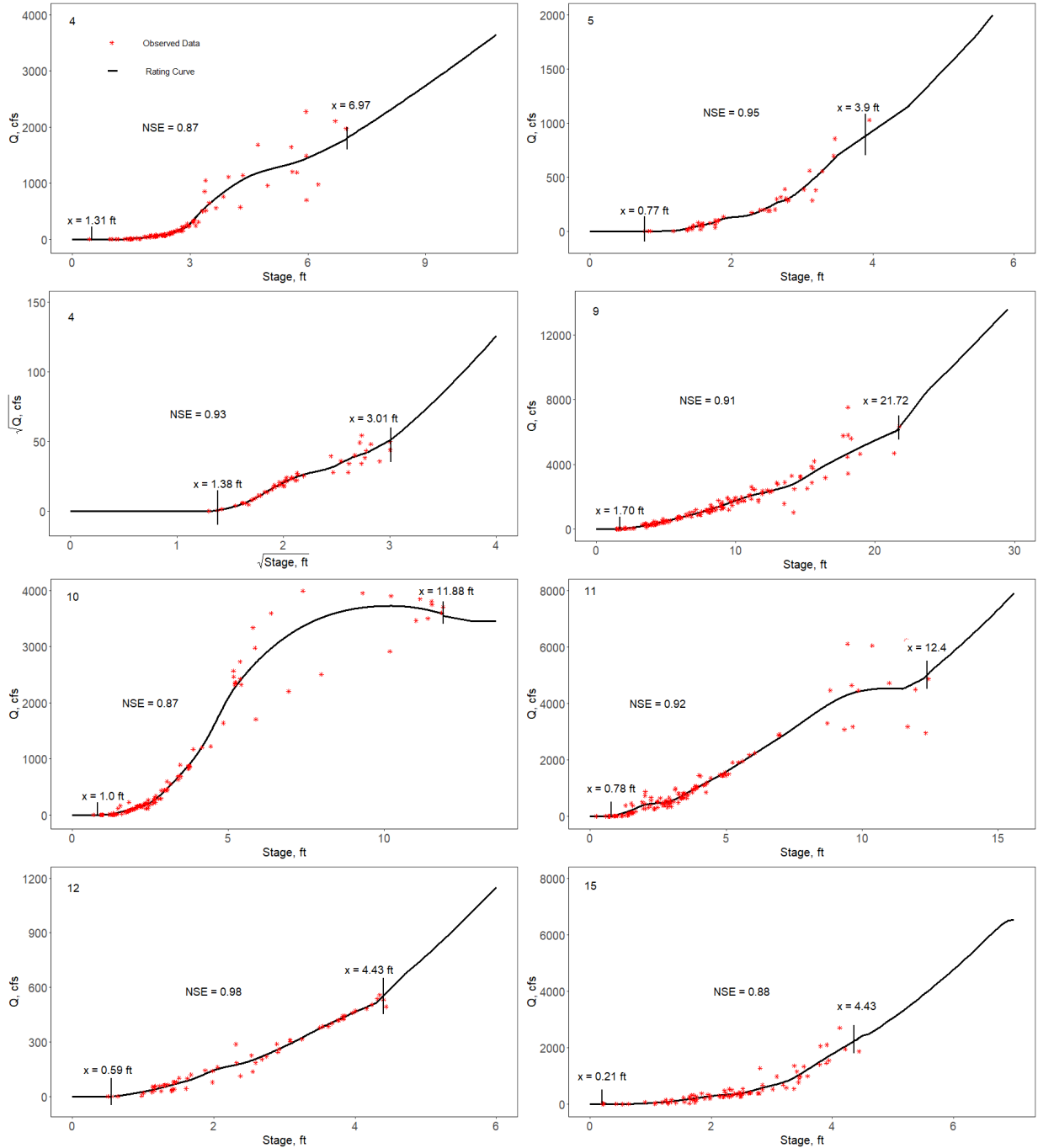


Figure 5: Final rating curves for all non-USGS sites with measured flow data. The bold value in the top left corner of each plot corresponds to site numbers in Table 1. Models were developed using LOESS regression across the range of measured flow data, 2-point regression to project flow less than the minimum measured value, and Manning's equation to project flow greater than the maximum measured value.

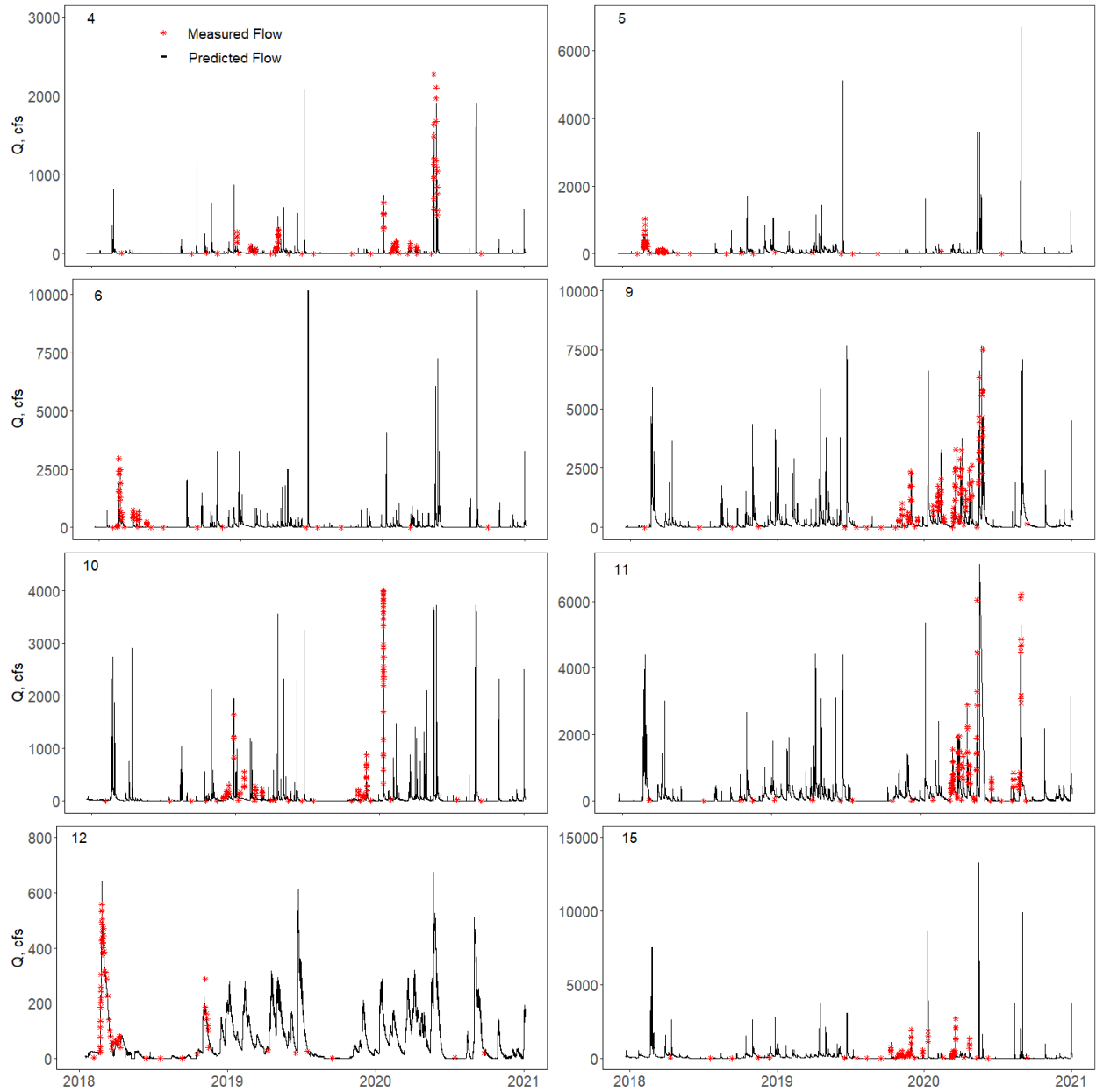


Figure 6: Manual and SonTek-IQ measured flows with predicted flows from rating curves. The bold value in the top left corner of each plot corresponds to site numbers in Table 1.

The performance of the rating curve models were evaluated by visualizing the predicted flows over time in conjunction with the measured flows (Figure 6). Additionally, Nash-Sutcliffe efficiencies for all sites ranged between 0.87 and 0.98 (Figure 5). Overall, model predicted flows well represented measured flows.

Constituent Load Estimations

Constituent loads were estimated at all sites where continuous records of flow were available (i.e., USGS stations and sites where a SonTek-IQ was deployed). For all sites, the range of measured stage data slightly exceeded the range of stages represented by water quality data. Therefore, constituent concentrations and loads must be projected when the stage is less than or greater than the range of stage data captured by water quality data. For sites where SonTek-IQ's were deployed, 95 to 99% of stage data were within the range of measured water quality data (Figure 4). At the USGS sites, 98 to 99% of stage data were within the range of water quality data. At all sites, less than 1% of stage data exceeded the maximum stage associated with water quality data, and less than 6% of stage data fell below the minimum stage associated with a water quality data. This is equivalent to less than 3 days of stage data exceeding maximum measured water quality data and less than 44 days of stage data below minimum measured water quality data throughout the 3 years of monitoring (Table 3).

The best fit GAM for each site was identified based on the lowest magnitude AIC, while also ensuring each predictor variable was significant ($p < 0.05$). Across all sites and parameters, GAM 1 most commonly outperformed other GAMs for each method (M1, M2, and M3), followed by GAM 3 (approximately 43% and 29% of the time GAM 1 and GAM 3 were best, respectively; Figure 7). GAM 2 was never the best fit model, and GAM 4 and 5 were the best fit model approximately 8 and 19% of the time, respectively. With best fit GAMs for each site and parameter, NSE and R^2 values were always greater than 0.85 and p values were always less than 0.01 (Appendix A).

When GAM 1 was not the best fit model for a certain site/parameter, GAM 1 was still always significant ($p < 0.01$), and NSE and R^2 values were still greater than 0.85 (Appendix A).

Additionally, R^2 and NSE values either didn't change or were less than 10% different compared to the best fit GAM, and AIC changed by a maximum of 50. Therefore, while the best fit GAM may not have always been GAM 1, GAM 1 was still significant and well predicted constituent loads; so, for consistency and simplicity, GAM 1 was applied across all sites, parameters, and methods (i.e., M1, M2 and M3).

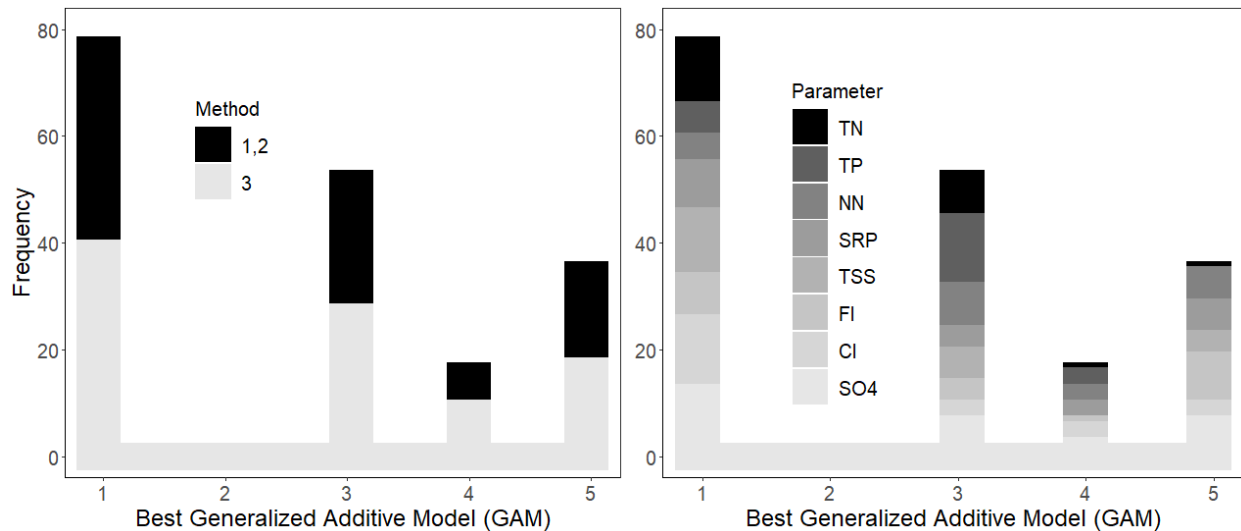


Figure 7: Frequencies of best fit generalized additive models (GAM) 1-5, corresponding to GAMs listed in Table 2, for each load estimation methods (1-3) and for each parameter: total nitrogen (TN), total phosphorus (TP), nitrate plus nitrite (NN), soluble reactive phosphorus (SRP), total suspended solids (TSS), fluoride (FI), chloride (Cl), and sulfate (SO₄).

Methods 1 and 2 for constituent load estimations applied the same data for GAM development (using Q_i), while M3 used Q_d . In general, GAMs using Q_i in M1 and M2 performed slightly better than GAMs using Q_d in M3, based on R^2 and NSE values (Appendix A). However, as stated previously, models were always significant and R^2 and NSE values were always above 0.85. When converting data back to non-log transformed, and comparing observed versus predicted data for each method, M1 still generally performed the best (average NSE = 0.80, range = 0.04 – 0.99). With M2, observed loads were estimated using constituent

concentrations and Q_d , and loads were predicted using GAM from M1 (with Q_i), but M2 almost always performed the most poorly (average NSE = 0.55, range = -0.59 – 0.97). Method 3 generally had higher NSE values compared to M2, but slightly smaller NSE values compared to M1 (average NSE = 0.76, range = -0.10 – 0.99). Plots of log transformed observed versus predicted daily loads from each method are shown in Appendix B.

An ANOVA and Tukey's HSD test were conducted to determine if the three methods of constituent load estimations produced significantly different means of daily loads. Across most sites and parameters, there were no significant difference among daily loads predicted by M1, M2, and M3 ($p > 0.05$). However, at site 14, M3 and M2 produced significantly greater daily loads compared to daily loads produced by M1 for TN, NN, SRP FI, Cl, and SO_4^{2-} . In general, M1 still produced greater NSE values for these parameters compared to M2 and M3. Daily loads for each method were then summed to estimate monthly and annual loads with 95% confidence intervals (Appendix C and D, monthly and annual loads, respectively). The difference in loads predicted by M1, M2 and M3 is evident for Site 14, but most other sites show minimal differences in loads and confidence intervals.

Discussion

Rating Curve Development

Continuous discharge measurements are imperative towards water resources management, and currently these data are limited or nonexistent on small-scale streams. Over the last couple decades, efforts to predict flow in ungauged watersheds have been an active area of research (Hauet et al. 2008; Royem et al. 2012; Atieh et al. 2017; Tegegne and Kim 2020), with techniques often involving hydrologic models (Gitau and Chaubey 2010; Tegegne and Kim

2020), instantaneous flow measurements and rating curves (Harmel et al. 2006b), or regression relationships between watershed/stream characteristics and flow (Chen and Chiu 2004; Gianfagna et al. 2015). However, these efforts can be data intensive (Razavi et al. 2013), unreliable (e.g., with indirect measurements), or logistically unfeasible across numerous, remote sites. The proposed methods discussed in this study provide an opportunity to fill this data gap by collecting continuous records of flow across multiple, remote, small-scale watersheds.

A variety of methods have been used to successfully collect flow measurements for use in rating curve development. The most common flow measurement techniques include direct measurement methods (e.g., timed volume), velocity-area methods (e.g., float method, dilution gaging, trajectory method, current meters, acoustic Doppler current profilers, and electromagnetic method), formed constriction methods (e.g., weirs and flumes), and non-contact methods (e.g., remote sensing and particle image velocimetry) (Gravelle 2015; Dobriyal et al. 2017). Direct and formed constriction methods are impractical across numerous sites, and these can be expensive and difficult to operate. Non-contact methods not only are costly, but do not directly measure streamflow, and require extensive ground-checking and validation.

While acoustic Doppler instruments (e.g., the SonTek-IQ) are costly, they are highly accurate, and the proposed method allows for direct installation of the instrument into the stream, removing the need for technicians to measure instantaneous flow during dangerous conditions. Additionally, the SonTek-IQs can be rotated among numerous sites between flood events, so a SonTek-IQ does not have to be purchased for every monitoring site of interest. The proposed method also removes the logistical hindrance of trying to measure peak flows at numerous, remote sites, when often peak flows are maintained for only a couple hours or less in small-scale streams.

Nonlinear regression analyses are common practice for rating curve development (Westphal et al. 1999; Reitan and Petersen-øverleir 2008; Fenton 2018; Tamagnone et al. 2019), but few studies have applied the use of locally weighted regressions such as LOESS. The benefit of locally weighted regression is the ability to fit the curve-linear shape of measured stage and discharge data, as well as compute uncertainty bounds around the predictions. Across 500 streams in United Kingdom, nonparametric LOWESS regression was used to fit rating curves and estimate discharge uncertainty, which resulted in a robust and versatile framework for hydrologic analyses (Coxon et al. 2015). Additionally, for a low-gradient subcatchment in Louisiana, the use of artificial neural networks (ANN) and local nonparametric regression (LOESS) were compared for modelling rating curves. While the ANN performed slightly better than LOESS, both techniques agreed well with the observed discharge measurements (Habib and Meselhe 2006).

Extension of rating curves outside the range of measured data is often necessary when developing continuous records of flow. When a SonTek-IQ was deployed this study, at least 89% of all stage measurements were captured by flow data, meaning less than 11% of the time were flow measurements required to be predicted outside the range of measured data. Extension of rating curves is often done using the existing model, developing a new model using watershed/stream characteristics, or using Manning's equation (Sivapragasam and Muttill 2005). Since Manning's equation is a common practice for predicting flow in ungauged streams, and hydrological information can be estimated from existing stage-discharge relationships, Manning's equation was chosen for the purpose of extending rating curves in this study. While rating curves and extrapolation with Manning's equation has often been adapted (Leonard et al.

2000; Leon et al. 2006; Pan et al. 2016), the need for extrapolation in the proposed methods could be reduced with continued or extended deployments of the SonTek-IQs.

The downfall of many typical rating curve techniques is the inability to accurately represent hysteresis in the stage-discharge relationships. As occurred in this study, hysteresis typically appears as higher flows at a given stage on the rising limb of a hydrograph compared to the same stage on the falling limb, creating a loop in the rating curve. This can be observed in Figure 5 for site 8, where the majority of data points from the largest storm event were included (i.e., measurements above 6 ft stage) to increase the sample size on the higher end. Historically, two methods have been used to incorporate hysteresis into rating curves including 1) separate rating curves for the rising and falling limbs of hydrographs, and 2) the Jones formula (Jones 1916). The first method of developing separate rating curves often produces separation in the discharge hydrograph (Tawfik et al. 1997), so the Jones formula has been widely applied to adjust a single rating curve for unsteady flow (Perumal et al. 2004; Petersen-øverleir 2006). However, the Jones equation requires accurate identification of hydraulic parameters such as channel resistance, bed slope, channel length and friction law, and has shown significant error near peak flow where large hysteresis occurs (Perumal and Raju 1999).

While the selection of data across the hydrograph and the use of LOESS regression in this study may not adequately capture hysteresis, it provides a method to essentially average the flows on the higher ends of measured stage. Additionally, the purpose of these data is to estimate daily flows for use in constituent load estimations and model calibration/validation (on a daily scale or larger). Therefore, the averaging of the instantaneous measurements seems acceptable. However, if the data are to be used on a finer times scale (i.e., hourly, 15-minute,

etc.), then a different approach to the rating curve models may be necessary to accurately represent hysteresis.

The purchase and installation cost of a typical USGS monitoring gage is around \$25,000, with a minimum operating cost of around \$15,000 per year (personal communication with Michael Norris, USGS). Therefore, to monitor 8 streams (i.e., the number of streams where SonTek-IQs were installed in this study), the total costs for 3 years would minimally be \$560,000. However, using the method developed in this study, a \$9,000 SonTek-IQ is not required for each site. Additional equipment and installation costs, besides the SonTek-IQ, is about \$1,200 per site. Therefore, assuming the purchase of 3 SonTek-IQs, 8 sites would cost about \$36,000 for purchase and installation. We also estimated operation and maintenance costs to be about \$110,000 for 3 years, assuming salary and benefits of a typical lab technician working half of their time maintaining this project, resulting in a total project cost of \$146,000. This is about 25% of the cost required if USGS gages systems were used, and may even be less, since minimum estimations were used for USGS estimations. Additionally, adding more sites to this monitoring method would only require HOBOS and equipment for HOBOS and SonTek-IQ installation (~\$1,200 per site), since SonTek-IQs can be rotated among sites. Therefore, the monitoring method developed in this study is a cost efficient way to develop continuous records of flow across numerous, small-scale streams.

Some limitations were recognized while implementing this monitoring method across the UPRW in Arkansas. No flow measurements were collected at sites 2 and 11, since the streams were too deep to wade through for baseflow discharge measurements and SonTek-IQ installation. Additionally, sites were limited to locations near bridge crossings in order to collect water samples. Therefore, monitoring sites must be investigated thoroughly before selecting, to

ensure the streams are an appropriate depth under baseflow conditions for equipment installation. Since this monitoring method seeks to fill the data-gap on small-scale streams, this should be feasible for most streams of interest.

Equipment malfunction and loss is always a risk in stream monitoring efforts, especially during flood events. At site 12, a SonTek-IQ was lost during a storm event in January of 2020 (Figure 6, where maximum flow occurred). The streambed at site 12 consists mostly of cobbles and boulders, and likely a large boulder shattered the concrete base where the SonTek-IQ was installed, allowing for pieces to break free and the SonTek-IQ to be washed away during the flood. Therefore, a different installation method for SonTek-IQs should be explored for sites with similar streambeds as site 12. A reinforced concrete base, with wire or rebar, may provide a stronger base under these conditions.

At site 1, a SonTek-IQ was installed for a short period of time before realizing the loose, shale sediment covered the SonTek-IQ during each high flow event. This caused poor and limited flow measurements from the SonTek-IQ, and a rating curve was not produced for this site. Therefore, streams with loose substrate similar to site 1 may not provide optimal conditions for monitoring with the proposed method. However, deployment time was limited at this site, and a longer deployment could have provided more usable data for rating curve development.

Long-term monitoring data is essential for understanding changes in natural environments, including trends, cycles and identification of rare events (Burt et al. 2014). However, due to fluctuations in streambeds and cross-sectional areas of streams over time, rating curve relationships can also change over time (Tomkins 2014). Using this monitoring method, SonTek-IQs would likely need to be redeployed in order to update rating curve relationships for long-term monitoring. Stage measurements can easily be continued for extended time periods,

and SonTek-IQ stations can remain in streams for simple removal and reinstallation when necessary.

Constituent Load Estimations

Water quality data and constituent load estimations are critical for managing surface water resources for both human and ecological health. A variety of methods have been applied for estimating constituent loads, including linear interpolation techniques (Migliaccio et al. 2010b), ratio estimators (Rousseau et al. 2006), and regression-based techniques (Lee et al. 2016). Many of the methods currently used were developed by the USGS, and are often multiple regression models relating constituent concentrations to daily discharge, time, and season (Runkel et al. 2004; Robertson and Saad 2011). However, the use of GAMs, while widely applied in environmental studies due to its ability to handle non-normal distributions (Ravindra et al. 2019), have rarely been applied to constituent load estimation techniques (Wang et al. 2011; Hagemann et al. 2016).

GAMs expand beyond regression models and generalized linear models by applying smoothing functions to predictor variables, as opposed to linear or polynomial functions (Wood 2017). In the Wachusett Reservoir Watershed (WRW) near Boston, the GAM framework improved explanatory and predictive capacity for estimating nitrate, TP, and total organic carbon, compared to linear models, and ultimately produced more accurate load estimations (Hagemann et al. 2016). The best fit GAMs for nitrate and TP in the WRW included a combination of sine and/or cosine of Julian day, smooth functions of Q_d and time, and a flow-derived function to capture hysteresis effects. In the present study, the GAM selected across all sites and constituents included solely smooth functions of Q and DOY. Our results suggested these explanatory variables were adequate, explaining at least 85% of the variance across all sites

and constituents. While a term to capture hysteresis was not explored in this study, as expressed in Hagemann et al., 2016, it could improve the performance of load estimations if adequate data is available across the rising and falling limbs of water quality hydrographs.

The use of Q_d as opposed to Q_i in load estimation techniques is a historically common practice (Haggard et al. 2003; Runkel et al. 2004; Migliaccio et al. 2010a; Lee et al. 2016). Often termed the “big river” approach for load estimations, using Q_d in load regression techniques assumes the instantaneous water quality samples represent the daily average concentration (Robertson and Roerish 1999). However, in small-scale streams, concentrations and streamflow can change rapidly (on a sub-daily scale), and an instantaneous water quality sample may not reflect daily concentrations. Similarly, mean daily flow may underestimate flow conditions if storm events occur on an hourly scale (as opposed to a daily scale for large rivers). Therefore, this study compared the use of Q_i and Q_d in load estimations for a wide range of stream sizes (watersheds ranging from 14 to 527 km², Table 1). GAMs using Q_i slightly outperformed GAMs using Q_d , but most sites and parameters showed no significant difference in daily loads predicted using Q_i and Q_d . Only one site (Site 14) showed significantly different means between M1 and M3 for all parameters except TP and TSS, with M3 (using Q_d) generally predicting greater constituent loads compared to M1. Therefore, while M1 generally performed better, both M1 and M3, with the use of Q_i and Q_d , respectively, are likely adequate for load estimations efforts.

Assessing the accuracy of load estimations can be difficult without high frequency water quality data. Therefore, loads can be compared by applying other methods using the same data set, or comparing to relevant sources in the literature (Rousseau et al. 2006). Constituent loads of TN, TP, NN, SRP and TSS at the three USGS sites in this study were compared to loads

estimated using the Weighted Regressions on Time, Discharge, and Season (WRTDS) model from Chapter 2. The WRTDS framework uses a weighted regression model with concentration, Q_d , and sine/cosine of time in decimal years (Hirsch et al. 2010; Hirsch and De Cicco 2015). At site 14, daily and monthly loads predicted by GAM-M3 and WRTDS agreed fairly well for all constituents (average NSE = 0.68; min NSE = 0.40; max NSE = 0.97). At site 8, daily and monthly loads predicted by GAM-M3 and WRTDS agreed well for all constituents except NN; NSE values for NN were less than one for daily and monthly loads, while all other constituents had NSE values greater than 0.70. At Site 1, constituent loads from GAM-M3 and WRTDS only agreed well for TP and TSS (NSE > 0.52). For TN, NN, and SRP, NSE values were always less than one, and generally differed the most on the higher end of load estimations. The lack of agreement between GAM-M3 and WRTDS for some sites and constituents is likely due to the difference in load estimation techniques and data used to develop models. While WRTDS and GAM-M3 use the same source of flow data from the USGS gages, the water quality data was collected and measured by two different entities. Additionally, the regression relationships developed in WRTDS are based on long-term data (20+ years), whereas the GAM relationships in this study use only 3 years of data. While the WRTDS and GAM results may not agree in all cases, the comparison was conducted to ensure similar order of magnitudes of load estimations. Ultimately, GAMs are beneficial for short-term data collection since WRTDS requires long-term datasets.

Nutrient and sediment loads were also quantified at sites 1 and 8 between 2011 and 2013 using the USGS Load Estimator (LOADEST) platform (McCarty et al. 2016). LOADEST develops regression models for estimating constituent loads based on time, discharge and/or season (Runkel et al. 2004), and similar to GAMs, can be used with short-term datasets. Over the

two year period of study in McCarty et al., 2016, the average annual TP and TSS loads at Site 1 were 43,000 kg and 25,050,000 kg, respectively, and 70,000 kg and 21,300,000 kg, respectively, at Site 8. Over the three year period in this study (using GAM-M3), the average annual TP and TSS loads at Site 1 were 61,200 kg and 26,100,000 kg, respectively, and 82,000 kg and 23,750,000 kg, respectively, at Site 8. Therefore, a similar magnitude of TP and TSS loads were found in this study as McCarty et al., 2016, providing a reasonable validation of the GAM load estimation technique. However, GAMs provide more flexibility compared to LOADEST and other regression models by relaxing the normal-distribution assumption and using smooth functions of predictor variables. Additionally, GAMs can simplify the model selection process, since LOADEST and other regression techniques often require selecting from numerous models with higher order predictor variables.

Finally, 95% confidence intervals were generated for constituent load estimations (Appendix C). In general, 95% confidence intervals were greater at higher magnitudes of monthly constituent loads across sites. The larger magnitude loads are often related to higher flows, where storm sampling introduces more levels of measurement uncertainty compared to base flow sampling (Harmel et al. 2006a). Additionally, when the largest magnitude of flows occur, water quality and flow data are more scarce compared to baseflow data (especially in short-term data collection projects), leading to a larger uncertainty in the load estimations. Therefore, it is important to capture water quality samples across the range of flow and in as many high flow events as possible, in order to minimize the error associated with loads under high flow conditions.

Conclusions

The purpose of this study was to introduce a cost-efficient method for remotely monitoring streamflow and estimating constituent loads in small-scale watersheds. Continuous stage measurements were collected from 12 sites across the UPRW using pressure transducers, and continuous discharge measurements were collected from 8 sites during high flow conditions using roving discharge stations, capturing at least 89% of stage measurements. Rating curves were developed for sites with stage and discharge measurements using LOESS regression, with NSE values greater than 0.88 across sites. Manning's equation and two-point regressions were used to predict flows above and below the range of measured flow, respectively. Rating curves were used to develop continuous records of flow across the three year monitoring period. Water quality samples were collected across the range of flow, and constituent loads were estimated using GAMs, where the best fit GAM was determined to be spline based smooth functions of Q and DOY. Additionally, Q_i and Q_d both well predicted constituent loads (NSEs > 0.87), and did not predict significantly different loads across sites (except site 14). Therefore, both Q_i and Q_d were considered adequate for load estimation methods. Ultimately, this study provides a cost-efficient method for collecting continuous discharge measurements and constituent load estimations across small-scale watersheds. This method can provide data for calibrating/validating watershed models at small-scales, and provide finer scale data for understanding land use impacts on water quality. Additionally, the data from this study will help to prioritize small watersheds of concern in the UPRW for watershed management.

References

- ADEQ, 2018. Arkansas's Final Impaired Waterbodies-303(d) List. Arkansas Department of Environmental Quality, North Little Rock.
- ANRC, 2018. 2018-2023 Nonpoint Source Pollution Management Plan. Arkansas Natural Resource Commission, Little Rock, Arkansas.

- Atieh, M., Taylor, G., Sattar, A.M.A., Gharabaghi, B., 2017. Prediction of flow duration curves for ungauged basins. *J. Hydrol.* 545, 383–394.
- AWRC, 2021. Arkansas Water Resources Center- Water Quality Lab.
- Aylward, B., Bandyopadhyay, J., Belausteguigotia, J.-C., Börkey, P., Cassar, A., Meadors, L., Saade, L., Siebentritt, M., Stein, R., Tognetti, S., Tortajada, C., Allan, T., Bauer, C., Bruch, C., Guimaraes-Pereira, A., Kendall, M., Kiersch, B., Landry, C., Rodriguez, E.M., Meinzen-Dick, R., Suzanne Moellendorf, Pagiola, S., Porras, I., Ratner, B., Shea, A., Swallow, B., Thomich, T., Voutchkov, N., Lead, C., Bruce, A., Authors, L., Bo, P., Moellendorf, S., Editors, R., Constanza, R., Jacobi, P., Rijsberman, F., 2005. Freshwater Ecosystem Services. *Ecosyst. Hum. Well-being Curr. State Trends* 213–255.
- Burt, T.P., Howden, N.J.K., Worrall, F., 2014. On the importance of very long-term water quality records. *Wiley Interdiscip. Rev. Water* 1, 41–48. <https://doi.org/10.1002/wat2.1001>
- Chen, X., Hao, Z., Devineni, N., Lall, U., 2014. Climate information based streamflow and rainfall forecasts for Huai River basin using hierarchical Bayesian modeling. *Hydrol. Earth Syst. Sci.* 18, 1539–1548. <https://doi.org/10.5194/hess-18-1539-2014>
- Chen, Y.C., Chiu, C.L., 2004. A fast method of flood discharge estimation. *Hydrol. Process.* 18, 1671–1684. <https://doi.org/10.1002/hyp.1476>
- Cohn, T.A., Delong, L.L., Gilroy, E.J., Hirsch, R.M., Wells, D.K., 1989. Estimating constituent loads. *Water Resour. Res.* 25, 937–942. <https://doi.org/10.1029/WR025i005p00937>
- Coxon, G., Freer, J., Westerber, I.K., Wagener, T., Woods, R., Smith, P.J., 2015. A novel framework for discharge uncertainty quantification applied to 500 UK gauging stations. *Water Resour. Res.* 51, 5531–5546. <https://doi.org/10.1002/2014WR016532>. Received
- Dai, A., Trenberth, K.E., 2002. Estimates of Freshwater Discharge from Continents: Latitudinal and Seasonal Variations. *J. Hydrometeorol.* 3, 660–687. [https://doi.org/10.1175/1525-7541\(2002\)003<0660:EOFDFC>2.0.CO;2](https://doi.org/10.1175/1525-7541(2002)003<0660:EOFDFC>2.0.CO;2)
- Dobriyal, P., Badola, R., Tuboi, C., Hussain, S.A., 2017. A review of methods for monitoring streamflow for sustainable water resource management. *Appl. Water Sci.* 7, 2617–2628. <https://doi.org/10.1007/s13201-016-0488-y>
- Dudgeon, D., Arthington, A.H., Gessner, M.O., Kawabata, Z.I., Knowler, D.J., Lévêque, C., Naiman, R.J., Prieur-Richard, A.H., Soto, D., Stiassny, M.L.J., Sullivan, C.A., 2006. Freshwater biodiversity: Importance, threats, status and conservation challenges. *Biol. Rev. Camb. Philos. Soc.* 81, 163–182. <https://doi.org/10.1017/S1464793105006950>
- Erwin, M.L., Hamilton, P.A., 2005. *Monitoring Our Rivers and Streams*. United States Geological Survey.
- Fenton, J.D., 2018. On the generation of stream rating curves. *J. Hydrol.* 564, 748–757. <https://doi.org/10.1016/j.jhydrol.2018.07.025>

- Gianfagna, C.C., Johnson, C.E., Chandler, D.G., Hofmann, C., 2015. Watershed area ratio accurately predicts daily streamflow in nested catchments in the Catskills, New York. *J. Hydrol. Reg. Stud.* 4, 583–594. <https://doi.org/10.1016/j.ejrh.2015.09.002>
- Gitau, M.W., Chaubey, I., 2010. Regionalization of SWAT Model Parameters for Use in Ungauged Watersheds. *Water* 2, 849–871. <https://doi.org/10.3390/w2040849>
- Gravelle, R., 2015. Discharge Estimation: Techniques and Equipment. *Geomorphol. Tech.* 5, 1–8.
- Habib, E.H., Meselhe, E.A., 2006. Stage – Discharge Relations for Low-Gradient Tidal Streams Using Data-Driven Models. *J. Hydraul. Eng.* 132, 482–492. [https://doi.org/10.1061/\(ASCE\)0733-9429\(2006\)132](https://doi.org/10.1061/(ASCE)0733-9429(2006)132)
- Hagemann, M., Asce, S.M., Kim, D., Park, M.H., Asce, A.M., 2016. Estimating Nutrient and Organic Carbon Loads to Water-Supply Reservoir Using Semiparametric Models. *J. Environ. Eng.* 142, 1–9. [https://doi.org/10.1061/\(ASCE\)EE.1943-7870.0001077](https://doi.org/10.1061/(ASCE)EE.1943-7870.0001077)
- Haggard, B.E., Soerens, T.S., Green, W.R., Richards, R.P., 2003. Using regression methods to estimate stream phosphorus loads at the Illinois River, Arkansas. *Appl. Eng. Agric.* 19, 187–194.
- Haritashya, U.K., Singh, P., Kumar, N., Singh, Y., 2006. Hydrological importance of an unusual hazard in a mountainous basin: flood and landslide. *Hydrol. Process.* 20, 3147–3154. <https://doi.org/10.1002/hyp>
- Harmel, R.D., Cooper, R.J., Slade, R.M., Haney, R.L., Arnold, J.G., 2006a. Cumulative Uncertainty in Measured Streamflow and Water Quality Data for Small Watersheds. *Trans. ASABE* 49, 689–702.
- Harmel, R.D., King, K.W., Haggard, B.E., Wren, D.G., Sheridan, J.M., 2006b. Practical Guidance for Discharge and Water Quality Data Collection on Small Watersheds. *Trans* 49, 937–948.
- Hauet, A., Creutin, J.D., Belleudy, P., 2008. Sensitivity study of large-scale particle image velocimetry measurement of river discharge using numerical simulation. *J. Hydrol.* 349, 178–190. <https://doi.org/10.1016/j.jhydrol.2007.10.062>
- Helsel, D.R., Hirsch, R.M., 1991. *Statistical Methods in Water Resources*. U.S. Geological Survey, U.S. Department of the Interior, United States of America.
- Hirsch, R.M., De Cicco, L.A., 2015. User Guide to Exploration and Graphics for RivEr Trends (EGRET) and dataRetrieval: R Packages for Hydrologic Data, in: *Hydrological Analysis and Interpretation; Section A, Statistical Analysis*. U. S. Geological Survey.
- Hirsch, R.M., Moyer, D.L., Archfield, S.A., 2010. Weighted Regressions on Time, Discharge, and Season (WRTDS), with an Application to Chesapeake Bay River Inputs. *J. Am. Water Resour. Assoc.* 46, 857–880.

- Hirsch, R.M., Slack, J.R., Smith, R.A., 1982. Techniques of trend analysis for monthly water quality data. *Water Resour. Res.* 18, 107–121.
- Jimenez Cisneros, B.E., Oki, T., Arnell, N.W., Benito, G., Cogley, J.G., Doll, P., Jiang, T., Mwakalila, S.S., 2014. Freshwater Resources, Climate Change 2014: Impacts, Adaption, and Vulnerability. Part A: Global and Sectoral Aspects. Contribution of Working Group II to the Fifth Assessment Report of the Intergovernmental Panel on Climate Change. <https://doi.org/10.2134/jeq2008.0015br>
- Jones, B.E., 1916. A method of Correcting River Discharge for a Changing Stage. *U.s. Geol. Surv. Water Supply Pap.* 375, 117–130.
- Lee, C.J., Hirsch, R.M., Schwarz, G.E., Holtschlag, D.J., Preston, S.D., Crawford, C.G., Vecchia, A. V., 2016. An evaluation of methods for estimating decadal stream loads. *J. Hydrol.* 542, 185–203. <https://doi.org/10.1016/j.jhydrol.2016.08.059>
- Leon, J.G., Calmant, S., Seyler, F., Bonnet, M.P., Cauhope, M., Frappart, F., Filizola, N., Fraizy, P., 2006. Rating curves and estimation of average water depth at the upper Negro River based on satellite altimeter data and modeled discharges. *J. Hydrol.* 328, 481–496. <https://doi.org/10.1016/j.jhydrol.2005.12.006>
- Leonard, J., Mietton, M., Najib, H., Gourbesville, P., 2000. Rating curve modelling with Manning's equation to manage instability and improve extrapolation to manage instability and improve extrapolation. *Hydrol. Sci. J.* 45, 739–750. <https://doi.org/10.1080/02626660009492374>
- Martin, D.M., Labadie, J.W., Poff, N.L., 2015. Incorporating social preferences into the ecological limits of hydrologic alteration (ELOHA): A case study in the Yampa-White River basin, Colorado. *Freshw. Biol.* 60, 1890–1900. <https://doi.org/10.1111/fwb.12619>
- McCarty, J.A., Haggard, B.E., Matlock, M.D., Pai, N., Saraswat, D., 2016. Post-model validation of a deterministic watershed model using monitoring data. *Trans. ASABE* 59, 497–508. <https://doi.org/10.13031/trans.59.11202>
- Migliaccio, K.W., Castro, J., Haggard, B.E., 2010a. Water Quality Statistical Analysis, in: Li, Y., Migliaccio, K.W. (Eds.), *Water Quality Concepts, Sampling and Analyses*. CRC Press, pp. 241–274.
- Migliaccio, K.W., Castro, J., Haggard, B.E., 2010b. *Water Quality Statistical Analysis*. pp. 241–274.
- OCC, 2018. HOB0 ® U20 Water Level Logger (U20-001-0x and U20-001-0x-Ti) Manual. 6,826,664.
- Pai, N., Saraswat, D., Daniels, M., 2011. Identifying priority subwatersheds in the Illinois River Drainage Area in Arkansas watershed using a distributed modeling approach. *Trans. ASABE* 54, 2181–2196. <https://doi.org/10.13031/2013.40657>

- Pan, F., Wang, C., Xi, X., 2016. Constructing river stage-discharge rating curves using remotely sensed river cross-sectional inundation areas and river bathymetry. *J. Hydrol.* 540, 670–687. <https://doi.org/10.1016/j.jhydrol.2016.06.024>
- Perumal, M., Raju, K.G.R., 1999. Approximate Convection-Diffusion Equations. *J. Hydrol. Eng.* 4, 160–164.
- Perumal, M., Shrestha, K.B., Chaube, U.C., 2004. Reproduction of Hysteresis in Rating Curves. *J. Hydraul. Eng.* 130, 870–878. [https://doi.org/10.1061/\(ASCE\)0733-9429\(2004\)130](https://doi.org/10.1061/(ASCE)0733-9429(2004)130)
- Petersen-øverleir, A., 2006. Modelling stage — discharge relationships affected by hysteresis using the Jones formula and nonlinear regression. *Hydrol. Sci. J.* 51. <https://doi.org/10.1623/hysj.51.3.365>
- Peterson, T.C., Heim, R.R., Hirsch, R., Kaiser, D.P., Brooks, H., Duffenbaugh, N.S., Dole, R.M., Giovannetone, J.P., Guirguis, K., Karl, T.R., Katz, R.W., Kunkel, K., Lettenmaier, D., McCabe, G.J., Paciorek, C.J., Ryberg, K.R., Schubert, S., Silva, V.B.S., Stewart, B.C., Vecchia, A. V., Villarini, G., Vose, R.S., Walsh, J., Wehner, M., Wolock, D., Wolter, K., Woodhouse, C.A., Wuebbles, D., 2013. Monitoring and understanding changes in heat waves, cold waves, floods, and droughts in the United States: State of knowledge. *Bull. Am. Meteorol. Soc.* 94, 821–834. <https://doi.org/10.1175/BAMS-D-12-00066.1>
- Poff, N.L., Richter, B.D., Arthington, A.H., Bunn, S.E., Naiman, R.J., Kendy, E., Acreman, M., Apse, C., Bledsoe, B.P., Freeman, M.C., Henriksen, J., Jacobson, R.B., Kennen, J.G., Merritt, D.M., O’Keefe, J.H., Olden, J.D., Rogers, K., Tharme, R.E., Warner, A., 2010. The ecological limits of hydrologic alteration (ELOHA): A new framework for developing regional environmental flow standards. *Freshw. Biol.* 55, 147–170. <https://doi.org/10.1111/j.1365-2427.2009.02204.x>
- R Core Team, 2016. R: A language and environment for statistical computing. Vienna, Austria.
- Ravindra, K., Rattan, P., Mor, S., Aggarwal, A.N., 2019. Generalized additive models: Building evidence of air pollution, climate change and human health. *Environ. Int.* 132. <https://doi.org/10.1016/j.envint.2019.104987>
- Razavi, T., Coulibaly, P., Asce, M., 2013. Streamflow Prediction in Ungauged Basins : Review of Regionalization Methods. *J. Hydrol. Eng.* 18, 958–975. [https://doi.org/10.1061/\(ASCE\)HE.1943-5584.0000690](https://doi.org/10.1061/(ASCE)HE.1943-5584.0000690).
- Reitan, T., Petersen-øverleir, A., 2008. Bayesian power-law regression with a location parameter, with applications for construction of discharge rating curves. *Stoch. Environ. Res. Risk Assess.* 22, 351–365. <https://doi.org/10.1007/s00477-007-0119-0>
- Robertson, D.M., Roerish, E.D., 1999. Influence of various water quality sampling strategies on load estimates for small streams. *Water Resour. Res.* 35, 3747–3759.

- Robertson, D.M., Saad, D.A., 2011. Nutrient inputs to the Laurentian Great Lakes by source and watershed estimated using Sparrow Watershed Models. *J. Am. Water Resour. Assoc.* 47. <https://doi.org/10.1111/j.1752-1688.2011.00574.x>
- Rousseau, A.N., Duchemin, M., Poulin, A., Quilbe, R., Gangbazo, G., Villeneuve, J., 2006. Selecting a calculation method to estimate sediment and nutrient loads in streams: Application to the Beaurivage River (Quebec, Canada). *J. Hydrol.* 326, 295–310. <https://doi.org/10.1016/j.jhydrol.2005.11.008>
- Royem, A.A., Mui, C.K., Fuka, D.R., Walter, M.T., 2012. Technical Note: Proposing a low-tech, affordable, accurate stream stage monitoring system. *Trans. ASABE* 55, 2237–2242. <https://doi.org/10.13031/2013.42512>
- Runkel, R.L., Crawford, C.G., Cohn, T.A., 2004. Load Estimator (LOADEST): a FORTRAN program for estimating constituent loads in streams and rivers, in: *Techniques and Methods, Book 4*. <https://doi.org/10.3133/tm4A5>
- Sala, O.E., Chapin, F.S., Armesto, J.J., Berlow, E., Bloomfield, J., Dirzo, R., Huber-Sanwald, E., Huenneke, L.F., Jackson, R.B., Kinzig, A., Leemans, R., Lodge, D.M., Mooney, H.A., Oesterheld, M., Poff, N.L.R., Sykes, M.T., Walker, B.H., Walker, M., Wall, D.H., 2000. Global biodiversity scenarios for the year 2100. *Science* (80-). 287, 1770–1774. <https://doi.org/10.1126/science.287.5459.1770>
- Silberstein, R.P., 2006. Hydrological models are so good, do we still need data? *Environ. Model. Softw.* 21, 1340–1352. <https://doi.org/10.1016/j.envsoft.2005.04.019>
- Sivapragasam, C., Muttill, N., 2005. Discharge Rating Curve Extension – A New Approach. *Water Resour. Manag.* 19, 505–520. <https://doi.org/10.1007/s11269-005-6811-2>
- Solans, M.A., García de Jalón, D., 2016. Basic tools for setting environmental flows at the regional scale: application of the ELOHA framework in a Mediterranean river basin. *Ecohydrology* 9, 1517–1538. <https://doi.org/10.1002/eco.1745>
- SonTek-IQ, 2017. SonTek-IQ Series Intelligent Flow Featuring SmartPulse User's Manual [WWW Document]. URL <https://www.sontek.com/sontek-iq-series> (accessed 1.16.20).
- Stein, E.D., Sengupta, A., Mazor, R.D., McCune, K., Bledsoe, B.P., Adams, S., 2017. Application of regional flow-ecology relationships to inform watershed management decisions: Application of the ELOHA framework in the San Diego River watershed, California, USA. *Ecohydrology* 10. <https://doi.org/10.1002/eco.1869>
- Tamagnone, P., Massazza, G., Pezzoli, A., Rosso, M., 2019. Hydrology of the Sirba River: Updating and Analysis of Discharge Time Series. *Water* 11, 1–15. <https://doi.org/10.3390/w11010156>
- Tawfik, B.M., Ibrahim, A., Fahmy, H., 1997. Hysteresis Sensitive Neural Network for Modeling Rating Curves. *J. Comput. Civ. Eng.* 11, 206–211.

- Tegegne, G., Kim, Y., 2020. Strategies to enhance the reliability of flow quantile prediction in the gauged and ungauged basins. *River Res. Appl.* 36, 724–734. <https://doi.org/10.1002/rra.3603>
- Tomkins, K.M., 2014. Uncertainty in stream flow rating curves: methods, controls and consequences. *Hydrol. Process.* 481, 464–481. <https://doi.org/10.1002/hyp.9567>
- Tripathi, M.P., Panda, R.K., Raghuwanshi, N.S., 2003. Identification and prioritisation of critical sub-watersheds for soil conservation management using the SWAT model. *Biosyst. Eng.* 85, 365–379. [https://doi.org/10.1016/S1537-5110\(03\)00066-7](https://doi.org/10.1016/S1537-5110(03)00066-7)
- Turnipseed, D.P., Sauer, V.B., 2010. Discharge measurements at gaging stations, U.S. Geological Survey Techniques and Methods Book 3, Chap. A8.
- USACE, 2016. HEC-RAS River Analysis System User's Manual. United States Army Corps of Engineers, Davis, California.
- USDA, 2017. National Agricultural Statistics Service. United States Department of Agriculture, United States Department of Agriculture.
- USEPA, 2006. TMDLs for Phosphorus, Copper, and Zinc for The Poteau River Near Waldron, AR. United States Environmental Protection Agency, Dallas, TX.
- USGS, 2016. National Land Cover Database [WWW Document]. URL <https://www.mrlc.gov/data?f%5B0%5D=category%3Alandcover&f%5B1%5D=year%3A2016> (accessed 10.2.20).
- USGS, 2001. National Land Cover Database. United States Geological Survey.
- Wang, Y., Wang, Y., Kuhnert, P., Henderson, B., 2011. Load Estimation with Uncertainties from Opportunistic Sampling Data – a Semiparametric Approach. *J. Hydrol.* 396. <https://doi.org/10.1016/j.jhydrol.2010.11.003>
- Welde, K., 2016. Identification and prioritization of subwatersheds for land and water management in Tekeze dam watershed, Northern Ethiopia. *Int. Soil Water Conserv. Res.* 4, 30–38. <https://doi.org/10.1016/j.iswcr.2016.02.006>
- Westphal, J.A., Thompson, D.B., Stevens, G.T., Strauser, C.N., 1999. Stage-discharge relations on the middle mississippi river. *J. Water Resour. Plan. Manag.* 125, 48–53.
- Wood, S.N., 2017. Generalized Additive Models: An Introduction with R, 2nd ed. Chapman and Hall/CRC.
- Zhang, Z., Balay, J.W., Bertoldi, K.M., MaCoy, P.O., 2016. Assessment of Water Capacity and Availability from Unregulated Stream Flows Based on Ecological Limits of Hydrologic Alteration (ELOHA) Environmental Flow Standards. *River Res. Appl.* 32, 1469–1480. <https://doi.org/10.1002/rra.2979>

Appendix

Appendix A: Best fit generalized additive model (GAM, from Table 2) for each site and parameter: total nitrogen (TN), nitrate plus nitrite (NN), total phosphorus (TP), soluble reactive phosphorus (SRP), total suspended solids (TSS), fluoride (Fl), chloride (Cl), and sulfate (SO₄²⁻). Where GAM 1 is not the best fit GAM, the statistics for GAM 1 are shown in the third column. P-values for GAMs were always less than 0.01, so they are not listed in the tables.

Constituent Load Methods 1 and 2:

Site	Parameter	Best Fit GAM				GAM 1			
		GAM	R ²	NSE	AIC	GAM	R ²	NSE	AIC
Site 1	TN	1	0.99	0.99	-135				
	TP	1	0.98	0.98	6				
	NN	4	0.97	0.97	77	1	0.96	0.96	108
	SRP	1	0.96	0.96	114				
	TSS	3	0.99	0.99	15	1	0.98	0.98	35
	Fl	3	0.94	0.96	107	1	0.91	0.92	150
	Cl	3	0.99	1.00	-198	1	0.99	0.99	-194
	SO4	3	0.99	0.99	-99	1	0.98	0.98	-75
Site 4	TN	5	0.97	0.98	16	1	0.98	0.98	14
	TP	1	0.97	0.98	50				
	NN	5	0.86	0.86	125	1	0.87	0.88	123
	SRP	1	0.94	0.95	109				
	TSS	5	0.95	0.95	70	1	0.96	0.97	64
	Fl	3	0.97	0.97	22	1	0.95	0.95	49
	Cl	3	0.99	0.99	-89	1	0.99	0.99	-79
	SO4	5	0.99	0.99	-91	1	0.99	0.99	-94
Site 5	TN	3	0.98	0.99	2	1	0.96	0.97	22
	TP	1	0.94	0.94	98				
	NN	1	0.92	0.93	58				
	SRP	1	0.90	0.93	133				
	TSS	1	0.96	0.97	71				
	Fl	3	0.98	0.99	-17	1	0.94	0.94	37
	Cl	1	0.99	0.99	-95				
	SO4	5	0.96	0.96	-38	1	0.96	0.97	-41
Site 6	TN	5	0.98	0.98	5	1	0.98	0.98	1
	TP	1	0.97	0.98	52				
	NN	5	0.87	0.87	132	1	0.88	0.89	128
	SRP	1	0.93	0.94	125				
	TSS	1	0.97	0.98	64				
	Fl	1	0.98	0.98	-23				
	Cl	1	0.99	1.00	-123				
	SO4	1	0.99	1.00	-102				

Constituent Load Methods 1 and 2, Continued:

Site	Parameter	Best Fit GAM				GAM 1			
		GAM	R ²	NSE	AIC	GAM	R ²	NSE	AIC
Site 8	TN	5	0.98	0.98	-96	1	0.98	0.98	-98
	TP	4	0.98	0.98	-39	1	0.98	0.98	-29
	NN	3	0.91	0.94	201	1	0.86	0.87	226
	SRP	3	0.95	0.95	111	1	0.95	0.95	117
	TSS	1	0.98	0.99	-14				
	FI	3	0.90	0.91	134	1	0.89	0.90	146
	Cl	5	0.87	0.87	74	1	0.87	0.88	74
	SO4	1	0.98	0.98	-89				
Site 9	TN	1	0.96	0.97	-16				
	TP	1	0.98	0.98	-10				
	NN	1	0.89	0.91	31				
	SRP	1	0.95	0.96	32				
	TSS	1	0.98	0.99	21				
	FI	1	0.97	0.97	1				
	Cl	3	0.96	0.96	-40	1	0.95	0.97	-31
	SO4	1	0.98	0.99	-68				
Site 10	TN	1	0.99	0.99	-39				
	TP	1	0.98	0.98	7				
	NN	1	0.92	0.92	137				
	SRP	1	0.96	0.97	72				
	TSS	3	0.99	0.99	13	1	0.97	0.98	37
	FI	1	0.98	0.98	-19				
	Cl	1	0.99	0.99	-69				
	SO4	4	0.99	0.99	-72	1	0.99	0.99	-66
Site 11	TN	1	0.99	0.99	-63				
	TP	3	0.98	0.98	-3	1	0.98	0.98	5
	NN	4	0.96	0.97	20	1	0.96	0.97	22
	SRP	5	0.97	0.97	33	1	0.97	0.98	28
	TSS	1	0.99	0.99	-6				
	FI	3	0.98	0.98	-13	1	0.96	0.98	29
	Cl	1	0.99	0.99	-81				
	SO4	1	0.98	0.98	-39				

Constituent Load Methods 1 and 2, Continued:

Site	Parameter	Best Fit GAM				GAM 1			
		GAM	R ²	NSE	AIC	GAM	R ²	NSE	AIC
Site 12	TN	3	1.00	1.00	-233	1	1.00	1.00	-233
	TP	3	0.99	0.99	-41	1	0.98	0.98	-28
	NN	3	0.98	0.98	30	1	0.97	0.98	45
	SRP	3	0.97	0.97	10	1	0.97	0.97	19
	TSS	5	0.98	0.98	-1	1	0.98	0.98	-5
	FI	3	0.92	0.93	130	1	0.92	0.92	136
	Cl	3	1.00	1.00	-255	1	1.00	1.00	-226
	SO4	3	0.99	0.99	-102	1	0.99	0.99	-104
Site 14	TN	5	0.99	0.99	-94	1	0.99	0.99	-98
	TP	1	0.96	0.96	31				
	NN	3	0.95	0.95	100	1	0.95	0.95	104
	SRP	1	0.94	0.95	97				
	TSS	3	0.97	0.97	33	1	0.97	0.87	38
	FI	3	0.89	0.91	162	1	0.88	0.89	175
	Cl	1	0.99	0.99	-195				
	SO4	4	0.98	0.98	-67	1	0.98	0.98	-64
Site 15	TN	5	0.99	0.99	-39	1	0.99	0.99	-39
	TP	5	0.94	0.94	68	1	0.94	0.95	68
	NN	5	0.96	0.97	21	1	0.96	0.97	23
	SRP	5	0.94	0.95	33	1	0.96	0.97	35
	TSS	5	0.85	0.86	140	1	0.85	0.86	141
	FI	4	0.89	0.91	79	1	0.89	0.90	80
	Cl	4	1.00	1.00	-121	1	1.00	1.00	-120
	SO4	5	0.99	0.99	-58	1	0.99	0.99	-56

Constituent Load Method 3:

Site	Parameter	Best GAM				GAM 1			
		GAM	R ²	NSE	AIC	GAM	R ²	NSE	AIC
Site 1	TN	4	0.99	0.99	-146	1	0.99	0.99	134
	TP	1	0.98	0.98	18				
	NN	4	0.97	0.98	73	1	0.96	0.96	107
	SRP	3	0.97	0.97	70	1	0.96	0.96	113
	TSS	3	0.98	0.98	62	1	0.97	0.98	76
	FI	3	0.94	0.95	113	1	0.91	0.92	149
	Cl	1	0.99	0.99	-194				
	SO4	3	0.99	0.99	-96	1	0.98	0.98	-76
Site 4	TN	5	0.98	0.98	13	1	0.98	0.98	10
	TP	1	0.97	0.98	42				
	NN	5	0.86	0.87	126	1	0.87	0.88	122
	SRP	1	0.94	0.96	106				
	TSS	1	0.95	0.96	66				
	FI	4	0.97	0.98	18	1	0.95	0.96	47
	Cl	1	0.99	0.99	-62				
	SO4	5	0.99	0.99	-92	1	0.99	0.99	-91
Site 5	TN	3	0.98	0.99	-15	1	0.96	0.97	20
	TP	4	0.94	0.96	93	1	0.93	0.94	99
	NN	1	0.90	0.92	64				
	SRP	1	0.91	0.94	138				
	TSS	1	0.95	0.96	88				
	FI	3	0.98	0.99	-15	1	0.95	0.97	37
	Cl	1	0.99	0.99	-83				
	SO4	5	0.96	0.96	-40	1	0.96	0.96	-41
Site 6	TN	1	0.98	0.99	-2				
	TP	5	0.96	0.97	57	1	0.97	0.97	52
	NN	5	0.86	0.86	133	1	0.87	0.89	128
	SRP	5	0.92	0.93	125	1	0.93	0.94	118
	TSS	5	0.96	0.96	82	1	0.96	0.97	76
	FI	1	0.98	0.98	-23				
	Cl	1	0.99	0.99	-118				
	SO4	1	0.99	1.00	-85				

Constituent Load Method 3, Continued:

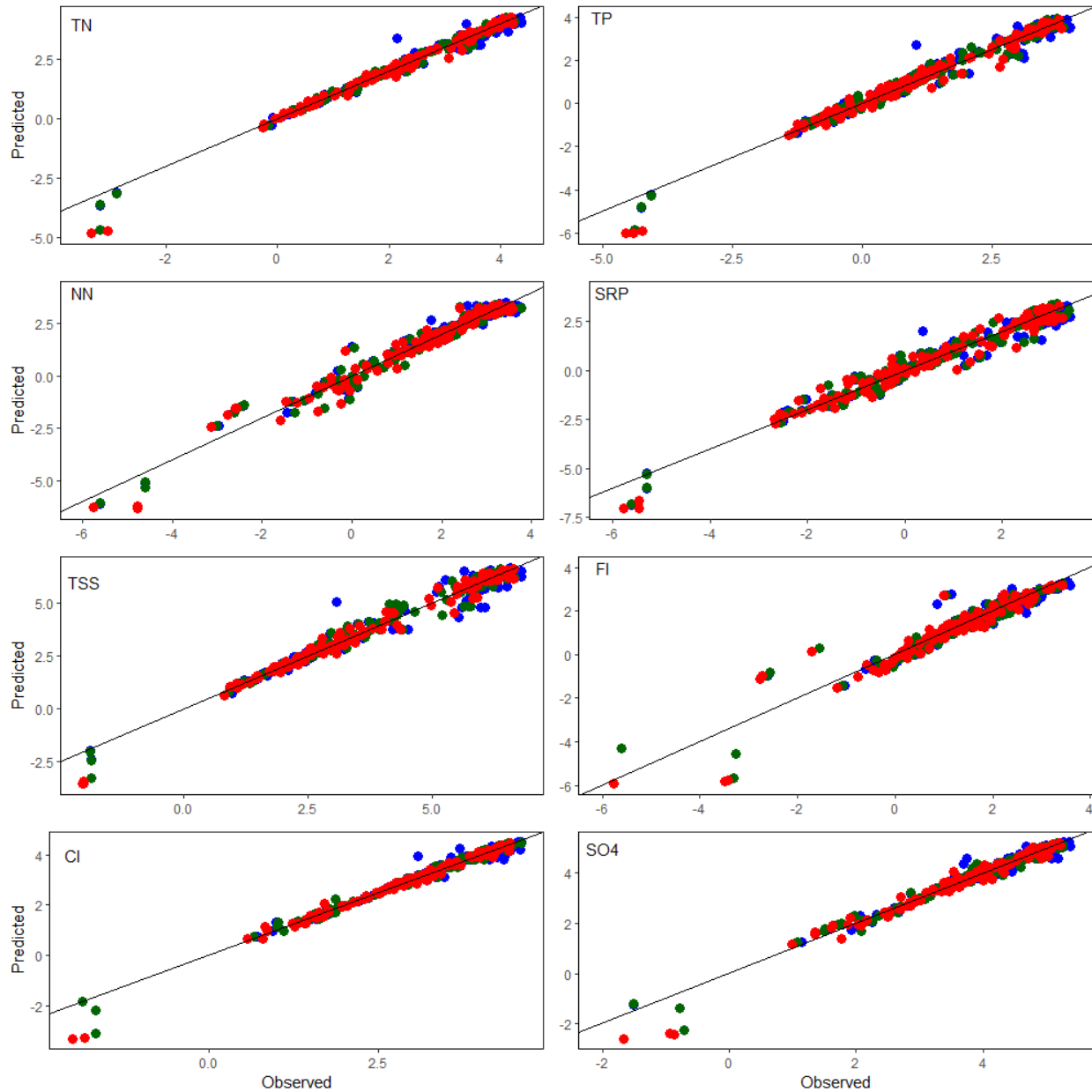
Site	Parameter	Best Fit GAM				GAM 1			
		GAM	R ²	NSE	AIC	GAM	R ²	NSE	AIC
Site 8	TN	5	0.98	0.98	-88	1	0.98	0.98	-91
	TP	4	0.98	0.98	-17	1	0.97	0.98	-12
	NN	3	0.90	0.93	202	1	0.85	0.86	225
	SRP	3	0.94	0.95	118	1	0.94	0.95	122
	TSS	1	0.98	0.98	12				
	FI	3	0.89	0.90	136	1	0.88	0.89	146
	Cl	3	0.88	0.89	67	1	0.87	0.87	74
	SO4	1	0.98	0.98	-89				
Site 9	TN	1	0.95	0.95	-3				
	TP	1	0.97	0.98	-5				
	NN	1	0.86	0.88	35				
	SRP	1	0.94	0.95	34				
	TSS	1	0.96	0.97	47				
	FI	1	0.97	0.97	-6				
	Cl	3	0.94	0.95	-36	1	0.93	0.95	-20
	SO4	1	0.978	0.981	-61				
Site 10	TN	3	0.99	0.99	-50	1	0.99	0.99	-42
	TP	1	0.98	0.98	4				
	NN	3	0.95	0.97	109	1	0.92	0.93	131
	SRP	1	0.97	0.97	57				
	TSS	3	0.96	0.97	45	1	0.96	0.96	57
	FI	4	0.98	0.99	-29	1	0.98	0.98	-24
	Cl	1	0.99	0.99	-75				
	SO4	1	0.99	0.99	-62				
Site 11	TN	1	0.99	0.99	-59				
	TP	1	0.98	0.98	6				
	NN	3	0.98	0.98	-6	1	0.96	0.97	13
	SRP	1	0.97	0.98	25				
	TSS	1	0.98	0.99	25				
	FI	3	0.98	0.98	-16	1	0.96	0.98	33
	Cl	1	0.99	0.99	-91				
	SO4	1	0.98	0.98	-38				

Constituent Load Method 3, Continued:

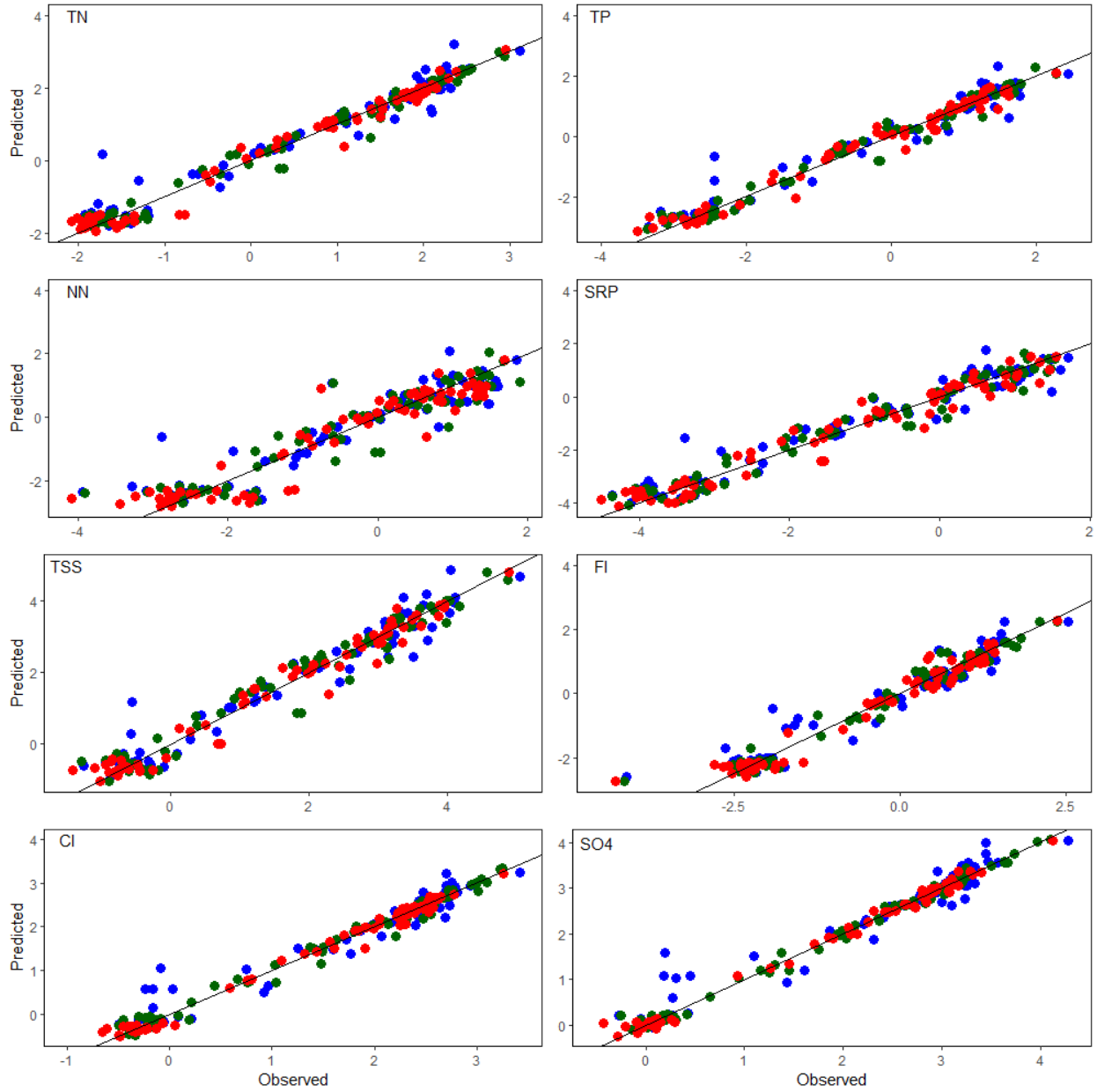
Site	Parameter	Best Fit GAM				GAM 1			
		GAM	R ²	NSE	AIC	GAM	R ²	NSE	AIC
Site 12	TN	1	1.00	1.00	-231				
	TP	3	0.98	0.99	-58	1	0.97	0.97	-26
	NN	3	0.96	0.97	22	1	0.96	0.97	37
	SRP	3	0.95	0.95	8	1	0.94	0.95	18
	TSS	4	0.96	0.96	-3	1	0.97	0.97	-4
	Fl	3	0.87	0.88	135	1	0.86	0.86	141
	Cl	3	1.00	1.00	-244	1	1.00	1.00	226
	SO4	5	0.99	0.99	-102	1	0.99	0.99	104
Site 14	TN	5	0.98	0.98	-86	1	0.98	0.99	-92
	TP	1	0.86	0.86	39				
	NN	3	0.95	0.95	99	1	0.94	0.95	104
	SRP	3	0.93	0.94	104	1	0.93	0.94	104
	TSS	1	0.96	0.97	60				
	Fl	3	0.89	0.91	162	1	0.87	0.89	175
	Cl	3	0.99	0.99	-212	1	0.99	0.99	198
	SO4	3	0.98	0.99	-81	1	0.98	0.98	-65
Site 15	TN	5	0.99	0.99	-32	1	0.99	0.99	-32
	TP	5	0.95	0.96	69	1	0.95	0.96	70
	NN	5	0.97	0.97	24	1	0.97	0.97	26
	SRP	5	0.96	0.96	33	1	0.96	0.96	35
	TSS	5	0.86	0.87	143	1	0.87	0.89	144
	Fl	1	0.93	0.94	69				
	Cl	1	1.00	1.00	-121				
	SO4	4	0.99	0.99	-60	1	0.99	0.99	-57

Appendix B: Measured versus predicted constituent loads from each method (M1 = red, M2 = blue, and M3 = green) for total nitrogen (TN), nitrate plus nitrite (NN), total phosphorus (TP), soluble reactive phosphorus (SRP), total suspended solids (TSS), fluoride (Fl), chloride (Cl), and sulfate (SO_4^{2-}) at each site. For M1, instantaneous loads are in g/m, and for M2 and M3, daily loads are in kg/day.

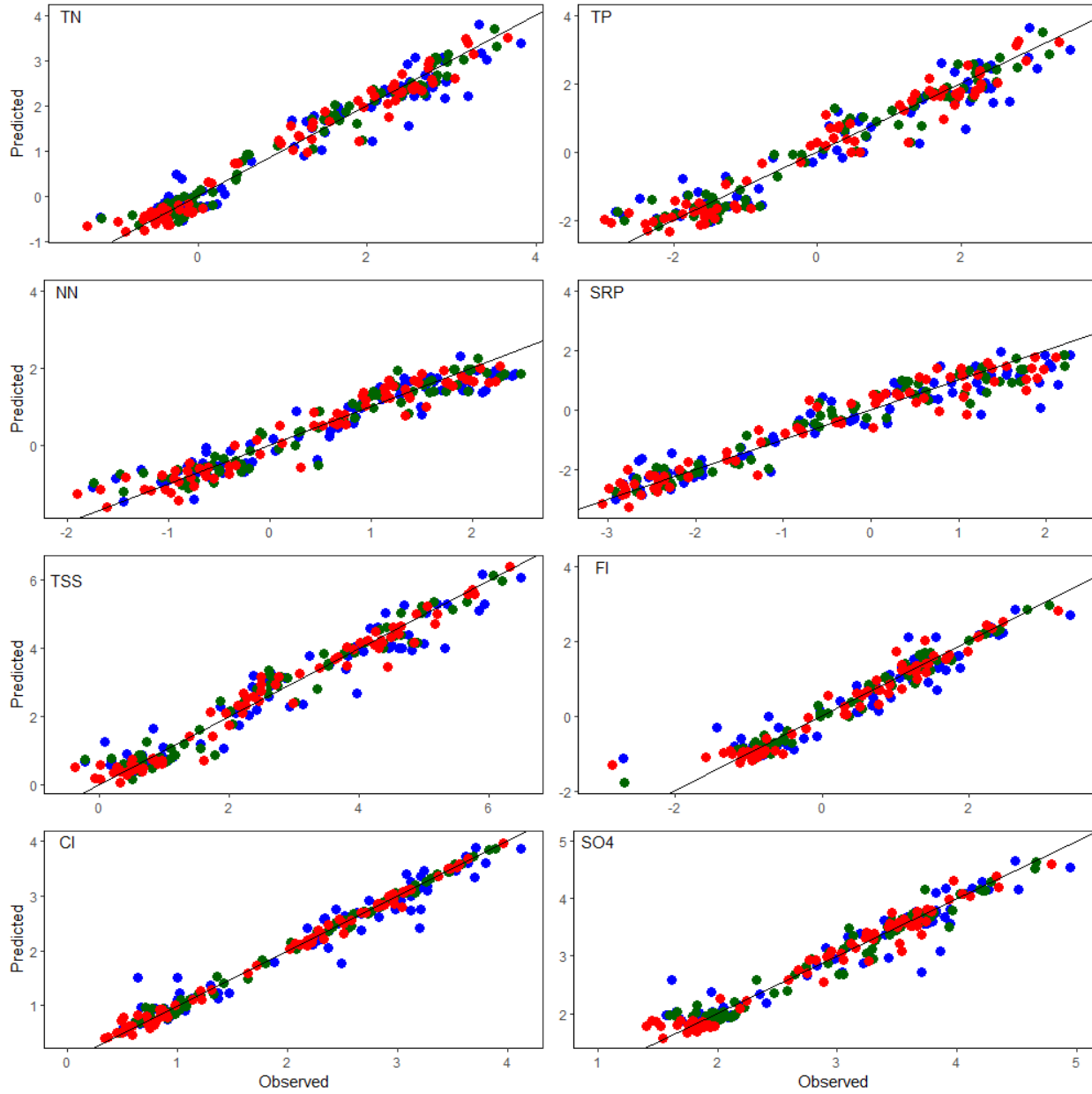
Site 1:



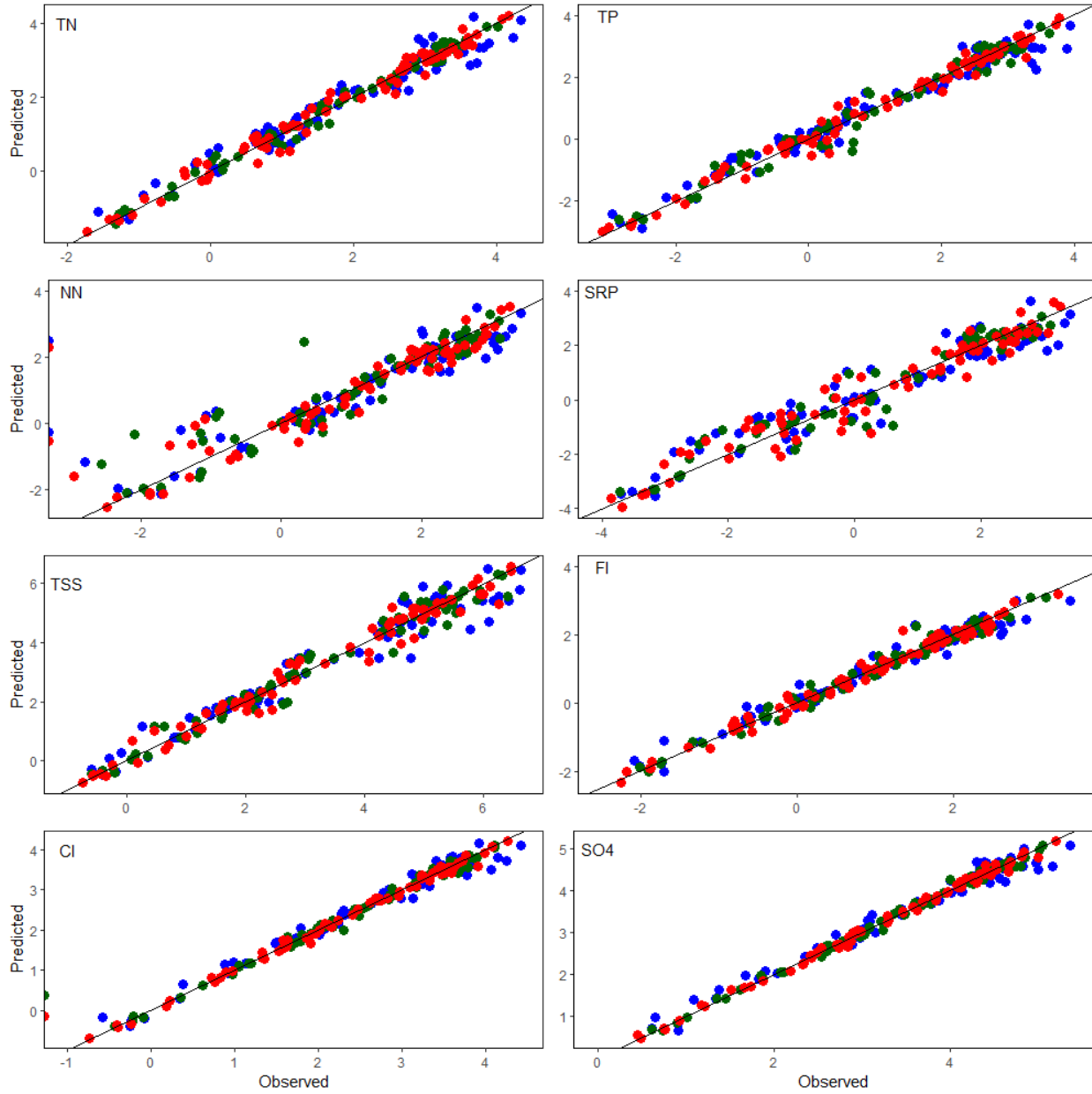
Site 4:



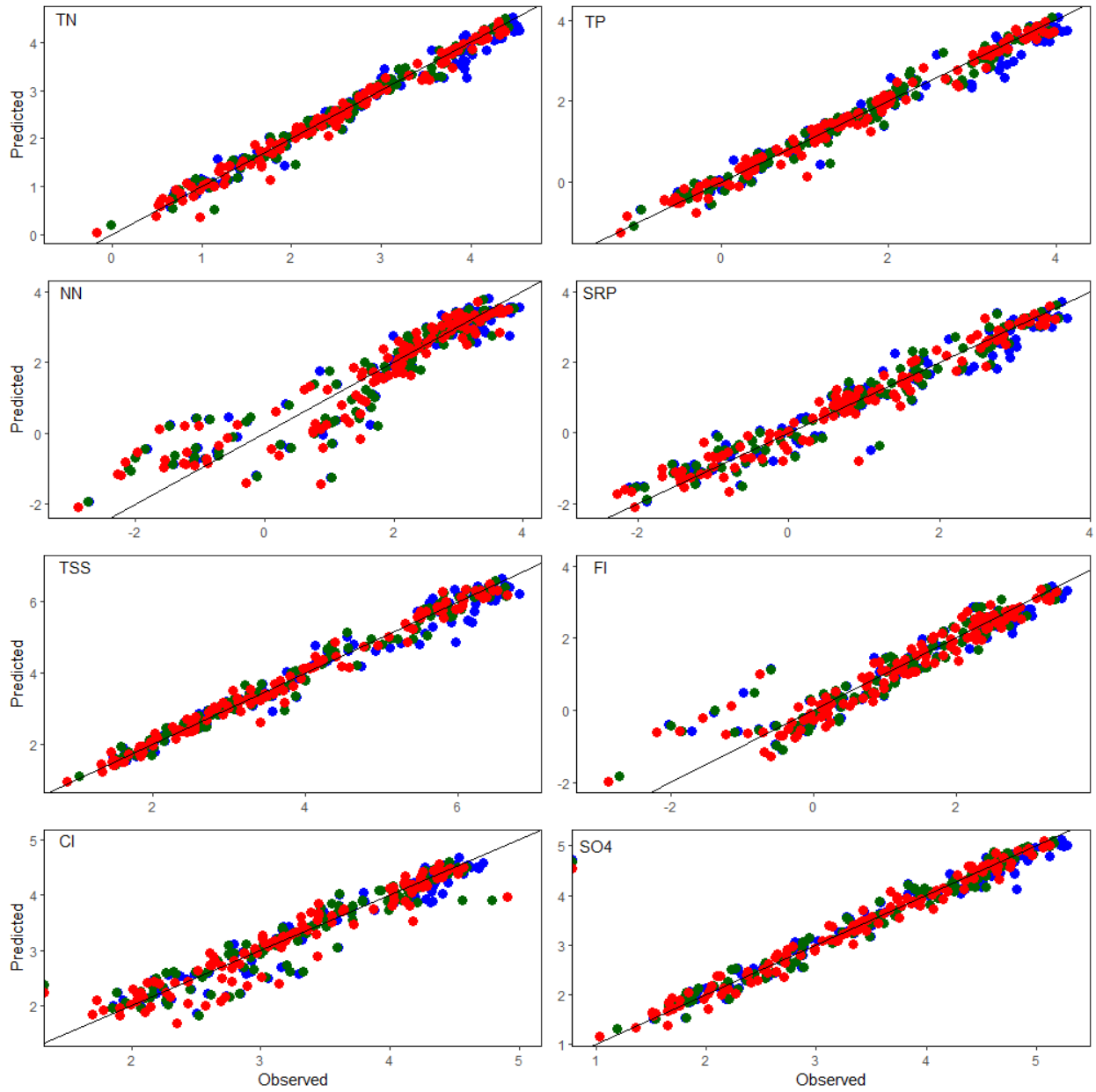
Site 5:



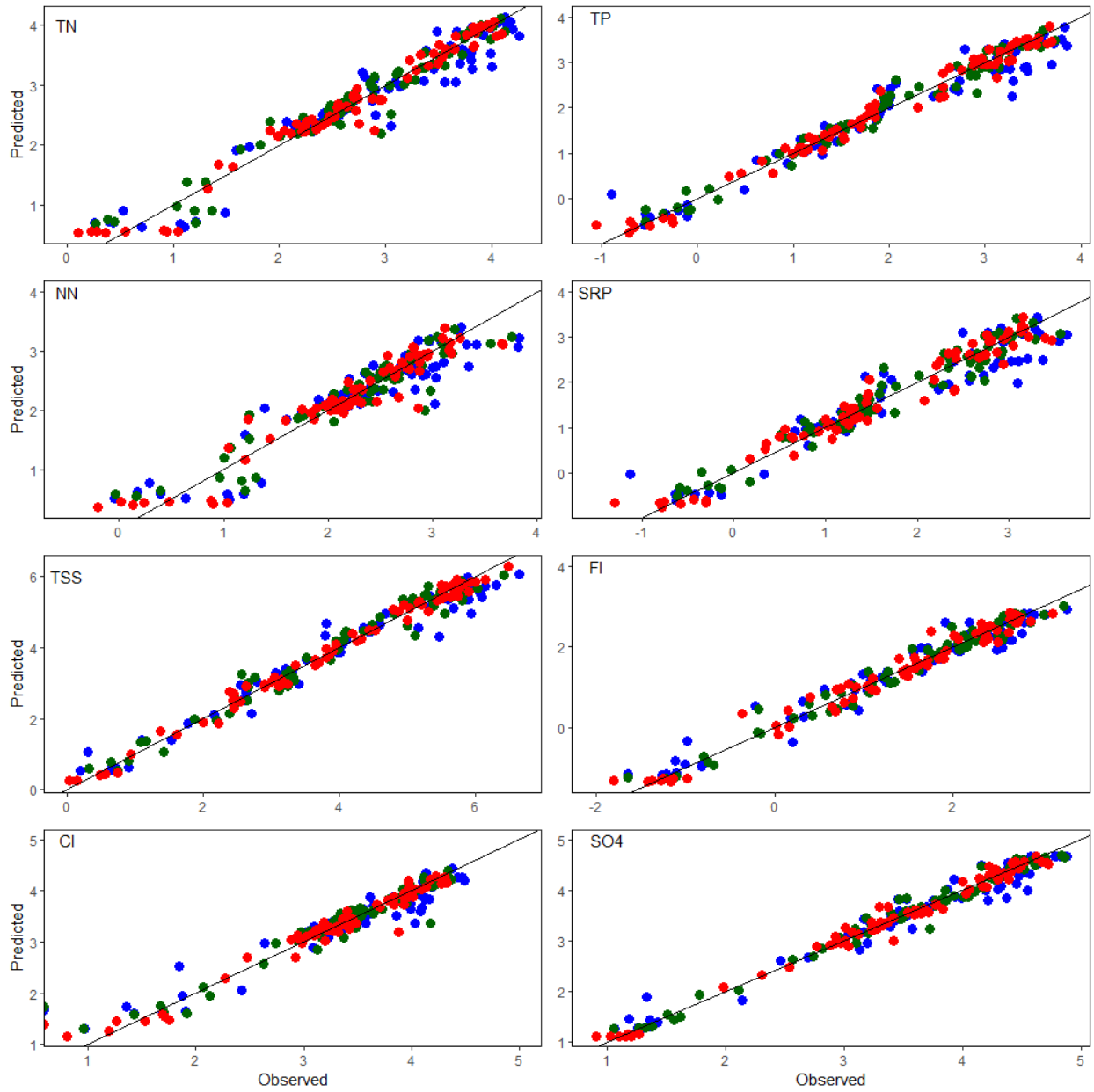
Site 6:



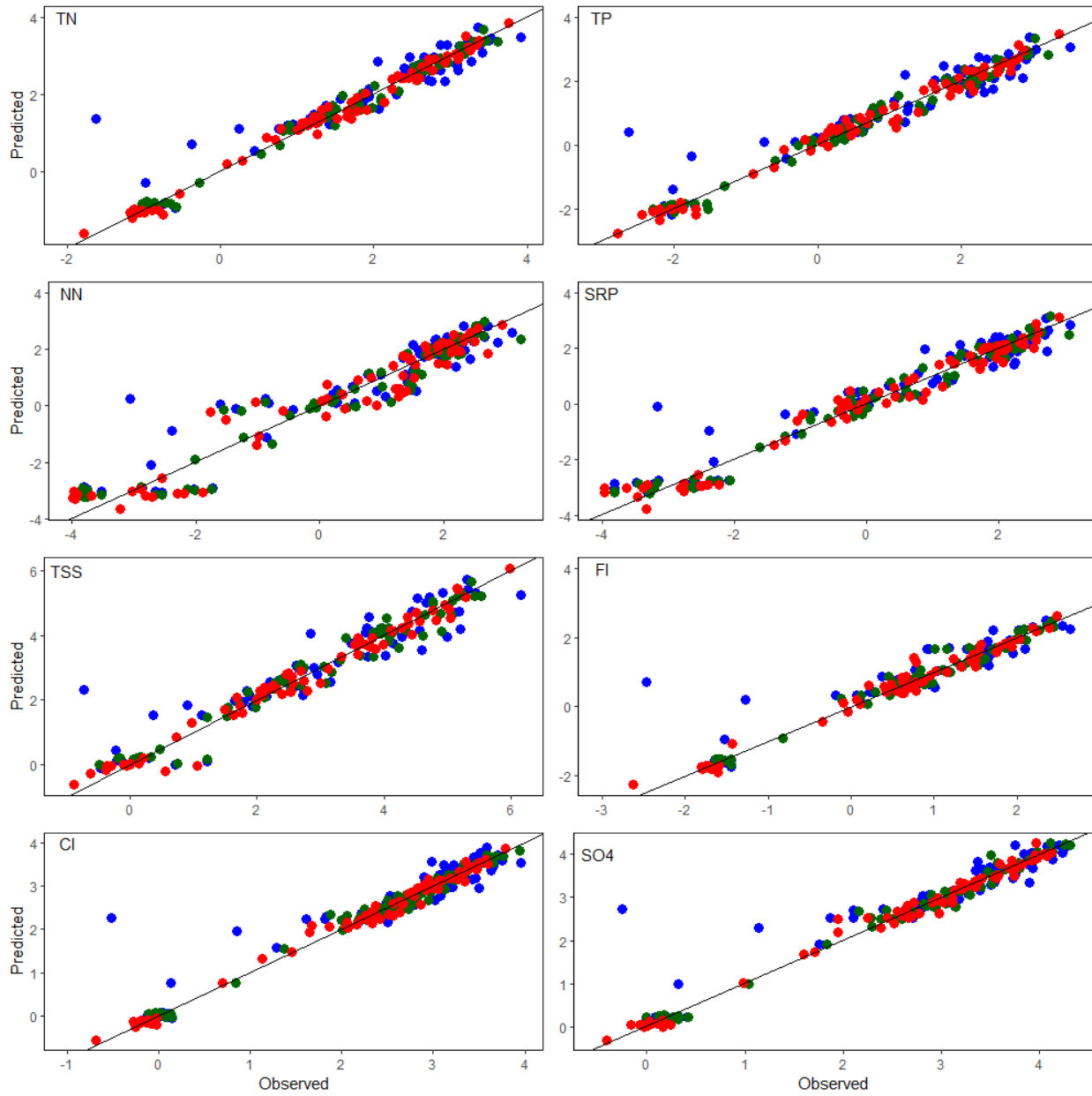
Site 8:



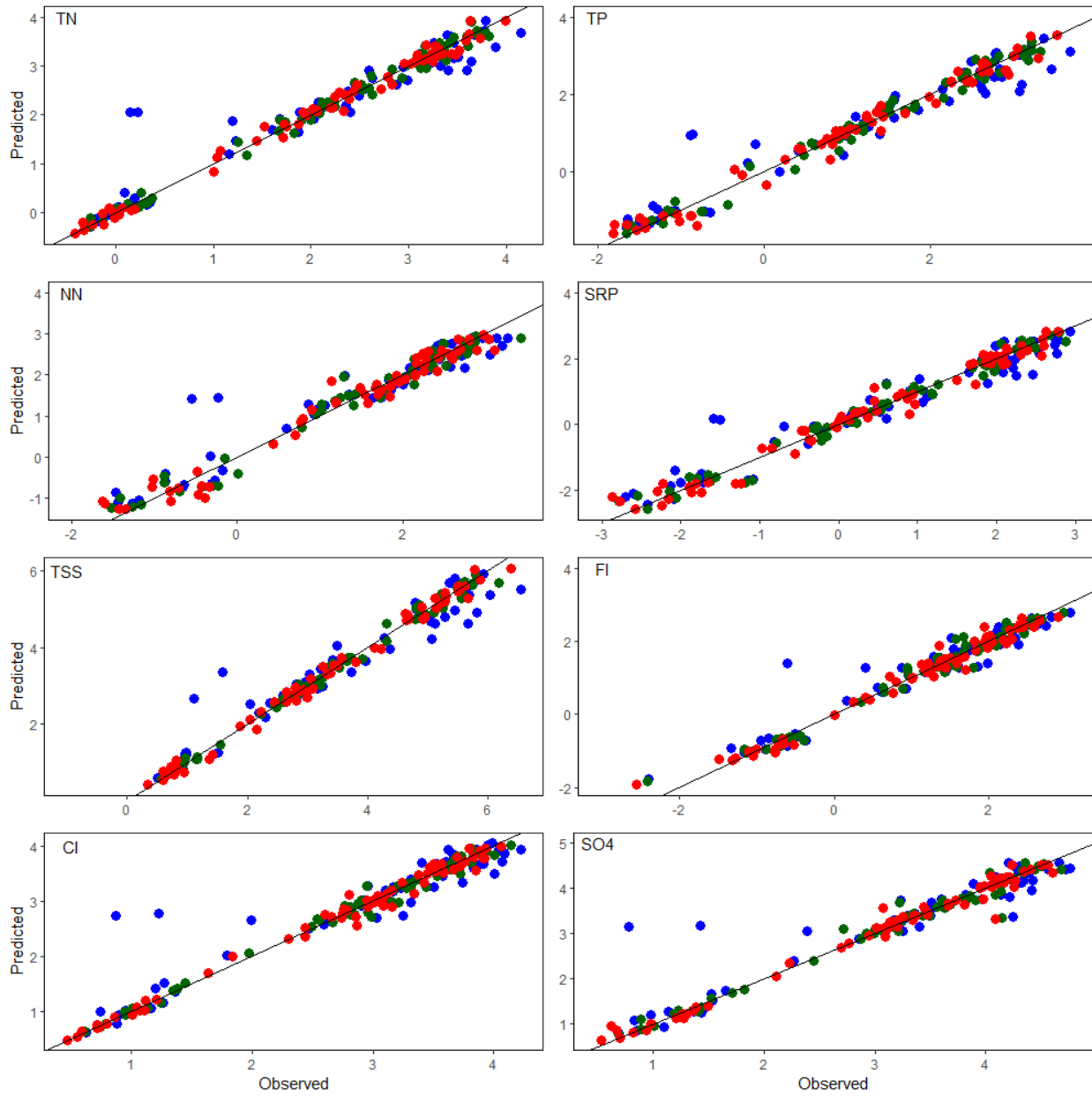
Site 9:



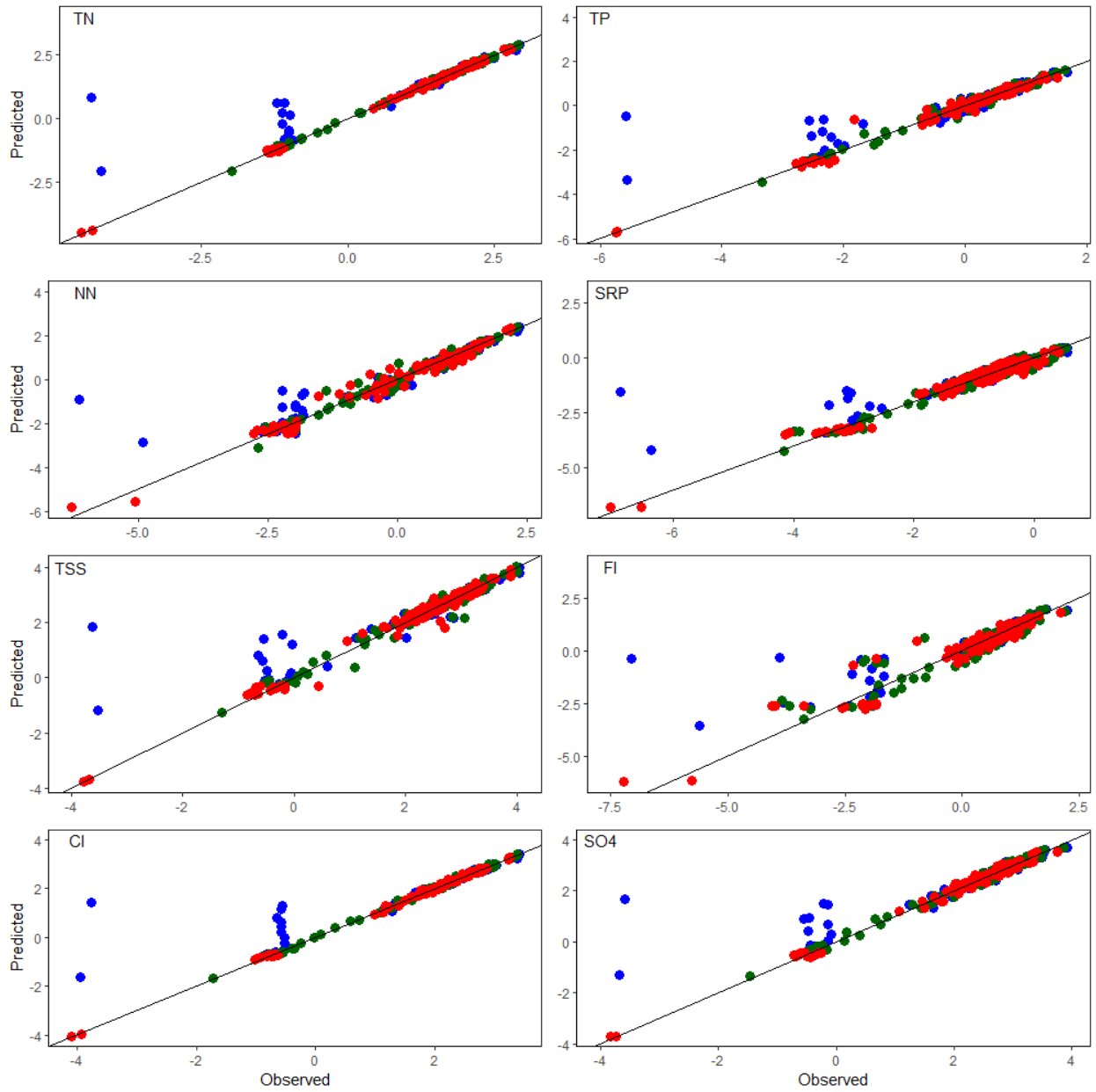
Site 10:



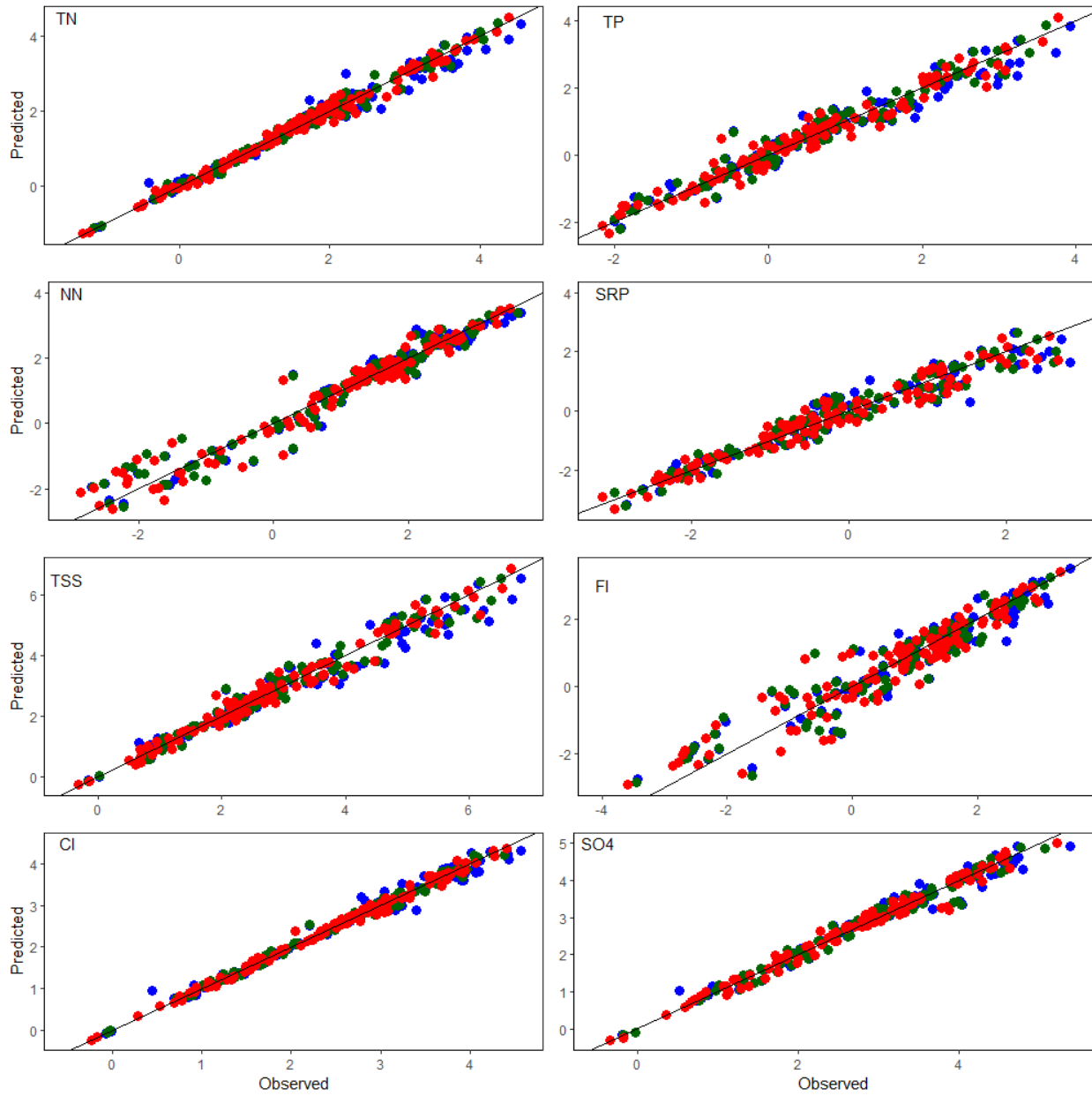
Site 11:



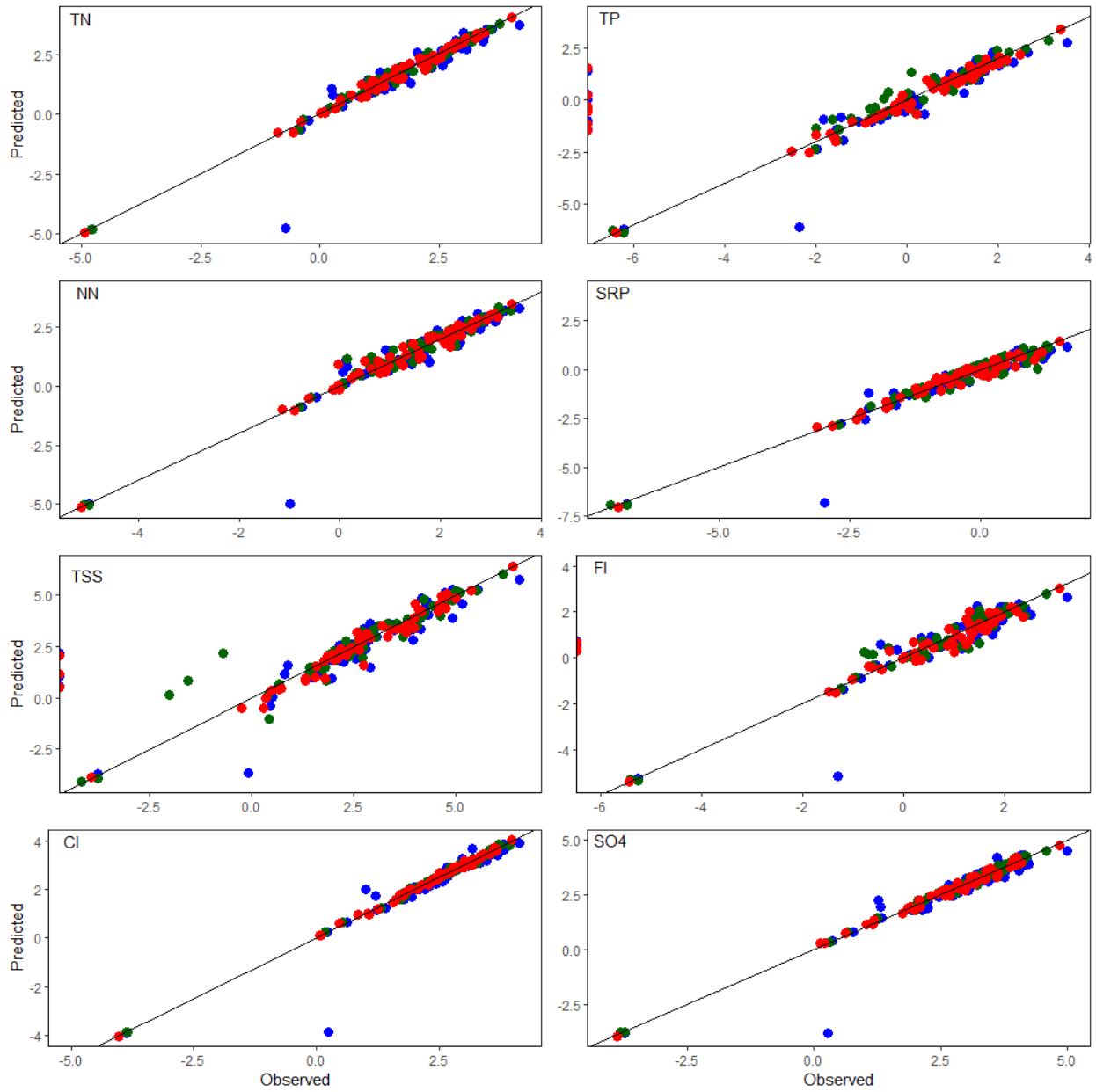
Site 12:



Site 14:

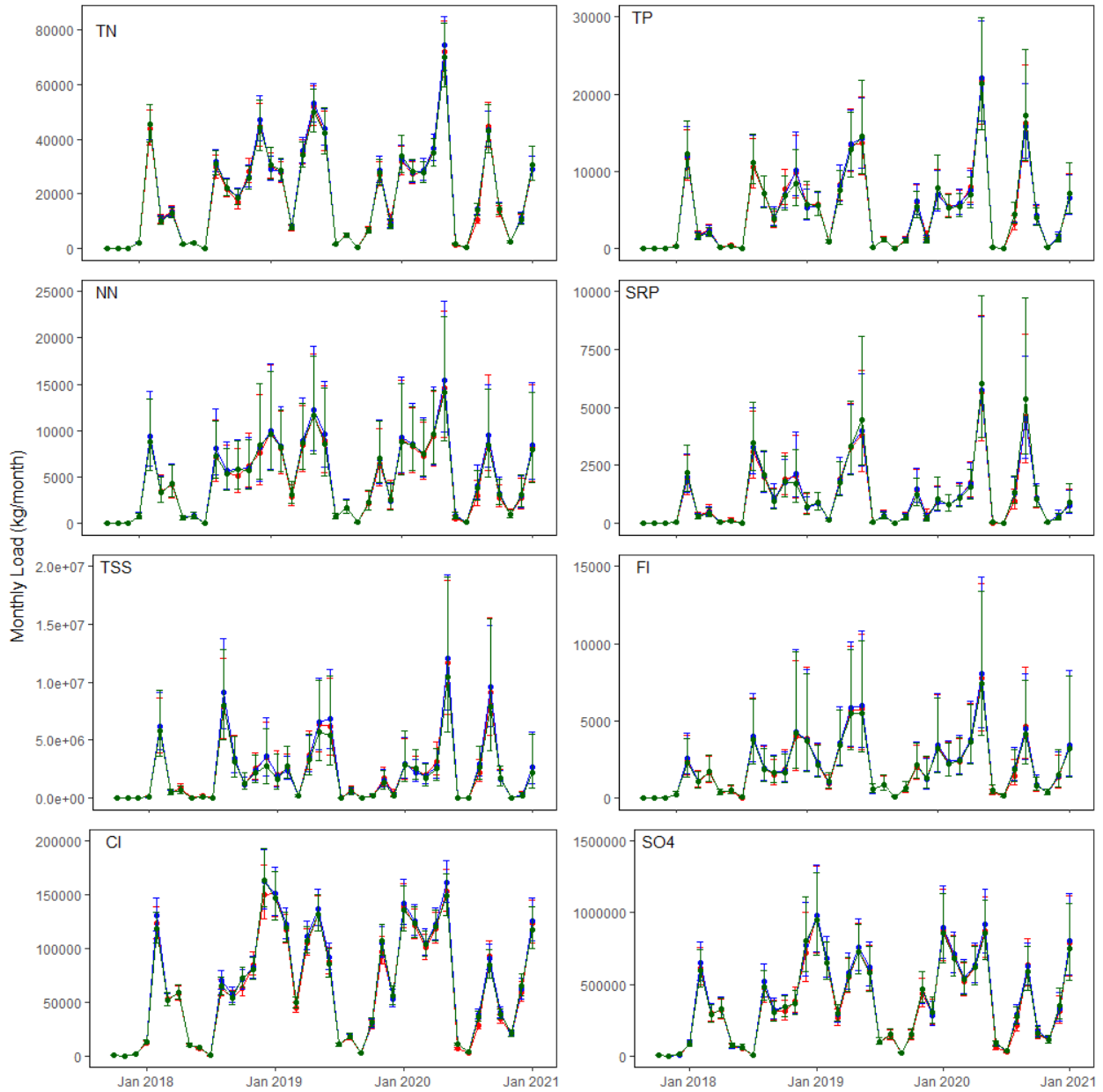


Site 15:

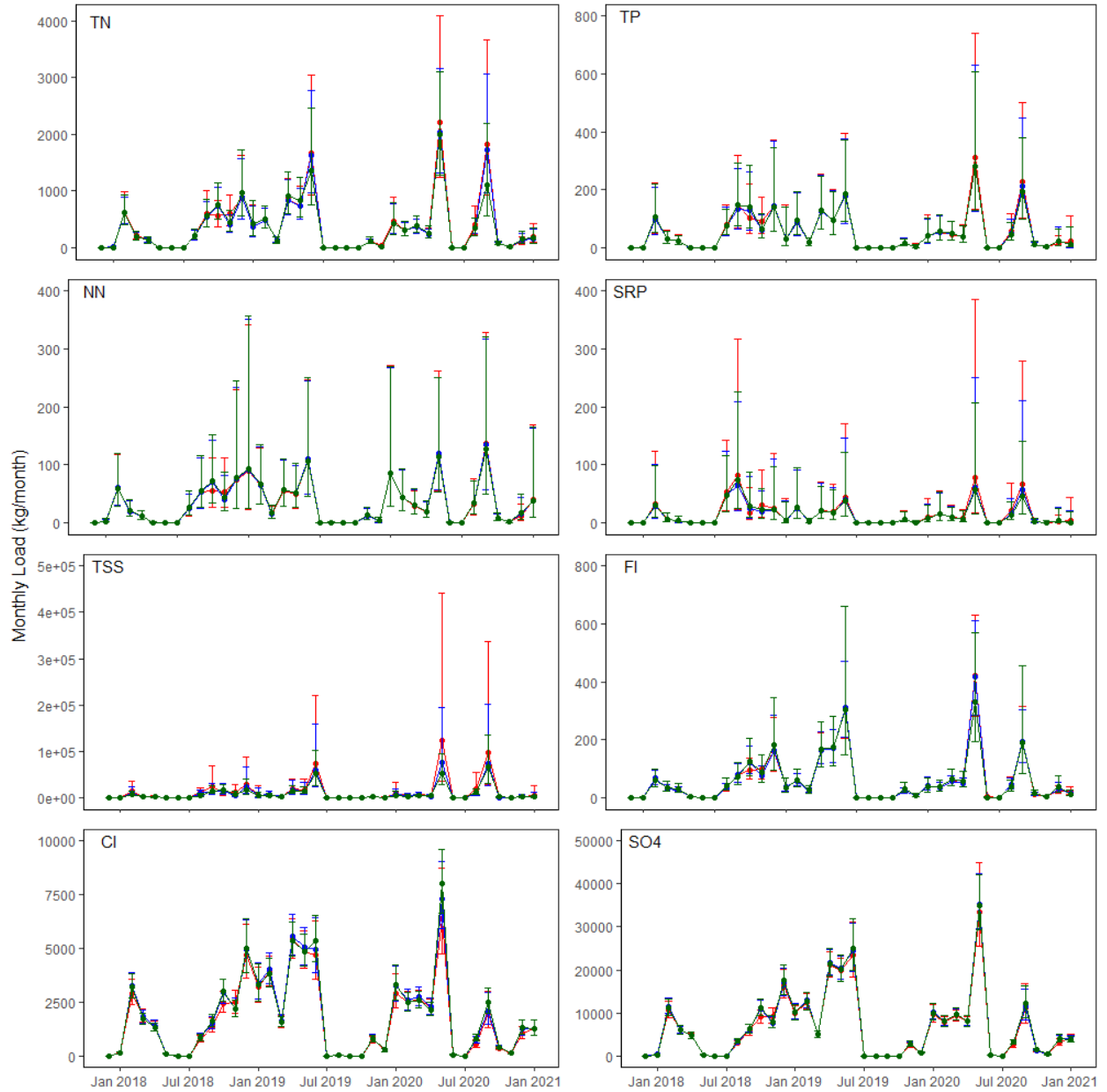


Appendix C: Monthly loads (kg/month) for each method (M1 = red, M2 = blue, and M3 = green) for total nitrogen (TN), nitrate plus nitrite (NN), total phosphorus (TP), soluble reactive phosphorus (SRP), total suspended solids (TSS), fluoride (Fl), chloride (Cl), and sulfate (SO_4^{2-}) at each site.

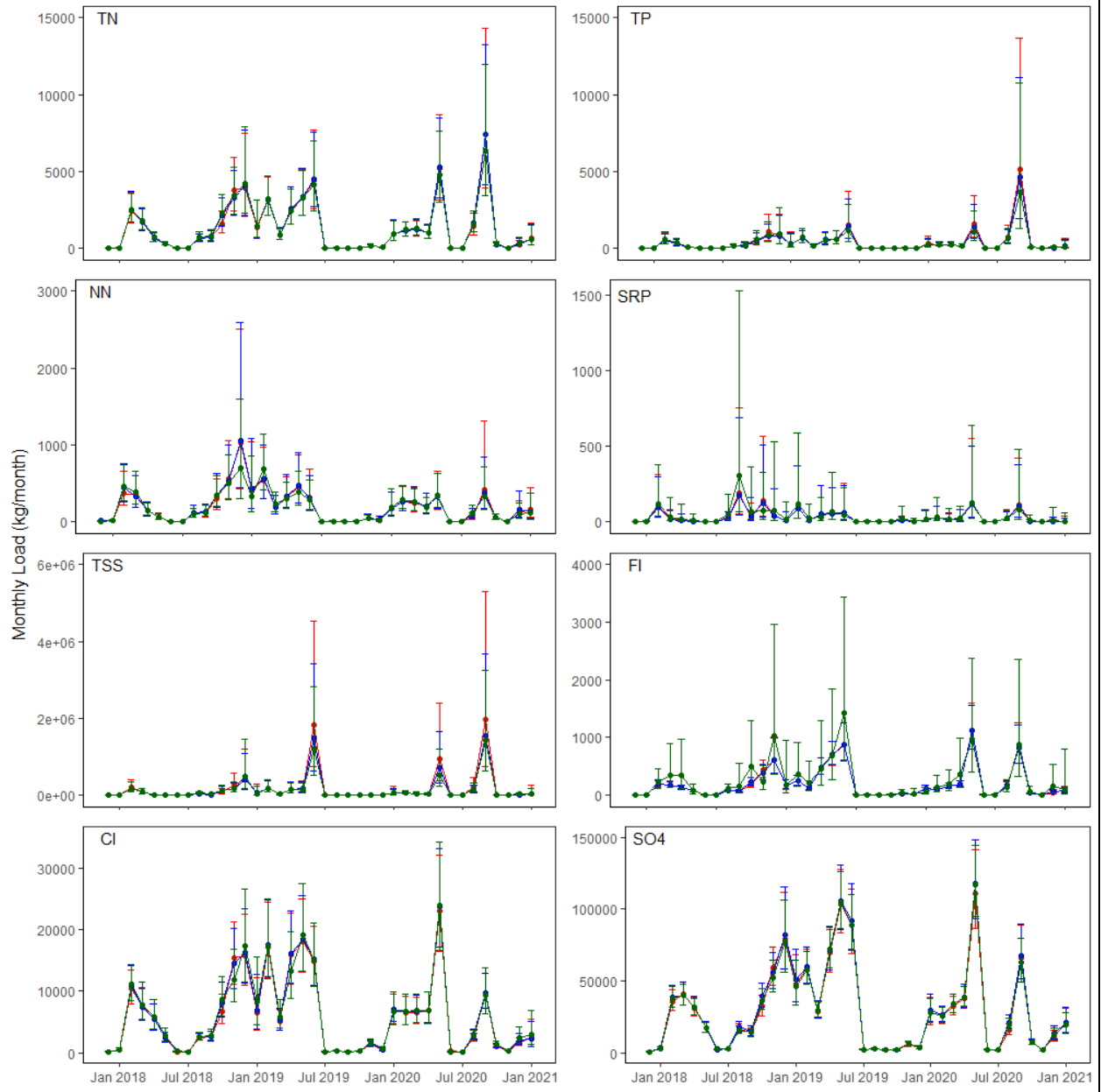
Site 1:



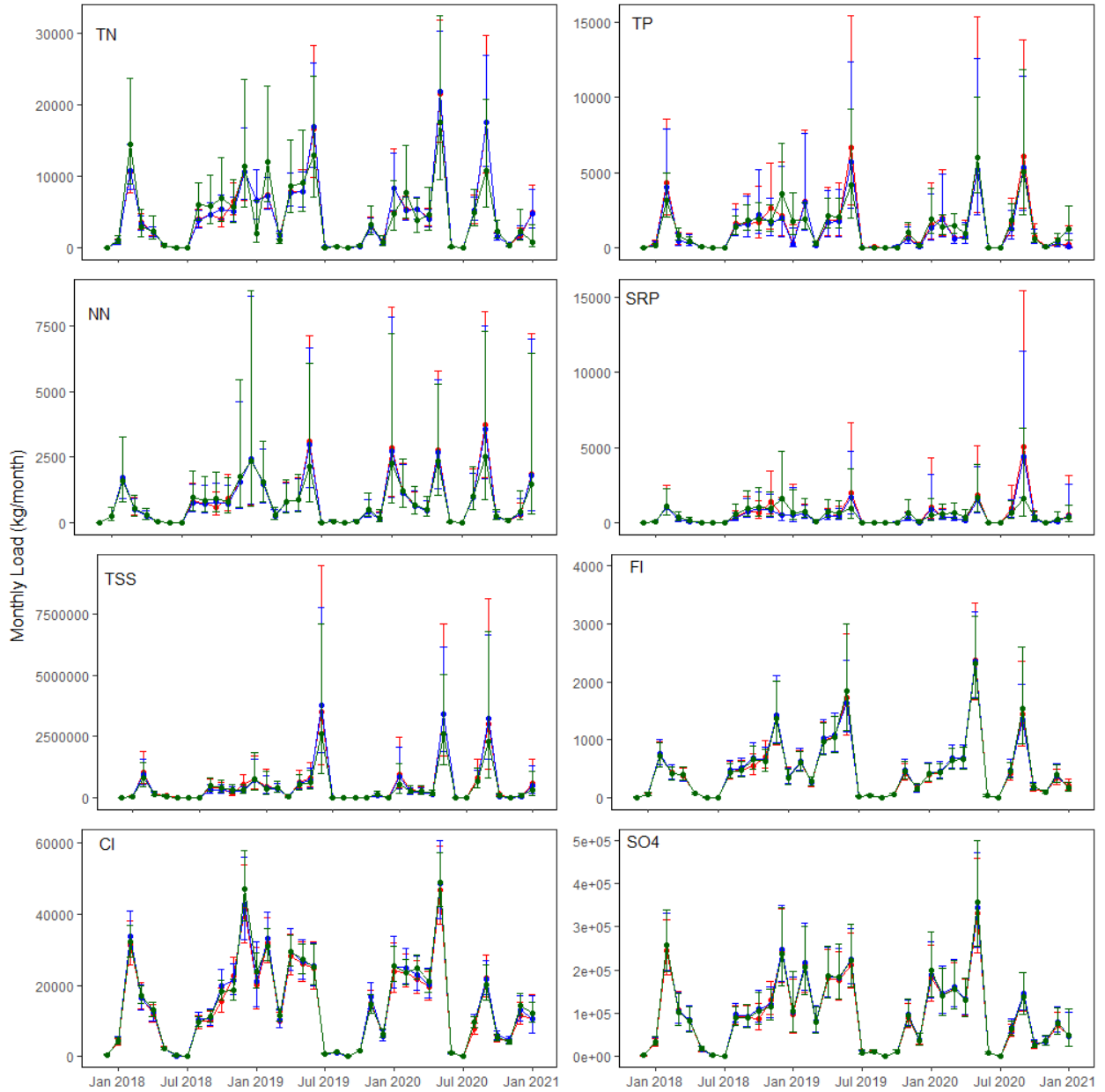
Site 4:



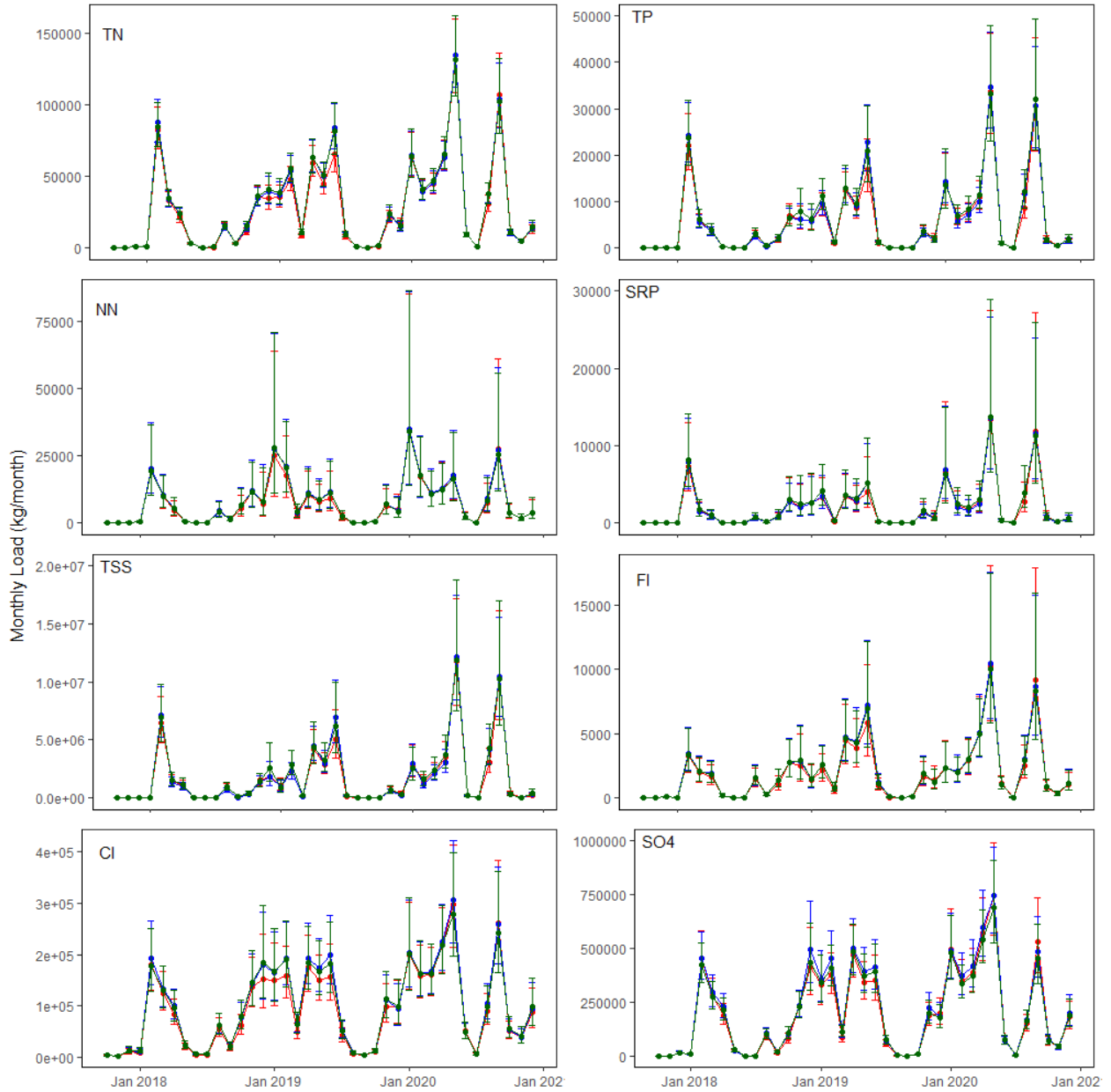
Site 5:



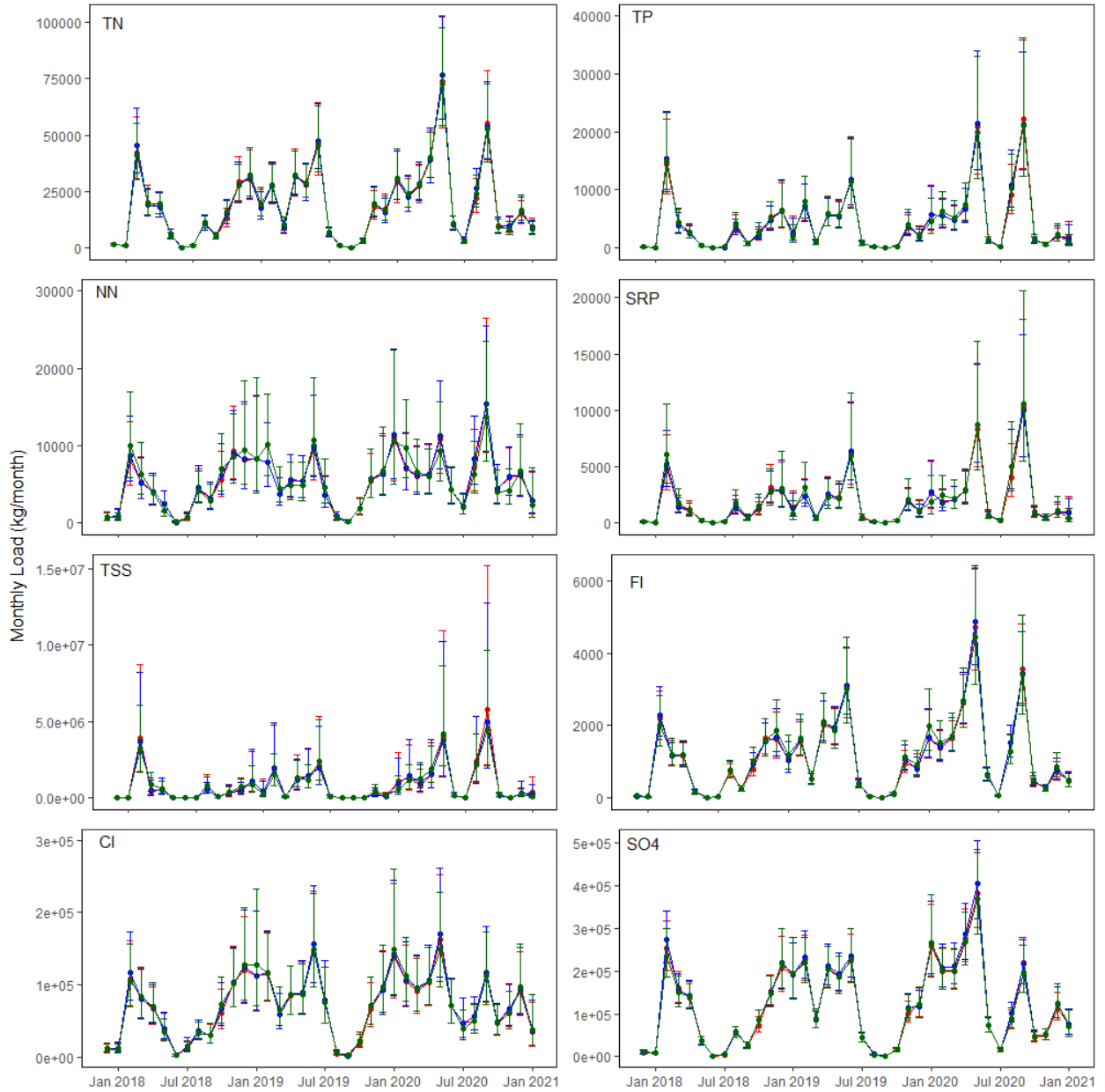
Site 6:



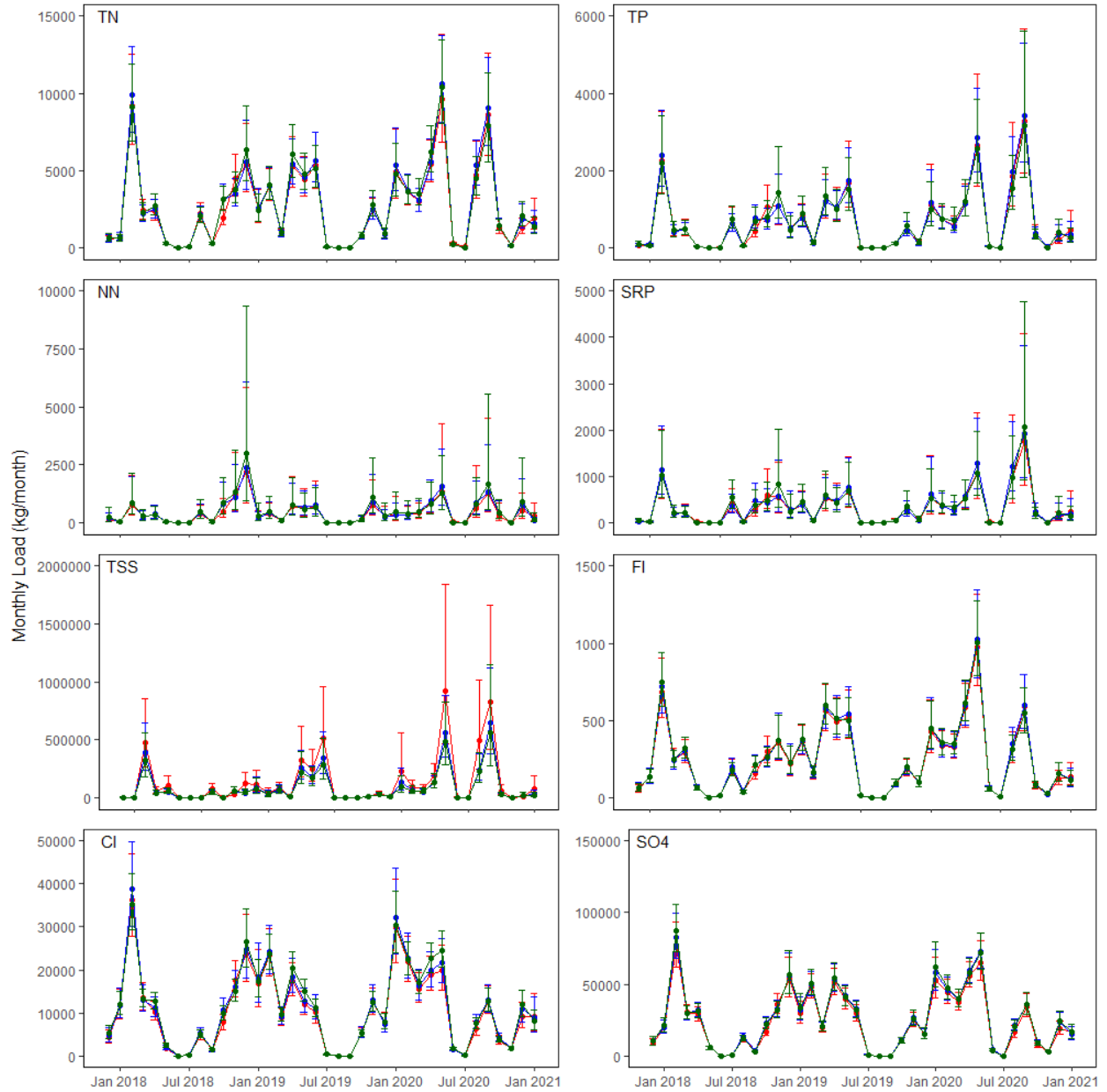
Site 8:



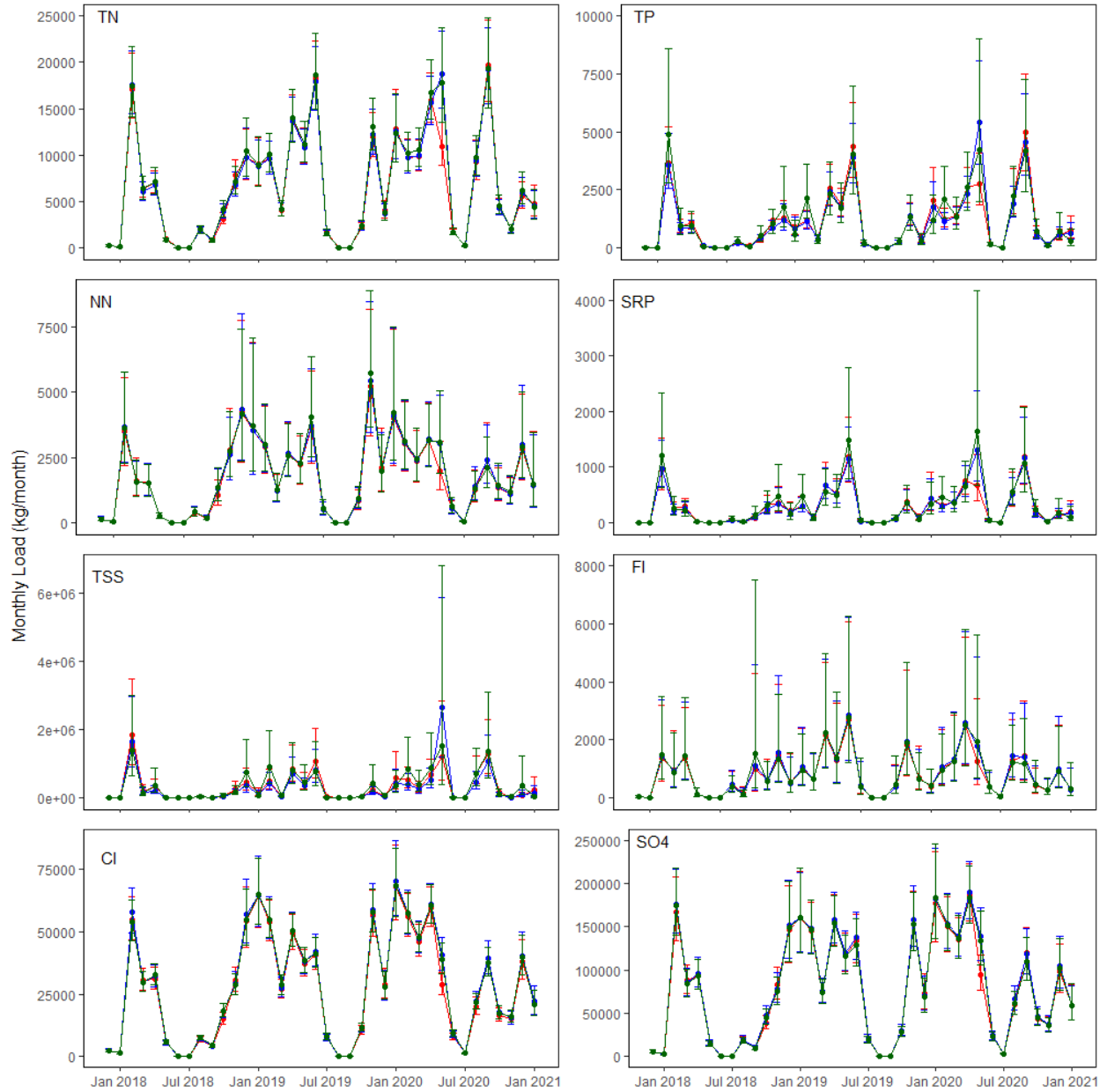
Site 9:



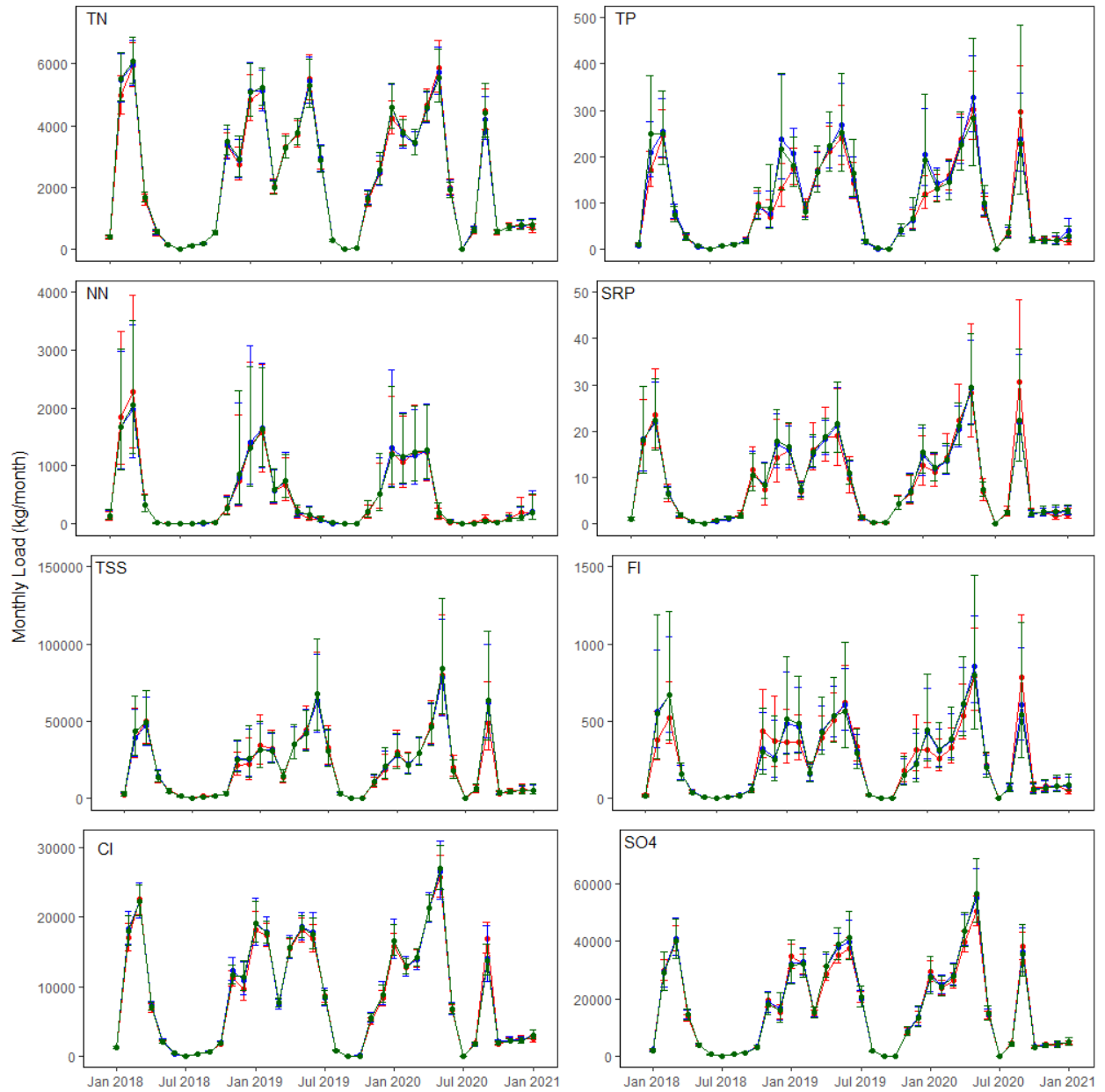
Site 10:



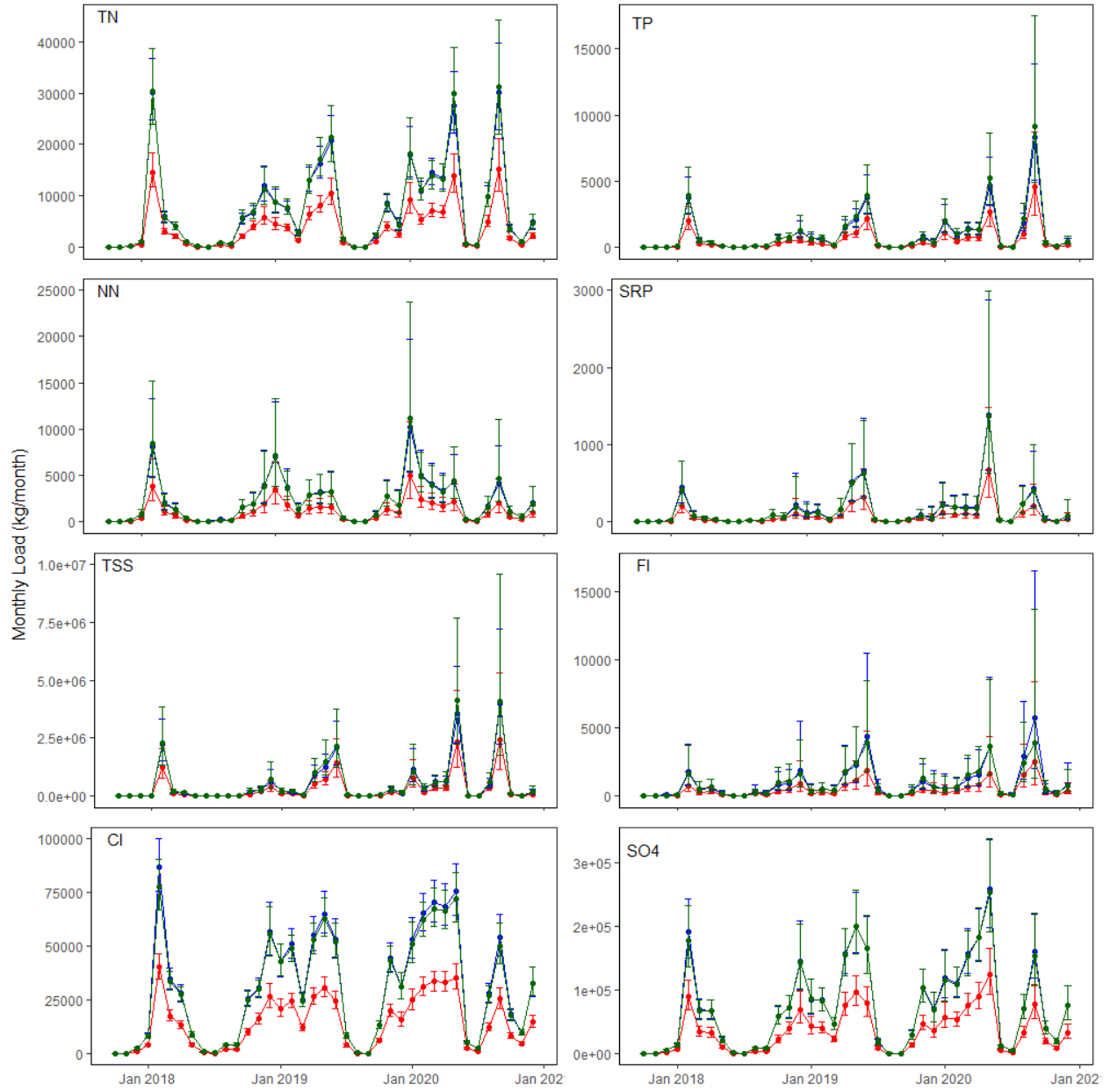
Site 11:



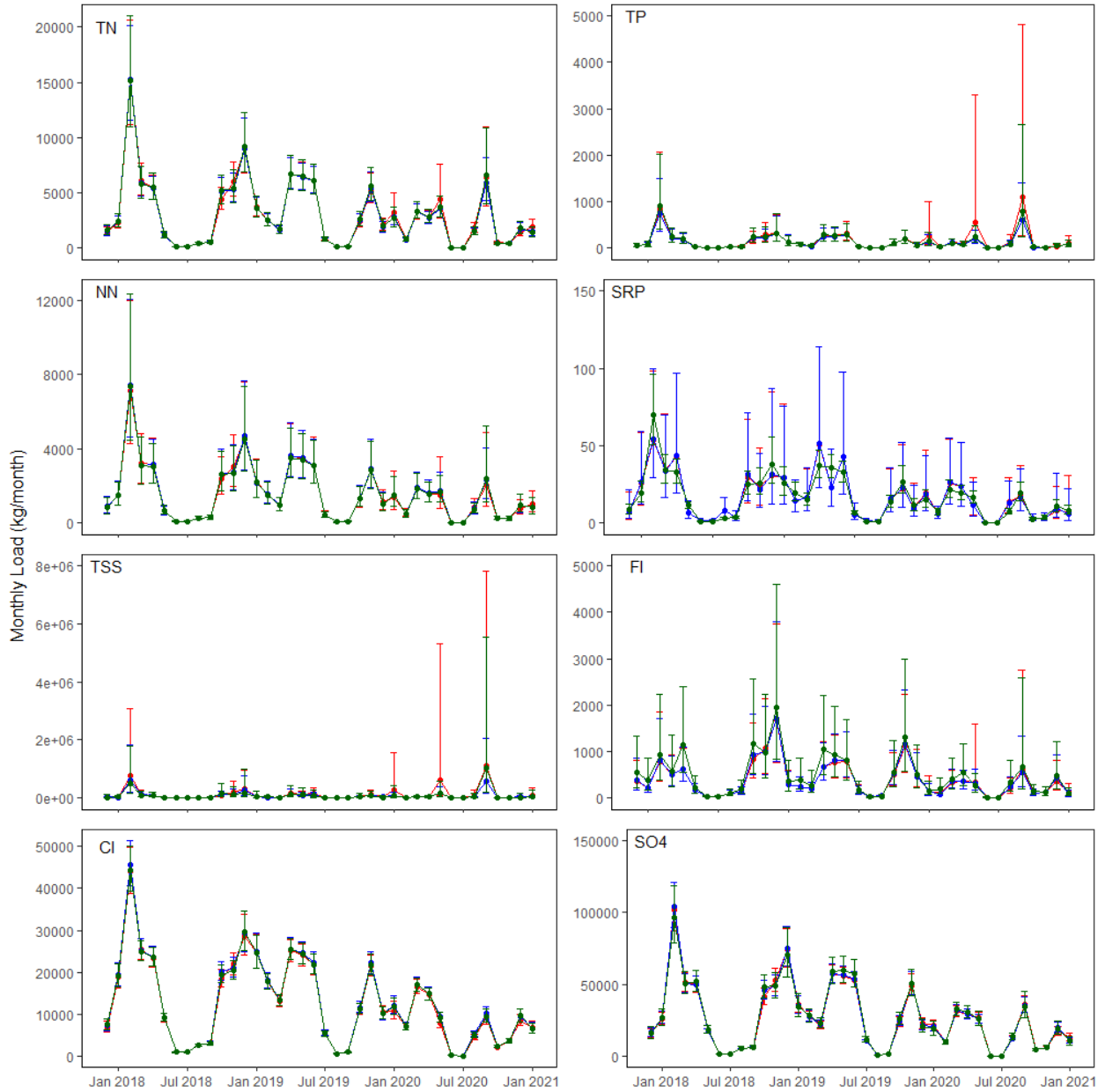
Site 12:



Site 14:

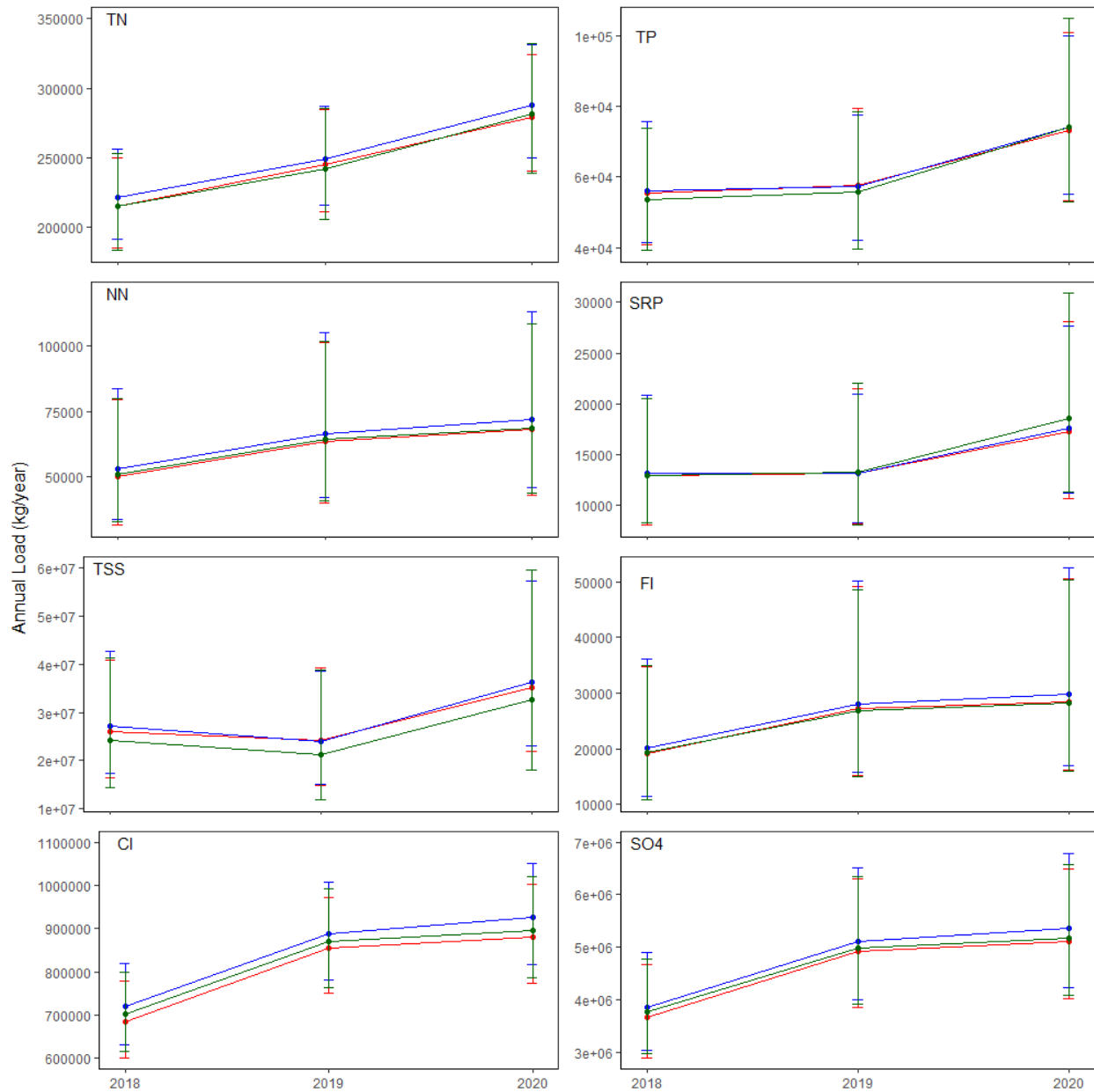


Site 15:

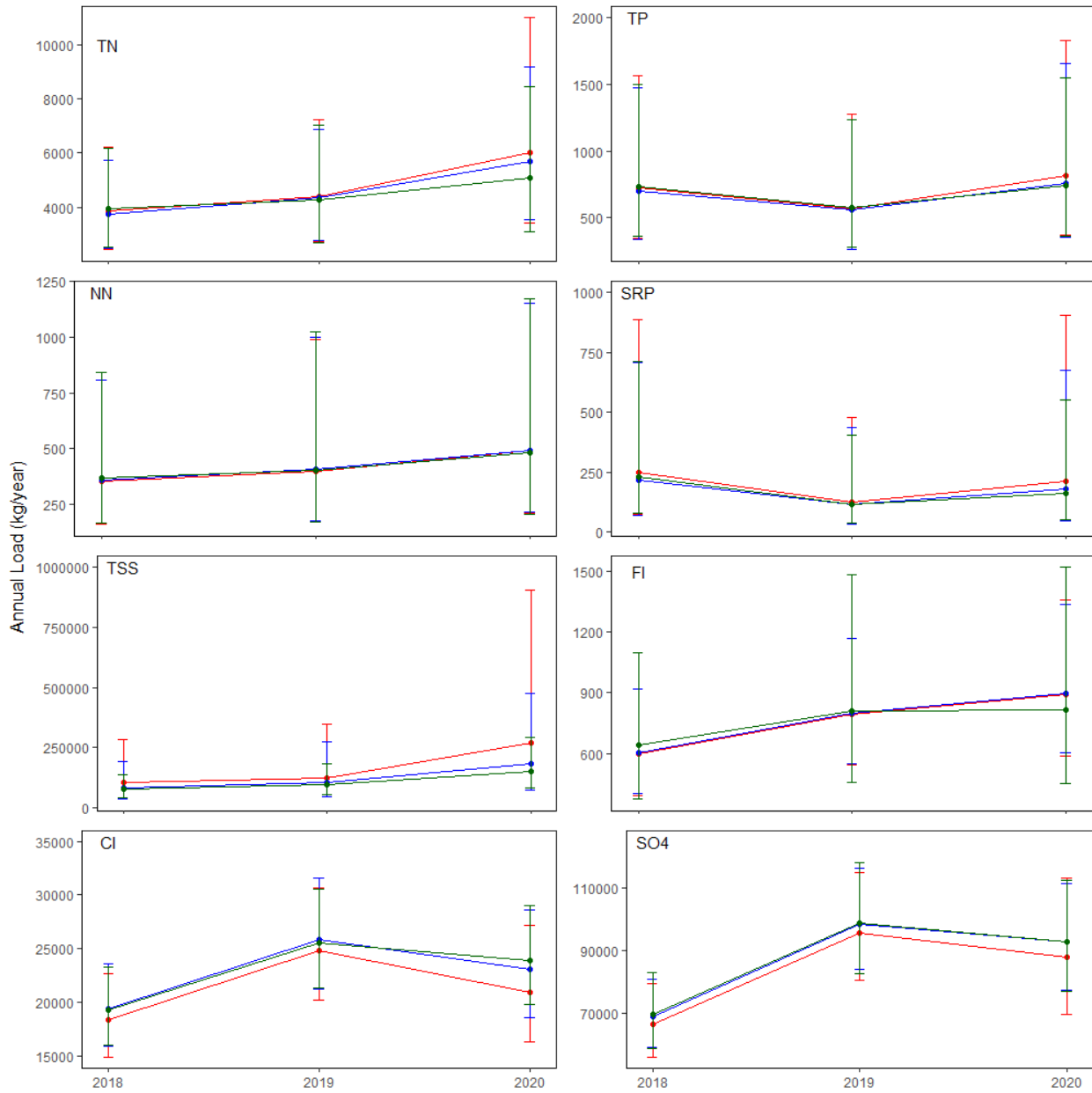


Appendix D: Annual loads (kg/year) for each method (M1 = red, M2 = blue, and M3 = green) for total nitrogen (TN), nitrate plus nitrite (NN), total phosphorus (TP), soluble reactive phosphorus (SRP), total suspended solids (TSS), fluoride (Fl), chloride (Cl), and sulfate (SO₄²⁻) at each site.

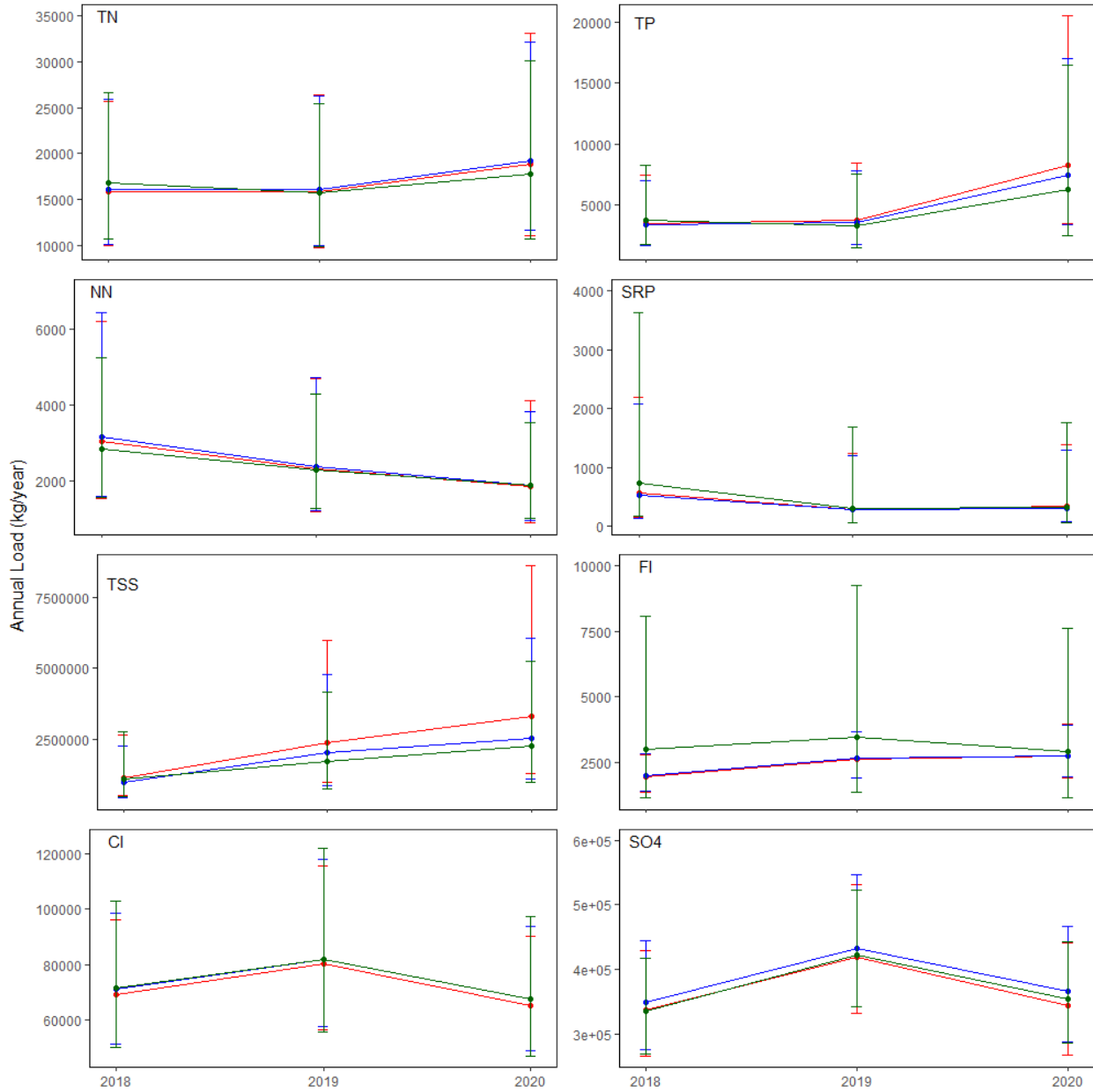
Site 1:



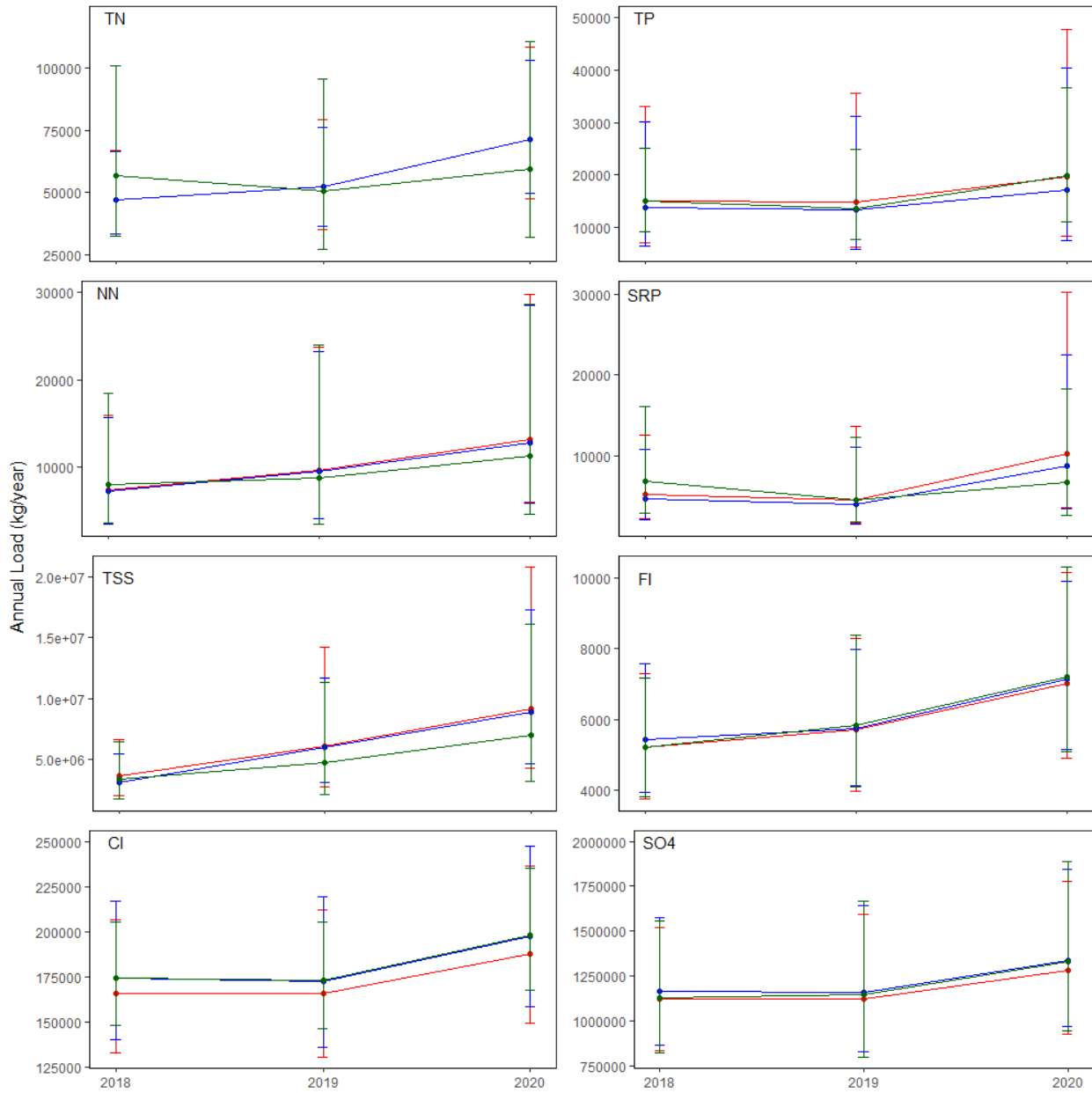
Site 4:



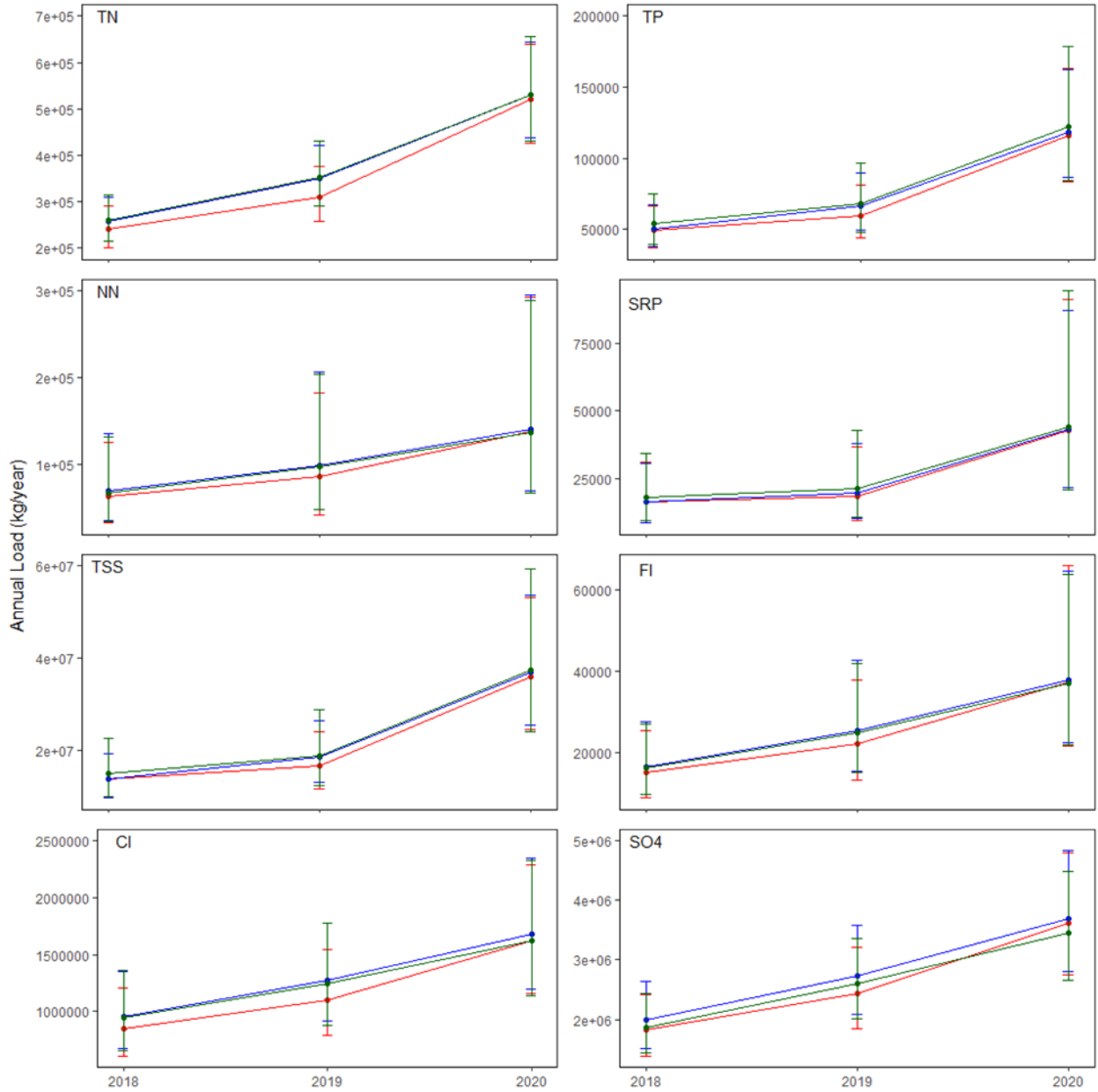
Site 5:



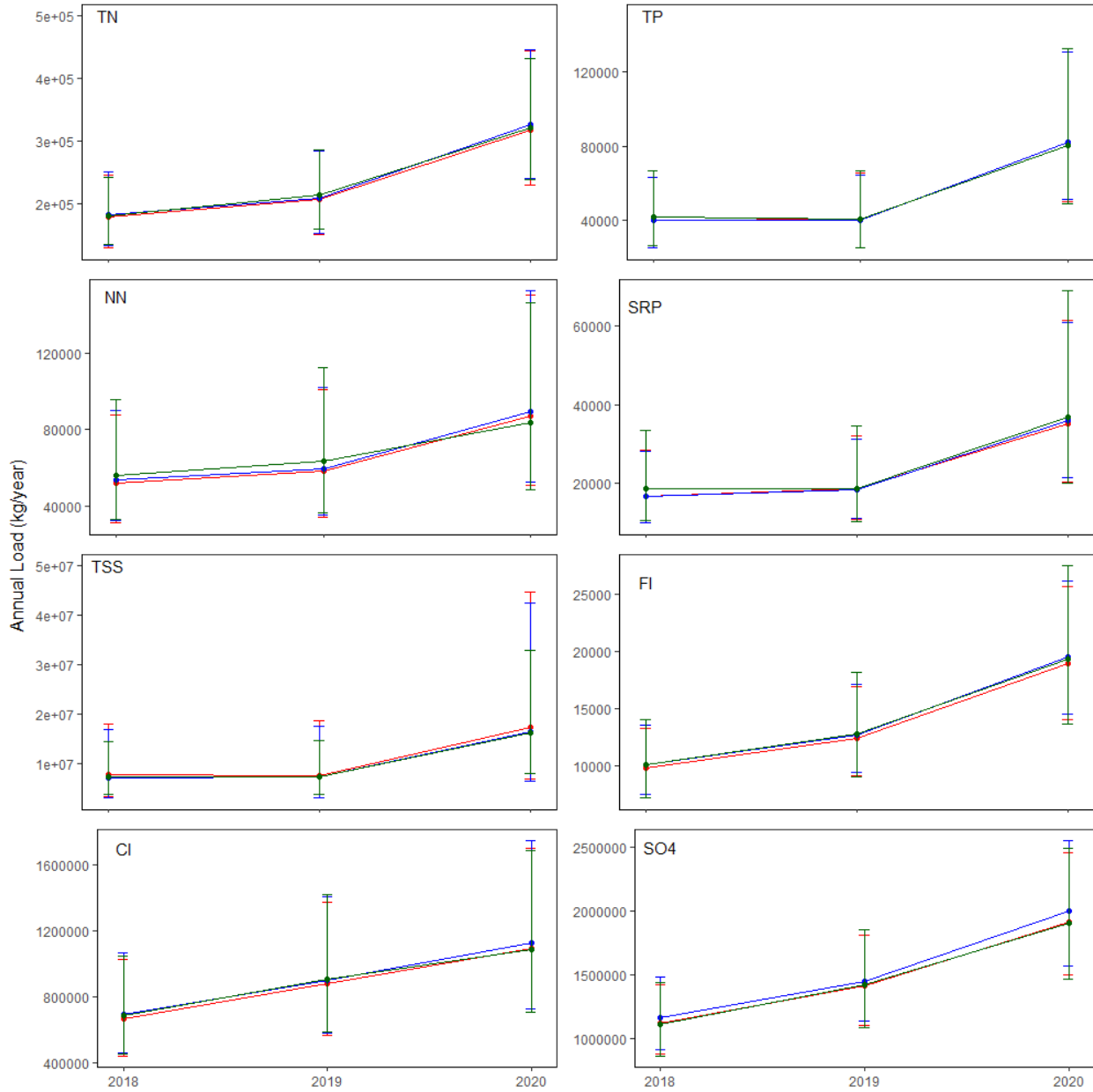
Site 6:



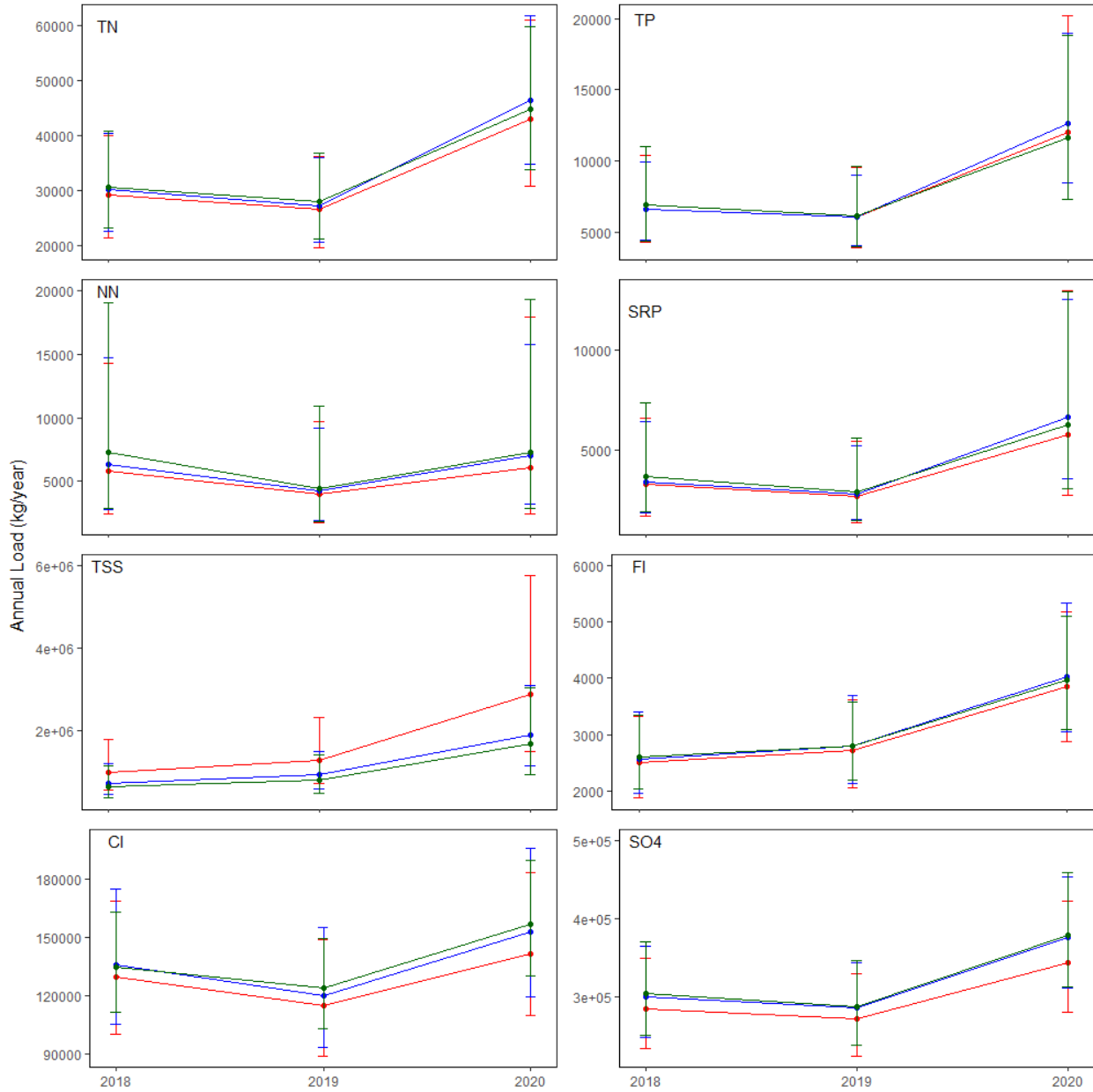
Site 8:



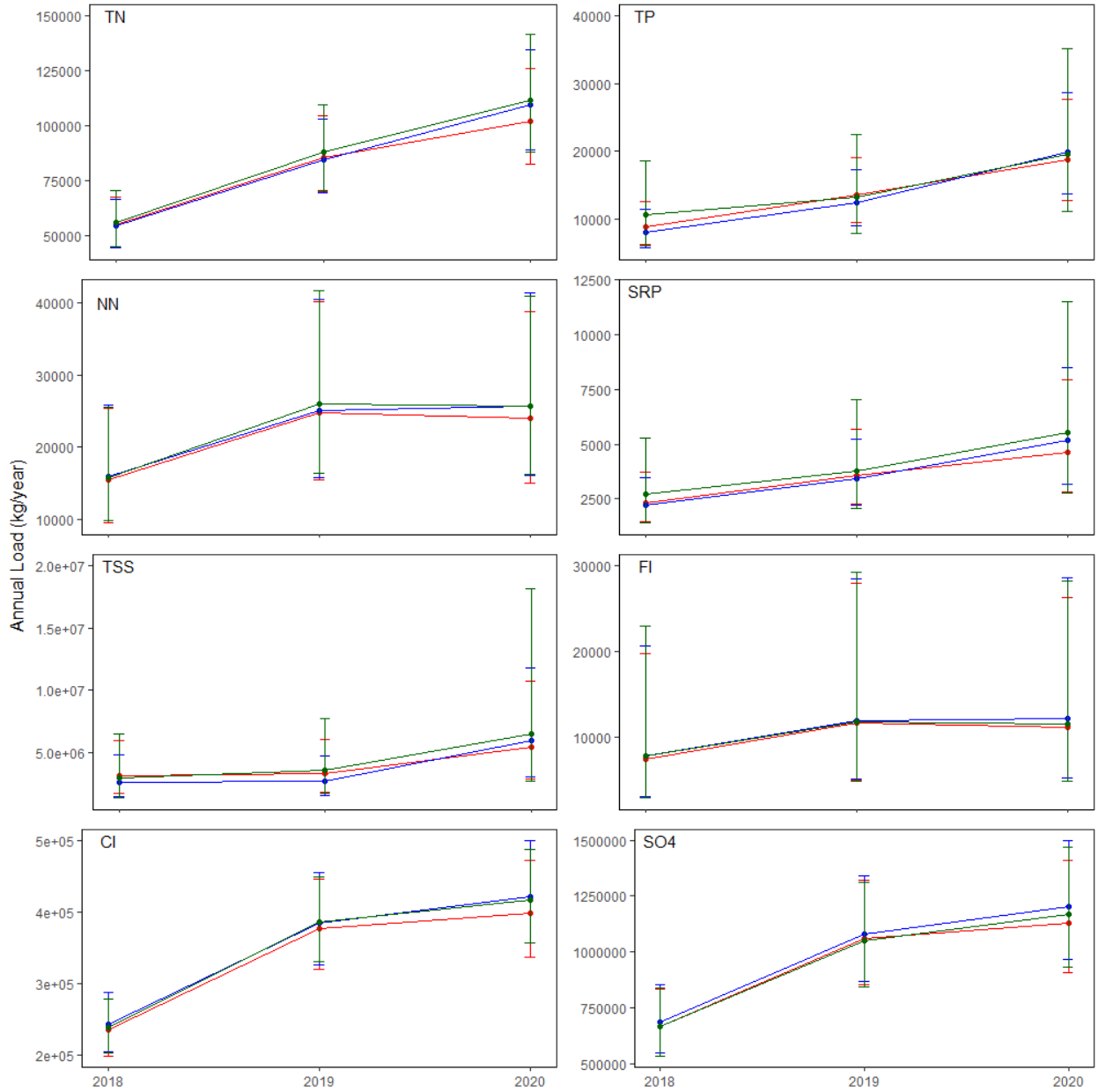
Site 9:



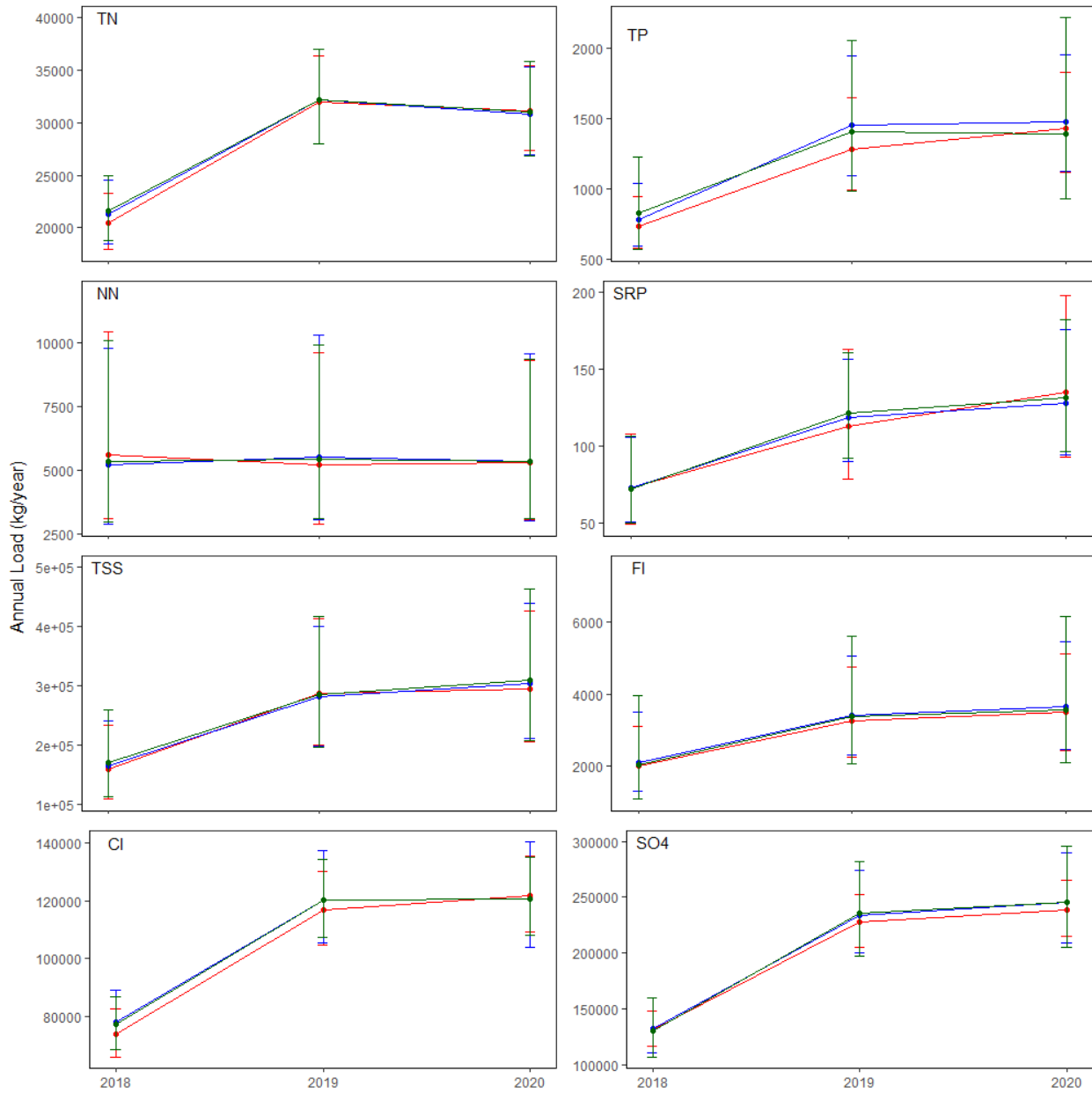
Site 10:



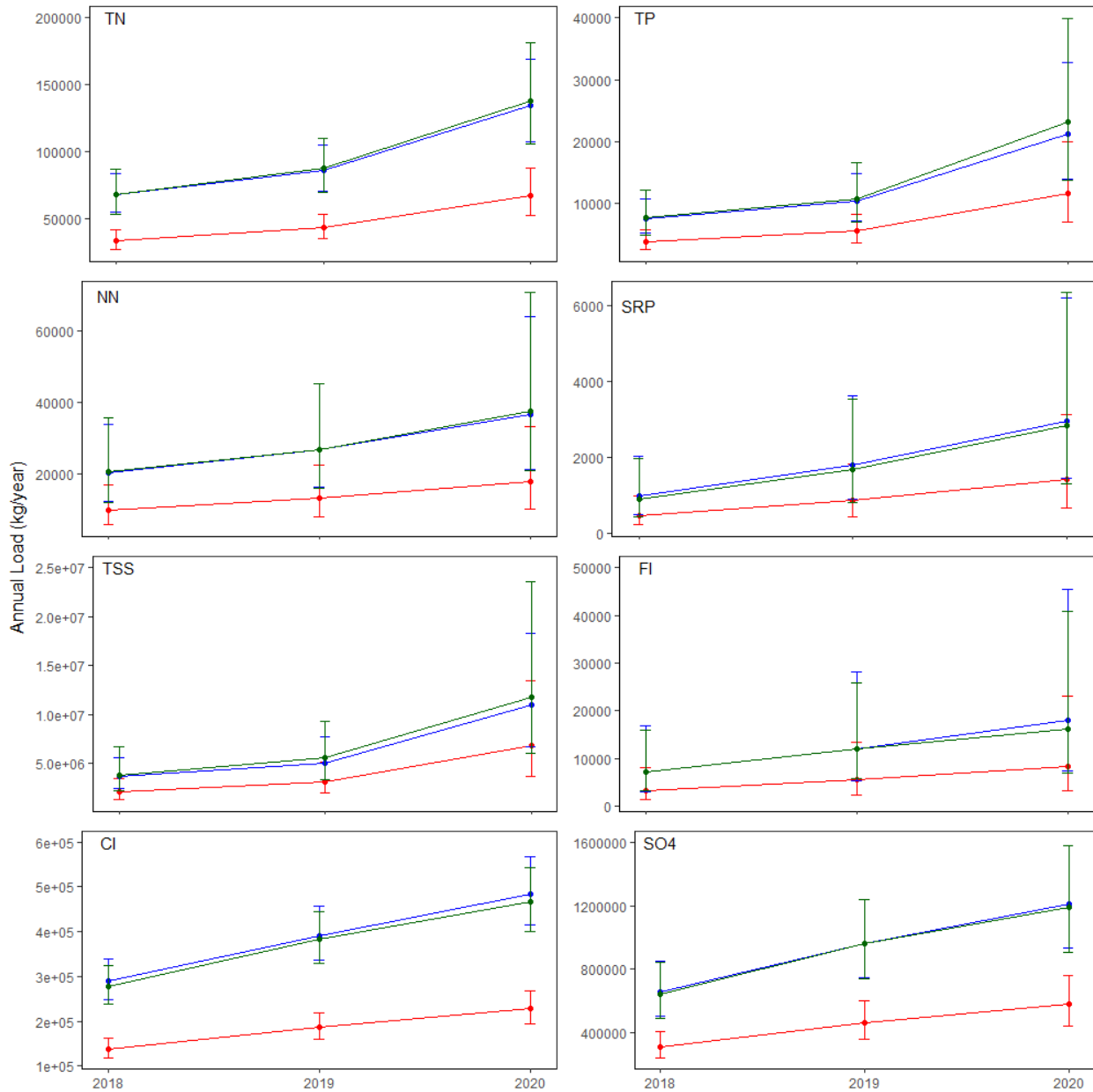
Site 11:



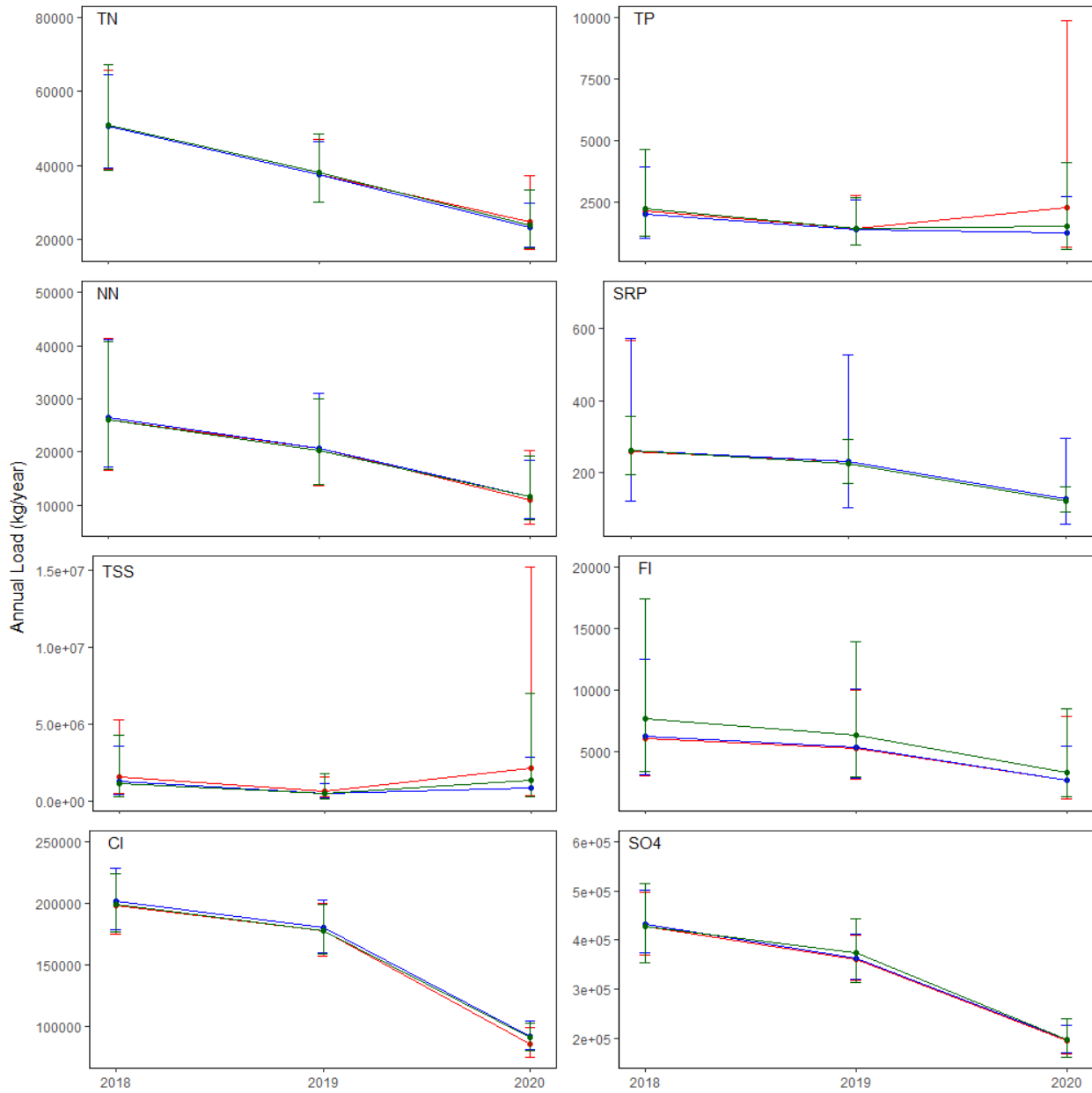
Site 12:



Site 14:



Site 15:



Chapter 6: Validation of the Soil Water Assessment Tool (SWAT) at Small-Scale Watersheds Mostly Unsatisfactory

Abbie Lasater¹, and Brian E. Haggard^{1,2}

¹Department of Biological and Agricultural Engineering, University of Arkansas, Fayetteville,
AR 72701

²Arkansas Water Resources Center, University of Arkansas, Fayetteville, AR 72701

Abstract

Due to cost and feasibility with water quality and discharge estimates, monitoring data is often limited or nonexistent on small-scale streams and watersheds. Therefore, watershed models are often calibrated on the subbasin scale or larger, constituent loads and flow conditions are predicted at the watershed scale or smaller, but data to calibrate or validate these small-scale model outputs are typically unavailable. The purpose of this study was to calibrate a SWAT model using larger watershed scale data (i.e., HUC-8/10) and validate the model with smaller watershed scale data (i.e., HUC-12/14), to analyze the ability of SWAT to predict flow and constituent loads at a small-scale watersheds where data is typically unavailable. Ultimately, the large-scale calibration was mostly satisfactory or better, but the small-scale validation was mostly unsatisfactory. With poor validation results at the HUC-12 and HUC-14 watershed scale, it is difficult to justify using the model outputs for subwatershed prioritization or other watershed modeling efforts (i.e., BMP evaluation and TMDL development). Therefore, it may be necessary to begin collecting more small-scale data for use in SWAT calibration/validation.

Introduction

Non-point source (NPS) pollution is a highly recognized threat to freshwater ecosystems, caused by diffuse sources transporting nutrients and sediments into waterbodies primarily through human alteration of landscapes (i.e., urban development and agricultural land use) (Daniel et al. 1998; Jonge et al. 2002; Sun et al. 2012). Fertilizers and other chemicals used in agricultural, residential and urban areas enter waterbodies through runoff and seepage, as well as sediments from construction sites and eroding streambanks. Excess inputs of nutrients and sediments jeopardize drinking water sources, aquatic life habitats, and aesthetic quality of freshwater ecosystems for recreation (Anderson et al. 2002). With increasing pressures of climate change and population growth, sustainable management of water resources becomes ever more imperative.

While point sources of pollutants are easily identified and highly regulated, NPS are more difficult to monitor and manage. In the 1987 amendment to the United States Clean Water Act, the scope of water quality improvements was expanded to NPS pollution, and states were required to develop management plans and implement programs to reduce runoff from agricultural lands, construction sites and urban areas (Copeland 2012). Since this initiative, there has been significant effort to accurately identify small-scale, diffuse pollutant sources for water quality improvement and best management practice (BMP) implementation (Katiyar et al. 2006; White et al. 2009; Tripathi et al. 2013).

Watershed prioritization is a process of ranking sensitive watersheds for applications of BMPs or restoration techniques, typically on the basis of subwatersheds within a larger watershed. Sensitive watersheds can include areas where ecosystem services need to be protected, where soil erosion rates are high, or where degradation is caused by human

disturbances (Malik and Bhat 2014; Fallah et al. 2016; Aguirre-Salado et al. 2017). Watershed modeling, especially the Soil Water Assessment Tool (SWAT), is a common technique used for subwatershed prioritization, where indicators such as sediment yield, nutrient loads, and land use help determine priority areas (White et al. 2009; Darwiche-Criado et al. 2017; Farhan et al. 2017; Ghafari et al. 2017). However, due to cost and feasibility with water quality and discharge estimates, monitoring data is often limited or nonexistent on small-scale streams and watersheds. Therefore, watershed models are often calibrated on the subbasin scale or larger, constituent loads and flow conditions are predicted at the watershed scale or smaller, but data to calibrate or validate these small-scale model outputs are typically unavailable (Pai et al. 2011b; Welde 2016; Chapter 4).

If small-scale model outputs are inaccurate, pollution sources and priority areas could be incorrectly identified, and time, effort, and funds invested in BMP implementation could be ineffective. Therefore, the purpose of this study is to calibrate a SWAT model using larger watershed scale data (i.e., HUC-8/10) and validate the model with smaller watershed scale data (i.e., HUC-12/14), to analyze the ability of SWAT to predict flow and constituent loads at a small-scale watersheds where data is typically unavailable.

Methods

Study Site Description

The Poteau River Watershed (HUC 11110105, PRW) originates on the western edge of Arkansas and flows into Oklahoma, south of the Arkansas River Valley (Figure 1). In Arkansas, the Poteau River Watershed drains an area of 1,400 km², which is 56% forested, 21% grassland, 19% transitional and 2% urban/suburban (Arkansaswater.org 2017). The headwaters of the

Poteau River originate near Waldron, Arkansas, flowing west into Oklahoma, near Loving, Oklahoma. The two main tributaries of the Poteau River within Arkansas are the Black Fork and the James Fork (to the south and north, respectively).

The PRW has been listed as a priority watershed within the Arkansas Nonpoint Source (NPS) Pollution Management plan since 1998, and thus has been the focus of trans-boundary water quality issues for the last several decades. Several reaches of the Poteau River have been identified as impaired on the 2018 303(d) list for dissolved oxygen, nutrients, anions and turbidity from municipal and industrial point sources and surface erosion (ADEQ 2018). The 2018-2023 NPS Pollution Management Plan aims at reducing pollutant loads in this priority watershed to decrease impairments and restore designated uses (ANRC 2018). For this study, water quality and streamflow data were collected from 8 sites on the outlets of HUC-12/14 subwatersheds and 3 sites at USGS stations on the outlets of HUC-8/10 subwatersheds within the Upper PRW (UPRW) (Figure 1, Table 1). Data collection methods are detailed in Chapter 5.

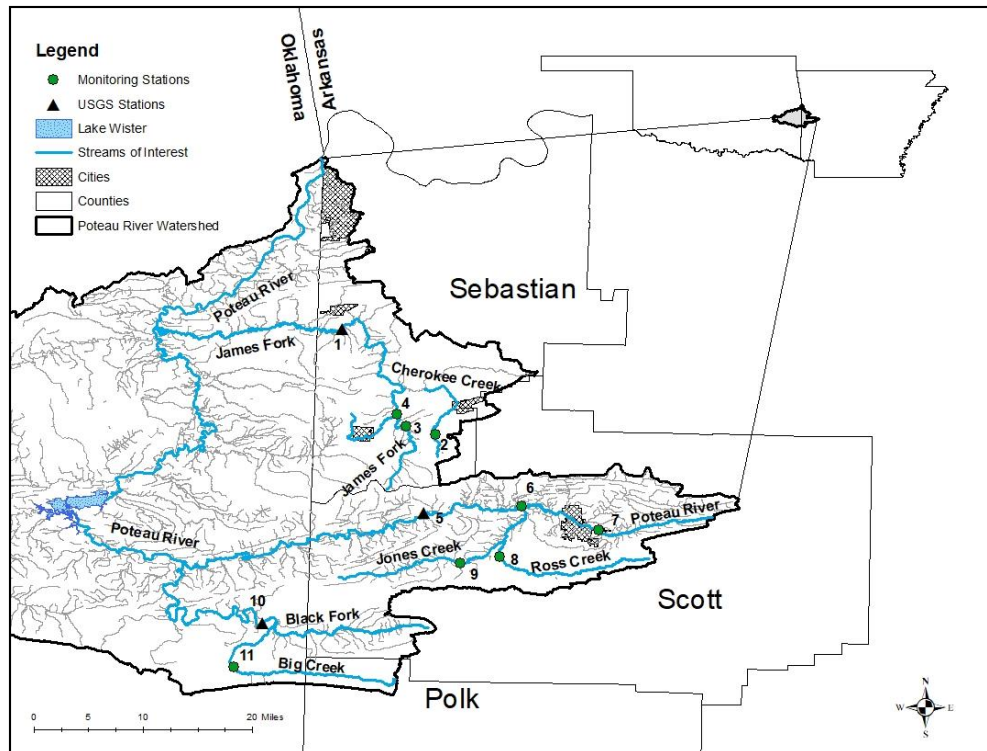


Figure 1: Monitoring sites in the Upper Poteau River Watershed in Arkansas; numbers near streamgages correspond to site ID's in Table 1.

Table 1: Monitoring site ID's (corresponding to Figure 1), names, locations, watershed areas, and land use in the Upper Poteau River Watershed.

Site ID	Site Name	Lat N	Long W	Watershed Area (km ²)	%F ¹	%U ²	%AG ³	%G ⁴
James Fork Watershed- HUC 1111010508								
1	USGS 07249400- James Fork	35 09.755	94 24.424	381	49.7	4.8	33.2	10.9
2	Cherokee Creek Headwaters	35 01.379	94 16.985	14	84.5	1.1	9.4	2.8
3	James Fork Headwaters	35 01.984	94 19.315	39	84.7	1.2	8.9	2.4
4	Lower James Fork	35 02.820	94 20.302	95	69.9	3.5	18.3	6.9
Headwaters Poteau River Watershed- HUC 1111010501								
5	USGS 07247000- Poteau River	34 55.129	94 17.918	527	63.7	5.6	21.3	7.8
6	Lower Poteau River	34 55.666	94 10.124	193	51.6	7.7	32.0	7.7
7	Poteau River Headwaters	34 53.769	94 03.975	39	52.7	5.5	33.1	8.6
8	Ross Creek	34 51.647	94 11.910	77	71.8	4.6	13.9	9.3
9	Upper Jones Creek	34 51.895	94 12.835	73	84.8	2.7	2.2	4.4
Black Fork Watershed- HUC 1111010502								
10	USGS 07247250- Black Fork	34 46.428	94 30.748	245	88.3	3.5	9.8	4.0
11	Big Creek	34 42.970	94 33.006	60	92.3	6.2	0.0	1.4

¹ % Forest (%F) includes deciduous, evergreen, and mixed forest; ² % Urban (%U) includes open space, low, medium and high intensity development; ³ % Agriculture (%Ag) includes pasture, hay, and cultivated crops; ⁴ % Grassland (%G) includes grassland and shrubs.

SWAT/QSWAT Model Description

The Soil Water Assessment Tool (SWAT) is a continuous-time, processed based river basin model used to assess nonpoint source problems around the globe (Gassman et al. 2007). SWAT operates on a basin scale and predicts the impacts of land management and agriculture on water resources. Primary components of the SWAT model include weather, hydrology, soil properties, plant growth, nutrients, pesticides, bacteria, pathogens and management practices. Watersheds are divided into subwatersheds in SWAT, and further divided into hydrologic response units (HRUs) to analyze water resources (Arnold et al. 2012). SWAT has been used for a variety of applications including total maximum daily load (TMDL) development (Borah et al. 2006), assessing effectiveness of conservation activities (Arabi et al. 2008), and prioritizing subwatersheds to address water quality issues (Pai et al. 2011b). QSWAT is a QGIS interface for SWAT and was used in this study (Dile et al. 2020).

QSWAT Model Setup

Topography of the UPRW was defined using a digital elevation map (DEM) at 10 m spatial resolution from the USGS National Elevation Dataset. The average elevation was 162 m, with a minimum of 120 m and a maximum of 812 m. The average slope across the watershed was about 11%, and 24% of the watershed fell within the 0-2% slope class, 33% of the watershed fell within the 2-8% slope class, and 43% of the watershed fell within the >8% slope class.

The entire PRW was simulated in QSWAT, since an individual outlet must be selected to delineate the watershed, but the focus of this study was on the upper portion of the watershed in Arkansas. A DEM-based approach was used to delineate subwatersheds and HRUs within the PRW. A threshold of 2 km² was used, which is the area required to form a stream (i.e., a cell in

QSWAT was made into a stream if it had at least the threshold area draining into it). Subbasins were defined as the areas draining into each stream reach, and a total of 1,313 subbasins were delineated in the PRW. QSWAT created HRUs using all unique combinations of soil, land cover, and slope in each subwatershed, with slope bands defined as 0-2%, 2-8%, and >8%. A threshold of 10 acres was used to merge non-dominant HRUs with dominant HRUs, and a total of 15,953 HRUs were generated across the PRW. Currently, there is no universally accepted method for HRU thresholds, but higher computational power is required with more HRUs. Therefore, there must be a balance between computational cost and representation of spatial variability across the watershed (Gitau 2003).

Land use and land cover data were obtained from the 2016 National Land Cover Database. Land use changes over time can be simulated in QSWAT to simulate processes such as runoff and pollutant loads in response to changes in land use. However, the period of interest for this study was 2017 to 2020, and land use data past 2016 was not available. Therefore, it was assumed that land use remained the same from 2016 through 2020.

Soil characteristics were obtained from the Soil Survey Geographic (SSURGO) soil database, as SSURGO is the most comprehensive soils database currently for Arkansas. The soil series are classified into hydrologic groups, and 23% of the watershed was group A, 62% of the watershed was group B, and 15% of the watershed was group D. Infiltration rates decrease as hydrologic groups move from A to D.

Weather data was obtained from the National Oceanic and Atmospheric Administration (NOAA) Climate Data Online (CDO) for years 2012 through 2020. Weather stations were located in Abbott, Waldron, and Fort Smith, Arkansas, where Waldron and Fort Smith contained precipitation and temperature data, while Abbott only contained precipitation data. An inverse

distance weighted spatial interpolation method was used by QSWAT to determine daily precipitation at the centroid of each subwatershed. Other climatic inputs including solar radiation, relative humidity, and wind velocity were generated by QSWAT's weather generator, and evapotranspiration was simulated using the Penman-Monteith method (Penman 1948; Monteith 1965).

Ponds were simulated in QSWAT using the National Hydrography Dataset from the USGS, identifying 10,894 ponds/waterbodies in the PRW. However, QSWAT only allows one pond per subwatershed, therefore, pond properties (i.e., surface area, volume, and drainage area) were aggregated for each subwatershed. Ponds were assumed to have a depth of 2 m, based on the average minimum depth of water (Deal et al. 1997), and were 75% full at the start of the simulation. Drainage areas of the ponds were assumed to be 0.00131 ha per m³ of storage of ponds (Deal et al. 1997; Saraswat et al. 2009).

Point sources identified and operating in the UPRW between 2012 and 2020 included waste water treatment plants (WWTPs) in Waldron, Huntington and Mansfield, and Tyson, Inc. in Waldron. The Waldron plants discharge into a tributary of the Poteau River upstream from monitoring site 6, and the Huntington and Mansfield WWTPs discharge into Cherokee Creek downstream of site 2. Point source effluent data were acquired from the Arkansas Department of Environmental Quality, which began prior to 2012, but only 2012 through 2020 was used for this study. The frequency of data varied across facilities, so to avoid bias, data were aggregated on an annual scale.

Constituents used to characterize point source inputs in QSWAT include flow, total suspended solids (TSS), organic and mineral phosphorus (P), ammonia (NH₃-), nitrate (NO₃-) and organic- nitrogen (N), carbonaceous biochemical oxygen demand (CBOD), and dissolved

oxygen (DO). Assumptions for point source effluents in Arkansas are described in Pai et al. 2011, where a review of nutrient forms in WWTP effluents was conducted. Total P (TP) effluent from WWTPs were assumed to be 20% organic and 80% inorganic P. Land application of sludge was not available, so it was not included in the model inputs. Nitrogen forms are typically reported as ammonia-nitrogen from point sources, so $\text{NO}_3\text{-N}$ and organic N were estimated based on a ratio of 4:75:21 for $\text{NH}_4\text{-N}:\text{NO}_3\text{-N}:\text{organic N}$ (Pai et al. 2011b). However, it is understood that assumptions in point source effluents produce uncertainty in the model.

The monitoring locations in the UPRW are mostly forested followed by agriculture land and urban area. Default forest management was used, where forests were considered mature without harvest or planting operations. Since urban areas were less than 8% across the watershed, default urban management was also used, where Bermuda grass growing season and fertilization were scheduled by heat units.

Pasture management practices are outlined in Pai et al. 2011 for Benton and Washington counties in Arkansas, and these methods for grazing and poultry litter application were adapted for Scott, Sebastian and Polk counties in this study. In 2017, the total cattle population in Scott, Sebastian and Polk counties were 21,968, 27,875, and 37,916, respectively (USDA-NASS 2018). Based on the percentage of watershed falling within each county, the watershed cattle population was 8,809, 9,756, and 834 in Scott, Sebastian and Polk counties, respectively. Intake averages while grazing on Bermuda were 10.88 kg d^{-1} and 10.43 kg d^{-1} while grazing on Tall Fescue. Total daily consumption rate of grass in a subwatershed was obtained by multiplying the daily consumption rate by the number of cows in each subwatershed, and then divided by the pasture area to obtain grazing density ($\text{kg day}^{-1} \text{ ha}^{-1}$). Grazing densities were 5.2, 5.7, and $0.5 \text{ kg day}^{-1} \text{ ha}^{-1}$ for Scott, Sebastian, and Polk counties, respectively (Table 2). Grazing was scheduled for

105 days starting May 15, 59 days starting October 1, and 43 days starting March 1. Manure deposition was estimated at 4.32 kg day⁻¹, which was converted to 2.0, 2.3, and 0.2 for Scott, Sebastian, and Polk counties, respectively (Table 2). Poultry litter was uniformly applied across pasture area at a rate of 2.6 Mg ha⁻¹ year⁻¹ (Sharpley et al. 2009).

Three to 5 years of warmup is typical for SWAT model simulations (Rostamian et al. 2008; Pai et al. 2011b; Bressiani et al. 2015; Mengistu et al. 2019). Historic weather data (prior to 2012) was used to run QSWAT with a variety of warmup periods in the PRW. Five years of warmup did not produce different results for total flow and constituent loads compared to lengths longer than 5 years (i.e., up to 30 years where weather data was available). Therefore, the model was run from 2012 to 2020, with the first 5 years as warmup.

QSWAT Model Sensitivity Analysis, Calibration, and Validation

Sensitivity analysis, calibration, and validation of the SWAT model was conducted using the SWAT-Calibration and Uncertainty Program (SWAT-CUP). SWAT models contains a large number of calibration parameters, so it is important to identify parameters that greatly impact the outputs. Therefore, a global sensitivity analysis was done using the Latin hypercube (LH) method in SWAT-CUP, where a t-test is used to identify the relative significance of each parameter, and then the parameters are ranked from least to most sensitive. Sensitivity analyses were conducted individually for each site and constituent of interest with a total of 53 parameters used across the literature for SWAT calibration (Appendix A) (Santhi et al. 2001; White and Chaubey 2005; Ahl et al. 2008; Ndomba et al. 2008; Saraswat et al. 2013; Shawul et al. 2013; Wallace et al. 2018; Mengistu et al. 2019).

Calibration was conducted using daily flow and constituent loads (i.e., TP, TN, and TSS) at each monitoring location between 2018 and 2020. Streamflow was calibrated first, followed by sediment, then TN and TP. Some calibration parameters are at the whole watershed scale (Appendix A) and had to be manually adjusted to minimize error across the calibration sites (e.g., parameters related to sediment routing, ADJ_PKR and SPCON). Similarly, some calibration parameters impacted multiple outputs (e.g., flow and sediments) and had to be manually adjusted to minimize error across outputs. All three years of data were used for calibration and validation. While more years of monitoring data may improve model performance, several studies have used three year calibration/validation techniques in SWAT due to data availability (Reungsang et al. 2007; Karamouz et al. 2008; Andrade et al. 2013). To test the significance of the small-scale watershed data, the SWAT model was calibrated on the larger scale (i.e., the 3 USGS gauges) and validated at the small-scale (HUC-10/HUC-12 subwatersheds, remaining 8 sites). Calibration and validation was evaluated based on recommended model evaluation statistics (i.e., Nash-Sutcliffe efficiency (NSE), percent bias (PBIAS), and the root mean square error standard deviation ratio (RSR). Additionally, daily observed and simulated outputs (i.e., flow, sediment, TN and TP) were summed on a monthly and annual time scale and compared with NSE, PBIAS, and RSR values. Thresholds and their evaluation criteria (Table 2) will be used for each statistic (Moriassi et al. 2007). This information was used to determine the ability of SWAT to predict flow and constituent loads in small-scale watersheds (i.e., HUC-10/HUC-12).

Table 2: Performance ratings for evaluating model results (Moriassi et al. 2007)

Rating	NSE	RSR	PBIAS (%)		
			Flow	Sediment	TN, TP
Very Good	0.75 - 1.00	0.00 - 0.50	$\leq \pm 10$	$\leq \pm 15$	$\leq \pm 25$
Good	0.65 - 0.74	0.51 - 0.60	$\pm 10 - \pm 15$	$\pm 15 - \pm 30$	$\pm 25 - \pm 40$
Satisfactory	0.50 - 0.64	0.61 - 0.70	$\pm 16 - \pm 25$	$\pm 31 - \pm 55$	$\pm 41 - \pm 70$
Unsatisfactory	< 0.50	> 0.70	$> \pm 25$	$> \pm 55$	$> \pm 70$

Results

Calibration at Site 1

The top five sensitive parameters for flow, sediments, TN and TP at Site 1 (Table 3) were used as starting points for calibration. For streamflow, the top five parameters were related to groundwater, stream channel, and overland flow processes and included the baseflow alpha factor (ALPHA_BF), hydraulic conductivity in the main channel alluvium (CH_K2), Manning's n for the main channel (CH_N2) curve number (CN2), and Manning's n for the overland flow (OV_N), and were all adjusted on the HRU or subwatershed scale based on the calibrated value (Table 3). Daily streamflow calibration was considered satisfactory (Table 4, Figure 2), while monthly and annual comparisons were unsatisfactory (Table 4, Figures 3 and 4). The lowest model performance occurred at Site 1 (Table 4) compared to the other calibration sites, and flows were typically over predicted within the lower range of flows.

Table 3: Top five sensitive parameters (descriptions in Appendix A) for each process (flow, sediments, total nitrogen (TN), total phosphorus (TP)), calibration method, and calibrated values at Site 1.

Process	Top 5 Sensitive Parameters	Calibration Method*	Calibrated Value
Flow	ALPHA_BF	Replace	0.996
	CH_K2	Replace	119.9
	CH_N2	Replace	0.020
	CN2	Relative	-0.099
	OV_N	Relative	0.459
Sediments	USLE_K	Replace	0.776
	USLE_P	Replace	0.743
	ADJ_PKR	Replace	2.620
	BIOMIX	Replace	0.145
	SPCON	Replace	0.018
TN	NPERCO	Replace	0.198
	CDN	Replace	2.610
	SOL_CRK	Replace	0.670
	SDNCO	Replace	0.110
	ERORGN	Replace	0.830
TP	P_UPDIS	Replace	39.00
	PHOSKD	Replace	101.0
	SOL_BD	Replace	1.316
	ERORGP	Replace	0.960
	RS5	Replace	0.006

*Calibration methods in SWAT-CUP are either relative (parameter is multiplied by 1 + calibrated value), replace (parameter is replaced by calibrated value), or additive (calibrated value is added to parameter).

Table 4: Calibration statistics at Site 1 for each constituent (flow, sediments, total nitrogen (TN), total phosphorus (TP)) and average simulated and observed values on the daily, monthly and annual scale.

Scale	Process	NSE	PBIAS	RSR	Average Simulated	Average Observed
Daily	Flow (cms)	0.52	30.2	0.69	9.9	7.6
	Sediments (tons)	0.29	-40.2	0.84	50.1	83.8
	TN (kg)	0.32	0.2	0.82	652.0	650.5
	TP (kg)	0.48	-0.3	0.72	164.0	164.7
Monthly	Flow (cms)	0.48	30.2	0.71	302	231
	Sediments (tons)	0.38	-40.4	0.77	1519	2551
	TN (kg)	0.24	0.2	0.87	19851	19803
	TP (kg)	0.70	-0.3	0.54	4996	5014
Annual	Flow (cms)	-0.24	30.2	0.91	3634	2782
	Sediments (tons)	-2.50	-40.4	1.53	18312	30618
	TN (kg)	-0.85	0.2	1.11	238212	237643
	TP (kg)	0.77	-0.3	0.39	59961	60169

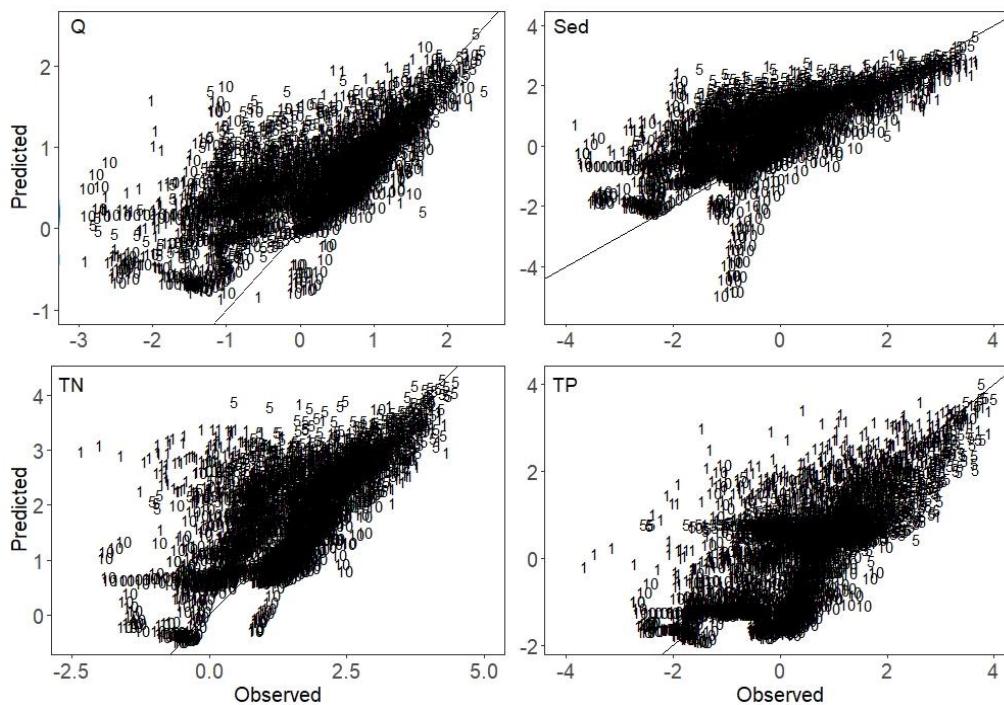


Figure 2: Observed daily streamflow, sediment, total nitrogen (TN), and total phosphorus (TP) loads versus SWAT simulated values at calibration sites; numbers represent Site IDs listed in Table 1.

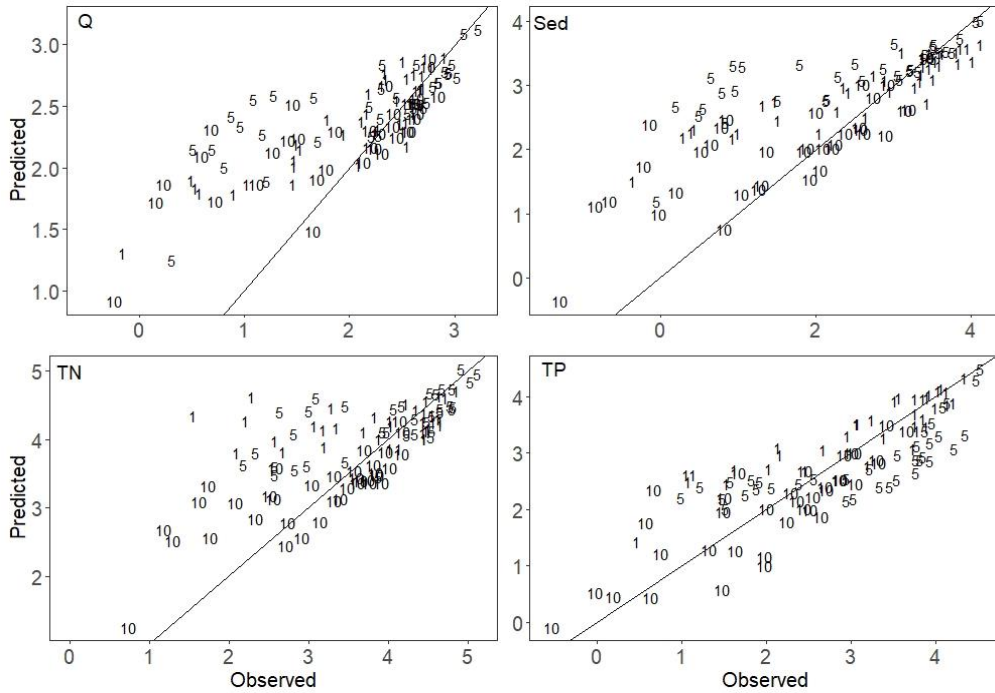


Figure 3: Observed monthly streamflow, sediment, total nitrogen (TN), and total phosphorus (TP) loads versus SWAT simulated values at calibration sites; numbers represent Site IDs listed in Table 1.

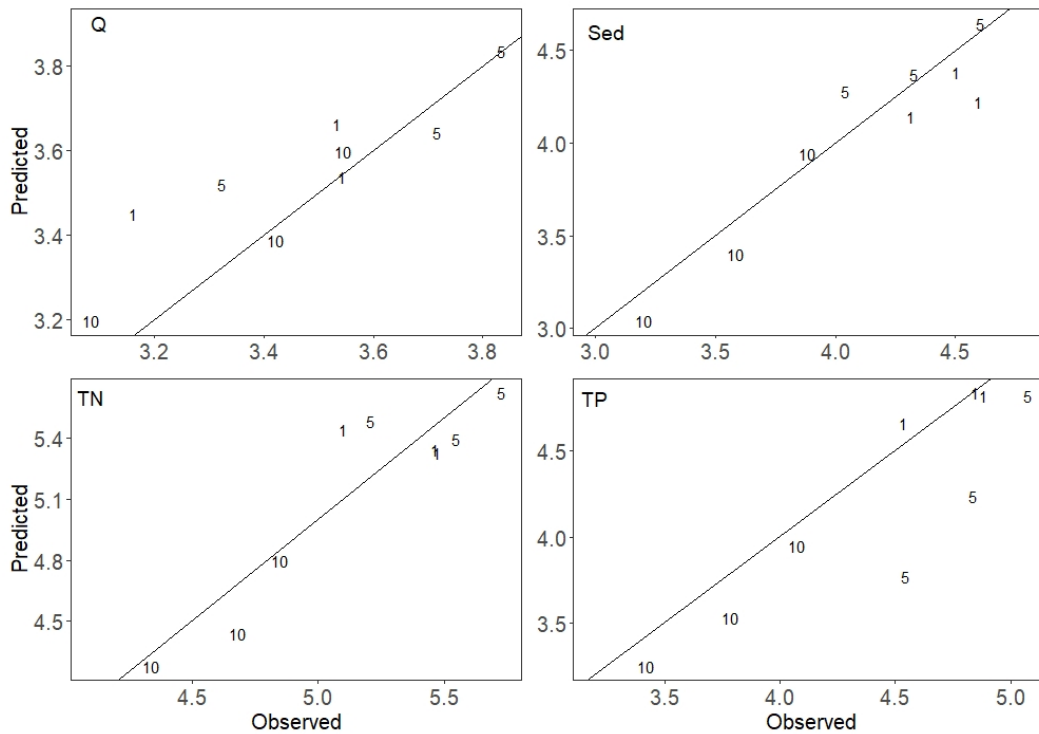


Figure 4: Observed annual streamflow, sediment, total nitrogen (TN), and total phosphorus (TP) loads versus SWAT simulated values at calibration sites; numbers represent Site IDs listed in Table 1.

The top five sensitive parameters for sediment (Table 3) were related to both upland and channel erosion, including the universal soil loss equation (USLE) k factor (USLE_K), the USLE support practice factor (USLE_P), the peak rate adjustment factor for sediment routing in the subbasin (ADJ_PKR), the biological mixing efficiency (BIOMIX), and linear parameter for the maximum amount of sediment that can be re-entrained during channel sediment routing (SPCON). Parameters ADJ_PKR and SPCON are on the whole watershed scale, so they were manually adjusted to optimize all sites, and the final values were 1.0 and 0.008, respectively. In addition to the lowest model performance occurring at Site 1, sediment performance specifically had the lowest performance. Sediment calibration was considered unsatisfactory on the daily, monthly and annual scale (Table 4, Figures 2-4). The best performance occurred on the monthly scale, but was still considered unsatisfactory.

The top five sensitive parameters for TN (Table 3) were related to denitrification, infiltration, and sediment loading, including the nitrate percolation coefficient (NPERCO), denitrification exponential rate coefficient (CDN), potential crack volume of the soil profile (SOL_CRK), denitrification threshold water content (SDNCO), and the organic N enrichment ratio for loading with sediment (ERORGN). Parameters CDN, SDNCO and NPERCO are on the watershed scale, so these were adjusted manually to optimize outputs across all sites, and a final value of 0.01, 0.71 and 0.01 were used, respectively. TN calibration was considered unsatisfactory based on NSE and RSR, but satisfactory based on PBIAS on all time scales (Table 4, Figures 2-4).

Finally, the top five sensitive parameters for TP (Table 3) were related to plant uptake of P, soil properties, runoff, and in-stream processes, including the P uptake distribution parameter (P_UPDIS), P soil partitioning coefficient (PHOSKD), moist bulk density of the soil (SOL_BD), phosphorus enrichment ratio for loading with sediment (ERORGP), and the organic P settling

rate in the reach (RS5). Watershed scale parameters, PHOSKD and P_UPDIS, were adjusted manually to optimize outputs across all sites, and values of 196.5 and 0.5 were used, respectively. While TP performance was slightly better than TN, it was still considered unsatisfactory at the daily scale based on NSE and RSR, but satisfactory based on PBIAS (Table 4). However, on the monthly and annual scale, TP was considered satisfactory.

Calibration at Site 5

For streamflow, the top five parameters (Table 5) were related to soil properties, stream channel, and overland flow processes and included CN2, available water capacity of the soil layer (SOL_AWC), OV_N, saturated hydraulic conductivity (SOL_K), and average slope length (SLSUBBSN), and were all adjusted on the HRU or subwatershed scale based on the calibrated value. Daily streamflow calibration was good based on NSE and RSR and very good based on PBIAS (Table 6). Additionally, monthly and annual calibration were good and very good, respectively.

Table 5: Top five sensitive parameters (descriptions in Appendix A) for each process (flow, sediments, total nitrogen (TN), total phosphorus (TP)), calibration method, and calibrated values at Site 5.

Process	Top 5 Sensitive Parameters	Calibration Method*	Calibrated Value
Flow	CN2	Relative	-0.175
	SOL_AWC	Relative	0.895
	OV_N	Relative	0.028
	SOL_K	Relative	0.963
	SLSUBBSN	Relative	-0.418
Sediments	USLE_K	Replace	0.638
	CH_N2	Replace	0.015
	USLE_P	Replace	0.589
	ESCO	Replace	0.136
	EPCO	Replace	0.722
TN	NPERCO	Replace	0.390
	CDN	Replace	0.015
	SDNCO	Replace	0.695
	ANION_EXCL	Replace	0.825
	ERORGN	Replace	0.955
TP	SOL_BD	Replace	1.100
	PHOSKD	Replace	151.0
	ERORGP	Replace	0.725
	P_UPDIS	Replace	17.00
	RS5	Replace	0.002

*Calibration methods in SWAT-CUP are either relative (parameter is multiplied by 1 + calibrated value), replace (parameter is replaced by calibrated value), or additive (calibrated value is added to parameter).

Table 6: Calibration statistics at Site 5 for each constituent (flow, sediments, total nitrogen (TN), total phosphorus (TP)) and average simulated and observed values on the daily, monthly and annual scale.

Scale	Process	NSE	PBIAS	RSR	Average Simulated	Average Observed
Daily	Flow (cms)	0.71	2.9	0.54	13.3	12.9
	Sediments (tons)	0.77	19.4	0.48	79.0	66.1
	TN (kg)	0.50	-6.5	0.63	893.0	956.0
	TP (kg)	0.60	-60.0	0.65	81.2	203.2
Monthly	Flow (cms)	0.69	2.9	0.55	404	392
	Sediments (tons)	0.83	19.5	0.41	2402	2010
	TN (kg)	0.62	-6.5	0.61	27187	29077
	TP (kg)	0.50	-60.0	0.70	2473	6179
Annual	Flow (cms)	0.81	2.9	0.36	4856	4711
	Sediments (tons)	0.81	19.5	0.36	28862	24129
	TN (kg)	0.38	-6.5	0.64	326248	348934
	TP (kg)	-0.79	-60.0	1.09	29676	74148

The top five sensitive parameters for sediment (Table 5) were related to both upland and channel erosion, including USLE_K, CH_N2, USLE_P, the soil evaporation compensation factor (ESCO), and the plant uptake compensation factor (EPCO). Sediment calibration was considered very good based on NSE and RSR and good based on PBIAS on the daily, monthly and annual scale (Table 6, Figures 2-4). In general, sediments were slightly over predicted by the model.

The top five sensitive parameters for TN (Table 5) were related to denitrification, infiltration, and sediment loading, including NPERCO, CDN, SDNCO, the fraction of porosity which anions are excluded (ANION_EXCL), and ERORGN. TN calibration was considered satisfactory based on NSE and RSR, and very good based on PBIAS on all time scales (Table 6, Figures 2-4).

Finally, the top five sensitive parameters for TP (Table 5) were related to plant uptake of P, soil properties, runoff, and in-stream processes, including SOL_BD, PHOSKD, ERORGP,

P_UPDIS, and RS5. TP calibration was considered satisfactory on the daily and monthly scale (Table 6, Figure 2 and 3), but TP was unsatisfactory on the annual scale, where TP was under predicted by the model (Figure 4).

Calibration at Site 10

For streamflow, the top five parameters (Table 7) were related to soil properties, stream channel, and overland flow processes including CN2, SOL_K, SLSUBBSN, SOL_AWC, and ESCO, and were all adjusted on the HRU scale based on the calibrated value (Table 7). The ESCO factor was sensitive for both streamflow and sediments, so it was manually adjusted to a value of 0.678 to optimize both processes. Streamflow calibration was good based on NSE and RSR and very good based on PBIAS on the daily scale (Table 8, Figure 2). On the monthly and annual scales, streamflow calibration was very good (Figure 3 and 4).

Table 7: Top five sensitive parameters (descriptions in Appendix A) for each process (flow, sediments, total nitrogen (TN), total phosphorus (TP)), calibration method, and calibrated values at Site 10.

Process	Top 5 Sensitive Parameters	Calibration Method*	Calibrated Value
Flow	CN2	Relative	-0.089
	SOL_K	Relative	0.866
	SLSUBBSN	Relative	-0.366
	SOL_AWC	Relative	0.184
	ESCO	Replace	0.678
Sediments	USLE_K	Replace	0.891
	USLE_P	Replace	0.841
	CH_N2	Replace	0.052
	ESCO	Replace	0.906
	EPCO	Replace	0.196
TN	CDN	Replace	2.355
	ERORGN	Replace	0.525
	ANION_EXCL	Replace	0.985
	SDNCO	Replace	0.215
	NPERCO	Replace	0.361
TP	ERORGP	Replace	0.960
	SOL_BD	Replace	1.316
	PHOSKD	Replace	101.0
	P_UPDIS	Replace	39.00
	PPERCO	Replace	15.90

*Calibration methods in SWAT-CUP are either relative (parameter is multiplied by 1 + calibrated value), replace (parameter is replaced by calibrated value), or additive (calibrated value is added to parameter).

Table 8: Calibration statistics at Site 10 for each constituent (flow, sediments, total nitrogen (TN), total phosphorus (TP)) and average simulated and observed values on the daily, monthly and annual scale.

Scale	Process	NSE	PBIAS	RSR	Average Simulated	Average Observed
Daily	Flow (cms)	0.65	8.5	0.60	7.3	6.7
	Sediments (tons)	0.61	-5.6	0.63	11.3	12.0
	TN (kg)	0.63	-22.1	0.61	99.7	127.9
	TP (kg)	0.62	-32.2	0.61	12.8	18.8
Monthly	Flow (cms)	0.55	8.5	0.66	222	204
	Sediments (tons)	0.77	-5.6	0.47	343	363
	TN (kg)	0.58	-22.1	0.64	3035	3896
	TP (kg)	0.68	-32.2	0.56	388	573
Annual	Flow (cms)	0.86	8.5	0.31	2664	2456
	Sediments (tons)	0.82	-5.6	0.34	4122	4367
	TN (kg)	0.60	-22.1	0.52	36422	46761
	TP (kg)	0.60	-32.2	0.53	4664	6881

Besides ESCO, the other top sensitive parameters for sediment were USLE_K, USLE_P, CH_N2, and EPCO (Table 7). All parameters were adjusted on the HRU scale, except for Manning's n, which was on the subwatershed scale. Sediment calibration was considered satisfactory based on NSE and RSR and good based on PBIAS on the daily scale. (Table 8, Figure 2). On the monthly and annual scales, sediment calibration was very good (Figure 3 and 4).

The top five sensitive parameters for TN (Table 7) were related to denitrification, infiltration, and sediment loading including CDN, ERORGN, ANION_EXCL, SDNCO, and NPERCO. TN calibration was considered satisfactory based on NSE and RSR and very good based on PBIAS on the daily and monthly scale (Table 8, Figure 2 and 3). On the annual scale, TN was considered satisfactory based on NSE, very good based on PBIAS, and good based on RSR (Table 8, Figure 4).

Finally, the top five sensitive parameters for TP were related to plant uptake of P, soil properties, and runoff including ERORGP, SOL_BD, PHOSKD, P_UPDIS, and P percolation coefficient (PPERCO). TP calibration was considered satisfactory based on NSE and RSR and good based on PBIAS on the daily scale (Table 8, Figure 2). On the monthly and annual scale, TP calibration was considered good (Table 8, Figure 3 and 4).

Validation at Small-Scale Watersheds

Once calibration the large scale was considered acceptable, validation was conducted at eight sites on small-scale watersheds over the same 3-year time span. Validation on the daily scale was variable across sites and calibration statistics (NSEs ranged from < -100 to 0.60), and the lowest validation performance occurred at site 9 (Table 9, Figure 5). Based on NSE and RSR, streamflow validation was unsatisfactory at all sites except for sites 6 and 7, where streamflow calibration was satisfactory (Table 9). Sediment validation was satisfactory at sites 6, 7 and 8, but unsatisfactory at the remainder of sites. TN validation was only satisfactory at site 6, but the remainder of the sites were unsatisfactory. Finally, TP validation was only satisfactory at site 7. However, based on PBIAS, several sites and constituents were considered satisfactory or better (Table 9).

Table 9: Validation statistics for each constituent (flow, sediments, total nitrogen (TN), total phosphorus (TP)) and average simulated and observed values on the daily scale.

Site	Process	NSE	PBIAS	RSR	Average Daily-Simulated	Average Daily-Observed
2	Flow (cms)	0.38	35.00	0.79	0.4	0.3
	Sediments (tons)	-2.19	208.90	1.79	1.5	0.5
	TN (kg)	0.17	-36.50	0.91	8.3	13.2
	TP (kg)	0.25	19.60	0.85	2.3	1.9
3	Flow (cms)	0.32	10.60	0.83	1.2	1.1
	Sediments (tons)	0.04	-53.50	0.98	0.3	7.0
	TN (kg)	0.09	-60.80	0.95	18.2	46.9
	TP (kg)	0.04	-75.50	0.98	0.4	14.3
4	Flow (cms)	0.37	29.60	0.79	0.3	2.2
	Sediments (tons)	0.21	3.00	0.89	19.5	19.2
	TN (kg)	0.17	-41.70	0.91	91.2	158.2
	TP (kg)	0.22	-36.50	0.88	28.7	45.8
6	Flow (cms)	0.57	-31.50	0.65	4.4	6.4
	Sediments (tons)	0.59	-34.80	0.64	21.3	32.8
	TN (kg)	0.54	-33.60	0.68	425.0	640.5
	TP (kg)	0.45	-69.80	0.74	45.3	146.9
7	Flow (cms)	0.50	-32.50	0.70	0.9	1.4
	Sediments (tons)	0.59	-23.60	0.64	4.0	5.3
	TN (kg)	0.45	-18.40	0.74	74.4	91.6
	TP (kg)	0.50	-63.50	0.70	8.5	22.9
8	Flow (cms)	0.46	-52.70	0.85	2.2	4.5
	Sediments (tons)	0.60	-2.60	0.63	12.2	12.1
	TN (kg)	0.39	-31.40	0.92	159.0	223.7
	TP (kg)	0.33	-77.80	0.78	9.3	37.7
9	Flow (cms)	-1.39	20.10	1.55	2.2	1.8
	Sediments (tons)	-22342	7515	150	5.6	0.7
	TN (kg)	-0.27	-79.10	1.15	16.1	77.2
	TP (kg)	-23.50	-25.70	4.69	2.4	3.2
11	Flow (cms)	0.39	-44.70	0.78	1.9	3.4
	Sediments (tons)	0.36	-64.90	0.80	1.5	4.4
	TN (kg)	0.16	-80.80	0.92	19.8	103.1
	TP (kg)	0.39	-67.60	0.78	1.7	5.4

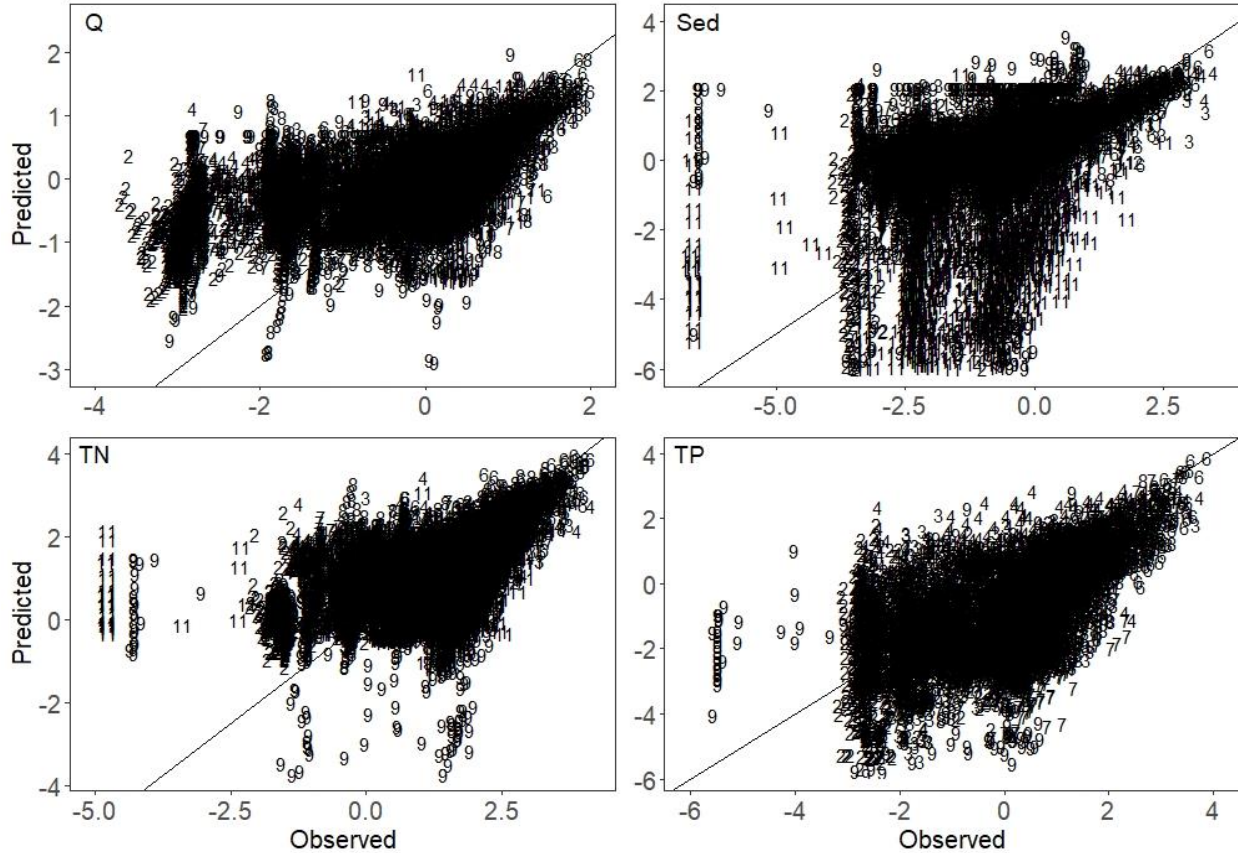


Figure 5: Observed daily streamflow, sediment, total nitrogen (TN), and total phosphorus (TP) loads versus SWAT simulated values at validation sites; numbers represent Site IDs listed in Table 1.

Validation at the small-scale watersheds on the monthly scale typically had lower performances across sites compared to daily validation. Based on NSE and RSR, streamflow validation was unsatisfactory at all sites, but based on PBIAS, streamflow validation was satisfactory at site 3 and 9 (Table 10, Figure 6). Sediment validation was good at site 7 and very good at site 8 based on all statistics. However, sediment validation was unsatisfactory at the remainder of sites. TN validation was satisfactory at site 7 based on NSE and RSR, and very good based on PBIAS. The remainder of the sites were unsatisfactory based on NSE and RSR, but some sites were satisfactory or better based on PBIAS. At site 2, TP validation was satisfactory based on NSE and RSR, and very good based on PBIAS, but the remainder of the

sites were unsatisfactory. Similar to TN, some sites were satisfactory or better based on PBIAS for TP (Table 10).

Table 10: Validation statistics for each constituent (flow, sediments, total nitrogen (TN), total phosphorus (TP)) and average simulated and observed values on the monthly scale.

Site	Process	NSE	PBIAS	RSR	Average Monthly-Simulated	Average Monthly-Observed
2	Flow (cms)	0.42	35.70	0.75	13	10
	Sediments (tons)	-2.87	209.10	1.94	47	15
	TN (kg)	0.26	-36.10	0.84	254	397
	TP (kg)	0.55	19.80	0.64	70	58
3	Flow (cms)	0.42	11.60	0.75	38	34
	Sediments (tons)	0.01	-53.30	0.98	98	209
	TN (kg)	-0.05	-60.70	1.01	553	1405
	TP (kg)	-0.07	-75.50	1.02	105	429
4	Flow (cms)	0.43	30.50	0.75	87	66
	Sediments (tons)	0.26	2.90	0.85	591	574
	TN (kg)	0.17	-36.10	0.98	2777	4741
	TP (kg)	0.32	-36.30	0.81	873	1371
6	Flow (cms)	0.46	-31.40	0.73	133	195
	Sediments (tons)	0.54	-35.00	0.67	648	997
	TN (kg)	0.38	-33.60	0.77	12940	19499
	TP (kg)	0.25	-75.20	0.88	1381	4472
7	Flow (cms)	0.37	-32.00	0.78	28	41
	Sediments (tons)	0.72	-23.30	0.52	121	158
	TN (kg)	0.59	-17.50	0.63	2264	2745
	TP (kg)	0.19	-63.60	0.89	258	686
8	Flow (cms)	-0.04	-50.90	1.00	66	134
	Sediments (tons)	0.75	1.60	0.49	370	364
	TN (kg)	0.07	-28.30	0.95	4832	6742
	TP (kg)	-0.21	-80.50	1.08	284	1137
9	Flow (cms)	-0.11	20.00	0.85	68	56
	Sediments (tons)	-1174	7510	106	1730	22
	TN (kg)	-0.60	-79.10	1.25	484	2320
	TP (kg)	-1.56	-29.60	1.58	71	96
11	Flow (cms)	-1.84	-44.70	1.08	58	104
	Sediments (tons)	0.36	-64.90	0.78	47	134
	TN (kg)	-0.55	-80.80	1.23	602	3139
	TP (kg)	0.21	-67.60	0.88	53	163

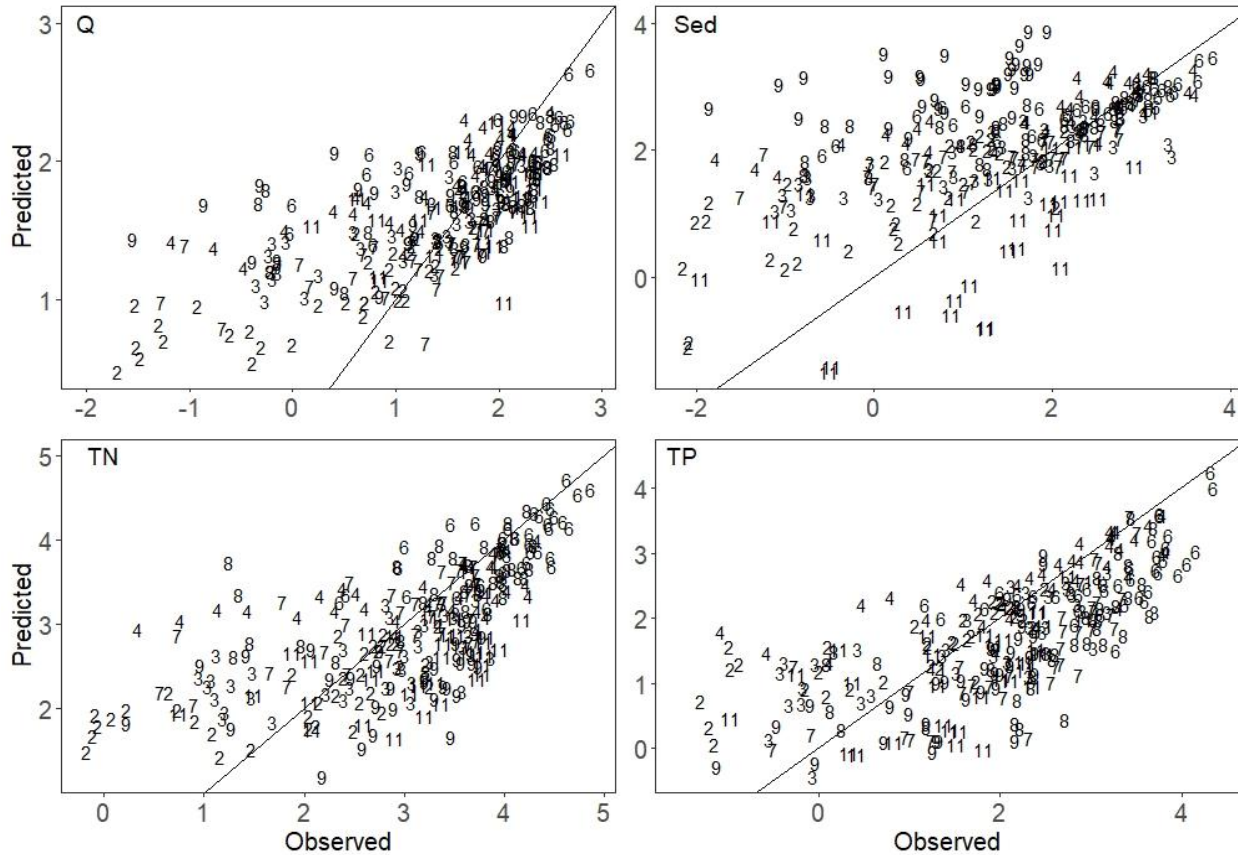


Figure 6: Observed monthly streamflow, sediment, total nitrogen (TN), and total phosphorus (TP) loads versus SWAT simulated values at validation sites; numbers represent Site IDs listed in Table 1.

On the annual scale, validation statistics were poor across most sites and constituents. However, at site 7, sediment validation was considered good based on NSE and PBIAS, and very good based on RSR (Table 11). Additionally, sediment validation at site 8 were very good across all calibration statistics. The remainder of the sites were considered unsatisfactory across all constituents, except for some sites and constituents using PBIAS (Table 11, Figure 7). In general, TN and TP were under predicted by the model on the annual scale.

Table 11: Validation statistics for each constituent (flow, sediments, total nitrogen (TN), total phosphorus (TP)) and average simulated and observed values on the annual scale.

Site	Process	NSE	PBIAS	RSR	Average Annual-Simulated	Average Annual-Observed
2	Flow (cms)	-7.21	35.70	2.34	156	115
	Sediments (tons)	-23.80	209.10	4.06	562	182
	TN (kg)	-4.17	-36.10	1.86	3043	4766
3	TP (kg)	-1.62	19.80	1.33	842	703
	Flow (cms)	-2.15	11.60	1.45	455	408
	Sediments (tons)	-2.14	-53.30	1.45	1175	2519
4	TN (kg)	-53.56	-60.70	6.03	6634	16869
	TP (kg)	-3.17	-75.50	1.67	1263	5147
	Flow (cms)	-5.71	30.50	2.11	1046	801
6	Sediments (tons)	-0.82	2.90	1.10	7097	6896
	TN (kg)	-5.62	-41.40	2.10	33322	56901
	TP (kg)	-7.24	-36.30	2.10	10476	16457
7	Flow (cms)	-0.41	-31.40	0.97	1605	2341
	Sediments (tons)	0.09	-35.00	0.78	7779	11964
	TN (kg)	-117.00	-33.60	1.20	155279	233988
8	TP (kg)	-2.93	-69.10	1.67	16569	53674
	Flow (cms)	-2.31	-32.00	1.49	338	497
	Sediments (tons)	0.69	-23.30	0.45	1453	1894
9	TN (kg)	0.32	-17.50	0.68	27177	32943
	TP (kg)	-2.86	-63.30	1.60	3098	8238
	Flow (cms)	-3.78	-50.90	1.78	795	1619
11	Sediments (tons)	0.99	1.60	0.07	4440	4371
	TN (kg)	-1.58	-28.30	1.31	58011	80895
	TP (kg)	-5.62	-75.00	2.10	3406	13648
11	Flow (cms)	-0.62	20.00	1.04	810	675
	Sediments (tons)	-97666	7510	255	20759	272
	TN (kg)	-17.50	-79.10	3.66	5805	27837
11	TP (kg)	-4.56	-29.60	1.93	852	1147
	Flow (cms)	-3.28	-44.70	1.69	693	1253
	Sediments (tons)	-1.69	-64.90	1.34	563	1607
11	TN (kg)	-9.09	-80.80	2.59	7225	37663
	TP (kg)	-12.53	-67.60	3.00	634	1957

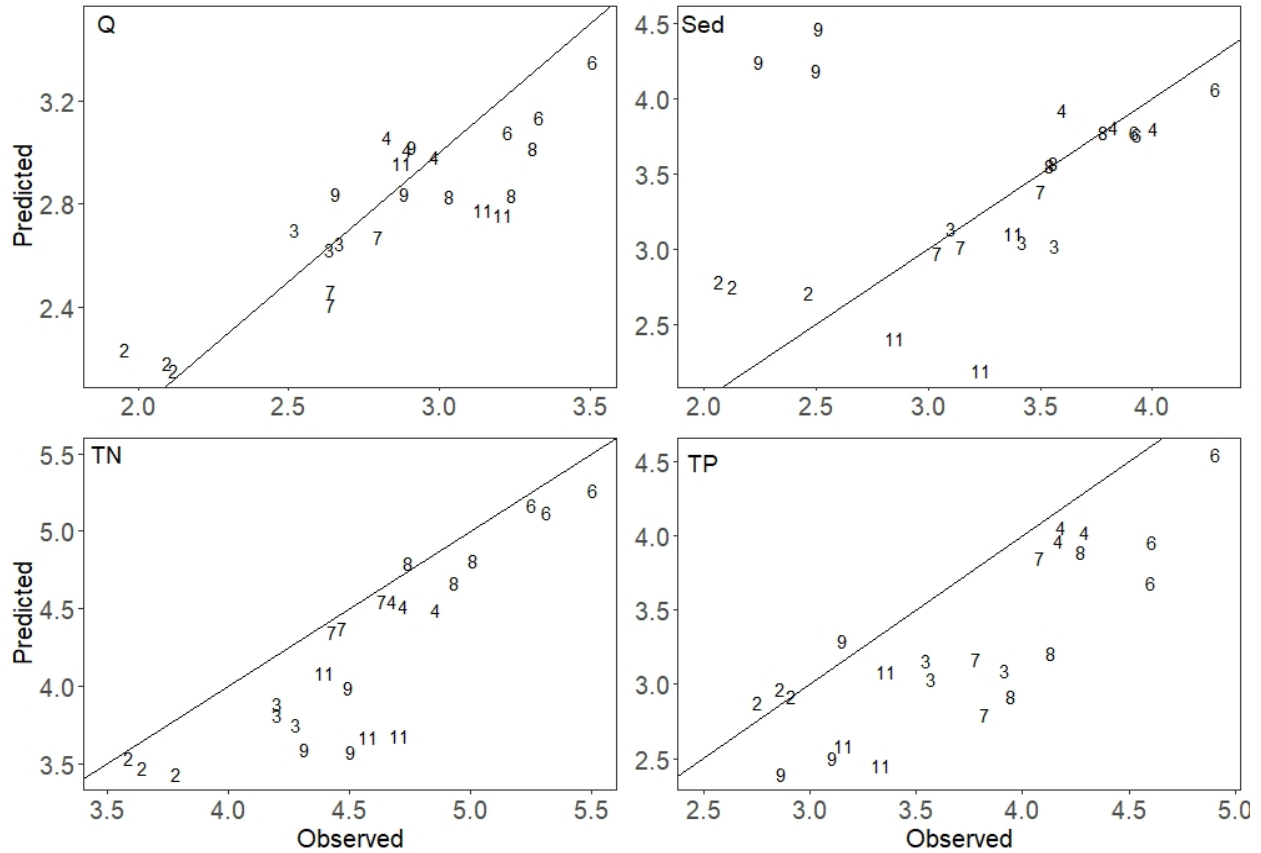


Figure 7: Observed annual streamflow, sediment, total nitrogen (TN), and total phosphorus (TP) loads versus SWAT simulated values at validation sites; numbers represent Site IDs listed in Table 1.

Discussion

Watershed models are often calibrated at the HUC-8 or HUC-10 scale where monitoring data is frequently available. However, model outputs are often used on the HUC-12 scale or smaller without data to validate the model at this scale (e.g., see Chapter 4). Therefore, this study sought to calibrate a watershed model at the large-scale and assess its performance on the small-scale through validation with HUC-12 and HUC-14 watershed data.

Sensitivity analyses in the UPRW identified numerous parameters representing several watershed processes, similar to many SWAT studies (Arabi et al. 2008; Dechmi et al. 2012; Jajarmizadeh et al. 2017). For streamflow, the most sensitive parameters were related to

Manning's roughness, hydraulic conductivity, and groundwater processes. Across all three sites, CN2 was highly sensitive, suggesting the importance of runoff for streamflow. For sediment loads, overland and instream erosion parameters were highly sensitive. All three sites expressed sensitivity toward denitrification, infiltration and sediment loading for TN. For TP, plant uptake, soil properties and runoff were sensitive. Instream processes for TP were sensitive at the James Fork and Poteau River, but not on the Black Fork.

Calibration was satisfactory or better at the Poteau River and Black Fork, but the James Fork did not perform as well. Streamflow at the James Fork was satisfactory on the daily scale, but based on NSE and RSR, sediments and nutrients were unsatisfactory. However, based on PBIAS, calibration of all parameters were satisfactory. Similar results occurred in a previously developed SWAT model for the Poteau River and James Fork, where the James Fork showed mixed results and was considered satisfactory based on PBIAS and NSE, but unsatisfactory based on R^2 and RSR (Saraswat et al. 2013). While model evaluation statistics developed by Moriasi et al. 2007 are widely used for SWAT modelling, based on evaluations developed by Parajuli et al. 2009, the daily calibration at the James Fork would be considered fair or better. Additionally, SWAT models have been developed and reported with calibration results similar to the James Fork (Santhi et al. 2001; White and Chaubey 2005; Parajuli et al. 2009).

Prior to calibration, the SWAT model performance at the James Fork produced NSE values between 0.15 and 0.46, PBIAS between ± 2 and 51, and RSR between 0.74 and 0.92 across constituents. Therefore, calibration efforts improved model predictions compared to the base model. Calibrated model outputs were generally under predicted at the upper end of observations and over predicted at the lower end of observations, occurring at greater magnitudes for sediment and nutrient loads compared to streamflow. Daily observed and predicted loads

were highly related to streamflow ($R^2 > 0.73$, $p < 0.001$), and calibration improvements of streamflow would also likely improve constituent load performances. Inadequate spatial coverage of precipitation data is often a source of poor calibration results (Arnold et al. 2012), and the James Fork monitoring site is around 40 km from the closest precipitation gage. Therefore, finer scale rainfall data could improve the James Fork calibration results.

While SWAT models have frequently been calibrated on the daily, monthly and annual scale, some studies have shown better calibration results at the monthly scale compared to daily (Golmohammadi et al. 2014). Across 31 studies calibrated on the monthly scale in Brazil, NSE values were considered satisfactory or better 94% of the time, but in 26 studies calibrated on the daily scale, NSE values were considered satisfactory or better 75% of the time (Bressiani et al. 2015). In the War Eagle Creek watershed in Arkansas, a SWAT model calibrated on the monthly scale outperformed a calibration on the daily scale (Sudheer et al. 2007). Therefore, it may be worth attempting calibration at the James Fork on the monthly scale to try and improve model performance.

At the Poteau River and the Black Fork, calibration was generally satisfactory or better across all constituents and scales. Evaluation statistics at the Poteau River were similar to the previously developed SWAT model for the Poteau River and James Fork, where calibration was also satisfactory or better on the monthly scale (Saraswat et al. 2013). Both the Black Fork and Poteau River fall within evaluation statistics of other SWAT models in the literature (Moriassi et al. 2015; Merriman et al. 2018; Mengistu et al. 2019), and specifically with SWAT models used for prioritization of subwatershed or critical source areas (Niraula et al. 2012; Kumar and Mishra 2015; Imani et al. 2019).

Overall, 77% of statistics were considered satisfactory or better, and on the daily scale (the scale of calibration) 80% of statistics were satisfactory or better. Therefore, the model calibration was considered acceptable. Only the James Fork had performances on the daily scale that were considered unsatisfactory, therefore, the model outputs in this watershed should be handled with caution.

When the model was validated at eight HUC-12 and HUC-14 watersheds over the same time period, only 24% of all statistics were considered satisfactory or better. According to PBIAS 47% were satisfactory or better, but for NSE and RSR, only 14% and 10%, respectively, were satisfactory or better. Typically SWAT models are temporally validated at one or more sites where calibration occurred, and validation performances are as good as or better than the calibration period (White and Chaubey 2005; Ahl et al. 2008; Shawul et al. 2013; dos R. Pereira et al. 2016; Bai et al. 2017). Therefore, the poor validation results at the small-scale watersheds are concerning.

The best validation results occurred at sites 6 and 7, where daily evaluations statistics were generally considered satisfactory. Sites 6 and 7 are upstream from the calibration site 5 on the Poteau River, and have similar land use distributions as site 5 (Table 1). However, the lowest validation performance occurred at site 9, which is just downstream of the Lake Hinkle dam in the Poteau River watershed. The model greatly over predicted sediment loads and under predicted nutrient loads at site 9, thus the model is not adequately representing reservoir impacts on this small stream. Since data is typically limited on small impoundments (as was true for Lake Hinkle), it can be difficult to calibrate small reservoir dynamics in SWAT. With monitoring data downstream of the Lake Hinkle dam, the dam outputs could be adjusted to improve model performance.

Both calibration and validation results were generally worse at the annual scale compared to monthly and daily. This could be due to the low sample size for evaluation statistics, since only 3 years of data were used in the study. Additionally, Sudheer et al., 2007 show that calibrating a SWAT model on the monthly scale and calculating the model's performance on the daily scale can be inaccurate. The same may be true for annual model performances in this study, since the model was calibrated on the daily scale.

There could be unfortunate implications if small-scale watershed outputs were used from this SWAT model calibrated at the large-watershed scale. If subwatersheds were prioritized based on nutrient and sediment loads, high priority could be designated to watersheds that are actually not a concern (e.g., Jones Creek would be high priority based on sediment loads, but monitoring data actually show low sediment loads). Therefore, time and money could be invested towards watershed management practices in areas that may not need improvements, and areas in need of management may be missed. To our knowledge, the majority of watershed models used for subwatershed prioritization are developed in this manner (Chapter 4), and could be inaccurately prioritizing areas of concern.

While actual monitoring data at the small-scale watershed would likely be the best method for validating model performances, small-scale watershed data is expensive and difficult to collect and is rarely available. Pai et al., 2011 validated SWAT model results in the Illinois River watershed by analyzing correlations between subwatershed pollutant concentrations and percentage of land use to confirm the expected trend of increasing concentrations with increasing pasture land. However, subwatersheds with point source discharges may deviate from this relationship (e.g., a forest dominated watershed could be high priority), so this validation metric must be used with caution when considering point and nonpoint pollution.

The previously developed SWAT model for the Poteau River watershed, which was calibrated at same locations on the James Fork and Poteau River as this study, was successfully validated temporally, and model outputs between 2008 and 2010 were used to prioritize critical source areas within the UPRW (Saraswat et al. 2013). Small-scale watershed data (HUC-12 scale) was then collected across the UPRW between 2011 and 2010, and baseflow concentrations were compared to the SWAT model outputs from the prioritization time period. Significant relationships were observed between monitoring data and model outputs for nitrate and TP, but not TSS, and the linear slopes were not close to one. However, the monitoring data and model outputs suggested the same sites as high or low priority, which the authors used as validation for the model's ability to prioritize HUC-12 subwatersheds (Massey et al. 2013). Therefore, it would be interesting to determine if small-scale monitoring sites in this study fell in the same prioritization categories as those determined from the SWAT model developed here.

Future Work

In this study, SWAT was calibrated at the large scale watershed and validated at the small-scale. The opposite scenario could be tested, where the model is calibrated at the small-scale watershed and validated at the large scale. Additionally, a spatial combination could be used, where some of the small and large scale watersheds are used for calibration and the rest for validation. Priority subwatersheds could then be compared across the different calibrated/validated models to determine the importance of the small-scale watershed data for prioritization using SWAT models.

The monitoring data in this study did not encompass the highly urban area in the northern portion of the UPRW. It would be interesting to select more monitoring sites on the HUC-12 and HUC-14 scale across the UPRW, including the urban dominated area, and compare priorities

determined from baseflow monitoring to SWAT outputs (similar to Massey et al., 2013, but with more monitoring sites encompassing more of the UPRW area and the HUC-14 scale).

Conclusions

Ultimately, the large scale calibration was mostly satisfactory or better, but the small-scale validation was mostly unsatisfactory. With poor validation results at the HUC-12 and HUC-14 watershed scale, it is difficult to justify using the model outputs for subwatershed prioritization or other watershed modeling efforts (i.e., BMP evaluation and TMDL development). Therefore, it may be necessary to begin collecting more small-scale data for use in SWAT calibration/validation.

References

- ADEQ (2018) Arkansas's Final Impaired Waterbodies-303(d) List. Arkansas Department of Environmental Quality, North Little Rock
- Aguirre-Salado C, Miranda-Aragón L, Pompa-García M, et al (2017) Improving Identification of Areas for Ecological Restoration for Conservation by Integrating USLE and MCDA in a GIS-Environment: A Pilot Study in a Priority Region Northern Mexico. *ISPRS Int J Geo-Information* 6:262. doi: 10.3390/ijgi6090262
- Ahl RS, Woods SW, Zuuring HR (2008) Hydrologic calibration and validation of SWAT in a snow-dominated Rocky Mountain watershed, Montana, U.S.A. *J Am Water Resour Assoc* 44:1411–1430. doi: 10.1111/j.1752-1688.2008.00233.x
- Anderson D, Glibert P, Burkholder J (2002) Harmful algal blooms and eutrophication: nutrient sources, compositions, and consequences. *Estuaries* 25:704–726. doi: 10.1016/j.hal.2008.08.017
- Andrade MA, Mello CR de, Beskow S (2013) Simulação hidrológica em uma bacia hidrográfica representativa dos Latossolos na região Alto Rio Grande, MG. *Rev Bras Eng Agrícola e Ambient* 17:69–76. doi: 10.1590/s1415-43662013000100010
- ANRC (2018) 2018-2023 Nonpoint Source Pollution Management Plan. Arkansas Natural Resource Commission, Little Rock, Arkansas
- Arabi M, Frankenberger JR, Engel BA, Arnold JG (2008) Representation of agricultural conservation practices with SWAT. *Hydrol Process* 22:3042–3055. doi: 10.1002/hyp
- Arkansaswater.org (2017) Poteau Watershed-11110105

- Arnold JG, Moriasi DN, Gassman PW, et al (2012) SWAT: Model Use, Calibration, and Validation. *Am Soc Agric Biol Eng* 55:1491–1508
- Bai J, Shen Z, Yan T (2017) A comparison of single- and multi-site calibration and validation: a case study of SWAT in the Miyun Reservoir watershed, China. *Front Earth Sci* 11:592–600. doi: 10.1007/s11707-017-0656-x
- Borah DK, Yagow G, Saleh A, et al (2006) Sediment and Nutrient Modeling for TMDL Development and Implementation. *Trans ASABE* 49:967–986. doi: 10.13031/2013.21742
- Bressiani D de A, Gassman PW, Fernandes JG, et al (2015) A review of soil and water assessment tool (SWAT) applications in Brazil: Challenges and prospects. *Int J Agric Biol Eng* 8:1–27. doi: 10.3965/j.ijabe.20150803.1765
- Copeland C (2012) CRS Report for Congress Clean Water Act: A Summary of the Law
- Daniel TC, Sharpley AN, Lemunyon JL (1998) Agricultural Phosphorus and Eutrophication: A Symposium Overview. *J Environ Qual* 27:251. doi: 10.2134/jeq1998.00472425002700020002x
- Darwiche-Criado N, Sorando R, Eismann SG, Comín FA (2017) Comparing Two Multi-Criteria Methods for Prioritizing Wetland Restoration and Creation Sites Based on Ecological, Biophysical and Socio-Economic Factors. *Water Resour Manag* 31:1227–1241. doi: 10.1007/s11269-017-1572-2
- Deal CJ, Edwards J, Pellmann RT, Woodward D (1997) Ponds- planning, design, construction. *Agricultural Handbook 590*. USDA Natural Resource Conservation Service, Washington, DC
- Dechmi F, Burguete J, Skhiri A (2012) SWAT application in intensive irrigation systems: Model modification, calibration and validation. *J Hydrol* 470–471:227–238. doi: 10.1016/j.jhydrol.2012.08.055
- Dile Y, Srinivasan R, George C (2020) QGIS 3 Interface for SWAT (QSWAT3) Version 1.1. October 2020.
- dos R. Pereira D, Martinez MA, Pruski FF, da Silva DD (2016) Hydrological simulation in a basin of typical tropical climate and soil using the SWAT model part I: Calibration and validation tests. *J Hydrol Reg Stud* 7:14–37. doi: 10.1016/j.ejrh.2016.05.002
- Fallah M, Kavian A, Omidvar E (2016) Watershed prioritization in order to implement soil and water conservation practices. *Environ Earth Sci* 75:1–17. doi: 10.1007/s12665-016-6035-1
- Farhan Y, Anbar A, Al-Shaikh N, Mousa R (2017) Prioritization of Semi-Arid Agricultural Watershed Using Morphometric and Principal Component Analysis, Remote Sensing, and GIS Techniques, the Zerqa River Watershed, Northern Jordan. *Agric Sci* 08:113–148. doi: 10.4236/as.2017.81009

- Gassman PPW, Reyes MMR, Green CCH, Arnold JJG (2007) The Soil and Water Assessment Tool: historical development, applications, and future research directions. *Trans ASAE* 50:1211–1250. doi: 10.1.1.88.6554
- Ghafari H, Gorji M, Arabkhedri M, et al (2017) Identification and prioritization of critical erosion areas based on onsite and offsite effects. *Catena* 156:1–9. doi: 10.1016/j.catena.2017.03.014
- Gitau MW (2003) A quantitative assessment of BMP effectiveness for phosphorus pollution control: The Town Brook watershed, New York. Pennsylvania State University
- Golmohammadi G, Prasher S, Madani A, Rudra R (2014) Evaluating three hydrological distributed watershed models: MIKE-SHE, APEX, SWAT. *Hydrology* 1:20–39. doi: 10.3390/hydrology1010020
- Imani S, Delavar M, Niksokhan MH (2019) Identification of Nutrients Critical Source Areas with SWAT Model under Limited Data Condition. *Water Resour* 46:128–137. doi: 10.1134/S0097807819010147
- Jajarmizadeh M, Sidek LM, Harun S, Salarpour M (2017) Optimal Calibration and Uncertainty Analysis of SWAT for an Arid Climate. *Air, Soil Water Res* 10:1–14. doi: 10.1177/1178622117731792
- Jonge VN de, Elliott M, Orive E (2002) Causes, historical development, effects and future challenges of a common environmental problem: eutrophication. *Hydrobiologia* 475–476:1–19. doi: 10.1023/A:1020366418295
- Karamouz M, Taheriyoun M, Emami F, Rouhanizadeh B (2008) Assessment of watershed nutrient load input to reservoir, a case study. *World Environ Water Resour Congr 2008 Ahupua'a - Proc World Environ Water Resour Congr 2008* 316:. doi: 10.1061/40976(316)543
- Katiyar R, Garg PK, Jain SK (2006) Watershed Prioritization and Reservoir Sedimentation Using Remote Sensing Data. *Geocarto Int* 21:55–60. doi: 10.1080/10106040608542393
- Kumar S, Mishra A (2015) Critical Erosion Area Identification Based on Hydrological Response Unit Level for Effective Sedimentation Control in a River Basin. *Water Resour Manag* 29:. doi: 10.1007/s11269-014-0909-3
- Malik MI, Bhat MS (2014) Integrated Approach for Prioritizing Watersheds for Management: A Study of Lidder Catchment of Kashmir Himalayas. *Environ Manage* 54:1267–1287. doi: 10.1007/s00267-014-0361-4
- Massey LB, McCarty JA, Matlock MD, et al (2013) Water quality monitoring for selected priority watersheds in Arkansas, Upper Saline, Poteau and Strawberry Rivers. Fayetteville, Arkansas
- Mengistu AG, Rensburg LD Van, Woyessa YE (2019) Techniques for calibration and validation of SWAT model in data scarce arid and semi-arid catchments in South Africa. *J Hydrol Reg Stud* 25:100621. doi: 10.1016/j.ejrh.2019.100621

- Merriman KR, Russell AM, Rachol CM, et al (2018) Calibration of a Field-Scale Soil and Water Assessment Tool (SWAT) Model with Field Placement of Best Management Practices in Alger Creek, Michigan. *Sustainability* 10:1–23. doi: 10.3390/su10030851
- Moriasi DN, Arnold JG, Van Liew MW, et al (2007) Model Evaluation Guidelines for Systematic Quantification of Accuracy in Watershed Simulations. *Trans ASABE* 50:885–900. doi: 10.1234/590
- Moriasi DN, Gitau MW, Pai N, Daggupati P (2015) Hydrologic and water quality models: Performance measures and evaluation criteria. *Trans ASABE* 58:1763–1785. doi: 10.13031/trans.58.10715
- Ndomba PM, Mtalo FW, Killingtveit A (2008) A Guided SWAT Model Application on Sediment Yield Modeling in Pangani River Basin: Lessons Learnt. *J Urban Environ Eng* 2:53–62. doi: 10.4090/juee.2008.v2n2.053062
- Niraula R, Kalin L, Wang R, Srivastava P (2012) Determining nutrient and sediment critical source areas with SWAT: Effect of lumped calibration. *Trans ASABE* 55:137–147. doi: 10.13031/2013.41262
- Pai N, Saraswat D, Daniels M (2011) Identifying priority subwatersheds in the Illinois River Drainage Area in Arkansas watershed using a distributed modeling approach. *Trans ASABE* 54:2181–2196. doi: 10.13031/2013.40657
- Parajuli PB, Nelson NO, Frees LD, Mankin KR (2009) Comparison of AnnAGNPS and SWAT model simulation results in USDA-CEAP agricultural watersheds in south-central Kansas. *Hydrol Process* 763:748–763. doi: 10.1002/hyp
- Reungsang P, Kanwar RS, Jha M, et al (2007) Calibration and validation of SWAT for the upper maquoketa river watershed. *Int Agric Eng J* 16:35–48
- Rostamian R, Jaleh A, Afyuni M, et al (2008) Application of a SWAT model for estimating runoff and sediment in two mountainous basins in central Iran Application of. *Hydrol Scie* 53:977–988. doi: 10.1623/hysj.53.5.977
- Santhi C, Arnold JG, Williams JR, et al (2001) Validation of the SWAT model on a large river basin with point and nonpoint sources. *J Am Water Resour Assoc* 37:1169–1188
- Saraswat D, Daniels M, Tacker P, Pai N (2009) A Comprehensive Watershed Response Modeling for 12-digit Hydrologic Unit Code “HUC” in Selected Priority Watersheds in Arkansas
- Saraswat D, Pai N, Daniels M, Riley T (2013) Development of Comprehensive Watershed Modeling for 12-digit HUCs in Selected Priority Watersheds in Arkansas- Phase II Poteau River Watershed (PRW)
- Sharpley A, Herron S, West C, Daniel T (2009) Outcomes of phosphorus-based nutrient management in the Eucha-Spavinaw Watershed. *Proc Farming with Grass Achiev Sustain Mix Agric Landscapes* 192–204
- Shawul AA, Alamirew T, Dinka MO (2013) Calibration and validation of SWAT model and estimation of water balance components of Shaya mountainous watershed, Southeastern

- Ethiopia. *Hydrol Earth Syst Sci Discuss* 10:13955–13978. doi: 10.5194/hessd-10-13955-2013
- Sudheer KP, Chaubey I, Garg V, Migliaccio KW (2007) Impact of time-scale of the calibration objective function on the performance of watershed models. *Hydrol Process*. doi: 10.1002/hyp
- Sun B, Zhang L, Yang L, et al (2012) Agricultural non-point source pollution in China: Causes and mitigation measures. *Ambio* 41:370–379. doi: 10.1007/s13280-012-0249-6
- Tripathi S, Soni SK, Maurya AK (2013) Morphometric Characterization & Prioritization of Sub Watersheds of Seoni River in Madhya Pradesh, Through Remote Sensing & Gis Technique. *Int J Remote Sens Geosci* 2:
- USDA-NASS (2018) Quick Stats. https://www.nass.usda.gov/Quick_Stats/. Accessed 5 Jun 2019
- Wallace CW, Flanagan DC, Engel BA (2018) Evaluating the Effects of Watershed Size on SWAT Calibration. *Water* 10:1–27. doi: 10.3390/w10070898
- Welde K (2016) Identification and prioritization of subwatersheds for land and water management in Tekeze dam watershed, Northern Ethiopia. *Int Soil Water Conserv Res* 4:30–38. doi: 10.1016/j.iswcr.2016.02.006
- White KL, Chaubey I (2005) Sensitivity Analysis, Calibration, and Validation for a Multisite and Multivariable SWAT Model. *J Am Water Resour Assoc* 41:1077–1089
- White MJ, Storm DE, Busteed PR, et al (2009) Evaluating Nonpoint Source Critical Source Area Contributions at the Watershed Scale. *J Environ Qual* 38:1654. doi: 10.2134/jeq2008.0375

Appendix

Appendix A: Parameters used in sensitivity analyses and calibration of SWAT model.

Parameter	Scale	Description	Model Range
CN2	HRU	Initial SCS runoff curve number for moisture condition II	0-11
Alpha_BF	Subwatershed	Baseflow alpha factor	0-1
GW_Delay	Subwatershed	Groundwater delay time	0-500
GWQMN	Subwatershed	Threshold depth of water in the shallow aquifer required for return flow to occur	-1000-2
ESCO	HRU	Soil evaporation compensation factor	0.01-1
OV_N	HRU	Manning's "n" for overland flow	0.001-0.5
SOL_AWC	HRU	Available water capacity of the soil layer	0-1
SURLAG	Watershed	Surface runoff lag coefficient	0-20
SOL_K	HRU	Saturated hydraulic conductivity	0-200
SLSUBBSN	HRU	Average slope length	0-100
HRU_SLP	HRU	Average slope steepness	0-1
GW_REVAP	Subwatershed	Groundwater "revap" coefficient	0.02-2
CH_K2	Subwatershed	Effective hydraulic conductivity in the main channel alluvium	0-200
SOL_ALB	HRU	Moist soil albedo	0-1
EPCO	HRU	Plant uptake compensation factor	0.01-1
CH_N2	Subwatershed	Manning's "n" for the main channel	0.001-0.50
BIOMIX	HRU	Biological mixing efficiency	0-1
RSDIN	HRU	Initial residue cover	0-100
SPCON	Watershed	Maximum amount of sediment that can be reentrained during channel sediment routing	0.0001-0.01
USLE_P	HRU	USLE equation support practice factor	0-1
PRF_BSN	Watershed	Peak rate adjustment factor for sediment routing in the main channel	0-2
SPEXP	Watershed	Exponent parameter for calculating sediment reentrained in channel sediment routing	1-2
CH_COV1	Subwatershed	Channel erodibility factor	0-1
USLE_K	HRU	USLE equation soil erodibility K factor	0-1
CH_ERODMO	Subwatershed	Erosivity of channel	0-1
REVAPMN	HRU	Threshold depth of water in the shallow aquifer for percolation to the deep aquifer	0-2
ANION_EXCL	HRU	Fraction of porosity (void space) from which anions are excluded	0-1

Appendix A (cont.)

ERORGP	HRU	P enrichment ratio for loading with sediment	0.0-1
PPERCO	Watershed	P percolation coefficient	10-17.5
PSP	Watershed	P availability index	0.0-1
SOL_BD	HRU	Moist bulk density	1.1-1.9
AI2	Watershed	Fraction of algal biomass that is phosphorus	0-1
BC4	Watershed	Rate constant for decay of organic P to dissolved P	0.01-0.70
CMN	Watershed	Rate factor for humus mineralization of active organic nutrients (N and P)	0.001-0.1
RS5	Subwatershed	Organic P settling rate in the reach at 20°C	0.001-0.1
PHOSKD	Watershed	P soil partitioning coefficient	0-500
P_UPDIS	Watershed	P uptake distribution parameter	0-100
SOL_CRK	HRU	Potential or maximum crack volume of the soil profile	0-1
NPERCO	Watershed	Nitrate percolation coefficient	0.01-1
CDN	Watershed	Denitrification exponential rate coefficient	0-3
SNDCO	Watershed	Denitrification threshold water content	0-2
ADJ_PKR	Watershed	Peak rate adjustment factor for sediment routing in the subbasin	0-1
CH_N1	Subwatershed	Manning's "n" for the tributary channels	0.001-0.5
CH_K1	Subwatershed	Effective hydraulic conductivity in tributary channel alluvium	0-200
RCN	Watershed	Concentration of N in rainfall	0-50
SHALLST_N	HRU	Initial concentration of nitrate in shallow aquifer	0-100
RS4	Subwatershed	Rate coefficient for organic N settling in the reach at 20°C	0.001-0.1
BC2	Subwatershed	Rate constant for biological oxidation of NO ₂ to NO ₃ in the reach	0.1-1
RCHRG_DP	HRU	Deep aquifer percolation fraction	0-1
ERORGN	HRU	Organic N enrichment ratio for loading with sediment	0-1
HLIFE_NGW	HRU	Half-life of nitrate in the shallow aquifer	0-30
BC1_BSN	Watershed	Rate constant for biological oxidation of NO ₂ to NO ₃	0.1-1
BC3_BSN	Watershed	Rate constant for hydrolysis of organic N to ammonia	0.02-0.4

Conclusions

In the UPRW, increasing OP at the James Fork and increasing TN at the James Fork and Poteau River must be managed. The relatively undisturbed Black Fork serves as a benchmark for watersheds with point and nonpoint sources, and is important to continue monitoring. The Poteau River contributes the largest amount of loads to Lake Wister, and while loads from the Fourche Maline are less, the increasing P concentrations on the Fourche Maline are a concern. Ultimately, the magnitude of loads from the LWW to Lake Wister is likely minimizing the effectiveness of alum treatments in the reservoir. After 5 alum treatments across 6 years, internal P fluxes were not different than prior to any alum treatments. Thus, it is important to address external P sources prior to or in conjunction with alum treatments.

When watershed models are used for subwatershed prioritization, model calibration is often conducted at minimal sites on the large watershed scale and model outputs on the subwatershed scale or smaller are used for prioritization, but little data exists to validate the small-scale model outputs. Therefore, a method was developed to monitor streamflow and estimate constituent loads in small-scale watersheds by using inexpensive pressure transducers to collect continuous records of stage, deploying SonTek-IQs during high flow events, and developing rating curves with a combination of simple linear regression, LOESS regression, and Manning's equation. Additionally, water quality samples were collected across the range of flow, and constituent loads were estimated using GAMs, where the best fit GAM was determined to be spline based smooth functions of Q and DOY. This method provides an opportunity to collect continuous records of flow across multiple, remote, small-scale watersheds, where data is typically unavailable.

When a SWAT model was calibrated using larger watershed scale data (i.e., HUC-8/10) and validated with the aforementioned smaller watershed scale data (i.e., HUC-12/14), the large scale calibration was mostly satisfactory or better, but the small-scale validation was mostly unsatisfactory. With poor validation results at the HUC-12 and HUC-14 watershed scale, it is difficult to justify using the model outputs for subwatershed prioritization or other watershed modeling efforts (i.e., BMP evaluation and TMDL development). Therefore, it may be necessary to begin collecting more small-scale data for use in SWAT calibration/validation.